Use of high-throughput sequencing for the characterization of extracellular RNA and to study the dynamics of bacterial RNA modification

Dissertation zur Erlangung des Grades

“Doktor der Naturwissenschaften”

Im Promotionsfach Pharmazie

am Fachbereich Chemie, Pharmazie und Geowissenschaften

Der Johannes Gutenberg-Universität Mainz

Adeline GALVANIN

Geboren am 07.05.1992 in Laxou

Mainz 2019

Supervisor:

Herr Mark Helm	Professor JGU
Herr Iouri Motorine	Professeur UL Nancy

Tag der mündlichen Prüfung:

17. September 2019

Foreword:

RNA are molecules that play roles far more important than a simple transfer of information from the head: the sacred stored genetic material to the working-class proteins. Indeed, RNA are not only the molecules which make the link between DNA and proteins, RNA are even in the centre, we can consider them at the wise of the cell. At the beginning of the life on Earth, they were there, pioneers, having catalytic activities before bequeathing them to enzyme proteins. At this time in the evolution, it was what we call "the RNA world" where these nucleic acids were ruling the whole cell, they were at the base for everything. Now, a lot of other molecular components took over but RNA are still strongly present in the cell and are involved in a multitude of essential functions. They have so much properties and attributions that it is impossible to list them in an exhaustive manner. If we add a layer of complexity and add RNA modification, splicing event in the equation, it becomes completely crazy.

This is why molecular biology and especially the study of RNA are a huge field in fundamental research where we never stop discovering new things. In a world where technology flows in our veins, where high throughput techniques allowed to make progress science, I am glad to contribute to this vast domain by writing my phD thesis.

"Our world is built on biology and once we begin to understand it, it then becomes a technology."

Ryan Bethencourt

Acknowledgement / Remerciements:

First of all, I would like to thank my director of thesis Yuri Motorin, for accepting me in master 1 internship and to have trusted in me since for master thesis and phD thesis. You gave me the opportunity to play a role in science. I thank you for your precious advises and the great supervision.

I thank my co-director of thesis Mark Helm. Thank for having welcomed me in your laboratory and supervising me during these periods. I could discover new and interesting methods for RNA analysis, another team, another culture!

I would like to thank all the members of the jury of my phD defense: Carine Tisne, David Coelho, Jessica Gobbo, Magali Frugier, Rolf Postina and Sophie Rome for your future important advises. I thank Stefano Marzi and David Coelho for being in my thesis advisory committee and for giving me good clues for the redaction and defense of my thesis.

I thank all the partners involved in my phD project and especially Alexander Dalpke and his team for the close collaboration we initiated together.

J'aimerais également remercier chaleureusement l'équipe ARN et de manière générale le Biopôle. J'avoue que la couleur verte pomme des murs ne va peut-être pas me manquer mais les personnes les côtoyant tous les jours c'est tout à fait différent. C'était un réel plaisir de travailler avec vous, de pouvoir compter sur beaucoup de personnes pour des questions de manips ou pas !

Je remercie la plateforme de séquençage UMS IBSLor 2008 dirigée par mon directeur de thèse Yuri Motorin et gérée par Virginie Marchand. Partie intégrante de mon projet de thèse, je me suis familiarisée et formée sur le séquençage à haut débit grâce à vous.

J'aimerais également remercie Emilie qui m'a beaucoup soutenue sur la partie vésicules extracellulaires. Des échanges enrichissants au point de vue scientifique mais pas uniquement.

J'aimerais remercier mes chères collègues Lilia et Valérie, toujours de bonne humeur et prêtes à m'aider quand j'en avais besoin. Lilia, ma voisine de bureau, merci pour tout le soutien que tu m'as apporté. Ensemble on se redonnait du baume au cœur.

Merci à mes amis thésards qui comprennent tant cette magnifique galère qu'est la thèse. Merci pour les moments de détente nécessaires aux pauses midi, en soirée ou autour d'un morceau de gâteau. Merci à ceux qui ont déjà terminé : Arnaud, Madhia, Yoann, Gabriel, Benjamin et à

ceux qui seront bientôt libérés : Liza, Timothé, Laeya, Fanny, Paul, Florent, Jean-Malo, Charbel …

Ich möchte mich bei der ganzen Mannschaft aus Mainz bedanken. Thank you for having welcomed me in the team and make increase the proportion of French members. A strong thank for Christina and Dominik, you taught me a lot of things and helped for many questions. I wish good luck to Larissa, you have to continue on these cursed tRNA isolation stuffs. Of course, I will not forget to thank Stephan, Florian, Kaouthar and Aurellia. It was a great pleasure to be with you for these few months. I made real friends and hope we will continue to see each other after! PS: je suis tellement dégoutée d'avoir cassé la boule à neige de Mainz …

Merci à toi Géraud, ensemble depuis le M1 et en « concurrence » pour la thèse. Au final, on s'est tous les deux retrouvés en thèse. Merci pour ton humour si particulier et pour toutes nos discussions sur la vie future. J'espère qu'on trouvera notre voie et qu'on sera épanouis.

Je te remercie Dafné, ensemble dans la même galère depuis le DUT ! On a beaucoup partagé pendant toutes ces années, nos joies, nos coups de mou, nos pétages de câble, nos excitations (qui parfois retombaient…), enfin tout quoi. Merci d'avoir été et d'être là. Petite mais énergique !

Je tiens à remercier ma famille et mes amis qui même s'ils n'ont toujours pas vraiment compris ce que je faisais, m'ont toujours soutenu dans mes projets d'étude et professionnels. Merci à mes parents, j'espère que vous serez fiers de moi. Merci notamment à Laurélia, nos rendez-vous du mercredi m'ont permis de tenir moralement dans des moments pas toujours faciles. Je ne suis pas médecin mais ça ne t'empêche pas de m'appeler pour tous tes petits bobos ^^.

Et enfin, à celui qui a dû me supporter au quotidien pendant ces trois années, qui m'a réconforté quand il le fallait, qui a su faire abstraction quand je stressais pour rien : « comme d'habitude ». Tu as été d'un soutien inébranlable, je ne suis pas sûre que j'aurais supporté cette étape de ma vie aussi bien sans toi. Merci à toi Loic…

Table of content:

Scientific achievements:

Posters:

- 2018 November 7-9th, Nancy (France), SifrARN 2018. ***A. Galvanin**, D. Jacob, L. Ayadi, V. Marchand, A. dalpke, M. Helm, I. Motorine*
  Dynamic changes in bacterial tRNA 2'-O-methylation profile revealed by RiboMethSeq

- 2018 June 11th, Strasbourg (France), RNA salon workshop. ***A. Galvanin**, D. Jacob, L. Ayadi, V. Marchand, A. dalpke, M. Helm, I. Motorine*
  tRNA 2'O-methylation analysis using next-generation sequencing

- 2017 November 6-7th, Paris (France), French Society of Extracellular Vesicles (FSEV). ***A. Galvanin**, G. Dostert, V. Marchand, P. Menu, E. Velot, I. Motorine*
  High-throughput analysis and biomedical applications of extracellular RNAs

- 2017 September 04-05th, Mainz (Germany), 1st Symposium on Nucleic Acid Modifications. ***A. Galvanin**, L. Ayadi, V. Marchand, A. Dalpke, M Helm, I. Motorine*
  tRNA 2'O-methylation analysis using next-generation sequencing (Illumina RiboMethSeq Protocol)

- 2017 March, Nancy (France), 1ère Journée Pharma Recherche. *G. Dostert, B. Mesure, **A. Galvanin**, V. Jouan-Hureaux, H. Louis, V. Deco, I. Motorine, P. Menu, É. Velot*.
  Mesenchymal stem cell exosomes preservation: a new opportunity for regenerative medicine.

- 2016 July 11-12th, Vandoeuvre-lès-Nancy (France), 6th International Symposium Europe China, First meeting of the CNRS GDRI France-China, *G. Dostert, B. Mesure, **A. Galvanin**, V. Jouan-Hureaux, H. Louis, V. Decot, I. Motorine, P. Menu, E. Velot*
  Mesenchymal stem cell exosomes preservation: a new opportunity for regenerative medicine?

- 2016 May 2nd, Strasbourg (France), Cancéropole Grand Est. ***A. Galvanin**, G. Dostert, V. Marchand, P. Menu, E. Velot, I. Motorine*
  Diversity of extracellular RNAs in human plasma and exosomes revealed by high-throughput sequencing

Talks:

- 2017 June 15th, Nancy (France), DocSciLor. ***A. Galvanin****, G. Dostert, V. Marchand, P. Menu, E. Velot, I. Motorine*
  High-throughput analysis and biomedical applications of extracellular RNAs
  Best talk price

- 2016 December 15th, Vandoeuvre-lès-Nancy, Journée de la FR CNRS UL 3209 BMCT « La médecine personnalisée ». ***A. Galvanin****, G. Dostert, V. Marchand, E. Velot, M. Helm, I. Motorine*
  L'analyse des ARN extracellulaires par séquençage à haut-débit pour des applications biomédicales

Scientific publications :

- **AlkAniline-Seq: Profiling of m7 G and m3 C RNA Modifications at Single Nucleotide Resolution**. Marchand V, Ayadi L, Ernst FGM, Hertler J, Bourguignon-Igel, **Galvanin A**, Kotter A, Helm M, Lafontaine DLJ, Motorin Y. *Angew Chem Int Ed Engl*. 2018 Dec

- **Mapping and Quantification of tRNA 2'-O-Methylation by RiboMethSeq. Galvanin A,** Ayadi L, Helm M, Motorin Y, Marchand V. *Methods Mol Biol*. 2019

- **RNA ribose methylation (2'-O-methylation): Occurrence, biosynthesis and biological function.** Ayadi L, **Galvanin A**, Pichot F, Marchand V, Motorin Y. *Biochim Biophys Acta Gene Regul Mech*. 2019 Mar

- **Absolute quantification of noncoding RNA by microscale thermophoresis.** Jacob D, Thüring K, Galliot A, Marchand V, **Galvanin A**, Ciftci A, Scharmann K, Stock M, Roignant JY, Leidel SA, Motorin Y, Schaffrath R, Klassen R, Helm M. *Angew Chem Int Ed Engl*. 2019 Mar

- **Diversity and heterogeneity of extracellular RNA in human plasma**. **Galvanin A**, Dostert G, Ayadi L, Marchand V, Velot E, Motorin Y. *Biochimie*. 2019 May

Figure list:

Table list:

Abbreviation list:

%: percentage

~: around

<: inferior

>: superior

°C: Celsius degree

µg: microgram

µm: microlitre

µm: micrometre

µmol: micromol

2D/3D: two or three dimensions

5'App: 5′ pre-adenylated

A: Adenosine

aaRS: amino acyl tRNA synthetase

ac^4C: N4-acetylcytidine

ACE: alternative current electrokinetic

acp^3U: 3-(3-amino-3-carboxypropyl)-uridine

Ala: alanine

Am: 2'-O-methyladenosine

APS: adenosine 5'phosphosulfate

APS: ammonium persulfate

Arg: arginine

Arg: arginine

Asn: asparagine

Asp: aspartate

ATP: Adenosine triphopsphate

B&W: binding and wash

bp: base pair

C: Cytosine

CCV: clathrin-coated vesicle

cDNA: complementary DNA

CLIP: Cross-Linking and Immuno-Precipitation

Cm: 2'-O-methylcytidine

CMCT: 1-cyclohexyl-(2-morpholinoethyl) carbodiimide metho-p-toluene sulfonate

$cmnm^5s^2U$: 5-carboxymethylaminomethyl-2-thiouridine

$cmnm^5U$: 5-carboxymethylaminomethyl-uridine

$cmnm^5Um$: 5-carboxymethylaminomethyl-2'- O-methyluridine

cmo^5U: uridine 5-oxyacetic acid

CMOS: complementary metal-oxide-semiconductor

Ctol: control

D: dihydrouridine

ddNTP: dideoxynucleotides triphosphate

deP/P: dephosphorylation/phosphorylation

DLS: dynamic light scattering

DNA: deoxyribonucleic acid

DNase: deoxyribonuclease

dNMP: deoxyribonucleotides monophosphate

dNTP: deoxyribonucleotides triphosphate

Dr.: Doctor

E. coli: *Escherichia coli*

EC_{50}: effective concentration for 50% of hybridization

EDTA: Ethylenediamine tetraacetic acid

emPCR: emulsion PCR

ESCRT: endosomal sorting complexes required for transport

ESI: electrospray ion

EV: extracellular vesicle

exRNA: extracellular RNA

F: fluorescence

Fast AP: thermosensitive Alkaline Phosphatase

FL: fluorescein

g: gram

G: Guanosine

Gln: glutamine

Glu: glutamate

gluQ: glutamyl-queosine

Gly: glycine

Gm: 2'-O-methylguanosine

Gm: 2'-O-methylguanosine

GTP: guanosine triphosphate

GW182: 182 kDa glycine-triptophane protein

h: hour

H2O2: Hydrogen Peroxide

HCV: Hepatitis C virus

HDL: high-density lipoprotein

His: histidine

hnRNPs: heterogeneous nuclear ribonucleoproteins

ho5C: 5-hydroxycytidine

HPLC: High Performance Liquid Chromatography

hsp: heat shock proteins

hY: fragment of human Y RNA

I: inosine

i^6A: N6-isopentenyladenosine

IFN: interferon

IFSET: ion-sensitive field-effect transistors

Ig: immunoglobulin

Ile: isoleucine

ILV: intra-luminal vesicle

Ini: initiator

IR: infra-red

ISTD: internal standard

JGU: Johannes Gutenberg Universität Mainz

k(k)Da: (kilo) Dalton

k^2C: 2-lysidine

kb: kilo base

K_D: dissociation constant

LB: lysogeny broth

LDL: low-density lipoprotein

LED: Light Emitting Diode

Leu: leucine

lncRNA: long non-coding RNA

Lys: lysine

m^1A: 1-methyladenosine

m^1G: 1-methylguanosine

m^1I: 1-methylinosine

m^2_2G: dimethyl- guanosine

m^2A: 2-methyladenosine

m^3C: N 3-methylcytidine

m5C: 5-methylcitidine

m6A: N6-methyladenosine

m^6t^6A: N6-methyl-N6-threonylcarba-moyladenosine

m^7G: 7-methylguanosine

MAMP: microbial associated molecular patterns

$mcmo^5U$: uridine 5-oxyacetic acid methyl ester

MeRIP-Seq: methylated RNA immunoprecipitation sequencing

Met: methionine

$MgCl_2$: Magnesium chloride

MHC: major histocompatibility complexe

miCLIP: m6A individual-nucleotide-resolution cross-linking and immunoprecipitation

min: minute

miRISC: miRNA induced silencing complex

miRNA: micro RNA

miscRNA: miscellaneous RNA

mL: millilitre

MMS: methyl methanesulfonate

mnm^5s^2U: 5-methylaminomethyl-2-thio-uridine

mnm^5se^2U: 5-methylaminomethyl-2-selenouridine

mnm^5U: 5-methylaminomethyluridine

MoTT: modification tunable transcript

mRNA: messenger RNA

MS: mass spectrometry

ms^2i^6A: 2-methylthio-N6-isopentenyl-adenosine

MST: microscale thermophoresis

MTase: methyltransferase

MVB: multivesicular body

MVE: multivesicular endosome

N.A.: not applicable

NaAsO2: Sodium arsenite

NaCl: sodium chloride

NaOCl: Sodium Hypochlorite

ncRNA: non-coding RNA

NEB: New England Biolabs

ng: nanogram

NGS: Next Generation Sequencing

NH_2: primary amine

NHS: N-Hydroxysuccinimide

nm: nanometre

NP1: nuclease P1

nSMase2: neural sphingomyelinase

nt(s): nucleotide(s)

NTA: Nanoparticle Tracking Analysis

OD: Optical Density

OH: hydroxyl

ONT: Oxford Nanopore technologies

osRNA: other miscellaneous RNA

P: phosphate

PacBio: Pacific Bioscience

PAGE: Polyacrylamide gel electrophoresis

PBMC: peripheral blood mononuclear cells

PBS: Phosphate-Buffered Saline

PCR: polymerase chain reaction

PDE: Snake Venom Phosphodiesterase

PE: paired-end

PEG: polyethylene glycol

phD: Doctor of Philosophy

Phe: phenylalanine

piRNA: piwi RNA

PK: Proteinase K

pmol: picomol

PPi: pyrophosphate

Pr. : Professeur

Pro: proline

PS: Pentostatine

Q: queosine

QQQ: triple quadrupole

RISC: RNA-induced silencing complex

RNA: ribonucleic acid

RNase: ribonuclease

RNP: ribonucleoprotein particle

ROS: reactive oxygen species

rpm: rotation per minute

rRNA: ribosomal RNA

RT-(q)PCR: real-time quantitative polymerase chain reaction

RT: retro-transcription

RTD: rapid tRNA decay

S. cer: *Saccharomyces cerevisiae*

S^2C: 2-thiocytidine

S^4U: 4-thiouridine

SAM: S-adenosyl-L-methionine

SBL: sequencing by ligation

SBS: sequencing by synthesis

scaRNA: small cajal-bodies RNA

Sec or s: second

SEC: size exclusion chromatography

Sen: selenocysteine

Ser: serine

SIL-IS: isotope-labelled internal standard

siRNA: small-interference RNA

snoRNA: small nucleolar RNA

SNP: nucleotide polymorphism

snRNA: small nuclear RNA

SR: single read

SSC: saline-sodium citrate

ssDNA: single stranded DNA

T: Thymidine

t^6A: N6-threonylcarbamoyl-adenosine

TBE: Tris Borate EDTA

tDR: transfer-derived small RNA

TEM: tetraspanins enriched microdomains

TEM: Transmission electron microscopy

TEMED: N,N,N,N'-Tetramethyl ethylenediamine

Thr: threonine

THS: Tetrahydro uridine

TLC: thin Layer Chromatography

TLR: Toll-like receptor

Tm: 2'-O-methylribothymidine

Tot tRNA: total tRNA

tRNA: transfer RNA

tRNA: tRNA-derived fragments

tRNase: tRNA ribonuclease

Trp: triptophane

tT: ribothymidine

Tyr: tyrosine

U : unity

U: Uridine

UL: Université de Lorraine

Um: 2'-O-metyluridine

UMS: Unité Mixte de Service

UV: ultra violet

V : volt

Val: valine

WNV: West Nile virus

ZMV: zero-mode waveguide

ZV: Zika virus

Ψ: pseudouridine

General introduction

I. Ribonucleic acids: RNA

Together with proteins, lipids and complex polysaccharides, nucleic acids are the most important macromolecules and are essential for the life and cell functions. The major functions of these biomolecules are the storage of genetic information for deoxyribonucleic acid (DNA) and the conversion of the genetic information to active biomolecules for ribonucleic acid (RNA). Nucleic acids are composed of nucleosides consisting of a sugar deoxyribose (DNA) or ribose (RNA) connected to the nucleobase via a glycosidic bond. Adenosine (A) and Guanosine (G) belong to the purine family while Uridine (U)/ Thymidine (T) and Cytosine (C) are pyrimidines. Nucleosides are attached to a ribose-phosphate chain. In contrast to DNA which is structured in a rigid double stranded helix (1,2) in order to keep stability for storage of genetic information, RNA are single stranded, but can form complex 2D and 3D structures via hydrogen bonding between complementary bases: A-U (2 hydrogen bonds) or C-G (3 hydrogens bonds) (1).

The genetic code, stored as DNA, is transcribed in coding RNA: messenger RNA (mRNA) and further is translated to proteins with the help of non-coding RNA species, namely the transfer RNA (tRNA) and ribosomal RNA (rRNA). Besides their role in translation, ncRNA are involved in a multitude of other important biological processes. Some of them, like the small nuclear RNA (snRNA) are involved in splicing, while small nucleolar RNA (snoRNA) and small cajal-bodies RNA (scaRNA) play a role in nucleotide modifications (methylation and pseudouridylation) of rRNA and snRNA, respectively. Among small ncRNA, there are also interference RNA that regulate gene expression, such as microRNA (miRNA), piwi-interacting RNA (piRNA) and small-interference RNA (siRNA). There are also various long ncRNA (lncRNA, size > 200 - 300 nt). For instance, there are RNA playing a role in epigenetic regulation by chromatin modification (e.g. RNA Xist responsible for X chromosome inactivation, Air and HOTAIR (HOX transcript antisense) RNA...), or in regulation of gene expression by acting on transcription (7SK RNA) or on translation (7SL RNA) (3–5).

II. Nucleic acids sequencing from 60s to now and later

The strong diversity of RNA makes their study a real challenge. Since decades, scientists strive to characterize their sequences and optimize DNA/RNA sequencing.

a. 1st Generation

In 1953 Watson and Crick determined the 3D structure of DNA but reading their sequenced remained impossible for some years. Techniques used for protein sequence determination were not transposable since DNA had only 4 different nucleobases with a longer sequence than proteins (6). This is why, researchers had to find other strategies. First, they combined the techniques used for nucleic acid composition determination with treatment by selective ribonucleases to get information of their order via specific produced fragments. In 1965, Robert Holley and colleagues were able to sequence a whole alanine-specific tRNA from *S. cerevisiae* (7). In parallel Frederick Sanger developed a method based on the detection of radiolabelled fragments that were partially digested and fractionated by two-dimensional gel coupled with thin layer chromatography (TLC) (8). Using this method Sanger's and then Fier's laboratories sequenced a first pool of ribosomal and tRNA sequences as well as, few years later, the whole bacteriophage MS2 RNA in 1972 (9–15). Then, Ray Wu and Dale Kaiser used DNA polymerase with radioactively-labelled nucleotide triphosphates. They managed to determine the sequence by measuring the radioactivity of the labelled nucleotides added one by one (16,17). However, this required a considerable amount of analytical chemistry and the necessity to use sophisticated 2-D fractionation techniques (electrophoresis coupled to chromatography).

Better resolution in a single separation step was achieved by the use of polyacrylamide gels. Two protocols were simultaneously developed: Alan Coulson and Frederick Sanger created the "plus and minus" system in 1975 while Allan Maxam and Walter Gilbert used chemical cleavage techniques (18,19). "Plus and minus" technique is an optimization of the previously described method where two DNA polymerisation experiments are done in parallel. The "plus" reaction uses only one labelled nucleotide triphosphate and thus all sequences seen on the gel end by this nucleotide. The "minus" reaction uses the three other nucleotide triphosphates. In contrast, Maxam and Gilbert used radiolabelled DNA treated with chemicals able to cleave DNA at specific bases. This last technique was considered as the first generation for nucleic acids sequencing.

The major event in this field occurred in 1977 with the development of the protocol which we call now Sanger sequencing by chain termination (20). This protocol uses dideoxynucleotides triphosphate (ddNTP) which are analogues of deoxyribonucleotides triphosphate (dNTP) but lacking the 3' hydroxyl group and thus preventing further extension of the DNA chain. Radiolabelled ddNTP are added to DNA extension reaction containing standard dNTP at higher

concentration and provoke termination of DNA chains at all possible lengths, since ddNTP are randomly incorporated. On the polyacrylamide gel, one can read the sequence by following the DNA bands for all four nucleotides in parallel like it is shown in the figure 1. For years, Sanger sequencing became the most used technology to sequence DNA. Since 70s, several improvements were proposed such as the use of fluorophores instead of radioactivity (allowing to use all four fluorophores together in one experiment) or the detection of DNA chains by capillary based electrophoresis (21–26). These improvements considerably change the way analyses were performed and sequencing could be automatized with machines (27).

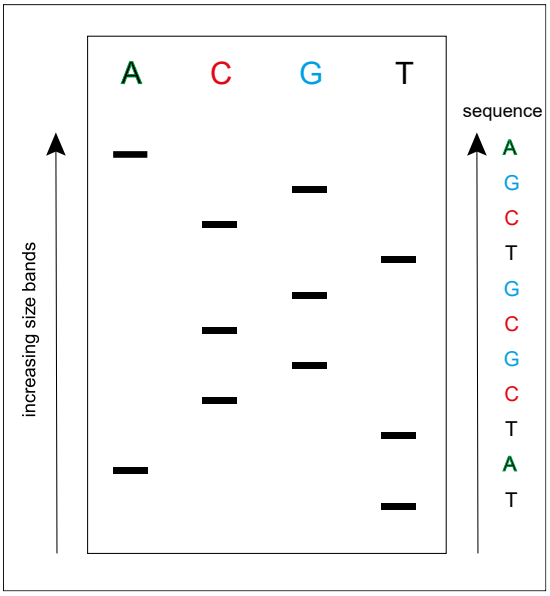

Figure 1 Sanger sequencing

Sanger sequencing: generated fragments are visualized on a polyacrylamide gel. By following the increasing bands in size, one can determine the sequence because each fragment ends by labelled ddNTP. Here the sequence is TATCGCGTCGA.

b. 2nd Generation

For years and even decades, DNA sequencing was tedious and expensive. For instance, in 2003 the human genome sequencing costed around 2.2 billion euros (28). Now with the upcoming of 2nd generation of sequencing in the 2010s, cost decreases considerably to around 1,000 euros in 2016. The second generation of sequencing methods gathers all high-throughput methods including a phase of amplification of a given DNA in a restricted area in order to be able to detect its corresponding signal over background. Moreover, these methods are able to analyse only short reads: generally below 300 nts. One can distinguish two types of sequencing, the

sequencing by ligation (SBL) and the sequencing by synthesis (SBS) similar to Sanger Sequencing.

1. Amplification procedures

Before detecting signal from the sequencing, DNA amplification is required. Several strategies exist for the generation of clonal DNA template. Globally DNA is first fragmented in pieces and adapters are ligated to the extremities allowing their amplification and sequencing. For beads-based amplification, one of the adaptors is complementary to an oligonucleotide that is covalently attached to the beads. By doing an emulsion Polymerase Chain Reaction (emPCR): micelle droplets containing all reagents for PCR, single original DNA molecule is amplified and forms what we call polonies (29). Beads containing statistically a unique DNA population can be distributed on a glass surface (30) or arrayed on a PicoTiterPlate (31).

Alternative on-surface PCR amplification (32) avoids the use of emPCR since DNA is directly amplified on a surface (33). Both adaptors (one at the time) can hybridize to oligonucleotides covalently bound to the surface. This is called a “bridge amplification” since the new synthetized DNA strand has to arch over to rich the neighbouring primer for the next cycle of polymerisation (32,34,35).

The last type of amplification used is the one which can be done in solution and employs to the rolling circle amplification process (36) leading to DNA nanoballs. In that case, DNA undergoes a ligation, circularization and cleavage process to create a circular template. Nanoballs are then distributed on a slide such as the polonies.

2. Sequencing by ligation (SBL): SOLiD

SBL approaches consist in the hybridization and ligation (37) of labelled probes to a DNA strand. In SOLiD system (figure 2), once the probe is bound to DNA template coming from emPCR amplification, imaging of the fluorescence is performed and one can identify two nucleotides. A new cycle begins after cleavage of the probe in order to remove the fluorophore. SOLiD is composed of a series of probe binding, ligation, imaging, cleavage cycles to elongate the complementary strand. Since determined dinucleotides are not next to each other, it is important to use other probes with first part offset of one nucleotide to ensure sequencing of every base.

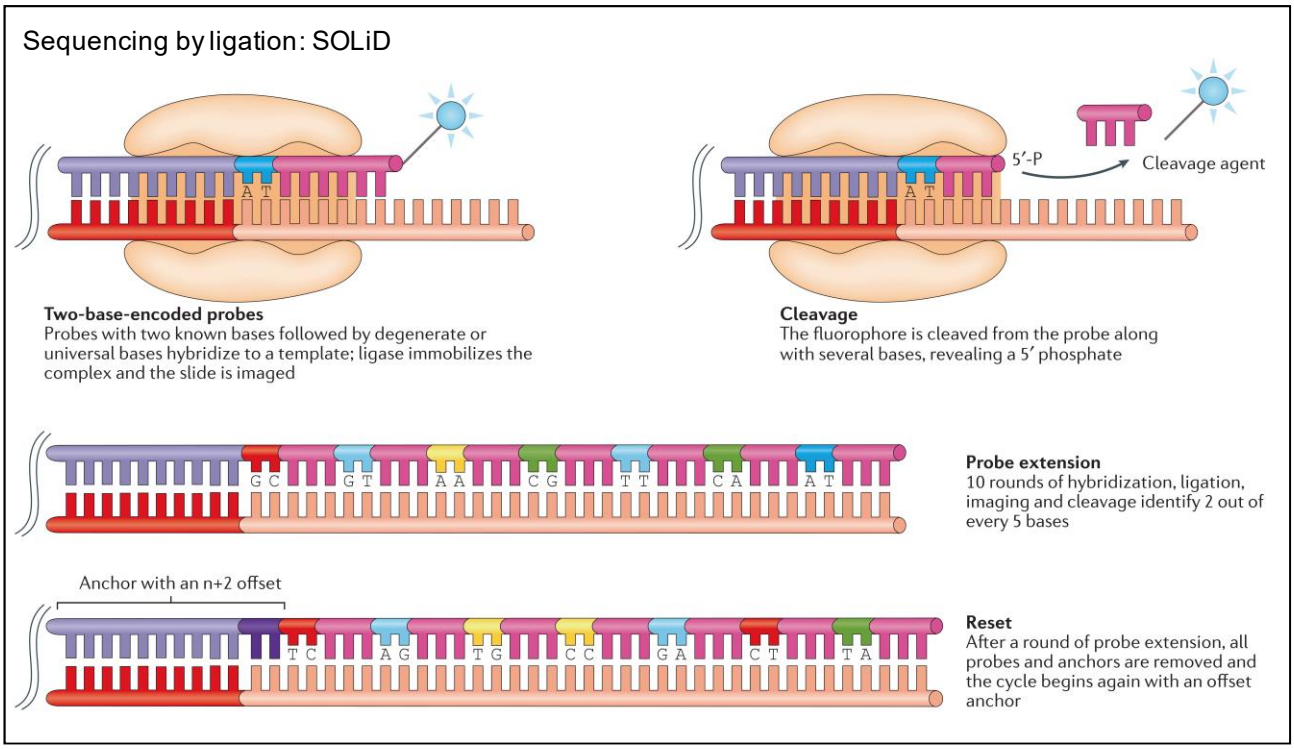

Goodwin et al, 2016. Nature Reviews (38)

Figure 2 Sequencing by ligation: SOLiD

After library amplification on beads, fragments are sequenced by ligation. A probe encoded with two known bases (blue) and several degenerated and universal nucleotides (pink) are labelled with a fluorophore and is added to the libraries. The two bases probe is ligated onto the anchor (light purple) that is complementary to a 5' adaptor (red). Fluorescence is detected and the two first bases are identified. The probe is cleaved and the fluorophore and a part of the degenerate and universal nucleotides are released. The process is repeated ten times. Then, the entire strand is reset by removing all the ligated probes and the anchor. A novel anchor with a N+1 offset is ligated and another cycle of ligation, imaging and cleavage is performed. This continues with until N+4 offset anchor in order to read the whole sequence.

3. Sequencing by synthesis

Sequencing by synthesis groups all the methods using DNA polymerase. Some techniques use single nucleotide addition (pyrosequencing and Ion torrent sequencing), while the others employ cyclic reversible termination (Illumina sequencing).

- Pyrosequencing and Ion torrent sequencing

In contrast to most described strategies, sequencing by single nucleotide addition doesn't rely on the detection of radioactivity or fluorescence. Here, a specific signal produced after the addition of a natural dNTP during polymerisation is measured. Thus, each of the four dNTP has to be added one by one to make sure the signal is specific to each nucleobase.

454 pyrosequencing (39), was the first system using this principle. After amplification by emPCR on beads, sequence is determined via direct nucleotide incorporation and an enzymatic cascade. Each time a dNTP is incorporated, a pyrophosphate (PPi) is produced as a by-product:

(40). The enzyme ATP sulfurylase converts PPi to ATP, which is then used as a substrate for luciferase leading to light emission which is proportional to the amount of pyrophosphate released (figure 3a).

Ion torrent sequencing (41) doesn't use an enzymatic system but directly detects the change of pH due to release of H+ ions when a dNTP is incorporated. Detection is done by the integrated complementary metal-oxide-semiconductor (CMOS) circuit (Figure 3b).

Major issue for these two techniques is the difficulty to sequence homopolymer regions since the signal detected is not completely proportional to the number of nucleotides incorporated.

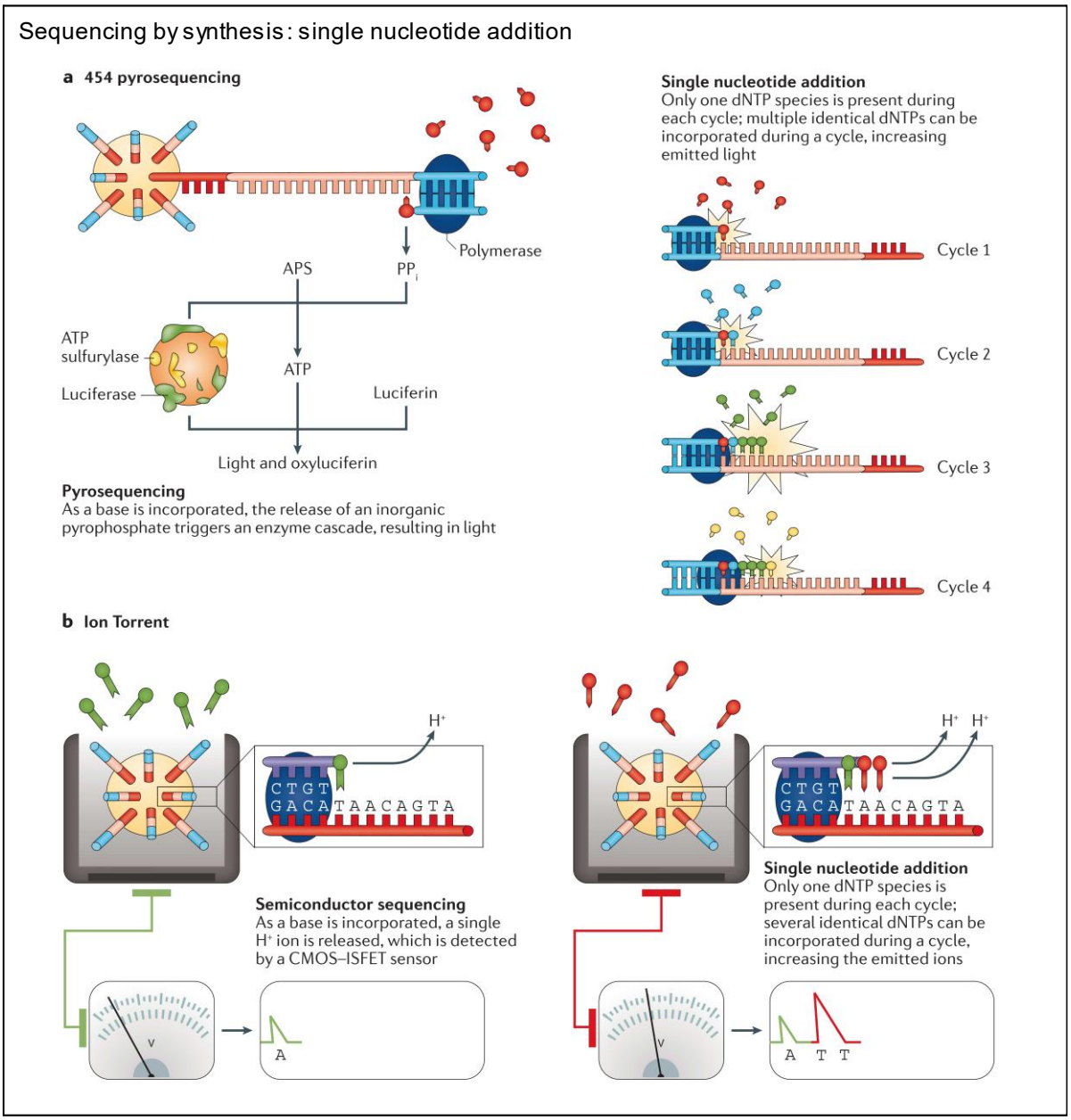

Goodwin et al, 2016. Nature Reviews (38)

Figure 3 Sequencing by synthesis: single nucleotide addition

a) 454 pyrosequencing. After library amplification on beads arrayed onto a microtitre plate along primers and beads containing an enzyme cocktail. A single nucleotide is added and each complementary base is incorporated in new synthetized strand. During the dNTP incorporation, pyrophosphate molecules are released. ATP sulfurylase transforms APS (adenosine 5'phosphosulfate) in ATP via pyrophosphates. Then, ATP, which is a cofactor, allows the conversion of luciferin to oxyluciferin by luciferase activity. Light is a by-product of the reaction and can be detected by a charge-coupled device (CCD) camera. Finally, apyrase degrades unincorporated dNTP and another base is added to the wells.

b) Ion Torrent. The principle is the same than 454 pyrosequencing except the fact that the by-product released during nucleotide incorporation is H+ leading to a change of pH that can be detected via an integrated complementary metal-oxide semiconductor (CMOS) and an ion-sensitive field-effect transistor (IFSET) device.

- Illumina sequencing (derived from Sanger sequencing)

Illumina sequencing is derived from the original Sanger protocol with the use of fluorescently-labelled dNTP blocked at 3'OH thus preventing the further cDNA elongation (42,43) (Figure 4). DNA templates are transformed into double stranded DNA with adaptors at both extremities. DNA clusters are performed via the bridge amplification directly on a flow cell. At every cycle, the four individually labelled and 3'-blocked dNTP are added. One is incorporated by the DNA polymerase where the three unbound are washed away. The surface is then imaged and the nature of incorporated dNTP into each DNA cluster is identified by specific fluorescent signal. The fluorophore and the blocking group are removed and another cycle begins. Illumina is also able to produce paired-end (PE) data where each DNA cluster can be sequenced from both extremities. Once a first sequencing by synthesis from a single stranded DNA bound to the flow cell is finished, sequencer changes its orientation by bridge amplification and starts another round from the opposite end. This provides a greater amount of data and improves accuracy, especially for repeated sequences.

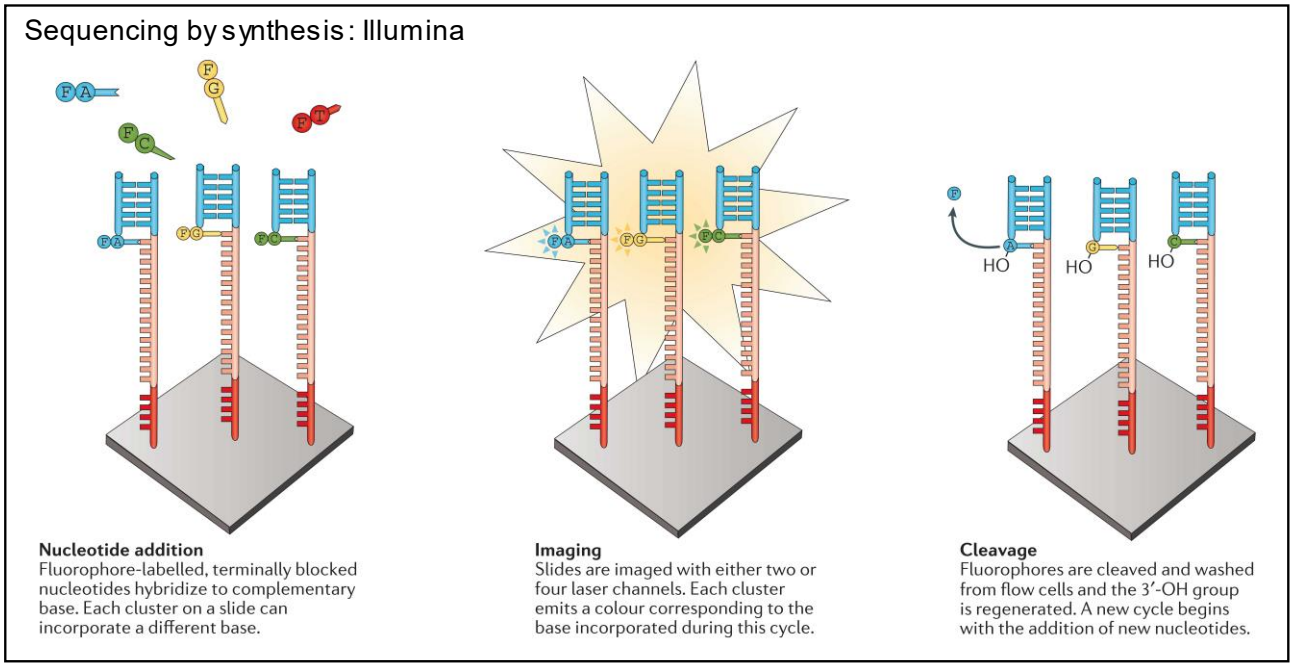

Goodwin et al, 2016. Nature Reviews (38)

Figure 4 Sequencing by synthesis: Illumina

After library amplification on a flow cell, a mixture of primers, DNA polymerase and labelled 3'-blocked ddNTP are added. At each cycle, only one ddNTP is incorporated due to the 3' blockage. Unincorporated bases are washed, fluorescence signal is measured and incorporated nucleotide is determined. The dye is then cleaved and the 3' group is regenerated by reduction. A new cycle of nucleotide addition, wash, imaging, cleavage, regeneration is possible.

4. Comparison of the different methods

Even if all these methods are rather accurate (> 99%), Sequencing by ligation (SOLiD) and pyrosequencing (454) are no longer commercialised due to their lower performance and especially a higher cost. In the field, Ion Torrent and especially Illumina sequencing are the pillars in the market and have the monopoly. In the table 1 specificities of each of the three methods are represented.

Table 1 Comparison between sequencing by ligation, sequencing by nucleotide addition and Illumina sequencing

Method	Read length (bp)	Comments
SBL: SOLiD	50-75	- under-representation of AT and GC rich regions as well as substitution errors - expensive (44,45)
SNA: 454 pyrosequencing and Ion Torrent	200-1000	- insertion and deletion errors when there are more than 6-8 identical following nucleotides (46) - 454 pyrosequencing is too expensive
Illumina	25-300	- High level of compatibilities with other platforms - technology mastery over decades since it derives from Sanger sequencing - some under-representation for AT and GC rich regions as well as some substitutions (44,47–49)

Whatever the technique used for 2nd generation of sequencing, reads are short (below 300 bp) and an amplification step is required. This amplification can lead to several uncontrolled biases due to polymerase errors or unequal amplification of fragments. That is why, it is crucial to develop new methods in this field in order to improve sequencing in term of accuracy, efficiency, sensitivity and cost.

c. 3rd Generation: Pacific bioscience and Nanopore Oxford Technology

The third generation of sequencing groups mostly techniques of single molecule sequencing and real time sequencing allowing the sequencing of long reads (several kb). Two major approaches were developed: Pacific Bioscience (PacBio) and Oxford Nanopore technologies (ONT).

Pacific Bioscience technology is also based on the detection of fluorescent dNTP incorporated by a polymerase but without bridge amplification (33,50–52). Here, DNA polymerase and template are attached to the bottom of a nanostructure called zero-mode waveguide (ZMW). These nanostructures exploit the properties of light passing through a window with a diameter

lower than the light wavelength. Thus, only the very bottom of the well is illuminated (where the DNA polymerase is attached). Then DNA polymerisation can be followed in real time since only the fluorescent dNTP that is incorporated can be detected. Pacific Bioscience process can sequence single molecules in a very short time. However, the level of sequencing errors is high and it becomes difficult for DNA templates longer than 3 kb.

Nanopore Oxford Technology (53) is based on the direct detection of DNA composition using a protein nanopore. DNA strand attached to a motor protein is translocated through a nanopore, modulating the electric current passing through. This change is called the squiggle space and shifts in voltage are characteristic of the particular DNA sequence in the pore. This very promising system is able to sequence up to 500 bp per second and read sequence of length up to 200 kb (54).

III. RNA-Sequencing

RNA sequencing relies on the same principles as DNA sequencing. With the exception of nanopore technology where extremely recent protocols propose to sequence directly RNA (55,56). All other methods convert RNA into cDNA via a retro-transcription (RT) step . Depending on the aim, target RNA species can be first enriched or non-target RNA can be depleted. In the case of transcriptome wide analysis, mRNA can be enriched via by a polyA selection with an oligo-dT oligonucleotide or rRNA (that represent more than 90% of a total RNA population) can be depleted using complementary oligonucleotides. Another possibility is to use the natural chemical properties at the extremity of some RNA for the ligation of adapters. For instance, miRNA have 5’phosphate and 3’OH extremities which allows direct adaptors ligation during library preparation.

High-throughput sequencing is widely applied in biomedical research and considerably contributed to advancement in transcriptomes knowledge over the last few years. A large set of applications can be performed using this technique. Two application areas can be distinguished: the exploratory domain and the comparison and quantification domain. On one hand, one can mention several RNA sequencing applications such as the discovery of new transcripts that can be involved in cell regulation (57–59), better knowledge of transcriptional start sites (60–64) or nucleotide polymorphisms (SNP) (65–68). On the other hand, RNA sequencing is also commonly used for the comparison of expression level of diverse target RNA under two (or more) different conditions.

RNA sequencing is not only used for RNA characterization, this technology is available for a lot of different purposes such as determination of RNA/protein interaction by all the Cross-Linking and Immuno-Precipitation (CLIP) procedures (69). Another example would be the detection and quantification of modified nucleotides by RNA sequencing that will be described in more details in the chapter II of this manuscript.

During my PhD thesis, I was working in tight collaboration with the Next Generation Sequencing core facility of the "Unité Mixte de Service" UMS2008 IBSLor directed and managed respectively by my Director of Thesis Pr. Iouri Motorine and Dr. Virginie Marchand. I could get better insights into Illumina sequencing system. In particular, I have used high-throughput sequencing in two projects that will be presented in the following chapters. The first one is about the characterization of extracellular RNA from human plasma and the second one is the dynamics of 2'O-methylation in *E. coli* under stress conditions.

CHAPTER I: Characterization of extracellular RNA by high-throughput sequencing

A. Literature review

I. Extracellular RNA: description

a. exRNA subpopulations

Besides intracellular RNA, it is now well established that a multitude of RNA is also circulating outside of the cell. These extracellular RNA (exRNA) are secreted by various cells via different mechanisms that are not yet fully understood. To be stable in such unfavourable extracellular environment rich in ribonucleases (RNases), circulating RNA require protection from nucleolytic degradation. This protection can be insured by two different ways.

On one hand, some RNA and especially miRNA are found in "soluble state" and are included in ribonucleoprotein (RNP) complexes, containing both ribonucleic acids and associated proteins (figure 5) (70), or, more rarely, as a part of particles such as low- and high-density lipoproteins (LDL and HDL) (71) or exomeres (72). However, it is still not clear if these RNA can really enter recipient cells and join the RNA-induced silencing complex (RISC) and how these RNA are recruited into lipoprotein vesicles.

On the other hand, RNAs are also found in another kind of particles released from the cell that are called extracellular vesicles (EV) (73–76). Extracellular vesicles are delimited by a double-leaflet membrane. There are evolving recommendations to characterize their subtypes particularly in biological fluids. To date, there is no consensus on specific markers of EV subtypes (77,78). Nevertheless, three major types of EV are mostly described according to their size and biogenesis (Figure 5): apoptotic bodies (79–81), microvesicles (or budding vesicles) (82,83) and exosomes (84–86). Apoptotic bodies are 1 - 5 µm vesicles and arise from apoptotic cells by invagination. They are composed predominantly of fragmented DNA and histones. Microvesicles, from 100 nm to ~1 µm in size, are formed by budding of the plasma membrane and their content depends on where the budding occurs. Their membrane composition is similar to the parental cells (87). Microvesicles are enriched in phosphatidylserin, lipid rafts, cell lineage markers and cell surface receptors (87–89). In contrast to apoptotic bodies which result from indiscriminate surface blebbing, nascent microvesicles come from a distinct blebbing mechanism leading to localized changes in plasma membrane protein and lipid composition. This modulates changes in membrane curvature and rigidity (90,91). Moreover, they carry proteins and nucleic acids components selectively enriched while others are excluded (89). The third type of EV called exosomes are particles of 50 - 150 nm in size (92) originating from

classical endocytic pathway with a specific biogenesis and cargo components recruitments (85,93).

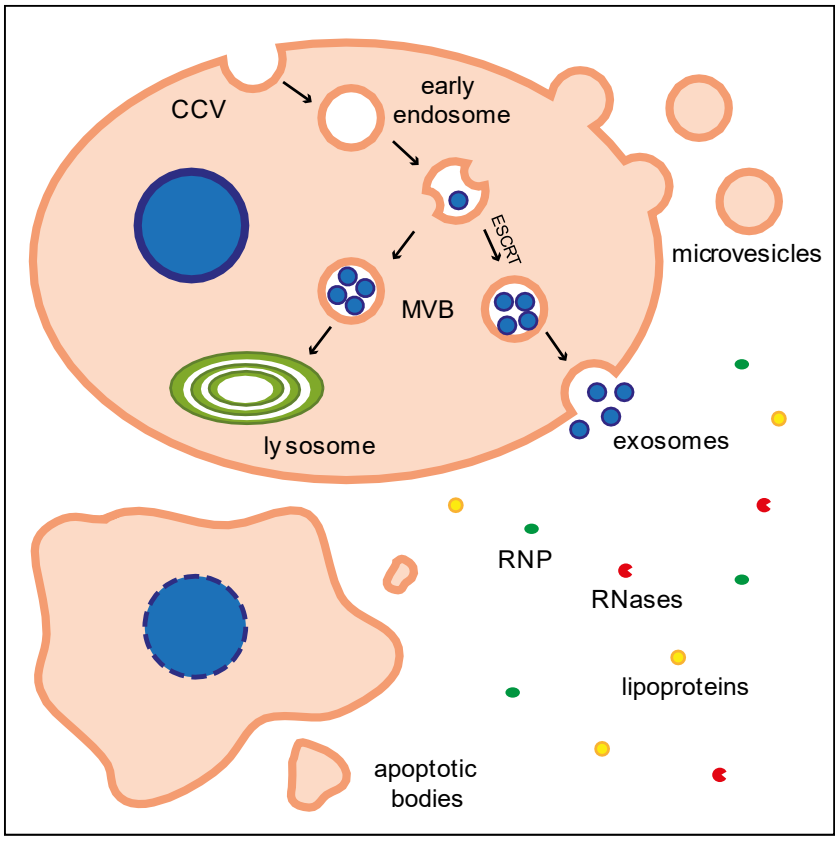

Figure 5 Extracellular RNA overview in plasma

Legend: CCV: clathrin-coated vesicle; ESCRT: endosomal sorting complexes required for transport; MVB: multivesicular body; RNP: ribonucleoprotein particle.

Extracellular RNA can be a part of extracellular vesicles. Apoptotic bodies 1-5 um arise from apoptotic cells by invagination, microvesicles 100 nm to 1µm are shed from the plasma membrane and exosomes 50-150 nm are secreted from the cell due to a specific biosynthesis. After endocytic pathway mediated by CCV, multivesicular bodies containing intraluminal vesicles are formed via the ESCRT and then fuse the plasma membrane in order to release exosomes. exRNA can also be part of RNP complexes or more rarely of lipoproteins.

Taking into account these multiple secretion pathways, exRNA composition is extremely diverse and heterogeneous (79,94). In addition, exRNA are attractive biomarkers of pathologies and diseases, with growing application in diagnostics and prognostics (95). Indeed, highlighting new biomarkers from theses populations that are present in the circulating blood could help for diagnostic by using liquid biopsy instead of classical invasive tissue biopsy. Among all these subpopulations, microvesicles and exosomes present a strong interest for the determination of disease biomarkers since they have a specific biogenesis, specific proteins and nucleic acids cargo recruitment and are known to play a role in different diseases such as cancers (92,96,97). We choose to focus our interest on exosomes because they are the most studied in the field.

Moreover, their small size allows them to cross the blood-brain barrier and tissue matrix, and thus to be harvested in biofluids (98,99).

b. Exosomes: biogenesis and composition

1. Biogenesis

Exosomes were first discovered nearly 45 years ago when vesicles were observed within the cartilage matrix (100,101) . Exosomes are now known to be secreted by almost any cell types (immune cells, cancer cells, stem cells, hepatocytes, neurons...) and are found in all biological fluids (plasma, urine, milk, amniotic fluids...) (see http://exocarta.com).

The general mechanism for secretion of exosomes outside the cell begins with a classical endocytic pathway commonly mediated via clathrin-coated vesicles (CCV). In the early endosomes, there is a formation of intraluminal vesicles (ILV) by invagination of the endosome membrane. These vesicles form multivesicular bodies (MVB). MVB often fuse with the lysosome where cellular waste products, proteins, lipids, carbohydrates and other macromolecules are cleaved down into simple compounds and recycled as new cell building material. Nevertheless, MVB can also fuse with the plasma membrane thereby releasing ILV, among which are found exosomes, to the extracellular space (Figure 5) (92,93,102,103).

The MVB fate, between lysosomal pathway and exosome release, depends on its biochemical composition. MVB rich in cholesterol and poor in lysobisphophatidic acid fuse with the plasma membrane and release exosomes while if their composition is inverted they are destined to the lysosome (104–106). Moreover, in the secretion pathway itself, there are two different options: the pathway involving the endosomal sorting complexes required for transport (ESCRT), and the lipid pathway (92,106–108). ESCRT complexes are implicated in the membrane remodelling that allows the formation of ILV. In the minor lipid pathway, exosome formation is independent from ESCRT complexes, but depends on the sphingomyelinase enzyme, which produces ceramide.

2. Composition

The molecular composition of exosomes does not reflect exactly the composition of the secreting cell (109,110). In fact, exosomes are enriched in specific proteins, lipids and RNA, while some other components are totally absent. Thus, sorting and recruitment of molecules into exosomes are controlled by specialized mechanisms.

Membranes of exosomes are enriched in specific lipids, like cholesterol, sphingolipids, glycerophospholipids and ceramides, but also in some proteins such as integrins, growth factor receptors or immunoglobulins (85) (Figure 6). The most abundant exosomal transmembrane proteins belong to the tetraspanin family (e.g. CD9, CD63 and CD81). They are organized in tetraspanins enriched microdomains (TEM) and have four transmembrane domains (111). Even if this protein family is also found on cell membrane, exosomes are highly enriched in tetraspanins (between seven to hundred times compared to cells and other vesicles). This makes tetraspanins good candidates to be specific biological markers for exosomes. Inside exosomes, other proteins are also found: heat shock proteins (hsp70, hsp90), cytoskeleton proteins (tubulin, actin), vesicle trafficking proteins (Rab GTPases, annexin, flotilin) required for MVB transport to the plasma membrane and ESCRT-related proteins (Alix, Tsg101) (112). Concerning RNA composition, this part will be described in more details in section (A. III. a. exRNA composition: state of the art).

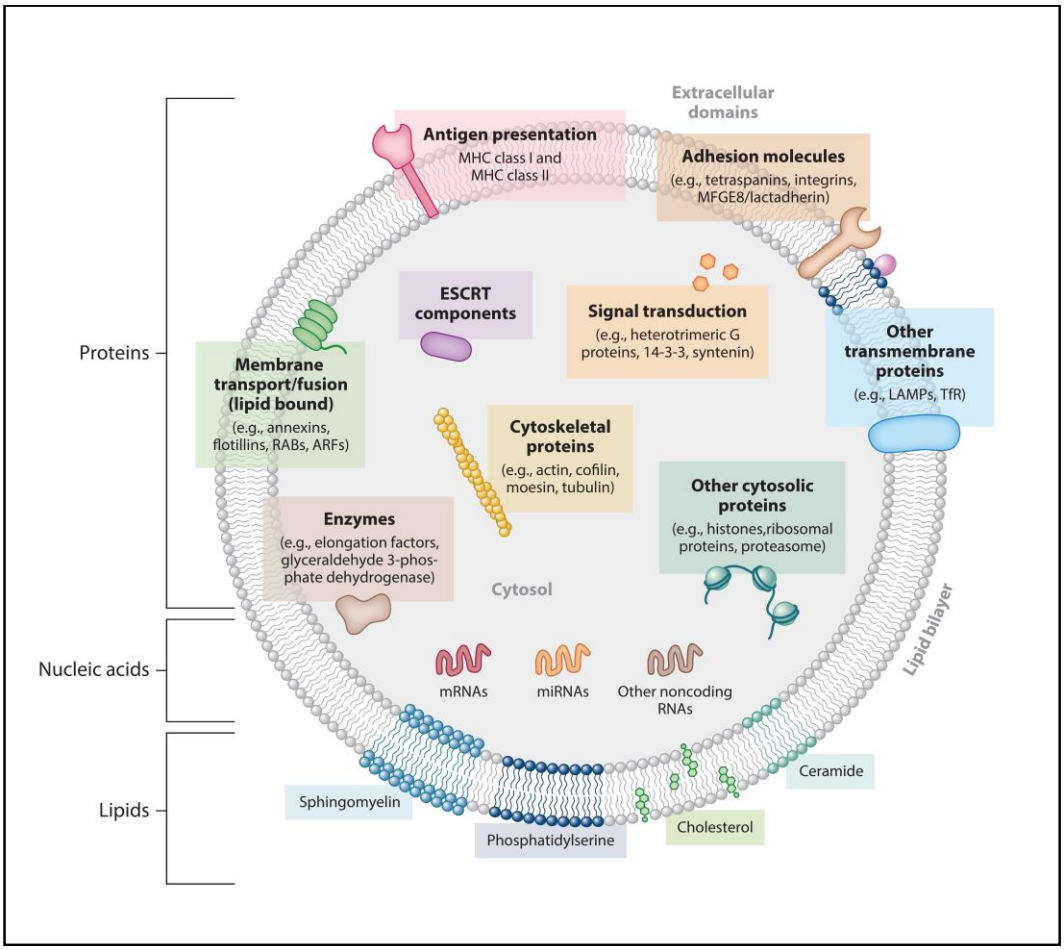

Colombo et al, 2014. Annu. Rev. Cell Dev. Biol (85)

Figure 6 Exosome composition

Legend: MHC/ Major histocompatibility complex; LAMPs/ Lysosomal-associated membrane proteins; TfR/ Transferrin receptor; ARF/ ADP ribosylation factors

Exosomes are composed of a lipid bilayer containing transmembrane proteins such as tetraspanins, integrins and several lipid components (ceramide, cholesterol or sphingomyelin). Inside the vesicle, we can find ESCRT components like Tsg101 and Alix proteins, cytoskeletal or signal transduction proteins. RNA molecules are also found into exosomes.

The exact mechanisms allowing protein recruitment into exosomes are not yet fully understood, even if the protein composition seems to be determined by the exosome secretion pathway. Since ESCRT complexes play a role in ILV budding, proteins that are able to interact with ESCRT complexes are preferentially sorted into ILV during their formation. In contrast, for production of ceramide-rich exosomes, ESCRT complexes are not involved. In this case, ceramide produced by the sphingomyelinase 2 is able to cause spontaneous curvature of the endosomal membrane to form ILV (113).

The existence of ESCRT-dependent and independent mechanisms for the loading of proteins into exosomes is not necessarily contradictory. Indeed, this heterogeneity allows the possibility to enhance or inhibit the secretion of only one sub-population of exosomes (114,115).

c. Functions

After their secretion, exosomes are released in the extracellular medium. While initial studies considered these EV as “garbage bags” of the cells (116,117), exosomes are now recognized to serve as “vehicles” for intercellular communication (118,119). This communication can be limited to cell-to-cell in close proximity or affect the whole organism by secreting signals such as hormones released from the cell and acting in autocrine and paracrine manner. How this regulation is insured? Exosomes can act through receptor-receptor interaction at the plasma membrane, but most probably their content is incorporated into the recipient cell. Exosomes can be either internalized entirely by endocytose into the cell and then join the lysosomes or they can fuse with the plasma membrane and deliver their molecules inside the cell (92,120) (Figure 7).

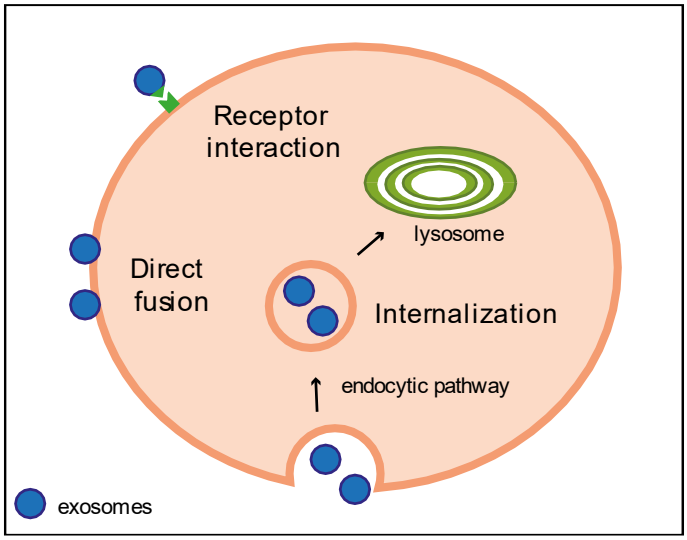

Figure 7 Exosome uptake in recipient cell

Exosomes can be internalized to the recipient cell by three potential different ways. They can fuse directly with the plasma membrane, interact with specific receptor or be internalized by the endocytic pathway, brought to the lysosome and release their content into the cell.

By this way, while the first reported function of exosomes was the elimination of outdated molecules in a catabolic pathway, exosomes have a lot of different functions, depending on their origin, their target cells, as well as on their composition. Exosomes can transfer specific proteins and nucleic acids (miRNA) to target cells for the delivery of signaling pathways and gene regulation (121–123). Exosomes affect the adaptive and innate immune system (124), they can bear peptide-major histocompatibility complexes (MHC) or antigen and activate T cell response or carry bacterial molecules that directly stimulate innate immune system (125–127). Moreover, depending on their producing cells, exosomes can protect recipient cells from tumor

invasion (128) or, in contrast, promote tumor invasion by enhancing angiogenesis, tumor cell migration in metastases and T cell inactivation by carrying immunosuppressive molecules (129,130). Thus, it has been reported that fibroblast-derived exosomes regulate the Wnt signaling pathway and promote breast cell cancer dynamic (131). They can also participate to myelin formation and in the propagation of prions in the brain (132). Some viruses such as human immunodeficiency virus type 1 and other pathogens use this secretion pathway to spread themselves in the recipient cells (133). Exosomes have a key role in intercellular communication and can act on different levels.

d. Use for biotechnologies: drug delivery system

Because liposomes look like exosomes, they were naturally exploited for drug delivery system. They have particular benefits such as specificity, safety, and stability. Due to their nanometric size, exosomes can be transferred between cells and are able to avoid phagocytosis. They fuse with the plasma membrane and bypass the lysosome pathway (134–136). Their lipid bilayer membrane protects their cargo containing bioactive molecules from degradation in the extracellular milieu (136). Moreover, exosomes show a lower immunogenicity and toxicity than other drug delivery system (136,136). By their intrinsic characteristics of intercellular communication, exosomes can deliver their cargo over a long distance with a strong stability in the blood under physiological and pathological conditions. In addition, exosomes have a hydrophilic core making them suitable to carry water-soluble drug (137).

Several methods are used to load cargos containing anticancer agents, siRNA or proteins. After their isolation from cell culture conditioned medium, exosomes are subjected to electroporation, sonication or they are simply incubated with the cargo to be mixed with it (138,139).

To target the recipient cells, either natural characteristics of exosomes can be used. For instance, exosomes bearing specific integrins can directly go to targeted organs (140). Otherwise, peptides have to be fused on the membrane surface (141). For instance, fused αv integrin-specific RGD (Arg-Gly-Asp) on exosome carrying anti-cancer drug, allow their uptake in αv integrin-positive cancer cells (142).

Most of application for exosome drug delivery is in the treatment of cancer diseases. As an example, this technique is used as a cell-free vaccine where cancer antigens are loaded in exosomes derived from autologous dendritic cells. By inducing natural killer activation, it facilitates the anticancer immune response in patients with non-small-cell lung cancer (143).

II. Studying extracellular RNA: from fractionation of subpopulations to RNA sequencing

a. Exosome isolation procedures

The gold standard for exosome isolation is differential centrifugation (144,145) (figure 8). This method consists in three steps: first, a low-speed centrifugation to remove cells and apoptotic debris, then a medium speed spin to eliminate larger vesicles and finally high-speed centrifugation (ultracentrifugation) to sediment exosomes. The second popular method is the polymer-driven precipitation proposed by several companies (figure 8). These precipitation kits such as Exoquick (System Biosciences), Total Exosome Isolation Reagent (Invitrogen), miRCURY™ Exosome Isolation Kit (Exiqon) are based on the formation of a mesh-like net that embeds EV with a size ranging from 60 to 180 nm (146). However, both of these procedures are barely suitable for complex and viscous biological fluids such as plasma or serum (147–149). Indeed, exosomes isolated from cell culture medium have a "simple" composition leading to a good yield and purity level. But due to their intrinsic characteristic, ultracentrifugation and precipitation methods lead to aggregation of proteins, RNP or lipids that are contaminating the exosome pellet and could prevent exosome detection due to high background (150). Thus, depending on the exosome source and their designed downstream applications, it may be important to use alternative methods to purify exosomes from other vesicles instead of only enriching them.

Among other proposed purification methods, size exclusion and ultrafiltration techniques bring much better purity (figure 8). For ultrafiltration protocol, after their enrichment by precipitation or ultracentrifugation, exosomes can be separated from other soluble proteins and aggregates using matrices with size exclusion limits (151,152). Concerning size exclusion chromatography (SEC), it has been shown that this technique avoids protein aggregation and subsequently allows EV purification without huge contamination. Due to pores of a diameter < 70 nm, proteins and RNP contaminants enter the beads and thus elute later than exosomes that are present in a void volume. Several comparative studies concluded SEC is the best method for EV isolation from plasma (153–155).

Immunoaffinity based protocol (150,156,157) target transmembrane proteins such as CD9, CD63 or CD81 and is the only one based on the biological properties of exosomes and not simply their size (figure 8). Here, there is no contamination by non-exosomal components, however, this kind of exosome enrichment is risky because some potentially important EV

populations without target marker protein may be excluded. In addition, this methods heavily relays on specificity and selectivity of antibodies used (158).

Other procedures that allow EV purification exist, but frequently require particular expertise and costly material/equipment. An often-used method is the density gradient/cushion centrifugation, where particles are separated by their floating density allowing separating soluble protein aggregates from EV. However, a swinging bucket ultracentrifuge is required (159–161). Another example among others is the technique proposed by Ibsen et al, 2017 (162) where EV are purified by an alternative current electrokinetic (ACE) microarray chip. This original method is certainly very promising but requires specific equipment.

Almost all theses procedures use the nanoscale size property of exosomes in order to enrich/isolate them. *De facto*, it is not possible to exclude other EV such as some microvesicles that may also have a nanoscale size. Moreover, depending on the target used in immunoaffinity-based methods, other EV can be isolated together with exosomes. For instance, tetraspanins are naturally found in the membrane of microvesicles since they come from a budding cell and therefore their membrane composition is similar to the parental cell containing tetraspanins (however, they are not enriched like it is the case for exosomes) (87). Nevertheless, this "contamination" remains relatively limited.

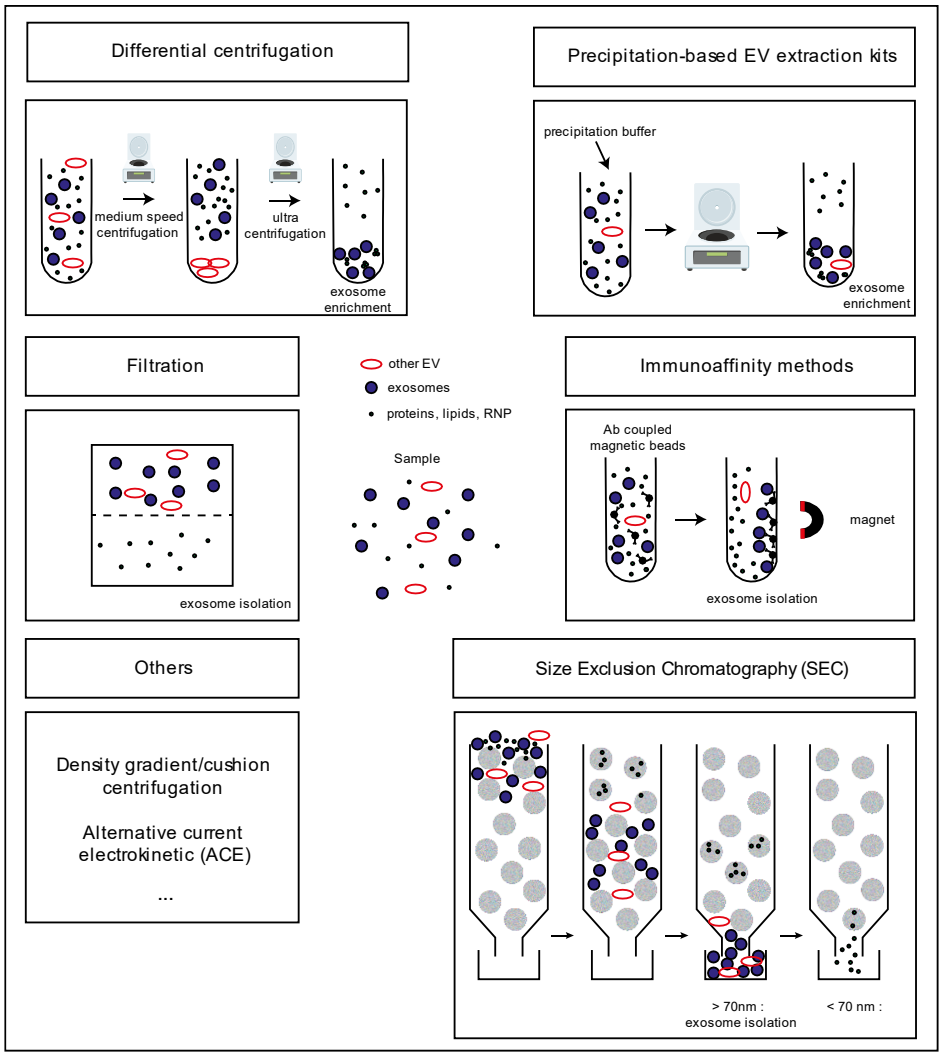

Figure 8 Methods for exosome isolation

Several methods are available for the isolation or at least the enrichment of exosomes. Differential centrifugation finishing by ultracentrifugation and methods based on exosomes precipitation are the most known. Filtration and size exclusion chromatography lead to a better purification like immunoaffinity beads. However, this last method can avoid certain subtypes of exosomes. Lastly, other methods are interesting but require specific material such as density gradient or alternative current electrokinetic (ACE).

b. Exosome characterization

After EV purification, it is crucial to validate that isolated particles are indeed exosomes. There are physical and biological validations based on different methods. However, while successfully applied to exosomes obtained from conditioned medium, all these methods are not entirely suitable for complex biological fluids such as plasma. The most popular is Nanosight system with a dedicated software called Nanoparticle Tracking Analysis (NTA) (163) that analyses videos captured giving a particle size distribution and particle count based upon tracking of each particle's Brownian motion. This tracking is due to the diffraction of a laser beam in contact with the particles. By this way, it is possible to analyse vesicles in solution and

to determine their size distribution and their concentration. This method is very helpful but does not make the difference between EV and protein aggregates. Thus, exosome concentrations are highly overestimated (154) when an inappropriate isolation method is used leading to protein and RNP contaminations. One can also mention dynamic light scattering (DLS) that gives size distribution, but does not provide information about particle concentration (164,165).

Transmission electron microscopy (TEM) (166–168) gives information about size and morphological characteristics such as lipid bilayer and shape. TEM can characterize EV but there is no information about their concentration. Moreover, it is not possible to make the difference between exosomes and microvesicles of the same size.

Biological validation includes immunoblotting targeting specific markers such as internal markers: Tsg101 (46kDa), Alix (96 kDa) or transmembrane proteins: tetraspanin CD63 (26 kDa), CD9 (26 kDa) and CD81 (26 kDa) for exosomes. This method is commonly used for exosome characterization (169–173). Unfortunately, when working with plasma one has to keep in mind that secondary antibodies may recognize intrinsic human immunoglobulins that are present in huge concentration in samples depending on the method used. This issue could prevent or disturb exosome marker detection. Light and heavy chain of immunoglobulins are 50 kDa and 25 kDa in molecular size and disturb specific EV marker detection. Even with Alix, the signal could be unspecific due to IgE or IgD.

Another option could be flow cytometry. However, because of their nanoscale, exosomes cannot be directly loaded on a classical flow cytometer in order to analyse the presence of specific markers on their surface. The sensibility of the cytometer is not appropriate for the analysis of these vesicles. To make EV detection possible, exosomes have to be bound to beads (4 µm in diameter) first (174). Now nanoscale flow cytometer exists (175,176) but require specific and expensive equipment.

c. RNA extraction

On whole plasma or with exosomes, it is well-established that exRNA are mostly below 200 nt in length (177,178). It has been shown that classical phenol/chloroform or TRIzol extraction is not efficient enough for this kind of RNA (179) because their yield is too low and small RNA (< 200 nt) are lost. Thus, the most important is to use a procedure that does not excludes some species: small and/or large RNA. Several kits are available on the market with more or less the same principle.

d. RNA sequencing

The first methods used for RNA characterization were mostly real-time quantitative polymerase chain reaction (RT-PCR) (70,180,181) or hybridization-based assays (70,182). However, these methods require the design of oligonucleotides recognizing known targets. Thus, it is not possible to analyse non-expected transcripts. Nowadays, high-throughput sequencing encounters this issue by sequencing all RNA in the sample.

III. exRNA: state of the art

In the field of liquid biopsies and diagnostic biomarkers determination, the most used biological fluid is blood: either plasma or serum. In this part, we will first describe how RNA are recruited into exosomes and then make an overview of exRNA content either from whole plasma/serum or from EV subpopulations.

a. Mechanisms of RNA recruitment into exosomes

Exosomal RNA composition is different to cellular total RNA of the donor cell (109). This means that in exosomes, there is a specific recruitment at least for some RNA species. At the moment, most studies were focused on miRNA, so only these specific recruitment mechanisms can be described in details, but it is clear that other RNA categories have dedicated recruitment mechanisms as well. For instance, ESCRT II and III were found to be RNA binding proteins that can contribute to the recruitment of various RNA into intraluminal vesicles ILV (183,184).

Four potential modes for miRNA recruitment into ILV, were described, although the underlying mechanisms still remain largely elusive (122). The first is the neural sphingomyelinase 2 (nSMase2)-dependent pathway. It was shown that overexpression of nSMase2 increases the amount of exosomal miRNA and, in contrast, its inhibition reduced exosomal miRNA number (185). The second mechanism is the miRNA motif and sumoylated heterogeneous nuclear ribonucleoproteins (hnRNP)-dependent pathway. hnRNPA1 is able to recognize a specific sequence in the 3’ portion of miRNA: GGAG (186). The third is the 3’-end of the miRNA sequence-dependent pathway. In fact Koppers-Lalic et al, 2014 (187) discovered that 3’-end adenylated miRNA are relatively enriched in cells (B cells), whereas 3’-end uridylated isoforms appear over-represented in exosomes derived from B cells or found in urine. According to the two last mechanisms, it seems that 3’-end of miRNA sequence is crucial for the recruitment into exosomes. Finally, the last mechanism is the miRNA induced silencing complex (miRISC)-related pathway. When Ago2 protein (main component of RISC) together with the

182 kDa glycine-triptophane protein: GW182 is inactivated, abundance of miRNA in exosomes drastically decreases (188).

b. exRNA composition in human blood

The initial studies on the composition of exRNA from extracellular vesicles showed the presence of miRNA and more than a thousand of different mRNAs (189). These mRNAs seem to be even functional because after transfer of mouse extravesicular RNAs into human mast cells, new mouse proteins were found to be produced in the recipient cell, indicating that transferred exosomal mRNA can be translated after entering another cell. Nevertheless, another study demonstrated that mRNA found in exosomes are mostly fragments from 3' untranslated region that could have functions other than translation, such as regulation stability or localization in recipient cells (190). However, in these studies authors used miRNA and mRNA specific microarrays for exRNA characterization. As mentioned before, these methods prevent the determination of unexpected RNA transcripts while high-throughput sequencing encounters this issue. In the last decade, more than a dozen of papers described exRNA content from plasma/serum and/or respective extracellular vesicles (94,170,191–199). Using RNA sequencing, almost all known RNA species were found in blood and extracellular vesicles: mRNA, rRNA, tRNA, miRNA, piRNA, snoRNA, vault RNA, Y RNA, lncRNA... However, the reported proportion of different RNA varies dramatically from one study to another (Table 2). For instance, protein coding RNA and miRNA are described at 24.5% and 8.8% respectively (170), while another study with similar design reported a proportion of 20% and 42% (192). Moreover, the proportion of rRNA was reported to be low (<10%) in (197), while the same rRNA was found to be a major species at ~50% in another study (193). This most probably reflects the extreme heterogeneity of sample preparation and the techniques used to isolate and characterize extracellular vesicle fractions (200). Discrepancies may also arise from the methods used in library preparation for sequencing, as well as from the bioinformatic pipeline used for data analysis and interpretation (201).

Analysis of human miRNAs, which are widely employed for biomarker discovery, may be highly biased, depending on the used purification procedures. The miRNA content of the exosomes isolated by centrifugation was shown to be very similar to RNA composition of the human plasma, demonstrating that inappropriate EV purification method yields preparations highly contaminated by non-exosomal RNA (202). In addition, several comparative studies highlighted strong differences in exosomal RNA content when extracellular vesicles were

isolated from the same biological sample by different methods (153,203–205). Not only the global miRNA content was found to be different (204), but also the level of individual miRNA such as let-7-d, miR-25, miR-127-3p, miR-16 and miR-451 (204,205). Such differences in exosomal RNA content were described for plasma-derived exosomes, and, surprisingly also for cell-derived exosomes obtained from rather well characterized cell-culture media (203). This demonstrates that biases related to exosomes purification methods may be important and may lead to lower quality results, even when the biological source is not a complex biofluid like plasma. In the study comparing ultracentrifugation, density gradient protocol and a precipitation based kit (153) only 40% of miRNAs were in common in the three protocols, moreover, mass spectrometry analyses pointed out that precipitation methods lead to contamination by polyethylene glycol (PEG) and serum proteins (206).

Globally, it is a real challenge to characterize exRNA content when plasma is used as source of exRNA (207). It is therefore critical to carefully design the study and to be aware of the possible contamination issues, which may affect sample composition.

Table 2 Published studies of human blood exRNA characterization.

Twelve studies on human blood exRNA characterization were compared by different parameters: type of sample and treatment, RNA extraction method, RNA sequencing and analysis method.

Galvanin et al, Biochimie. 2019 (208)

Sample type	**Blood treatment**	**RNA extraction methods**	**RNA seq methods**	**Studied RNA**	**Majors species found**	**Comments/Potential issues**	**Reference**
Exosomes from plasma	Exoquick (System Biosciences) +/- RNase A treatment	Qiagen miRNeasy micro kit	Illumina sequencing (NEBNext® Multiplex Small RNA Library Prep Set for Illumina and NEXTflex) - RNA sequencing kit (Bioo Scientific) - TruSeq Small RNA sample preparation kit (Illumina) Size selection of the libraries 140-160 bp	miRNA, rRNA, lncRNA, DNA,tRNA, miscRNA, piRNA, mRNA, snRNA, snoRNA, other	miRNA, rRNA	Kits based on precipitation include a lot of soluble extracellular RNA RNA from RNP or lipoproteins are not sensitive to RNase A	Huang et al, 2013 (197)
Exosomes from serum	Total exosome isolation (from serum) reagent (Invitrogen)	Total exosome RNA and protein isolation kit (Invitrogen)	Ion proton system (Ion Total RNA-Seq Kit v2 [Thermofischer])	miRNA, tRNA, rRNA, mRNA, snRNA, scaRNA, snoRNA, piRNA	miRNA, mRNA, tRNA	Kits based on precipitation include a lot of soluble extracellular RNA	Li et al, 2014 (193)
Plasma	N.A.	Exiqon miRCURY RNA Isolation Kit-biofluids	Ion proton system (Ion Total RNAseq kit v2 [Thermofischer])	rRNA removal miRNA, tRNA, snoRNA, piRNA, and other RNA RFam database	miRNA, piRNA, snoRNA		Freedman et al, 2016 (195)
Exosomes from plasma	Exoquick (System Bioscience) + RNase A treatment	Qiagen miRNeasy micro kit	Illumina sequencing (NEBNext® Multiplex Small RNA Library Prep Set for Illumina) Size selection of the libraries 140-160 bp	miRNA, piRNA, siRNA, lncRNA, mRNA, pseudogenes, antisense RNA, rRNA, snRNA, snoRNA, misc RNA other transcribed RNA, FLJ human cDNA and predicted RNA	miRNA, piRNA	Kits based on precipitation include a lot of soluble extracellular RNA RNA from RNP or lipoproteins are not sensitive to RNase A	Yuan et al, 2016 (192)
Serum	N.A.	- Qiagen Circulating Nucleic Acid Kit, - TRIzol LS Reagent, - Qiagen miRNeasy Serum/Plasma kit, - QiaSymphony RNA extraction kit - Exiqon miRCURY RNA Isolation Kit-biofluids	Illumina sequencing (TruSeq Small RNA sample preparation kit) Size selection of the libraries 5-40 bp	miRNAs, isomiRs, tDRs and osRNAs	osRNAs, tDRs, miRNA (including isomiR)	Serum: include RNA from platelets secretion: affects the composition of exRNA originally present in circulating blood	Guo et al, 2017 (194)

Sample type	Blood treatment	RNA extraction methods	RNA seq methods	Studied RNA	Majors species found	Comments/Potential issues	Reference
EV from plasma	Differential centrifugation, ultracentrifugation	Total RNA purification kit (Norgen Biotek) RNA fragmentation by RNase III	Ion proton system (Ion Total RNA-Seq Kit v2 [Thermofisher])	rRNA removal pseudogenes, mRNA, lncRNA, miRNA, tRNA, misc RNA, other	mRNA	Ultracentrifugation on viscous plasma procedure can co-pellet soluble extracellular RNA	Amorim et al, 2017 (170)
Whole platelet poor plasma, 16,000xg vesicles, 160,000xg vesicles and particles depleted in plasma	Differential centrifugation procedure	TRIzol reagent (Life Technologies) dephosphorylation/ phosphorylation treatment size selection on a gel for RNA > 19nt	SOLiD sequencing (SOLiD total RNA-Seq kit [Life Technologies])	Mitochondrial RNA, human genomic repeat consensus sequences, tRNA, rRNA, snRNA, small cytoplasmic RNA	rRNA, mRNA, mitochondrial RNA (for plasma and 16,000xg vesicles only)	Ultracentrifugation on viscous plasma procedure can co-pellet soluble extracellular RNA	Savelyeva et al, 2017 (94)
Plasma	N.A.	Thermofisher mirVana miRNA Isolation kit	Illumina sequencing (TruSeq Small RNA sample preparation kit) Gel purification: removal of dimers	rRNA, miRNA, tRNA, piRNA, RNA from ENSEMBL75 database, non-human RNA	Y RNA, miRNA		Yeri et al, 2017 (191)
Plasma	+/-Proteinase K treatment	Exiqon miRCURY RNA Isolation Kit-biofluids	Illumina sequencing (NEBNext® Multiplex Small RNA Library Prep Set for Illumina) Size selection of the libraries: RNA of 21-40 nt	rRNA, miRNA, tRNA, snoRNA, piRNA	rRNA, miRNA, tRNA		Danielson et al, 2017 (199)
Plasma and serum	Detergent and Proteinase K treatment	Personalized phenol/chloroform procedure	Illumina sequencing (personalized library preparation including RNA size selection)	miRNA, rRNA, tRNA, small cytoplasmic RNA, other cytoplasmic RNA, mRNA	Plasma: miRNA, mRNA, rRNA Serum: miRNA, scRNA, rRNA		Max et al, 2018 (196)

Abbreviations:

isomiRs- micro RNA isoforms, lncRNA – long non-coding RNA, miRNA – micro RNA, miscRNA – miscellaneous RNA, mRNA – messenger RNA, osRNAs – other miscellaneous RNA, piRNA – piwi RNA, rRNA – ribosomal RNA, siRNA – small interfering RNA, snoRNA – small nucleolar RNA, snRNA – small nuclear RNA, tDRs – transfer-derived small RNA, tRNA – transfer RNA

IV. Objectives

As it was mentioned before, exRNA can be found in almost every biological fluid and show a strong interest in the field of liquid biopsy. During the first period of my PhD thesis we decided to focus on the deep sequencing characterization of exRNA from blood due to its potential clinical interest. By having better knowledge on exRNA, we could use it to define diagnostic biomarkers in cancer, cardiovascular diseases or even infection by some viruses.

In this work, we approached the exhaustive characterization of exRNA from healthy human plasma using combination of extraction/characterization methods. We determined the exRNA composition from either whole plasma or from enriched or purified exosomes.

B. Results

I. Study design

a. Source for blood biological sample

Most common ways for blood pre-treatment consist in preparation of plasma or serum fractions. Plasma is obtained by centrifugation in the presence of anticoagulants, while serum is prepared by centrifugation of coagulated samples. Technically, working with serum is easier, but it is known that platelets release a lot of EV containing miRNA in response to coagulation (209) and this considerably affects the composition of exRNA originally present in circulating blood. This is the reason why plasma is the preferred source when studying exRNA as potential biomarkers (210). However, some popular anticoagulants, like heparin and EDTA, are not compatible with downstream applications (e.g. polymerase chain reaction, PCR) so we used citrate anticoagulant (211–213). Special care should be taken during these initial centrifugation steps to prevent release of platelet-derived EV (212).

b. Plasma treatment

Because plasma is a viscous and complex biological fluid, we had to first find the best method for exosome isolation since a lot of contaminants are commonly found in ultracentrifugation or precipitation-based kits procedures (148,149). The first part of this project was to compare several isolation methods including: kits based on precipitation, ultracentrifugation, density gradients and size exclusion chromatography. We also developed another method which consists in degrading soluble proteins in plasma with proteinase K treatment. Therefore, RNA from RNP are vulnerable while the one from EV are still protected by the lipid bilayer. Indeed, proteinase K is not able to make EV permeable. Then, non-protected RNA are degraded by RNase A treatment. This method should allow a good exosome purity by removing proteins and RNP contaminants (214).

c. Inclusion of degradation products

In the past decades, exosomes were thought to be only garbage bags of the cells but now this idea disappeared in the profit of intercellular communication function for EV. However, most of studies performed on RNA composition by deep sequencing include only maturation products. Indeed, when working with exRNA that mostly are below 200 nts in length, library preparation kits require 5’-P and 3’-OH extremities. However, degradation products probably present in whole plasma or exosomes have 5’-OH and 3’-P (or 3’-cyclophosphate) ends. Thus,

we decided to include theses RNA species in the analysis by adding a preliminary dephosphorylation/phosphorylation step that lead to the right extremities for all RNA present in the sample. Without any treatment, only maturation products are converted to library and sequenced, while degradation products are included only after this optional step. The goal is to perform the analysis with or without a dephosphorylation/phosphorylation step in order to compare maturation products to the pool of exRNA.

Nevertheless, we have to keep in mind that eukaryotic RNA are not only 5'P/3'OH or *vice et versa* (figure 9). While rRNA, tRNA, small RNA involved in regulation (miRNA, piRNA), most of snoRNA and scaRNA carry these extremities, this is not the case for mRNA, and most of lncRNA that carry a 5'm^7G-ppp cap and for snoRNA U3 that has a 5'm^{227}G-ppp cap. Even if exRNA is composed in majority of small transcripts (< 200nts), this does not exclude potential presence of RNA of a longer size. Thus, we have to be aware that potential extracellular mRNA, snoRNA U3 and most of lncRNA are excluded from the analysis because the alkaline phosphatase is not able to remove these caps.

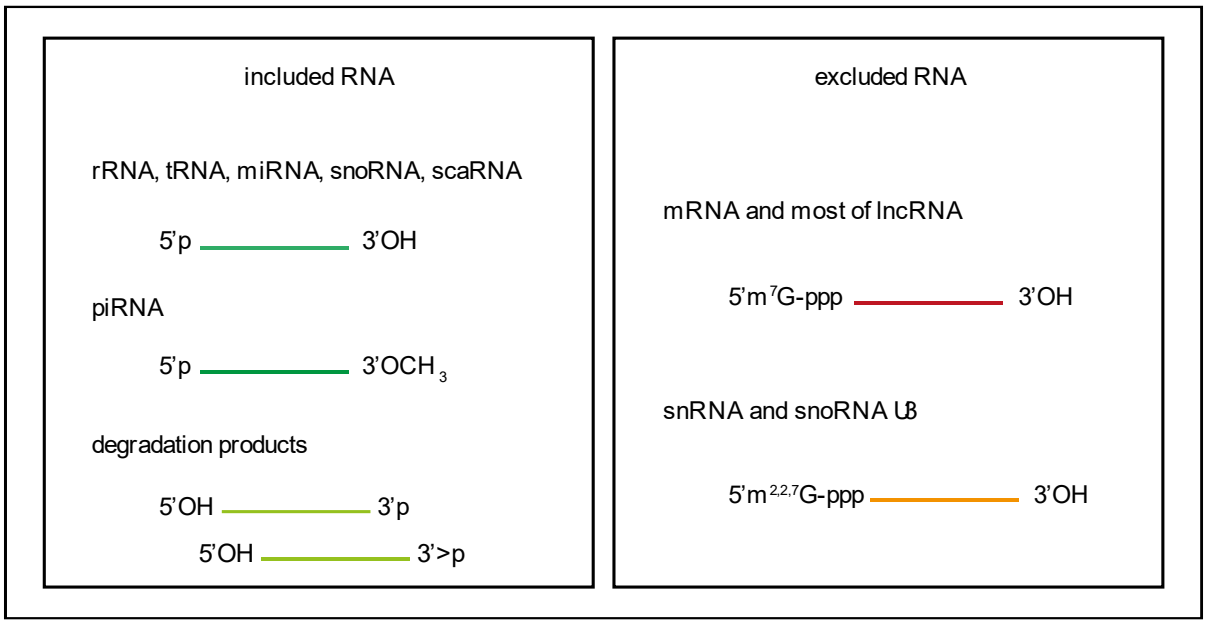

Figure 9 Types of RNA included or excluded in the analysis according to their extremities

Included rRNA, tRNA, miRNA, snoRNA, scaRNA have correct 5'P and 3'OH extremities, piwiRNA have 5'P and are 2'O-methylated in 3'extremities and degradation products have 5'OH and 3'P or cyclophosphate ends. In contrast excluded RNA are capped: mRNA and most lncRNA have a m^7G-ppp cap while snRNA and snoRNA U3 have a $m^{2,2,7}$G-ppp cap.

d. exRNA sequencing

Small RNA sequencing kits are the most appropriate to convert RNA fragments into sequencing libraries. Here is described the library preparation protocol proposed by New England Biolabs (NEB) that is compatible with widespread sequencing system: Illumina and is called NEBNext® Multiplex Small RNA Library Prep Set for Illumina (figure 10). To perform such library preparation, 5'-phosphate (5'-P) and 3'-hydroxyl (3'-OH) extremities of RNA are required. A 3' adaptor with a 5' pre-adenylated (App) and 3' blocked DNA sequence is ligated specifically to 3'OH extremities from RNA sample via a thermostable 5´ App DNA/RNA ligase enzyme which is ATP independent. The mutant ligase is unable to adenylate the 5´-phosphate of RNA or single stranded DNA (ssDNA), which reduces the formation of undesired ligation products (concatemers and circles). Then, the reverse transcription primer is hybridized on 3'adaptor. This step is important to prevent adaptor-dimer formation. The RT Primer hybridizes to the excess of 3´ single read (SR) Adaptor (that remains free after the 3´-ligation reaction) and transforms the single stranded DNA adaptor into a double-stranded DNA molecule that cannot be substrate for the T4 RNA ligase. Thus, during the ligation of 5'adaptor, none of them will hybridize to 3'-adaptor/RT primer dimer. Finally, the first complementary DNA (cDNA) strand is synthesized by a reverse transcriptase and an amplification by PCR is performed. Primers contain either P5 sequence either both a barcode and P7 sequence. P5 and P7 sequence are required to amplify libraries and fix them on the flow cell. The barcode is required to identify the library during demultiplexing after sequencing.

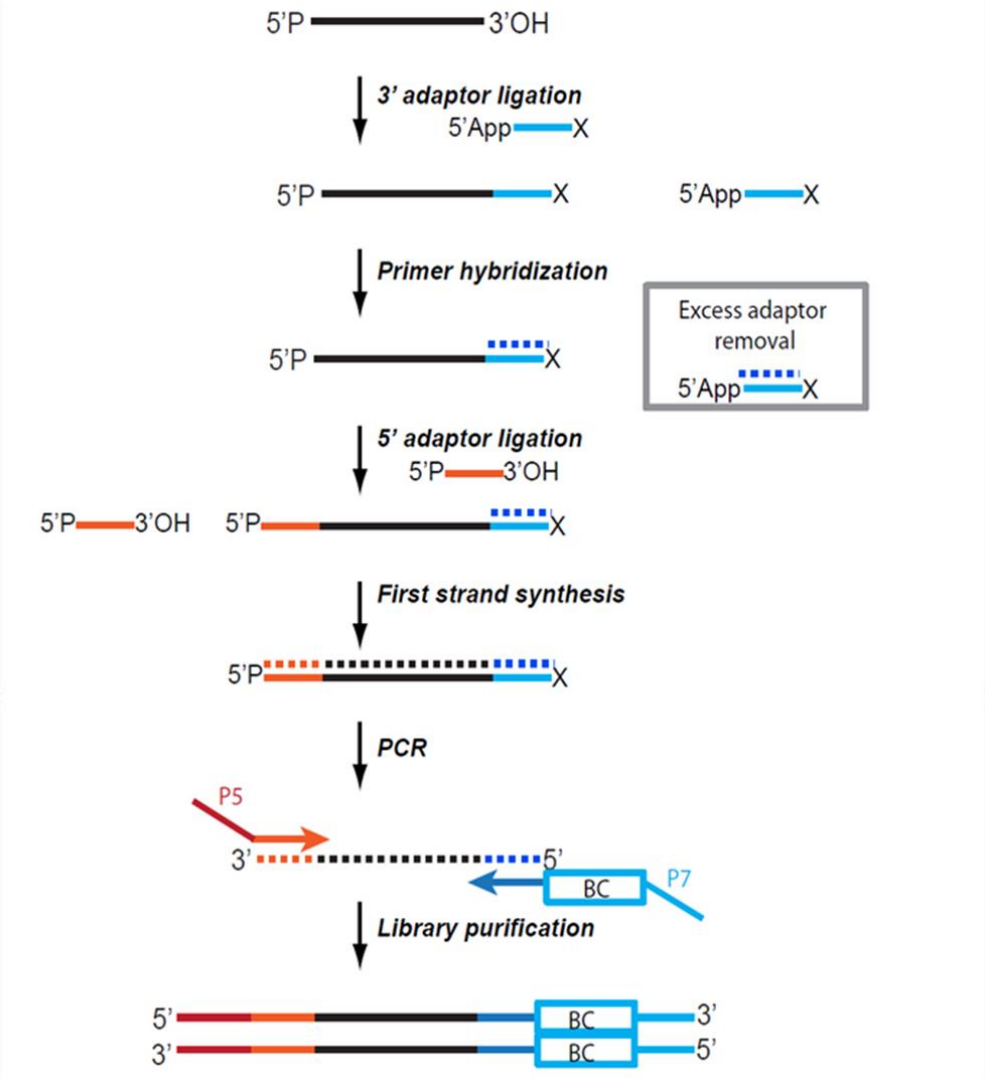

Figure 10 Library preparation adapted for small RNA

5'App: 5' pre-adenylated; X: 3'-blocked

A 3' adaptor with a 5' pre-adenylated (App) and 3' blocked DNA sequence is ligated specifically to 3'OH extremities from RNA sample. Then, the reverse transcription primer is hybridized on 3'adaptor. This step is important to prevent adaptor-dimer formation. After ligation of 5'adaptor, the first cDNA strand is synthesized by a reverse transcriptase and an amplification by PCR is performed. Primers contain either P5 sequence or both a barcode and P7 sequence. P5 and P7 sequence are required to amplify libraries and fix them on the flow cell. The barcode is required to identify the library during demultiplexing after sequencing.

II. Major Results

All data concerning this first project are reported in the article Galvanin et al "Diversity and heterogeneity of extracellular RNA in human plasma" published in *Biochimie* in May 2019 in the annexe 1 of this manuscript (208).

Briefly, exRNA preparations from whole healthy human plasma samples were isolated directly or plasma was first fractionated by ultracentrifugation, or by precipitation-based commercial kits. Two other treatments were performed on samples previously treated with a precipitation kit in order to enrich exosomes. These two methods are the size exclusion chromatography and the combination of proteinase K and RNase A treatments. For whole plasma and samples prepared by ultracentrifugation and precipitation-based kits, both mature RNA and degradation products were analysed, using prior deP/P treatment of exRNA species.

In this study, we demonstrated that exRNA are found in low amounts (between 1 to 8 ng of RNA/ mL of starting plasma) and have a similar profile on Bioanalyzer whatever were their treatment. In fact, exRNA are in majority below 200 nt and even below 70 nt in length.

Analysis of fragment size in whole plasma without further treatment highlighted the presence of two major peaks at 21 and 33 nt corresponding to miRNA and hY4 fragments respectively. When degradation products are included the profile changes with a broad peak of small fragment sizes that correspond mostly to rRNA fragments.

Ultracentrifugation or precipitation methods show a similar profile in fragment size and RNA composition than with whole plasma. The only difference was a moderate increase of nonhuman RNA in some preparations obtained by precipitation-based kits. These data demonstrate the inefficiency of both methods for the purification of exosomes and are in correlation with the literature describing how they contribute to contamination of other non exosomal RNA and proteins.

However, the profile of exRNA obtained from EVs purified by SEC or PK/RNase A treatment is completely different clearly indicating that another population of exRNA is present inside of exosomes. Here, size of RNA fragments is mostly over 50 nt without any characteristic miRNA or hY4 peaks. In addition, the proportion of nonhuman RNA considerably increases compared to the whole plasma without treatment.

III. Discussion and conclusion

In this article, we showed the real challenge for the analysis of exRNA from the complex and viscous biological fluid plasma, especially when one wants to enrich particular sub-populations like exosomes or microvesicles. Such issues are not encountered when working with cell secretome from cell culture, since its composition is much better controlled and exosome enrichment does not lead to contamination due to inappropriate treatment. However, in the field of liquid biopsies, biological fluids and more especially blood samples stay the only source available for diagnostics. Due to complexity of human plasma, it remains difficult to obtain pure extracellular vesicles such as exosomes. In the literature, a number of studies already suggested exosomes from blood as good candidates for definition of diagnostic biomarkers in term of proteins, but also RNA, like miRNA. One should pay attention on how these studies were designed, because discovered biomarkers may not belong to extracellular vesicles (215–220). When plasma is submitted to either SEC or PK/RNase treatment, a subpopulation of exRNA is highlighted with a completely different profile compared to the whole plasma and corresponds certainly to exosomal RNA. Here, miRNA are rare, but these data are not in correlation with the literature where lots of exosomal miRNA were pointed out as diagnostic biomarkers. Nevertheless, in term of clinical research, it does not really matter what is the exact origin of defined biomarkers, as far as they are able to discriminate healthy from unhealthy. Really promising studies even showed how extracellular RNA can be a marker for early stages of cancer (215,221,222). However, if the purpose is to study certain subpopulations of extracellular RNA, one should be really careful on the study design and be aware of potential contamination in samples.

In SEC or PK/RNase A treated samples, exRNA contains a huge proportion of nonhuman RNA species. This was also previously reporteded in Wang et al, 2012 (223). In addition, it has been demonstrated in the literature that viruses are able to use exosome biogenesis, release and uptake pathway in order to spread themselves into their host (133). Viruses enter the cell via clathrin-mediated endocytosis and hijack the ESCRT vesicular trafficking complex and then assimilate into exosomes (224–227). Inside intraluminal vesicles, viruses hide their genome and thus can persist in the host without activating the immune system. Hepatitis C virus (HCV), Zika virus (ZV), West Nile virus (WNV), and dengue viruses are able to antagonize the late endosome leading to the release of their genome to the cytoplasm. For HCV, viral genome can also stay in the multivesicular body and be secreted into exosomes. They can then perform as infectious particles (224,228,229) and infect specific targets through cellular contacts and

therefore creating a productive infection. Thus, exosomes or at least plasma treated with SEC or PK/RNase A could be used for the detection of several viruses.

The original point of our project is a pre-treatment of isolated RNA before library preparation for sequencing. This deP/P treatment allows to include RNA that don't have naturally 5'P and 3'OH, such as degradation products. In fact, most of studies don't perform this additional step and that's why miRNA (with the extremities compatible to direct ligation) are the most frequently found species in plasma. Finally, this represents a strong technical bias because many reported library preparation protocols don't take into account degradation products as well as all nucleic acid without 5'P such as capped RNA (mRNA, snRNA …).

Concerning soluble exRNA in plasma, the major species are miRNA included into RNP via interaction with Ago2 (230). These RNA represent a huge proportion of whole exRNA and our data are in perfect agreement with this observation. It could be of interest to isolate this population via Ago2 immunoprecipitation and compare their profile to data obtained with whole plasma and samples treated with ultracentrifugation and precipitation kits.

Regarding Y4 RNA, its role outside the cell is not well understood. This RNA exists in 4 isoforms between 83 to 112 nt in length (figure 11) and is composed by a loop domain, an upper and lower stem and a polyuridine tail. In the cell, Y RNA has two major functions. The upper stem is involved in DNA replication. The lower stem and the polyuridine tail bind to Ro60 and La proteins, respectively and are involved in RNA stability and quality control (231). However, in plasma, Y RNA is not found as a full-length RNA but mostly as fragments of 31 nt in length derived from the 5′-end (figure 12). These fragments are generated by cleavage within a predicted internal loop (232). Up to now, function(s) of the 5′-Y RNA fragment(s) is(are) unknown. However, the processing and secretion of specific 5'-Y RNA fragments in plasma are consistent with a signalling function of this RNA. Only one study provided an evidence for the potential role of hY4 RNA fragment that can form a 5'-half-tRNA-like structure and bind a target RNA to form a pre-tRNA-like structure in order to guide its cleavage by tRNase Z^L (233). Moreover, it has been shown that hY1 and hY3 isoforms are over-expressed in tumours such as carcinomas, while hY4 is the most abundant isoform in healthy cells (234). So, Y RNA fragments may be potential candidates for cancer biomarkers.

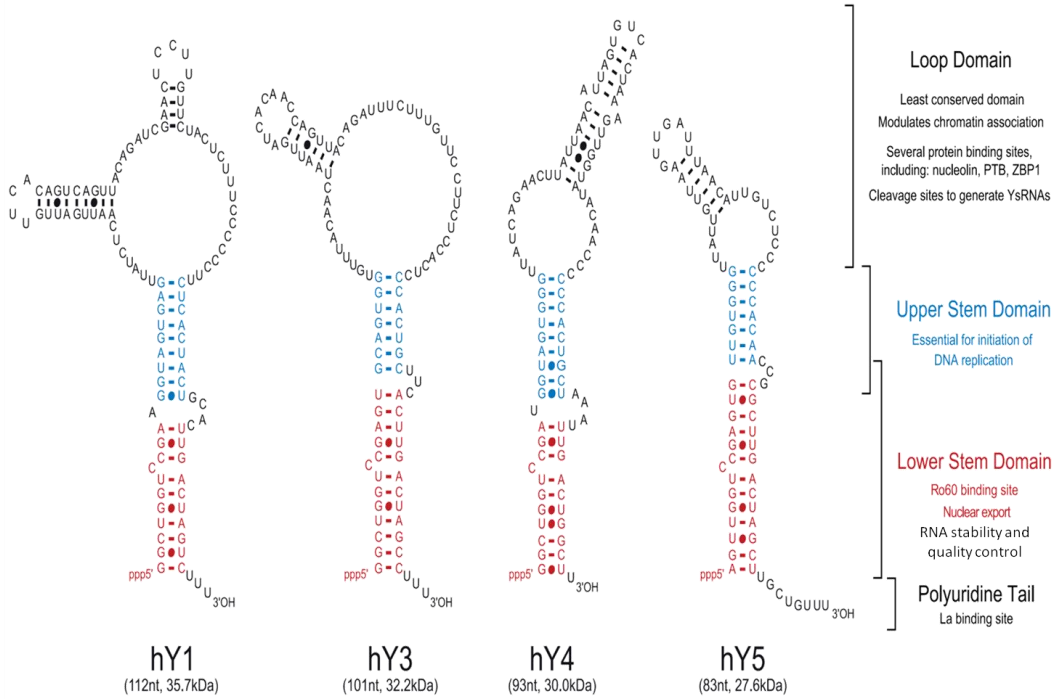

Kowalski and Krude, The international journal of biochemistry and cell biology, 2015 (231)

Figure 11: Structure of human Y RNA isoforms

In human cells, Y RNA has four isoforms hY1, hY3, hY4 and hY5 composed by a least conservative loop domain, a upper stem domain implicated in DNA replication, a lower stem domain and a polyuridine tail implicated in the interaction with Ro60 and La proteins playing a role in RNA stability and quality control.

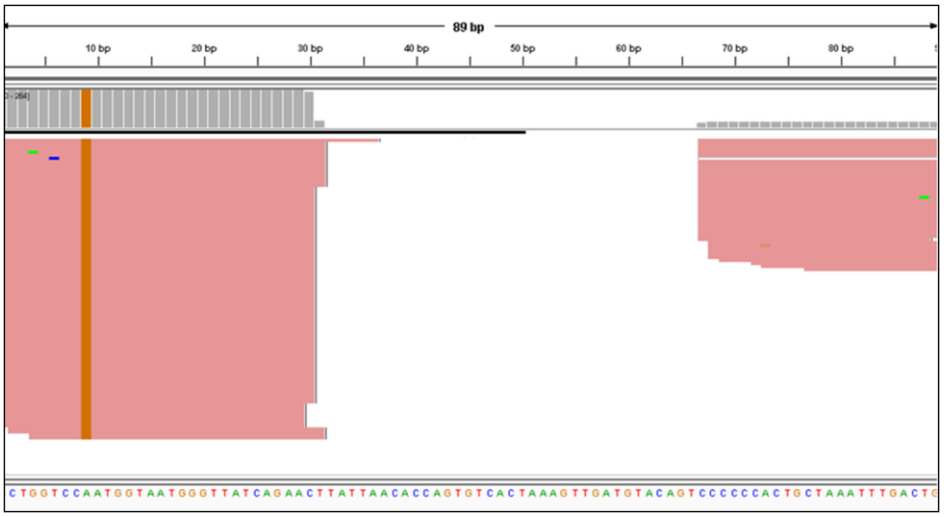

Figure 12: hY4 fragments found in plasma

Y RNA and mostly its hY4 isoform is found in plasma as fragments of 31 nt at the 5'-end and 22 nt at 3'-end.

To conclude, studying exRNA from plasma is really complicated and one must remember the study design is essential because little changes can strongly affect the resulting exRNA composition. Obtaining an exhaustive characterization of exRNA from either whole plasma or subpopulation (exosomes) is a real challenge. However, its use as diagnostic biomarkers in the field of liquid biopsies is very exciting and promising. Depending on the question asked, one can use whole plasma or subpopulation obtained by specific treatment (SEC or PK/RNase A). For instance, whole plasma (and not exosomes) is well appropriate for cancer diagnostics. On the contrary, samples enriched by SEC or PK/RNase A treatment can be used for detailed analysis of exRNA originating from the human microbiota.

CHAPTER II: Dynamics of *Escherichia coli* tRNA 2'O-methylations

A. Literature review

I. *E. coli* tRNA

tRNA are noncoding RNA playing a crucial role in translation. Individual tRNA are specific adaptors that results in the productive decoding of messenger RNA into proteins. They transfer the appropriate amino acid to an elongating polypeptide chain associated with the ribosome. After their transcription and processing, tRNA are strongly modified and then aminoacylated. The global structure of a tRNA consists in 5' monophosphate extremity followed by an acceptor stem, the D-loop, the anticodon loop, a variable loop and the TΨ loop. tRNA ends with the second strand of the acceptor stem and a 3'CCA-end (figure 14).

Historically, first studies on tRNA were done already in the 50s when Hoagland et al (235) discovered an enzyme able to activate amino acids and produce aminoacyl-adenylates in rat liver extract. Zamecnik' team demonstrated that this amino acceptor molecule was tRNA (235–238). The first tRNA sequence was described in yeast model (7,239) and with the increasing development of RNA sequencing (see general introduction on sequencing) most of tRNA sequences were determined in *E. coli*, *S. cerevisiae* and in human.

a. tRNA biosynthesis

In bacteria including *E. coli*, the genetic material encoding tRNA is mostly found in clusters where multiple gene copies for a single species are common (240). There are three different types of tRNA-encoding regions: units including only tRNA genes, those that contain tRNA genes between ribosomal RNA regions and tRNA operons including specific protein-encoding gene (241).

tRNA sequence varies significantly between each individual tRNA, but always respects a consensus of four (or five when there is a variable loop) inverted repeats that are responsible for stem-loop elements formation (242).

In contrast to eukaryotic system where 3'CCA sequence is added post-transcriptionally, tRNA genes of bacteria (including *E. coli)* encode directly this extremity feature (240). However, bacterial CCA-adding enzyme exist, they are not required for maturation, but contributes to efficient cell growth by restoring damaged CCA-ends (243,244).

1. Processing

Because tRNA genes are transcribed mainly in polycistronic regions, newly transcribed tRNA need first to be cleaved by endoribonucleases such as RNase E and RNase III in order to obtain smaller precursor molecules that will be then processed at 5’ and 3’ends (245–247) (figure 13). Both RNase E and RNase III play a role in the initial processing of tRNA precursors and give the accessibility for RNase P activity (required for 5’-processing), which is inhibited by long trailing regions, and for 3’-processing by exonucleases. Concerning the homodimer RNase III, compared to RNase E, its role in polycistronic tRNA transcript processing is less significant (248,249).

After endonucleolytic cleavage in the 3’-trailer region of the tRNA precursor, some extra nucleotides after the 3’CCA-end need to be removed. Final maturation at the 3’-end then requires an exonuclease that can trim right up to the critical CCA-end without disrupting it. RNase D plays this role and is not able to hydrolyse the CCA 3’-end (250,251) (figure 13).

5’-end tRNA processing is carried out by the ribonuclease RNase P (252) (figure 13). Bacterial RNase P is composed of one basic protein of 18 kDa (257,258) and one RNA. The catalytic activity carried by a 375-377 nt RNA and cleavage can be achieved without the protein component (257,258). However, the presence of the protein accelerates tRNA processing due to stabilization of RNase P RNA component (259–261). Three specific features in the tRNA substrate are required for an accurate recognition by the RNA of RNase P: the TΨ loop, the acceptor system and the CCA-end (262).

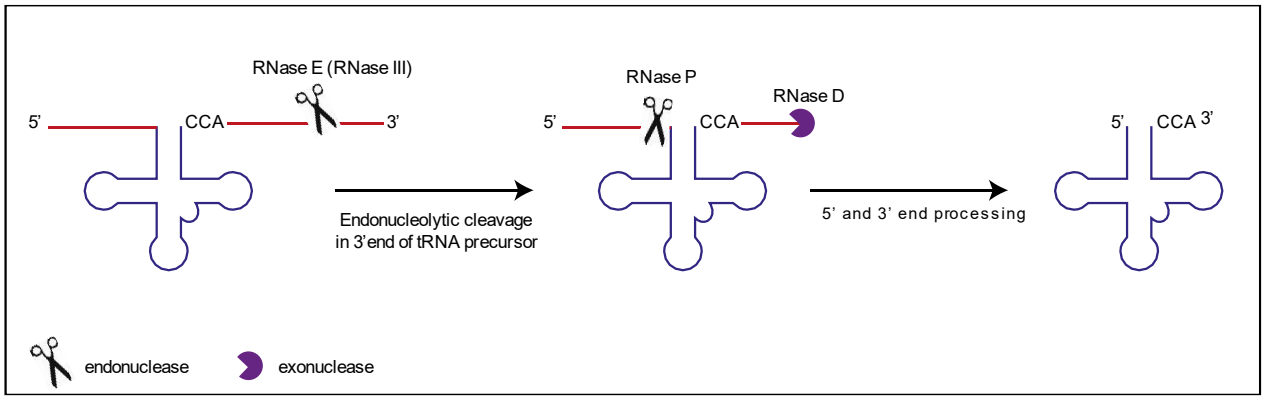

Figure 13 E. coli tRNA processing

Newly transcribed tRNA by RNA polymerase III are cleaved by endonucleases RNase E and in a minor way RNase III if they are polycistronic. 5’ processing removes the 5’ leader sequence via the endonuclease RNase P while 3’-end processing is performed by the exonuclease RNase D.

2. Modifications

Post- and co-transcriptional modifications on tRNA confer chemical diversity and increase tRNA functionality. Up to now, there are around 40 different chemical modifications reported in *E. coli* (figure 14), that generate various derivatives of the four classical nucleotides A, C, G and U. 1 to 10 % of the bacterial genome encodes for protein involved in tRNA modification process (263,264).

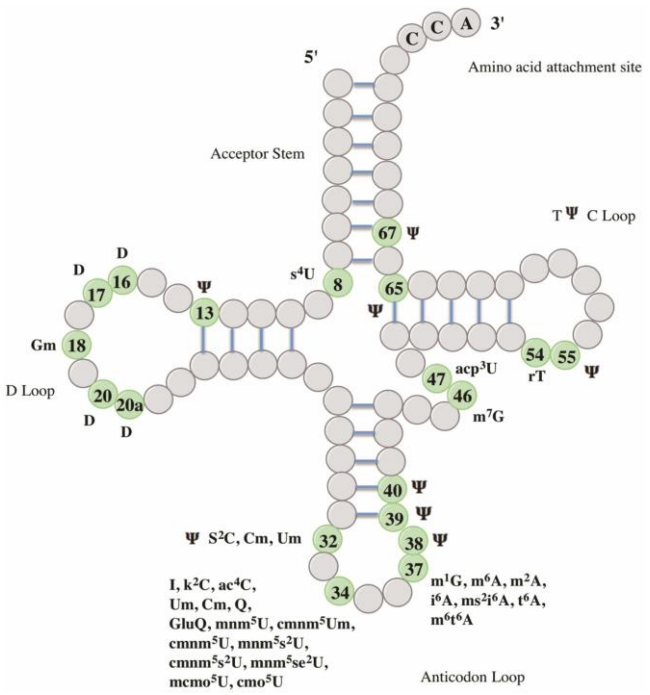

Position	Modification	Enzyme
8	S^4U	IscS, ThiI
13	Ψ	TruD
16	D	Dus A, B, C
17	D	Dus A, B, C
18	Gm	TrmH
20	D	Dus A, B, C
20a	D	Dus A, B, C
32	S^2C Cm, Um Ψ	IscS, TtcA TrmI RluA
34	I k^2C ac^4C Um, Cm Q, GluQ mnm^5U $cmnm^5Um$ $cmnm^5U$ mnm^5s^2U $cmnm^5s^2U$ mnm^5se^2U $mcmo^5U$ cmo^5U	TadA TilS TmcA TrmL FolE, QueDCEF, Tgt, QueA and G+YadB MnmC1 and C2+TrmL MnmE, GidA ? ? ? CmoA and B AroBDEKLAC
37	m^1G m^6A m^2A i^6A ms^2i^6A t^6A m^6t^6A	TrmD TrmN6? MiaA MiaB, IscS, IscU TsaC, D, B and E TsaA
38	Ψ	TruA
39	Ψ	TruA
40	Ψ	TruA
46	m^7G	TrmB
47	acp^3U	?
54	rT	TrmA
55	Ψ	TruB
65	Ψ	TruC
67	Ψ	TruC

Adapted from Shepherd and Ibba, 2015. FEMS Microbiology (240)

Figure 14 E. coli tRNA modification: positions and involved enzymes

Modified nucleosides can be found at several positions within tRNA sequence leading to differential functions but the highest frequency and diversity of modification is observed at positions 34 and 37 in the anticodon stem loop (262). Position 37 modifications are important for the maintaining of efficiency and fidelity of translation (265). Indeed, modifications are ensuring the maintenance of the correct reading frame. Thus, they allow a better stabilization of codon-anticodon interaction especially at the first base pair position (position 36) (264,265).. Position 34 modifications are involved in fidelity of translation by influencing codon choice and discrimination. This is really important when two amino acids correspond to two codons with only one of the three nucleotides is different. For example, Cm and Q modification at the

wobble position of $tRNA^{Trp}$ or $tRNA^{Tyr}$ respectively allow the discrimination between tryptophan (UGG) or Tyrosine (UAU and UAC) from stop codon (UGA, UAA or UAG) (48,264). In the anticodon loop another modification is important for translation fidelity, in the position 35 there is a pseudouridine in the $tRNA^{Tyr}$ (QΨA) (266)

Apart from the anticodon region, several other positions are known to be modified. Their main function is the stabilisation of the tRNA structure, as it was shown for pseudouridines, D and m^7G modifications among others (263,265). Other functions for tRNA modification are regulatory functions such as their role in the host immune response (267,268).

Prior studies demonstrated the importance of tRNA modification for translation or tRNA stability, but it is clear now that they play a role much more complex in cell regulation by providing connections to protein synthesis, metabolism and stress response. In the section (II. Stress and effect on tRNA) will be detailed how environmental stress can change tRNA modifications.

3. Aminoacylation

After tRNA transcription, processing and addition of their modifications, tRNA need to be aminoacylated at the 3'-end to be completely functional for translation on the ribosome. Aminoacylation is performed in two enzymatic steps by specific amino acyl tRNA synthetases (aaRS) corresponding each to a specific amino acid. First step consists in the formation of activated amino acid (aminoacyl-adenylate) in an ATP dependent manner leading to pyrophosphate release. Then, activated amino acids are transferred either at the 2' or 3' hydroxyl group of the terminal Adenosine that belongs to the CCA sequence of the acceptor tRNA. This leads to an aminoacyl-ester bond and to the release of the aminoacylated tRNA from the enzyme (269,270).

b. Focus on *E. coli* tRNA 2'O-methylation

This section is mainly inspired by the review entitled "RNA ribose methylation (2′-O-methylation): Occurrence, biosynthesis and biological functions" (271) where I had the opportunity to contribute essentially by writing the sections about tRNA 2'O-methylations, their enzymes and how this modification is involved in the innate immune system recognition.

tRNA molecules contain multiple 2'-O-methylated residues (272). In *E. coli* tRNA, three different 2'-O-methylated positions have been discovered (figure 15) (272). The major site is located in the D-loop at position 18, where the highly conserved G residue is converted to a 2'-

O-methylated guanine (Gm) in many tRNA species. The two other 2'-O-methylated residues located in the anticodon loop at positions 32 and 34 (tRNA wobble position) correspond to Cm and Um/cmnm^{5}Um residues and are present in a subset of tRNA.

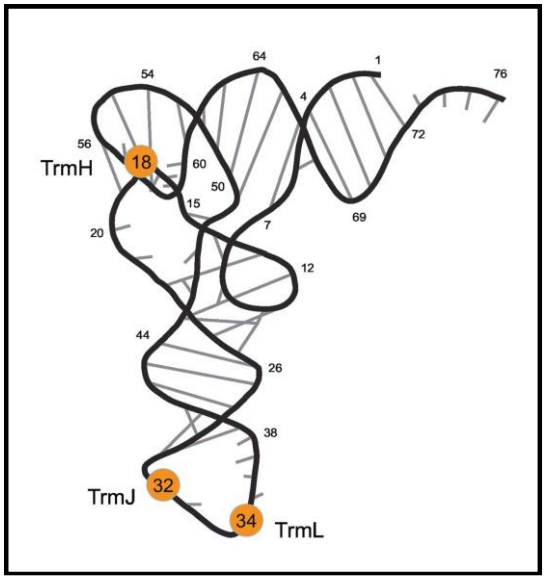

Adapted from Ayadi et al, 2019. Bbagrm (271)

Figure 15 E. coli tRNA 2'O-methylations: positions and enzymes involved

E. coli tRNA carry three modifications with methylated ribonucleotides at positions 18, 32 and 34. They are catalysed by the methyltransferases TrmH, TrmJ and TrmL respectively.

The addition of the methyl group to the ribose to form 2'O-methylation is performed by protein stand-alone enzymes: methyltransferases (MTases). They are specific to RNA and belong to a vast group of MTases that catalyze the transfer of a CH3- group (Me-group) from a methyl donor to a biomolecule (273–275). The almost universal methyl donor is S-adenosyl-L-methionine (SAM or AdoMet). All MTases share the same core structure of a mixed seven stranded β-sheets. Most 2'-OMTases belong to the superfamily of SPOUT MTases. In the past RNA 2'-O-MTases were separated into two groups: Rossman-like fold MTases (RMT) and SPOUT, but recently it has been demonstrated that they share a common evolutionary origin and they all form a single superfamily (274,276–278). Bacterial tRNA 2'-O-methyltransferases enzymes involved in tRNA 2'-O-methylation are rather well studied in *E. coli*. Each known position is formed by a specific tRNA MTase.

TrmH (or SpoU) is responsible for Gm18 and was found in the gmk-rpoZ-spoTspoU-recG operon (279,280). This enzyme is conserved in Gram negative species and in species living in harsh conditions such as *T. thermophilus* (281). Crystal structures of TrmH bound or not to

SAM have been established by extensive mutagenesis studies. Catalytic site and enzyme reaction mechanism have also been characterized. Four amino acids of the catalytic site (Asn35, Arg41, Glu124 and Asn152) are involved in tRNA binding. In addition, Asn35 is also responsible for SAM release (278,279,282).

TrmJ (or YfhQ or TrMet5Xm32) is involved in the formation of Cm32 in $tRNA^{Ser}$ 1 and $tRNA^{Gln}$ 2 (283). This enzyme also belongs to the SPOUT class of MTases (284). The 3D structure and catalytic site of *E. coli* TrmJ have been characterized. tRNA recognition by TrmJ involves not only SPOUT domain, but also additional parts of the protein (285).

TrmL (yibK) is responsible for 2'-O-methylation at position 34 in two *E. coli* $tRNA^{Leu}$ (anticodons CAA and UAA). Cm34 is formed in $tRNA^{Leu}$(CAA) and Um34 is introduced in an hypermodified nucleotide in another isoacceptor $tRNA^{Leu}$(cmnm5UmAA) (286). TrmL methylates only pyrimidine residues at position 34 and requires 2-methylthio-N 6 - isopentenyadenosine (ms^2i^6A) at position 37 for activity (287).

2'O-methylation affects the physico-chemical properties of the modified nucleoside. It does not change the base-pairing even if stabilization of the typical A-type RNA helix is observed (288,289) but it increases the stability of the nucleotide against alkaline (and even enzymatic) hydrolysis (290,291). Indeed, methylation at the 2'OH of the ribose prevent one hydrogen bound and abolishes de nucleophilic property of the O2'. In addition, tRNA modification are important for specific recognition between the tRNA acceptor and its cognate aminoacyl-tRNA synthetase (aaRS) (264). Another function for 2'O-methylation in position 18 in most of gram-negative bacteria, is its property of immunosuppressor. Indeed, Gm18 has been demonstrated to escape the innate immune system by inactivating Toll-like receptor (TLR) that are involved in the innate immune response (268)

II. Stress and effect on tRNA

tRNA are strongly regulated and can be influenced by environmental stresses such as change in temperature, nutrient deprivation or even oxidative conditions (292,293). There are documented cases of stress-induced regulation of tRNA from transcripts to translation. In addition, modifications may play discrete but elegant and essential role in fine tune of translation (292). Since few studies were done on *E. coli* or bacteria in general, both bacteria and eukaryotes will be considered in this section.

a. Transcriptional regulation of tRNA induced by stress

Eukaryotic tRNA transcription is performed by RNA polymerase III and, in yeast, is enhanced by a protein Maf1 that can be regulated by stress factors (294). In favourable conditions, Maf1 is phosphorylated and doesn't inhibit RNA polymerase III activity. However, in stress caused by DNA damage or nutrient deprivation for instance, Maf1 is not phosphorylated leading to the inhibition of the polymerase and thus reduced level of tRNA transcription (295–299). In human, the protein La is regulated by the same way: when it is not phosphorylated due to accumulating DNA damage, RNase P is inhibited and 5'processing is inhibited (300,301). Concerning 3-end processing, it has been demonstrated in *S. cerevisiae* that there is an accumulation of aberrant pre-tRNA under elevated temperatures or in glycerol-containing medium (302).

Translation fidelity certainly depends on the correct codon recognition by tRNA anticodon but also on the appropriate amino acid incorporation during aminoacylation process. In oxidative stress induced by reactive oxygen species (ROS), there is an increase of non-methionyl-tRNA charged with methionine (303,304). These misincorporations of methionine into nascent proteins allow a better detoxification capacity against ROS and belong to cellular mechanisms responsible for the protection against oxidative stress-induced damage.

In eukaryotes, tRNAs can also be cleaved into tRNA-derived ncRNAs (tRF) and this event generally occurs during stress conditions (305–311). When vertebrate tRNA are exposed to oxidative stress, heat shock and UV irradiation, the protein angiogenin is activated and cleaves tRNA in tRNA halves: sequences of 30-35 nucleotides in length derived from either 5'- or 3'-end of mature tRNA (312). In *S. cerevisiae*, Rny1 is responsible for this cleavage and is sensitive to oxidative stress, methionine starvation, extended growth and heat but not to UV irradiation and glucose starvation (307). Roles of tRNA halves are still poorly understood, but several of them are involved in the inhibition for translation initiation (313,314). Others inhibit stress-induced apoptosis by binding to cytochrome-c (315). tRNA can be also cleaved at other positions in the mature tRNA sequences leading to diverse set of tRNA-derived fragments (tRF) with a shorter length (between 13 to 32 nt). Some tRF, in higher eukaryotes, are associated with Argonaute proteins and play a role in gene expression regulation such as regulatory RNA (316,317).

In stress conditions, $tRNA^{Val}$ from archaea *Haloferax volcanii* is cleaved in tRF and then binds to small ribosome subunits in order to fine tune the rate of protein synthesis and regulate gene expression (318). Although *E. coli* is not producing tRNA halves or fragments, it has been

highlighted that bacterial tRNA instability could be a mechanism for stress response in nutrient/ amino acid deprivation condition (319). In addition to the regulation at the level of synthesis, tRNA could be subjected to demand-based regulation. However, further experiments require to be performed to validate this hypothesis.

b. Stress impact on tRNA modifications

While tRNA modification influence role in tRNA stability, maintaining the efficiency and fidelity of translation or play a role in the RNA recognition by innate immune system, they also have a more general role in cell regulation by being involved in cellular metabolism and mostly in the response to cellular and environmental stress (292,293). This is reinforced by the fact that several tRNA modifications were found to be modulated by environmental factors such as growth rate, oxygen level or temperature indicating that these modifications may play a role in stress response pathway (240).

In bacterial domain, relation between stress and tRNA modification is described. Several thermophilic bacteria showed an increase in the level of tRNA modifications when growth temperature changes (320). Concerning *E. coli*, TruB-effected pseudouridines 55 modification of tRNA is not essential, but contributes to thermal stress (321) . In addition to high temperature correlation, enzymes responsible for thiolated ms^2i^6A, τm^5s^2U tRNA modification are also necessary for oxidative stress survival (322). Content of thiolated tRNA correlates with growth rate (323). TruA-effected pseudouridines 38/39 are also important for high temperature growth (322) . However very few studies show the dynamic of these modifications for the regulation of stress conditions. For instance, *E. coli* ms^2i^6A mediated by MiaB has a role in response to stress by affecting the steady-state levels of RpoS. Indeed, the *rpoS* coding sequence is significantly enriched for Leu codons that use MiaA-modified tRNA ms^2i^6A (324). Moreover, a study on *Mycobacterium bovis* demonstrated that early hypoxia increases wobble cmo^5U in $tRNA^{Thr}$ (cmo^5UGU) inducing codon-biased translation. This allows the production of DosR protein required for hypoxia survival.

Concerning eukaryotes, similar findings were described. Some studies demonstrated that modification level changes upon elevated growth temperatures or under growth arrest conditions (325–328). In oxidative stress, Dedon's lab highlighted with an elegant method for tRNA modification detection and quantification by LC-MS/MS that *S. cerevisiae* Cm, m^5C and $m^2{}_2G$ are increasing after exposure to H_2O_2,but not in response to NaOCl: another oxidative stress-inducing agent (329). Moreover, when the strain lacks enzymes for the modification

responsible to oxidative stress, it shows a cytotoxic hypersensitivity to this stress. Thus, tRNA modification are involved in cell survival after ROS stress by playing a role in specific pathways.

Apart from oxidative stress, this very interesting high-throughput method reported change in *S. cerevisiae* modification level for 23 of the 25 analysed modification in response to the toxicants used such as $NaAsO_2$ (arsenite toxicity) or methyl methanesulfonate (MMS) (DNA damage) (329). This clearly demonstrate the importance of tRNA modification in response to stress event.

When modification dynamics is observed in the tRNA anticodon loop and more specifically at the wobble 34^{th} position, such as m^5C and mcm^5U, after certain stresses in *S. cerevisiae*, it has been demonstrated that this behaviour is crucial for codon-biased translation. The idea is that specific modifications are regulating gene expression. Indeed, these modification tunable transcripts called MoTTs may influence codon usage patterns. Peter Dedon's lab, demonstrated that modification on the wobble base is coordinated with stress-specific reprogramming leading to the translation of proteins involved in stress response (figure 16). Therefore, tRNA modifications serves as a regulatory system for translational control in stress response (292,329,330).

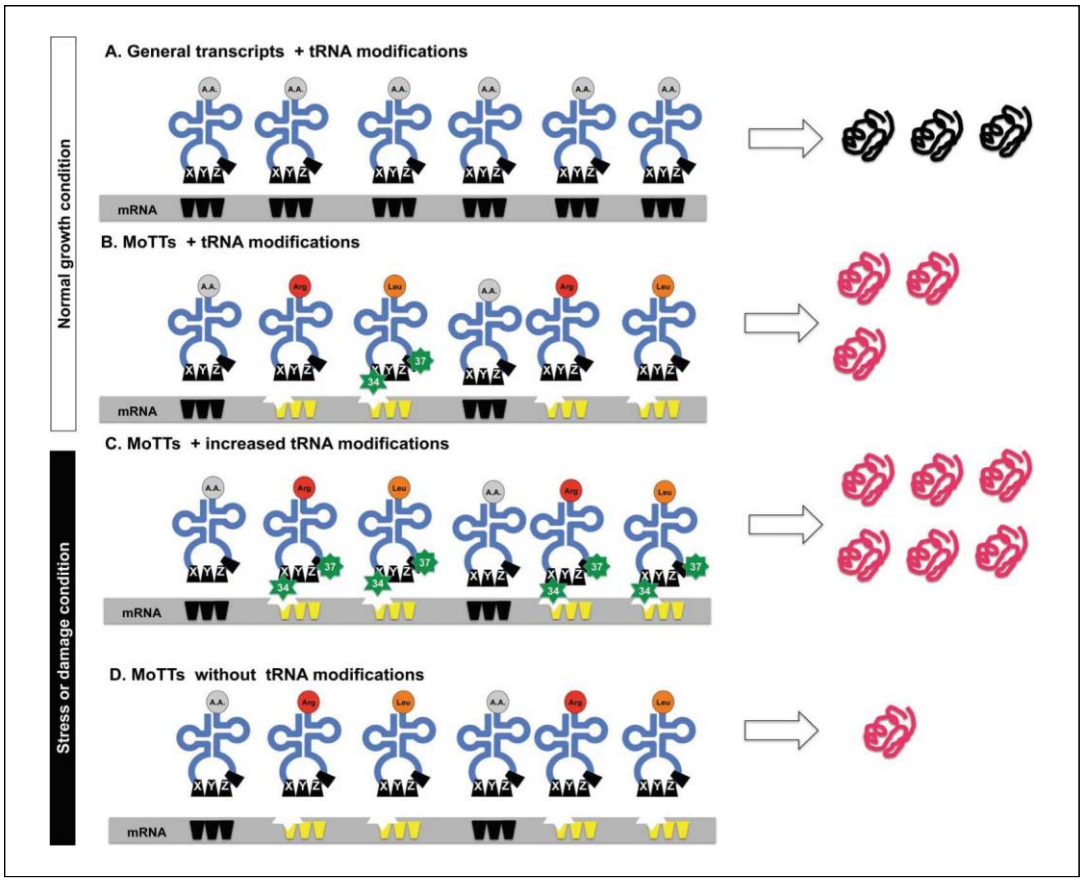

Endres et al, 2015. RNA Biology (292)

Figure 16 Model for the regulation of MoTT

When general transcripts are modified, a pool of proteins are translated. If tRNA are modified tunable transcripts (moTT), another pool of protein is translated. In stress condition, these modifications can be increased and lead to the more important production of the corresponding proteins. Without tRNA modification on moTT, fewer corresponding proteins are produced. Thus, depending on the level of modification on moTT, translation is regulated.

III. Detection of modified nucleosides

a. Methods for the detection of modification by high-throughput sequencing

Detection of RNA modification is performed for decades by various techniques of chromatography mostly by thin layer chromatography (TLC), but also high-performance liquid chromatography (HPLC) and combinations of liquid chromatography with mass spectrometry (LC-MS). However, these methods are not high-throughput and they don't give information about the position of the modification. This is why, detection of RNA modifications by deep sequencing becomes a very promising field and started less than 10 years ago (331–335). Three major principles are used for the detection of RNA modifications: targeting modifications with specific antibodies, using the RT signature induced naturally of after a particular chemical treatment or exploiting particular chemical properties of the RNA modifications.

1. Antibody based methods

This approach is widely used for the detection of m^6A and related modifications (331). The method called MeRIP-Seq and then improved leading to miCLIP technique (m^6A individual-nucleotide-resolution cross-linking and immunoprecipitation) (336) consists in the enrichment of RNA fragments containing the modification by immunoprecipitation with antibodies recognizing m^6A. Then, UV crosslinking treatment leads to formation of a covalent bound between antibody and targeted RNA fragment allowing a better enrichment of modified fragments, and also mapping of modification using the mismatch signature.

2. RT signature methods

Some modifications naturally cause a specific signature during the RT allowing to detect them by subsequent sequencing. Depending on the nature of the modification, it can either provoke a nucleotide misincorporation into cDNA or RT can be even aborted. m^3C, m^1A, m^1I, $m^2{}_2G$ and m^1G were detected using such approach called HAMR (High-throughput Annotation of Modified Ribonucleotides) (337).

Unfortunately, only limited number of post-transcriptional modifications naturally generate visible RT signature. Most of them are RT-silent but their RT signature can be enhanced by engineering of either the reverse transcriptase (338), dNTP chemical properties or the RNA template (339–341).

3. Methods based on modification of chemical properties

A multitude of chemical treatments can be performed on the RNA template before the synthesis of cDNA. These reagents can either act specifically on a given modification or selectively affect non-modified nucleotides. For example, m^5C can be detected using bisulfite treatment (342), while 1-cyclohexyl-(2-morpholinoethyl) carbodiimide metho-p-toluene sulfonate (CMCT) treatment allows the detection of pseudouridines (333,343–347).

Recently, Virginie Marchand and Yuri Motorin at the NGS core facility UMS IBSLor 2008 developed a method for the detection for m^7G, m^3C, but also D and ho^5C residues. The so-called AlkAnilineSeq method (348) relies on the enrichment of RNA fragments by selective ligation. First step is to make an alkaline hydrolysis that results in abasic sites for the mentioned modifications. This abasic site is then cleaved by aniline leaving 5'P at the N+1 nucleotide in

the sequence. Such RNA extremity is compatible with ligation of the 5'adaptor during library preparation. Thus, fragments containing the nucleotide N+1 to the modified residue in RNA are positively selected.

b. Specific detection of 2'O-methylation

Several methods were proposed for detection of 2'O-methylation. In particular conditions such as at low dNTP concentration , these modifications generate an RT signature by RT arrest (349). This method was extensively used for mapping of 2'O-methylation in rRNA and was now coupled to deep sequencing in a protocol called 2OMe-seq (350,351).

At normal dNTP concentration, 2'O-methylation don't create visible RT signature except if an engineered RT enzyme is used. In fact, engineered mutant of KlenTaq DNA polymerase is sensitive to ribose methylated residues, and generates RT stop (352). However, this method has not yet been applied in a high-throughput manner.

2'O-methylated ribose is more stable to $NaIO_4$ oxidation compared to unmodified ribose moiety. So, after $NaIO_4$ treatment, non-methylated riboses are unsuitable for 3' ligation during library preparation and only the modified one can be transformed in cDNA for sequencing. Two methods use this principle: the Nm-Seq (353) and RibOxi-Seq (354).

The last, and the most used, technique for 2'O-methylation detection relies on their chemical protective properties against alkaline cleavage. The protocol was first published by Nielsen lab in 2015 (355) and was further improved and optimized by the UMS IBSLor 2008 NGS core facility (356,357). The principle (represented in figure 19) relies on the protection of 3'-adjacent phosphodiester bond against alkaline hydrolysis of the nucleotide after the 2'O-methylation position. All other phosphodiester bonds remain sensitive to random alkaline cleavage, creating a more or less regular cleavage profile. So, the number of fragments that begin or finish at each position (5' and 3' end coverage) should be drastically low at N+1 to a ribose methylation. This method was further adapted for tRNA 2'O-methylation detection by optimizing the fragmentation step, non-redundant tRNA dataset for alignment with reduced number of ambiguously mapped reads and the bioinformatic pipeline for score calculation (357).

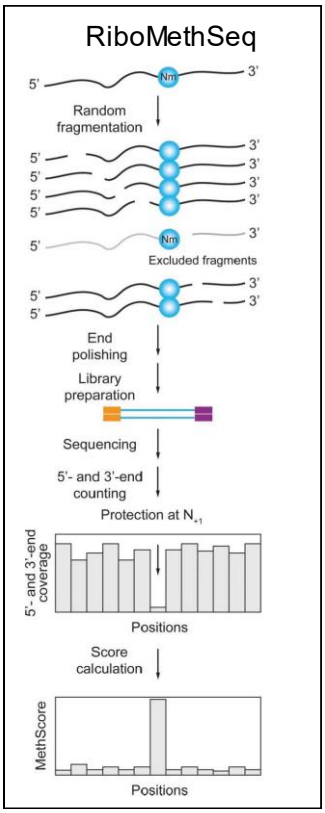

Adapted from Schwartz and Motorin, 2017. RNA Biology (358)

Figure 17 RiboMethSeq method

After alkaline random fragmentation, only methylated ribonucleosides are protected leading to a drop in the 5' and 3'end coverage after library preparation and sequencing. These drops can be transformed into MethScore thanks to appropriate score calculation.

c. Sequencing data validation

When working with deep sequencing for RNA modification detection and quantification, it is absolutely necessary to validate the results by alternative analytical approach since such high-throughput techniques always lead to multiple biases such as errors in the RT, library preparation, detection of the fluorescent signal or computational errors (359–361) .

For 2'O-methylation, several methods are commonly used for the validation of sequencing results. The first one is to perform sequencing gels after RT-PCR in low dNTP concentration leading to RT arrest visible on the polyacrylamide gel. However, this approach is not appropriate for tRNA, since their strong 2D structure gives false positive RT stop. Moreover, this technique is not appropriate for relative quantification of modifications.

Combination of liquid chromatography (LC) and tandem mass spectrometry (MS/MS) has become the method of choice for identification and quantification of RNA modifications,

providing high accuracy and sensitivity (362,363) and can also be used for validation of deep sequencing results. RNA samples are digested in nucleosides and analysed by LC-MS/MS where modifications are then determined according to their specific mass. Briefly, by feeding ^{13}C-glucose as sole carbon source, a stable isotope-labelled internal standard (SIL-IS) is generated and facilitates relative comparison of all modifications.

However, as mentioned above, the major issue of this technique is that RNA must be digested to nucleosides for quantitative LC-MS analysis and thus no information about the position of the modification can be obtained from this type of analysis. To overcome this problem, we first need to isolate RNA fragment containing only one modification. For tRNA species, it is necessary to purify individual tRNA priory to RNA digestion. Then, the obtained result will correspond to a specific position within the RNA sequence. Of note, it is possible to work with RNA sequences containing up to four 2'O-methylation modified residues as long as the methylation is carried by different nucleosides (Am, Gm, Cm and Um/Tm) because they have a specific mass. In the case of tRNA in *E. coli*, there are three potential methylated residues: Gm18, Cm/Um32 and Cm/Um34 but each individual tRNA carries always a unique 2'O-methylation for each of the three nucleosides pool in the sample. So, after appropriate and specific tRNA isolation, one can have information about the position and validate sequencing data.

IV. Objectives

In my PhD thesis project, in addition to characterization of the extracellular RNA content from human plasma, our aim was to explore the dynamics of bacterial tRNA modification by analysing levels of 2'O-methylation under several stress growth conditions. Most of studies addressing tRNA modification dynamics were performed on eukaryotes, so we focused our interest on the model bacteria *E. coli* and have chosen environmental stresses that could mimic the stress during host invasion. I first tested several common stress conditions such as change in temperature, oxygen level, nutrient limitation and non-lethal concentrations of antibiotics. As antibiotics, we have chosen several aminoglycosides affecting ribosomal translation either by modulating translation fidelity or by reduction of its speed. To detect and quantify these modifications, I used Illumina high-throughput sequencing coupled with the RiboMethSeq protocol adapted for tRNA (357). After a first screening, we highlighted modified tRNA positions of particular interest and stress conditions and performed experiments in biological replicates. RiboMethSeq data were then validated by LC-MS/MS measurements of the isolated and digested targeted tRNA. The LC-MS/MS part was performed in Mainz in the Institute of Pharmacy in the Johannes Gutenberg University where I was as part of my "cotutelle" PhD contract.

B. Results

I. High-throughput sequencing

a. Choice of stress conditions

Before applying any stress to growing *E. coli* culture, it was imperative to control growth conditions as strictly as possible. Indeed, cell physiology of the culture grown to the stationary phase is totally different from the one in the exponential phase of growth. To compare between control and stress conditions, it was necessary to establish first the exact growth conditions for the culture where only one parameter will change during the stress studied. We decided to use the *E. coli* laboratory strain DH5α at the exponential phase for all the cultures; in order to produce sufficient amount of cells without excessive stress linked to the lack of nutrients characteristic to stationary phase. Thus, the growth curve was systematically taken in order to determine the Optical Density (OD) at 600 nm corresponding to middle exponential phase. In the figure 18 (blue lane for both graphs) one notice that around $1OD_{600nm}$, *E. coli* cultures are still in the middle of the exponential phase under normal conditions. For all cultures, harvest of cells was done when OD_{600nm} reached 0.8 to 1.0. In order to achieve the best reproducibility, other growth parameters were also strictly controlled, the same incubator set to shaking speed of 190 rpm, as well as the same type of Erlenmeyer flasks (volume, shape: control of oxygenation level) were used. Seeding was performed at OD_{600nm} 0.01 - 0.05 from a preculture also grown to middle exponential phase. The same preculture was used for control and stress conditions for the same batch of experiments.

At beginning of the project, we performed a screening of several possible stress conditions in order to check if *E. coli* tRNA 2'O-methyation is affected. Thus, we tested varying temperatures (20°C, 37°C and 42°C), level of nutrients (standard LB medium, minimal medium M9 or starvation in Phosphate-Buffered Saline (PBS)). We also attempted to reduce the level of oxygen available in the medium (hypoxia-like conditions) or to induce antibiotic-driven stress using aminoglycosides affecting the ribosome (streptomycin, spectinomycin conditions). Some stress conditions were combined together such as low or high temperature with reduced level of oxygen or in M9 minimal medium. The table 3 describes all the conditions tested for the initial screening as well as growth parameters used.

In order to explore as much as possible potential impact of stress conditions, variants of previously reported protocols were also applied. For reduced oxygen level (hypoxia-like) conditions, we used bacteria grown in tightly closed glass bottles under normal agitation speed

(190 rpm). Under these conditions (protocol A) the level of oxygen is moderate since no oxygen can enter during the culture, but residual oxygen dissolved in a media and present in the air of the bottle can be used by bacteria. The protocol B relies on a culture without any agitation to prevent oxygenation. In addition, culture is grown in 50 mL plastic Falcon tubes completely filled by medium (no air in the Falcon). Only the oxygen initially dissolved in the medium was not removed. For these samples, OD_{600nm} was not checked regularly, in order to avoid disruption of the hypoxia-like conditions. This explains why for some samples the OD_{600nm} was inferior to expected 0.8-1.2 OD_{600nm}.

For non-lethal antibiotic stress conditions, protocol A consisted in growing the bacteria directly in the medium supplemented by non-lethal concentration of antibiotic. We selected a concentration leading to a growth delay around 30% (figure 18): 1.5 µg/mL for streptomycin and 2.5 µg/mL for spectinomycin. For the protocol B, the stress is more stringent. First cells are grown under normal conditions in LB at 37°C until middle exponential phase and are then submitted to stress with higher final antibiotic concentration, leading to a growth delay of around 90% (figure 18): 5 µg/mL for streptomycin and 10 µg/mL for spectinomycin.

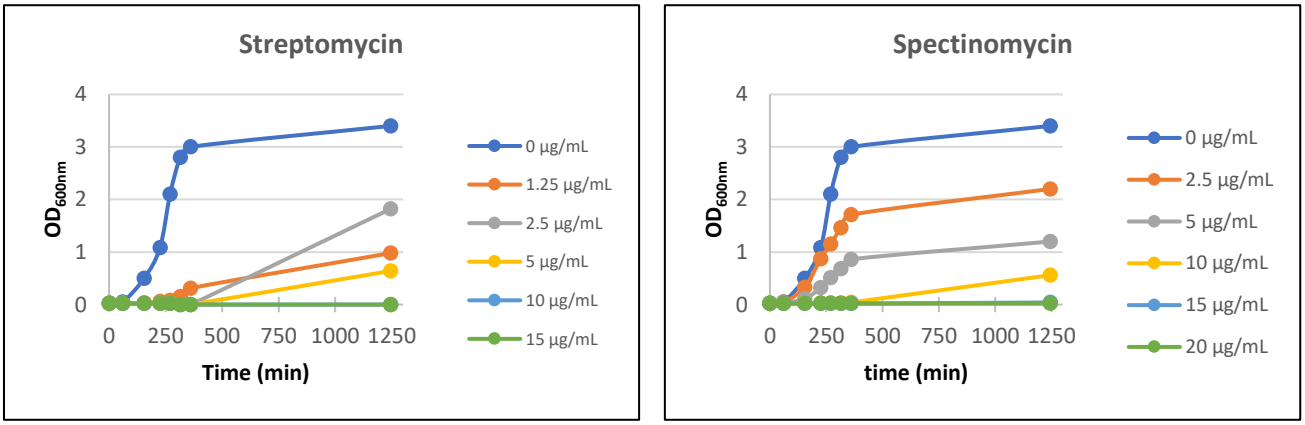

Figure 18 Growth curve in Streptomycin and Spectinomycin condition (protocol A)

Culture was seeded at 0.05 OD_{600nm} in a given antibiotic concentration. The OD_{600nm} was followed during 1250 min.

Table 3 Stress conditions for the first screening

Number (1,2,3) represent replicates for the same stress/ Letter (A or B) corresponds to two different protocols for a given stress/ H represents the conditions with a decrease level of oxygen (Hypoxia like condition)

Sample	Type of Stress	Seeding OD_{600nm}	Growing time	Final OD_{600nm}	Comments
LB 37°C control 1	/	0.05	3h	1.3	
LB 37°C control 2		0.05	3h	1.3	
LB 37°C control 3		0.05	3h	1.3	
LB 20°C	Temperature: 20°C	0.05	24h	1.4	
LB 42°C	Temperature: 42°C	0.05	3h	0.83	
M9 37°C	Nutrient level: minimal medium	0.05	24h	1.3	
M9 20°C	Nutrient level: minimal medium Temperature: 42°C	0.05	48h	1.26	
LB 37 H A	Hypoxia like condition	0.05	3h	0.83	*E. coli* was grown in a closed bottle under agitation
LB 37 H 1 B		0.02	24h	0.35	*E. coli* was grown in a closed full falcon without any agitation
LB 37 H 2 B		0.02	24h	0.36	
LB 37 H 3 B		0.02	24h	0.37	
LB 20 H A	Temperature: 20°C Hypoxia like condition	0.05	26h	1.6	*E. coli* was grown in a closed bottle under agitation
LB 20 H 1 B		0.02	24h	0.6	*E. coli* was grown in a closed full falcon without any agitation
LB 20 H 2 B		0.02	24h	0.63	
M9 37°C H A	Nutrient level: minimal medium Hypoxia like condition	0.05	24h	0.8	*E. coli* was grown in a closed bottle under agitation
M9 20°C H A	Nutrient level: minimal medium Temperature: 20°C Hypoxia like condition	0.05	48h	1.06	
Starvation 1	Nutrient level: starvation	0.05	3h	1.2	*E. coli* was grown in LB37°C until exponential phase, harvest and pellet was resuspended in PBS for 24h
Starvation 2		0.01	7h	1.4	
Streptomycin 1 A	Antibiotic	0.05	3h	0.8	*E. coli* was seeded at 0.01 or 0.05 OD_{600nm} in antibiotic concentration leading to growth delay of around 30%
Streptomycin 2 A		0.01	7h	1.4	
Spectinomycin 1 A		0.05	3h	0.76	
Spectinomycin 2 A		0.01	7h	1.6	
Streptomycin B		0.01	5h30	0.9 → 2.6	*E. coli* was grown in control condition until exponential phase, antibiotic was then added in a final concentration leading to a growth delay of around 90%
Spectinomycin B		0.01	5h30	0.82 → 2	

b. tRNA isolation and RiboMethSeq protocol

To measure the level of 2'O-methylation in *E. coli* tRNA by high-throughput sequencing RiboMethSeq protocol, appropriate total tRNA isolation procedure is essential. In order to provide the optimized total tRNA isolation protocol we performed the comparative analysis of available methods dedicated to tRNA isolation. We compared these approached in term of overall yield, purity and cost for *E. coli*, *S. cerevisiae* and human tRNA samples. The results of

this study were published in the manuscript entitled “Mapping and Quantification of tRNA 2'-O-Methylation by RiboMethSeq” appeared in *Methods in Molecular Bioliology (Springer)* in 2019 (364) (annexe 2).

In this work we demonstrated that the best method for isolation of total *E. coli* tRNA preparations compatible with downstream NGS applications is the TRIzol protocol on harvested bacterial cells. However, this method is not suitable neither for human tRNA, for which it gives a total RNA (not just tRNA) extraction, nor for *S. cerevisiae* tRNAs, since a highly biased composition of tRNA fraction was observed. TRIzol tRNA extraction from *E. coli* cells gives high purity and unbiased tRNA composition with a low cost. Indeed, the global proportions of individual tRNA species are not affected compared to a classical total RNA extraction protocol, such as acid phenol extraction.

After tRNA extraction, samples are submitted to RiboMethSeq protocol in order to measure 2’O-methylation level under control and stress conditions. The RiboMethSeq principle was explained in the section (chapter II, A, III, b : a. Specific detection of 2’O-methylation) and is also described in this article as well as in Marchand et al, 2017 (357).

For sequencing experiments, I prepared all the samples, performed library preparations and analysed data. Virginie Marchand, Lilia Ayadi and Valérie Igel-Bourguignon at the NGS core facility (UMS 2008 IBSLor) performed the sequencing and Pr Yuri Motorin conducted the bioinformatics analysis of the RiboMethSeq raw data.

c. High throughput sequencing: first screening

Our purpose was to determine what kind of growth stress can induce a change in level of tRNA 2’O-methylations in *E. coli*. The results of this initial screening of possible stress conditions are displayed on a heatmap (figure 19). Each square corresponds the MethScore (relative methylation level) normalised to the average value for a given modification in different samples. Thus, when it is blue, the 2’O-methylation level in the given condition is lower compared to the average, while if the square is in pink, the level of 2’O-methylation is higher than the average for the given stress condition. Data are shown for one, two or three biological replicates tested depending on the condition.

Heatmap shows that MethScore values, obtained for the majority of analysed tRNA 2’-O-methylated positions, remain stable even upon stress or their variation is not related to the

applied stress conditions. This is true for variable growth temperature, use of poor growth medium (M9), hypoxia-like conditions and protocol A for antibiotics. However, much stronger effect was observed for some of tRNA 2'-O-methylations under starvation in PBS, as well as for streptomycin and spectinomycin protocol B conditions. Here, over six methylated residues show increased methylation level under stress. For antibiotic stress, protocol A shows the same tendency, but clearly, the protocol B enhances strongly this effect of stress on tRNA 2'-O-methylation.

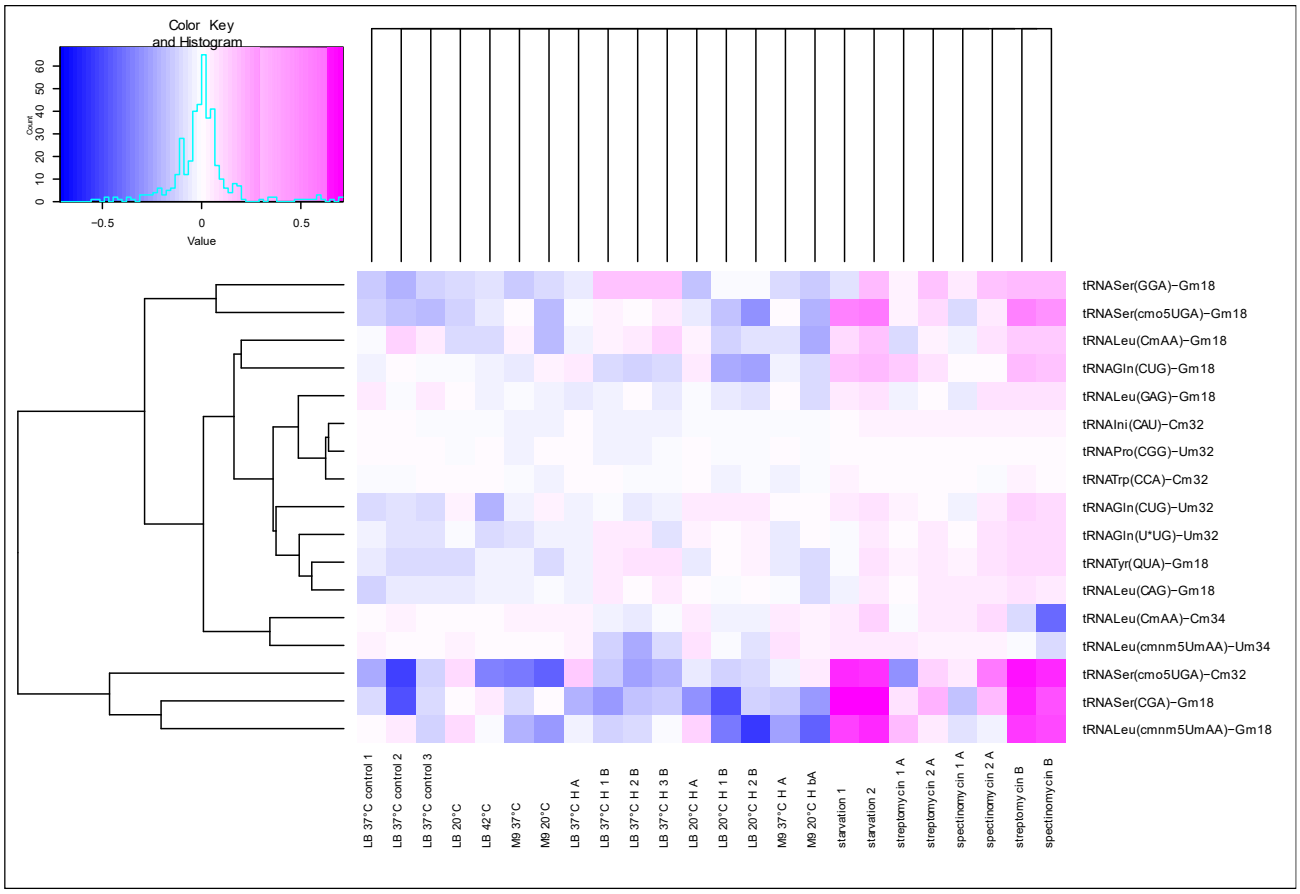

Figure 19 First screening: heat map representing MethScore levels under several stress conditions for a subset of analysed 2'O-methylations

Each square corresponds to the MethScore level normalised on the average value for a given modification.

d. Focus on starvation and antibiotics conditions

1. Study design

This first screening allowed us to focus our project on the most promising stress conditions like starvation in PBS and antibiotic treatment. To ensure reproducibility of observations, four biological replicates were tested (three replicates for chloramphenicol). Antibiotics streptomycin and spectinomycin belong to the aminoglycoside family, streptomycin decreases translation fidelity by binding to 16S rRNA and spectinomycin decreases translation speed by interfering with the binding of tRNA to the ribosome (365). We also decided to include chloramphenicol as example of non-aminoglycoside substance but still affecting ribosome translation. Chloramphenicol binds to the large sub-unit of the ribosome and inhibits the peptide bond formation by preventing peptidyl transferase activity. Like streptomycin and spectinomycin condition (protocol B), we determined optimal working concentration for chloramphenicol (figure 20), which is 5 µg/mL

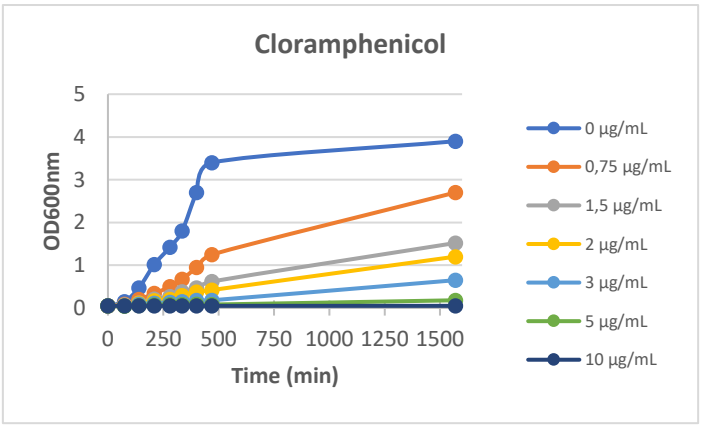

Figure 20 Growth curve in the presence of varying concentrations of chloramphenicol

Culture was seeded at 0.05 OD_{600nm} in a given chloramphenicol concentration. The OD_{600nm} was followed during 1600 min.

Finally, we performed "return-back" experiment in order to check if the level of tRNA 2'-O-methylation in bacteria under stress conditions can come back to the level observed for control phenotype when source of stress is not there anymore.

The whole experimental design is summarized in the figure 21.

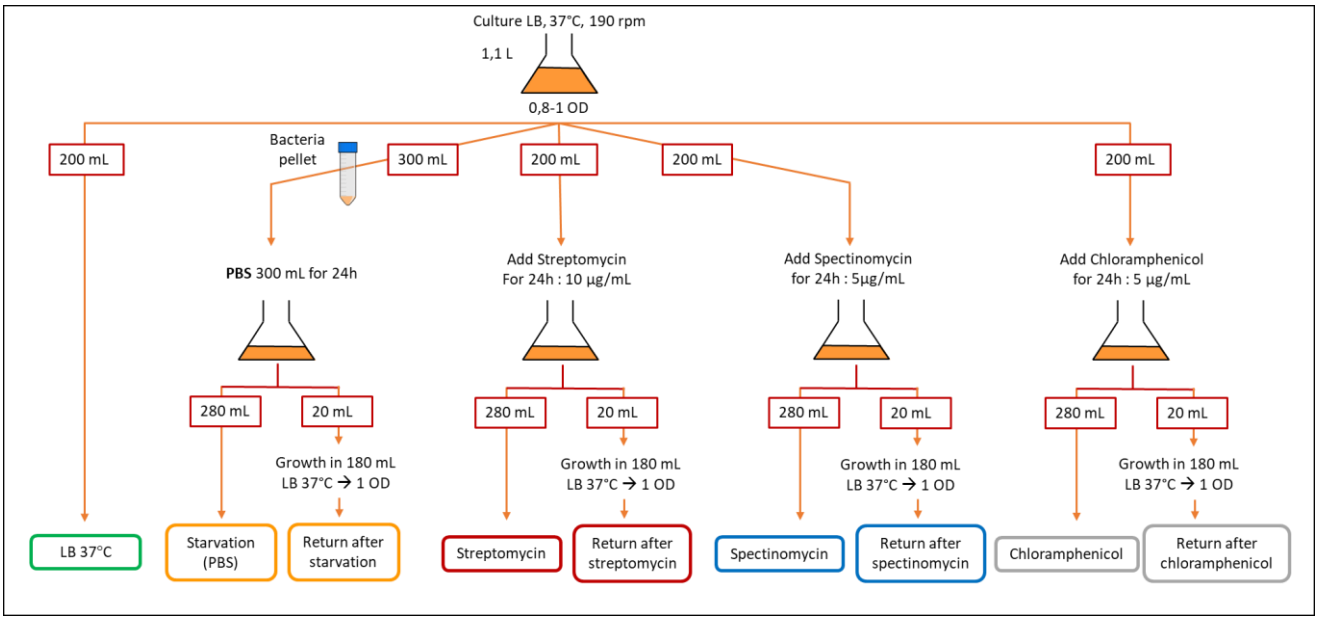

Figure 21 Study design for starvation and antibiotics conditions and restoration experiments

A large volume of control culture was grown in LB at 37°C until 1 OD_{600nm}, 200 mL were harvest and used for control condition while the rest of the culture was split for the four stress conditions. 300 mL was centrifuged and the pellet resuspended and incubated for 24h in PBS 1x. For antibiotics conditions, the appropriate concentration of antibiotics was added to the 200 mL of culture and the culture was incubated for 24h. After, one day 20 mL of each culture is seeded in 180 mL of LB medium and cultured until 1OD_{600nm} for "return-back" experiments. The rest of the culture is pelleted for the stress conditions.

In the table 4, is listed the different cultures parameters.

Table 4 Stress conditions for biological replicates

Sample	Seeding	Growing time	OD_{600nm} before stress	OD_{600nm} after 24h stress
LB 37°C control 1	0.02	6h	0.96	/
LB 37°C control 2	0.02		1	
LB 37°C control 3	0.02		1	
LB 37°C control 4	0.05		0.98	
Starvation 1	0.02	6h + 24h incubation	0.96	0.53
Starvation 2	0.02		1	0.55
Starvation 3	0.02		1	0.52
Starvation 4	0.05		0.98	0.52
Streptomycin 1	0.02		0.96	1.39
Streptomycin 2	0.02		1	1.32
Streptomycin 3	0.02		1	1.31
Streptomycin 4	0.05		0.98	1.21
Spectinomycin 1	0.02		0.96	1.51
Spectinomycin 2	0.02		1	1.54
Spectinomycin 3	0.02		1	1.5
Spectinomycin 4	0.05		0.98	2.7
Chloramphenicol 1	0.05		0.98	1.06
Chloramphenicol 2	0.05		0.94	1.05
Chloramphenicol 3	0.05		0.87	1.07

2. Major results

Results for biological quadruplates or triplicates for starvation and antibiotics conditions are presented in the figure 22 as a heatmap. MethScore levels were normalized to the average as described previously. Three different behaviour profiles can be described. The first one groups together almost the half of studied positions where there are no visible differences between control and stress conditions (bottom part of the heatmap). As already noticed in the initial screening, several modifications (Nm32 and Gm18) are not impacted when a growth stress is induced. However, in the upper part of the heatmap, two dynamics profiles are clearly visible. First, six tRNA modifications ($tRNA^{Ser}$ (cmo^5UGA)-Cm32, $tRNA^{Ser}$ (CGA)-Gm18, $tRNA^{Leu}$ ($cmnm^5UmAA$)-Gm18, $tRNA^{Ser}$ (cmo^5UGA)-Gm18, $tRNA^{Gln}$ (CUG)-Gm18 and $tRNA^{Leu}$ (CmAA)-Gm18) show an increase in their 2'O-methylation level in all stress conditions compared to the control one. Modifications concerned are mostly Gm18 (5/6) and predominantly on $tRNA^{Ser}$ or $tRNA^{Leu}$, which are tRNA with a long variable loop. Out of the 9 Gm18 positions studied, more than the half (5) show such behaviour. On the contrary, out of the 6 studied modifications at the position 32, only one Cm32 was found to be increased under stress conditions. The second profile for response to stress is observed for positions 34: $tRNA^{Leu}$ (CmAA)-Cm34 and $tRNA^{Leu}$ ($cmnm^5UmAA$)-Um34. Here the profile is different.

Modification at those two positions is not affected in starvation and spectinomycin stress. Only a slight decrease for Cm34 in $tRNA^{Leu}$ (CmAA) was observed in upon spectinomycin stress. However, under streptomycin stress and particularly under chloramphenicol-induced stress, the level of these two 2'O-methylations was substantially decreased.

Thus, this experiment highlights two possible behaviours: a global increase of certain Gm18 and Cm32 modifications and a specific decrease for position 34 under streptomycin and chloramphenicol stress conditions.

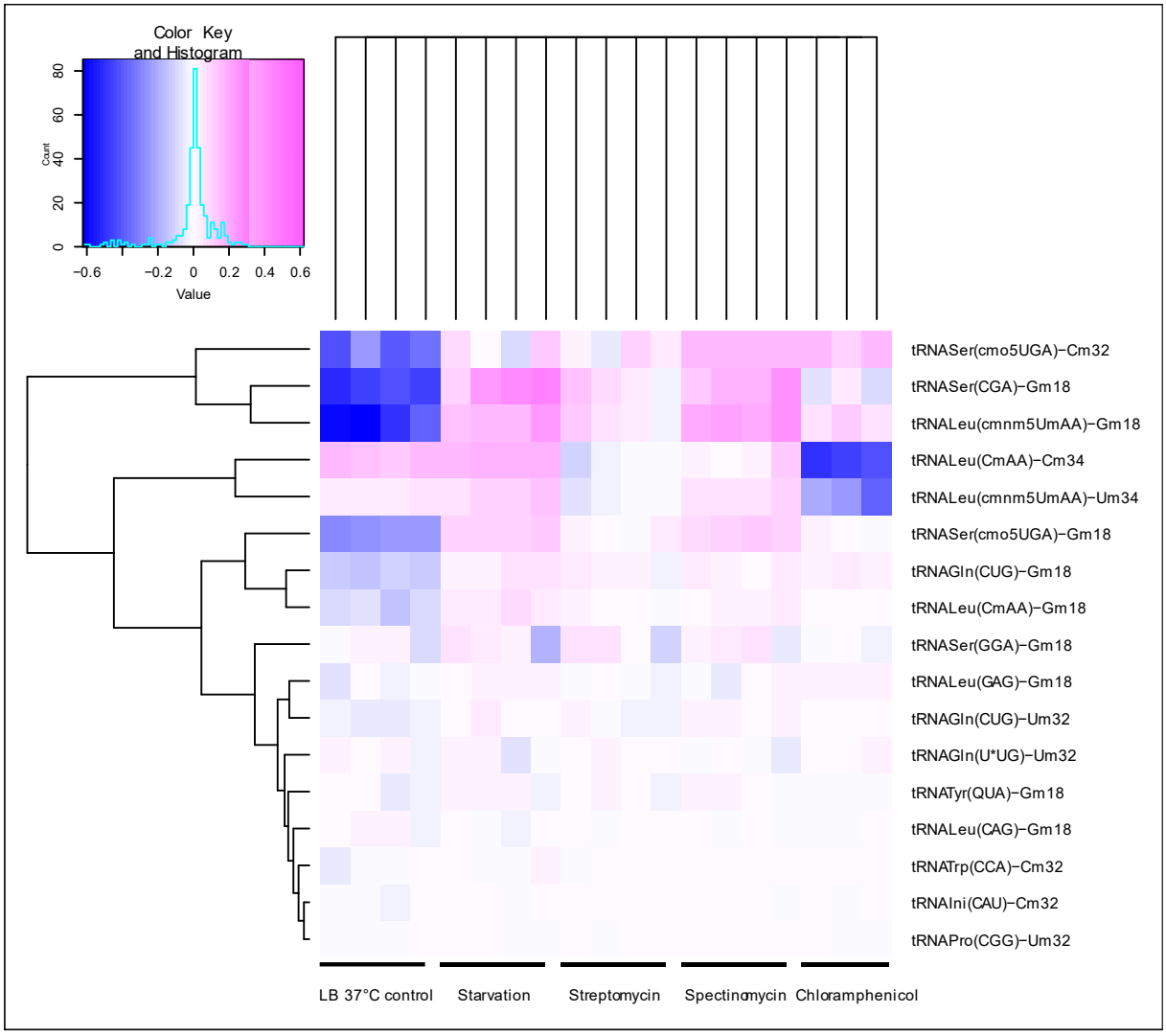

Figure 22 Global heatmap: heat map representing MethScores in starvation and antibiotics conditions performed in biological replicates

The figure 23 represents a boxplot for the 8 most affected positions. Here, MethScore levels are not normalised to the average deviation, but raw values are used. This allows a better individual analysis (position per position) and better illustrates variability between biological replicates. Clearly, for all studied methylations, the figure shows a significant difference between MethScore levels observed in controls and under stress conditions.

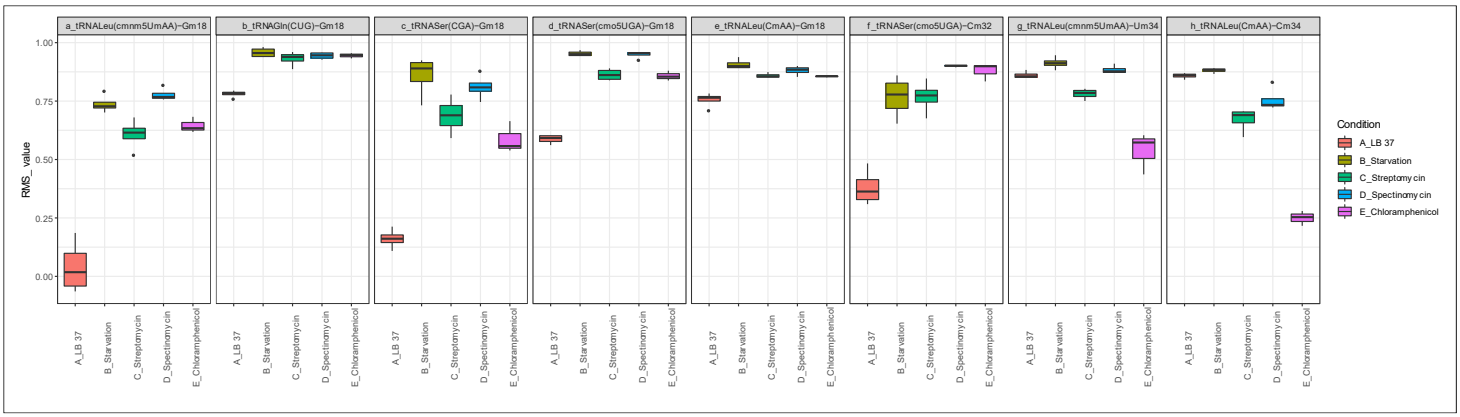

Figure 23 Box plot on 8 interesting positions leading to a modification dynamism

Rectangle in the box plot represents data from 1st to 3rd quartile and is cut by the median. Segments (or dots) in the extremities show the extreme values.

3. "Return-back" experiment

Finally, we tested if the observed stress-related changes in profile of tRNA 2'-O-methylation are reversible. Thus, after growth under stress conditions the cells were placed back to standard LB medium and grown at 37°C as for the control conditions. The figure 24 shows a heatmap of MethScore values obtained for "return-back" experiments. As seen before, Gm18 and one Cm32 methylation levels are increased under stress conditions, while methylations at position 34 are decreased in the presence of streptomycin and chloramphenicol. However, after "return-back" growth in LB at 37°C, the MethScore values are rather similar to control values in LB 37°C cultures. Thus, we can consider that the response to stress involving modulation of tRNA 2'O-methylation is reversible. These data highlight the fact that modifications in *E. coli* tRNA are dynamically regulated in response of stress and this may be a regulation mechanism allowing adaptation to growth environment.

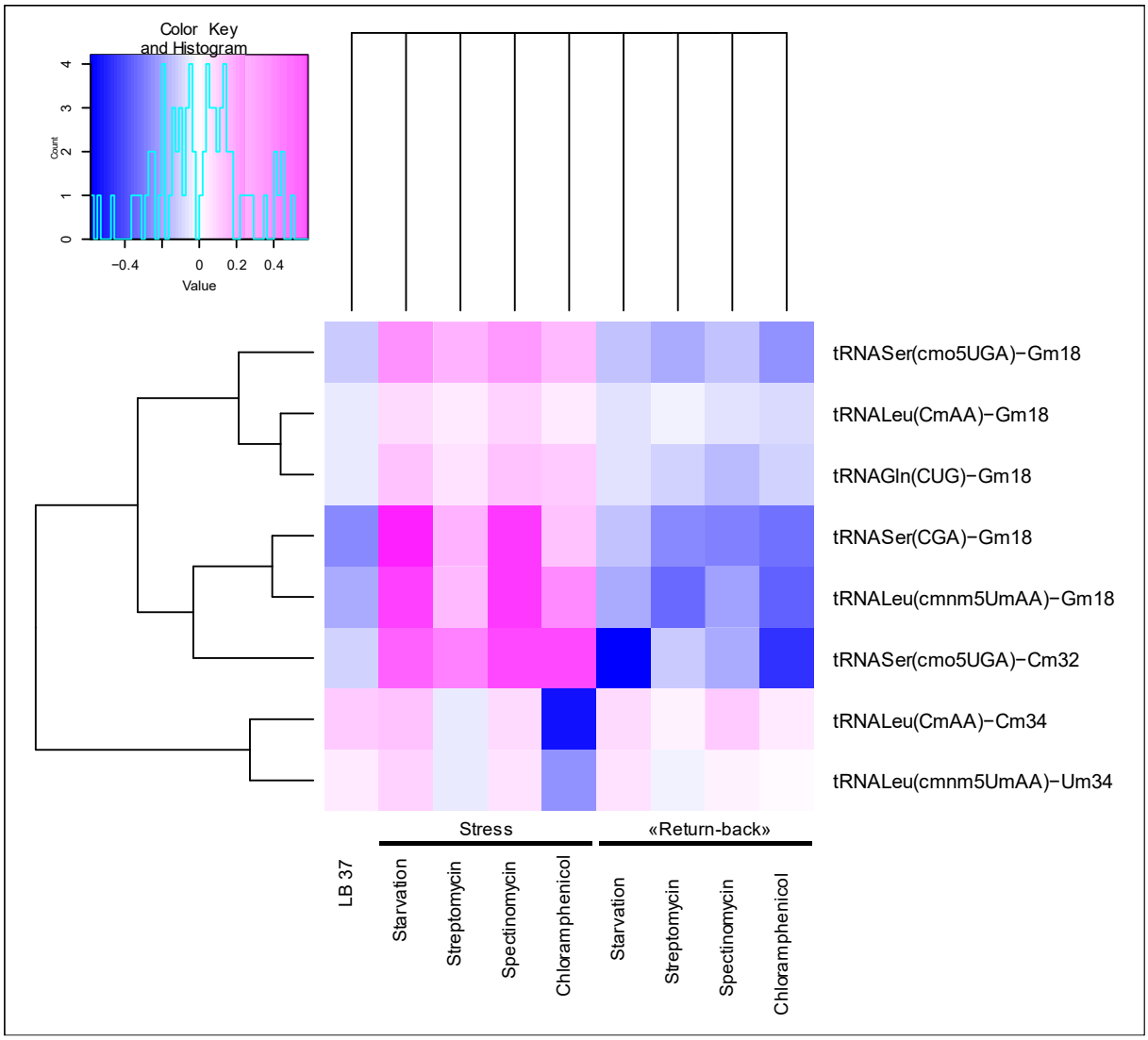

Figure 24 Heat map representing "Return-back" experiment

II. LC-MS/MS validation experiment

Since 2'O-methylation analysis by RiboMethSeq is based on deep sequencing which is a high-throughput technology, it is necessary to validate such data by alternative technology. We have chosen RNA nucleoside analysis by liquid chromatography coupled to mass spectrometry. This method is capable of performing relative quantification of RNA modified nucleotides between control and stress samples. Normalization is done using a stable isotope-labelled internal standard (SIL-IS) obtained *in vivo*, by feeding yeast cells with ^{13}C-glucose as sole carbon source.

All experiments were performed in the laboratory of Pr. Mark Helm. In the framework of my "cotutelle" contract, I stayed several months in Mainz in order to conduct these validation

experiments. I prepared all samples, digested RNA and Dominik Jacob from M. Helm group performed the LC-MS/MS quantification and coached me for data analysis.

a. total tRNA samples

First, we analysed the global 2'O-methylation content of total tRNA samples obtained under different conditions. Even if tRNA preparations from different organisms are always contaminated by fragmented rRNA pieces, *E. coli* rRNA is relatively poor in Nm residues (3 only) and thus does not interfere much with these measurements. The figure 25 represents the relative level of Gm, Cm, Um and pseudouridine compared to the sample obtained in control conditions for starvation, streptomycin and spectinomycin stress conditions. One can notice a significative increase of the total Gm content, in all stress conditions compared to the control. This result is really impressive since from RiboMethSeq data we know that only a half of Gm18 are modulated by stress response and because tRNA carrying these modifications are not very well represented in the whole tRNA pool. As expected, global level of Cm and Um modifications remain stable. Indeed, only few modifications were observed to respond under stress condition (two Cm and only one Um residue) in RiboMethSeq data, this is also why their level is considerably lower than the one for Gm modification. Secondly, concerning Cm we had opposite results for position 32 (increase) and position 34 (decrease). So, it is anticipated to have only a minor change at the global modification level. Pseudouridine level was also analysed as a control and no substantial changes were observed. Since pseudouridine residues are mostly used for tRNA structure stabilization, they are not expected to respond to environmental stress.

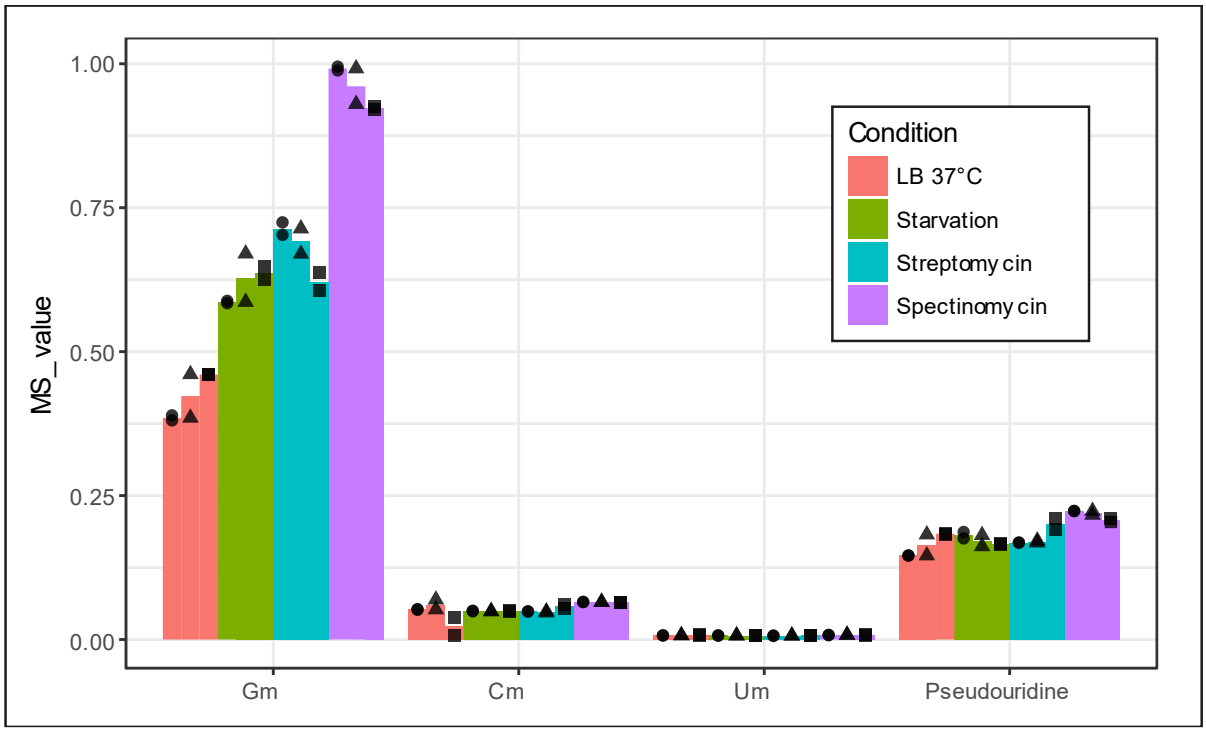

Figure 25 Relative quantification on MS signal from tot tRNA samples

MS values were reported between 0 and 1. 1 represents the highest MS value. Black circles, triangles and rectangles represents first, second and third biological replicates respectively. Each sample was analysed in technical duplicates.

b. Individual tRNA isolation procedure

Observed global changes in Gm content in total tRNA fractions obtained under stress conditions were encouraging for further validation using individual purified tRNA species. For this analysis it was necessary to isolate specific tRNA species before proceeding to nucleic acid fragmentation and LC-MS/MS quantification. It is highly important to use only pure preparations of each tRNA of interest in order to assign the quantified modifications. Since all tRNA species have similar size (74-90 nt) and physico-chemical properties, they cannot be efficiently purified to homogeneity neither by polyacrylamide gel electrophoresis (PAGE), nor by classical chromatography techniques. During my phD thesis I applied two different protocols for isolation of individual tRNA. The first protocol was already optimized in Mark Helm's lab and consists in hybridization of the tRNA of interest to a fully complementary DNA oligonucleotide 5'-end conjugated to biotin. Coupling these biotinylated DNA oligos to streptavidin-coated magnetic beads allows specific retention and isolation of individual tRNA. The second protocol relies on the same hybridization principle but here oligonucleotides have 3'NH_2 extremity that forms a covalent link with N-Hydroxysuccinimide (NHS) group of pre-activated agarose, placed into Hi Trap column (figure 26).

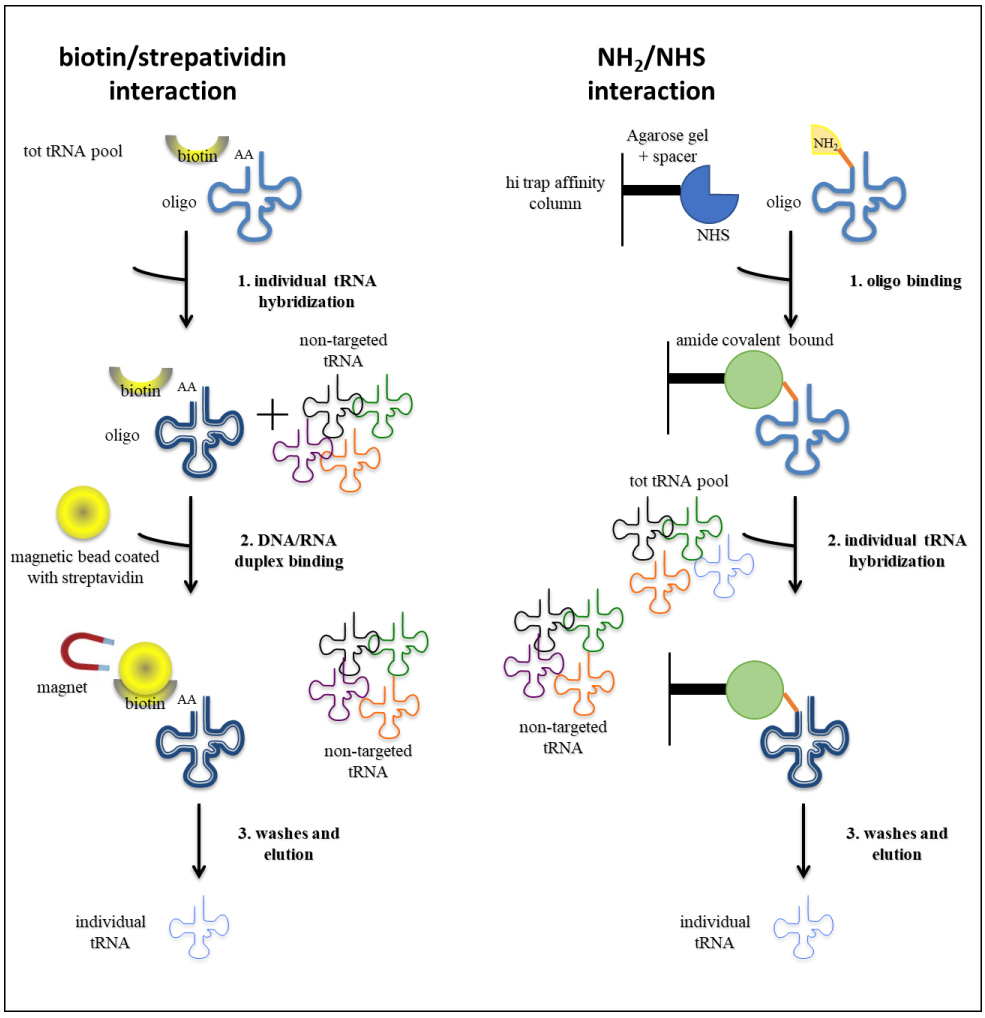

Figure 26 Two methods for individual tRNA isolation

Both methods rely on the hybridization of the target tRNA to DNA oligonucleotide. The method on the left consists in the interaction of biotin coupled to the oligo with streptavidin-coated magnetic beads. Using a magnet, beads with specific tRNA are retained and the non-targeted species are washed away. The second method (on the right) uses DNA oligonucleotide with a primary amine at the 3'-end that reacts with NHS-activated agarose placed in the HiTrap column. Then by passing a total tRNA sample through the column, only the targeted one will stay in the column and can then be eluted by decreasing salt concentrations.

To perform isolation of individual tRNA species for LC-MS/MS validation of Nm content, we ordered four oligonucleotides targeting altogether six 2'O-methylations as described in the table 11 in the section (Chapter II, C, I, c: Oligonucleotides). These modifications showed most prominent increase under stress condition for Gm18 and Cm32 position in RiboMethSeq data, while substantial decrease was observed for Cm34 under chloramphenicol and streptomycin stress. For application of biotin/streptavidin protocol, DNA oligonucleotides were fully complementary to the target tRNA with a biotin coupled at the 5'-end and a fluorescein at the 3'-end. For NH_2/NHS-agarose protocol, DNA oligonucleotides were of 40 nt in length with complementarity to the 3'-end of the target tRNA and were carrying a primary amine at the 3'-end.

1. Optimization of the biotin/streptavidin method

Since our goal was to isolate several tRNA species for analysis, we decided to optimize the isolation protocol for parallel isolation of different individual tRNA from one total tRNA sample. DNA oligonucleotide is first bound to magnetic beads via the biotin/streptavidin interaction and then, total tRNA sample is added to the beads for hybridization. Beads containing individual tRNA are sedimented in the magnetic field, washed to remove unspecific contaminants and bound material eluted in buffer with low salt concentration.

- Determination of the best DNA/RNA ratio for hybridization

The first step was to determine the best ratio between DNA oligonucleotide and amount of total tRNA. Analysis of RNA/DNA duplex was performed by separation on native polyacrylamide gel followed by detection of the fluorescence signal emitted by fluorescein attached to the 3'-ends of DNA oligonucleotides. In the native gel the RNA/DNA duplex and free DNA have different migration behaviour, and thus can be distinguished.

To determine the optimal tRNA amount, constant amount of DNA oligonucleotide (2 pmol) was titrated by increasing amount of total tRNA preparation. Optimal amount was defined as the point insuring 100% of hybridization for DNA oligonucleotide. Figure 27 illustrates this principle for $tRNA^{Leu}$ ($cmnm^5UmAA$) where 3,5 µg of total tRNA fraction was sufficient for complete binding with 2 pmol of DNA oligonucleotide. The table 5 shows the different amounts of total tRNA required for complete binding of all four DNA oligonucleotides used. Amount of total tRNA thus depends on individual tRNA content in the pool. For tRNA Ser CGA, due to its low concentration in total tRNA pool, the point of 100% of hybridization was not reached even with 12 µg of total tRNA. For this tRNA, isolation was done with 12 µg of tot tRNA leading to a lower hybridization level (and lower yield).

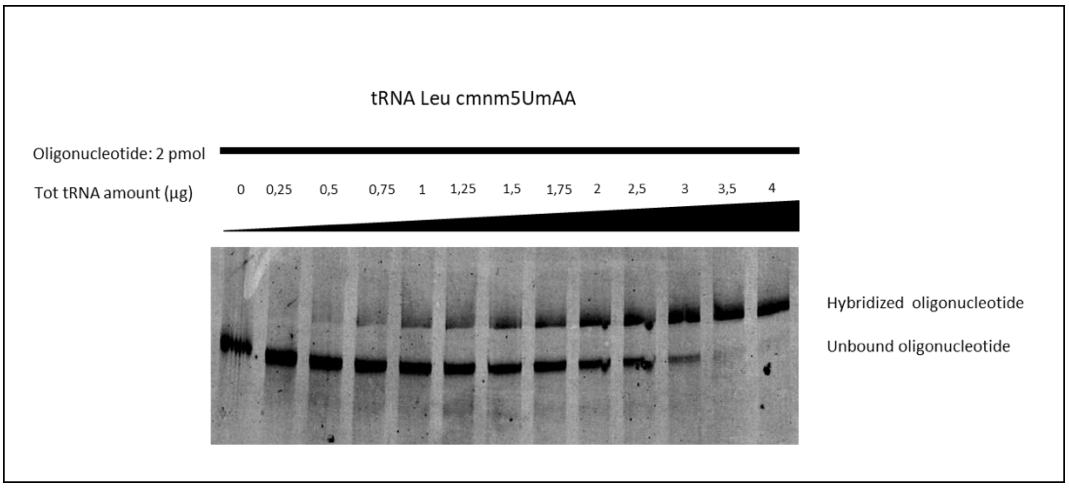

Figure 27 Determination of DNA/RNA optimal ratio for individual tRNA hybridization

2pmol of oligonucleotide complementary to tRNA^{Leu} (cmnm^{5}UmAA) was hybridized with an increasing amount of total tRNA preparation and loaded on a native gel. Upper shift observed after measuring fluorescein signal corresponds to oligonucleotide hybridized to the target tRNA (RNA/DNA duplex) while the lower band represents the free DNA oligonucleotide. 3.5 µg of tot tRNA is the minimal amount to obtain 100% of hybridization.

Table 5 Determined DNA/RNA ratios for the four studied tRNA

tRNA	**Tot tRNA amount for 100% hybridization with 2 pmol of oligonucleotide**
tRNA^{Leu} (cmnm^{5}UmAA)	3,5 µg
tRNA^{Ser} (cmo^{5}UGA)	3,5 µg
tRNA^{Leu} (CmAA)	6 µg
tRNA^{Ser} (CGA)	> 12 µg

- Optimization to limit DNA leakage in flow-through fractions

After the determination of DNA/RNA ratio, we performed the isolation procedure consecutively with four DNA oligonucleotides with a unique total tRNA preparation, to limit amount of sample required. We first isolated tRNA^{Leu} (cmnm^{5}UmAA) and used the flow-through containing all other tRNA for tRNA^{Ser} (cmo^{5}UGA) isolation. To continue in this direction, isolation of tRNA^{Leu} (CmAA) was performed from total tRNA depleted for tRNA^{Leu} (cmnm^{5}UmAA) and tRNA^{Ser} (cmo^{5}UGA) and the last tRNA^{Ser} (CGA) on a pool of tRNA depleted for all three previously isolated tRNA. In this procedure the risk is the leakage of DNA oligonucleotides into the flow-through and thus contamination of consecutive fractions by other tRNA species.

The figure 28 a) shows that the flow-through from tRNA^{Leu} (cmnm^{5}UmAA) isolation still contains DNA oligonucleotide after one, two or even three consecutive washes. This result shows that biotin/streptavidin binding is not sufficiently stable and there is a substantial leakage

of bound DNA oligonucleotide into the non-target tRNA fraction. As a consequence, the second isolated tRNA is contaminated by the tRNA isolated in the first round (figure 28 b)).

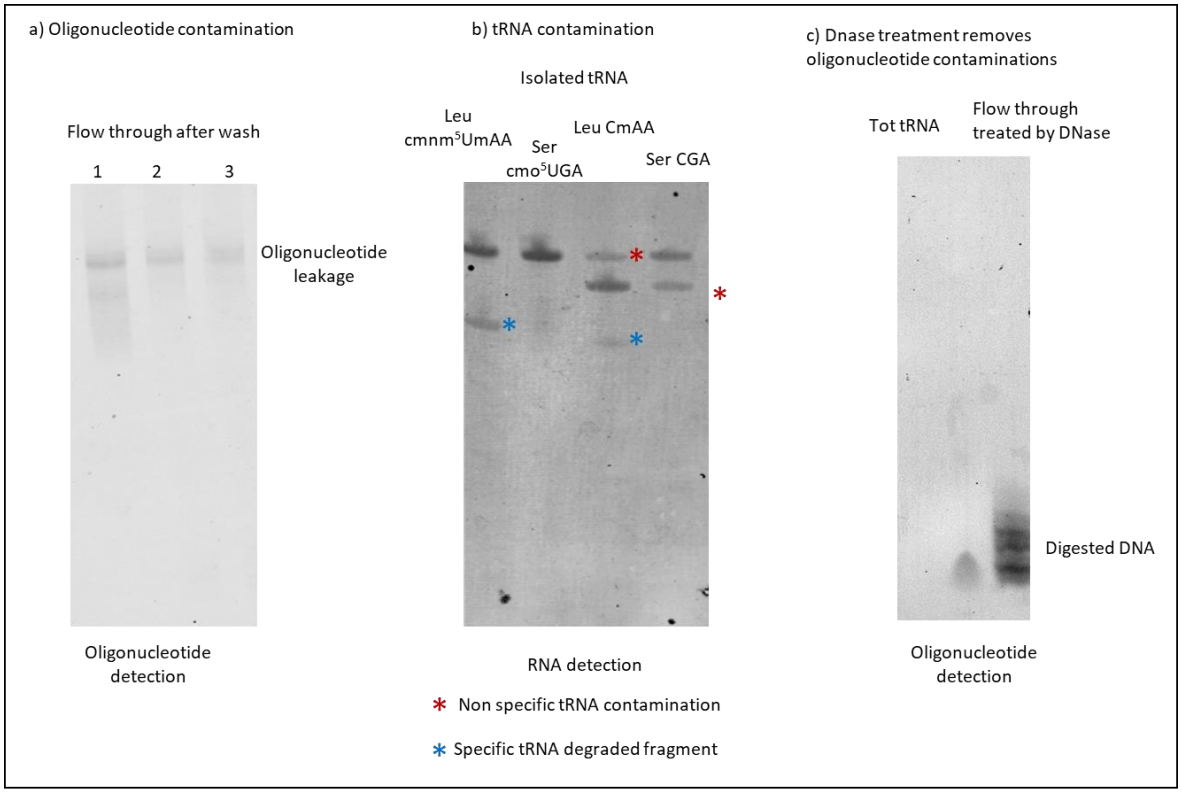

Figure 28 Leakage of oligonucleotides leads to cross-contamination

a) 100µg of tot tRNA were used for $tRNA^{Leu}$ ($cmnm^5UmAA$) isolation. First, second and third washes are loaded on a denaturing gel and the potential presence of oligonucleotides is detected by measuring the fluorescein fluorescence. We can see a DNA leakage in all washes

b) Serial isolation of first $tRNA^{Leu}$ ($cmnm^5UmAA$), $tRNA^{Ser}$ (cmo^5UGA), $tRNA^{Leu}$ (CmAA) and finally $tRNA^{Ser}$ (CGA) using at each time the flow through containing tot tRNA minus previously isolated tRNA. Samples were loaded on a denaturing gel and RNA was detected via gel red staining. Red star corresponds to non-targeted tRNA isolation while green star represents the degradation of the specific isolated tRNA

c) After DNase treatment and loading on a denaturing gel, there is no more full-length oligonucleotides but only digested nucleotides.

It is essential to have strictly purified tRNA. Indeed, LC-MS/MS measurement require the digestion of RNA sample and if individual tRNA are not purified, we wouldn't be able to attribute the signal to a particular modification. Thus, we couldn't use this protocol with a DNA leakage. This is why we decided to treat the flow-through with DNase in order to digest oligonucleotides so that they can't be involved in further contaminations. Because the buffer composition in the flow-through (SSC 5X : 0,75 M NaCl; 75 mM trisodiumcitrate pH7) inhibits DNase enzyme, we first had to precipitate the flow-through and then proceed to DNase

treatment. The figure 28 c) shows that there are no more full-length oligonucleotides in DNase treatment sample but only digested nucleotides.

The last step before the next cycle of individual tRNA isolation is the removal of deoxyribonucleotides monophosphates (dNMP), DNase and buffer. We performed this step using MEGAclear™ kit which is normally designed for rapid purification of RNA longer than 100 nt. Since tRNA of interest are shorter, the ethanol concentration was adjusted accordingly, to retain tRNA on the hydrophobic filter (675 µL instead of 250 µL recommended for longer RNA). In this optimized protocol the estimated loss of total tRNA preparation is 15% - 25% between two cycles.

The global yield observed for these four isolations is described in the table 6. Observed differences between four tRNA is due to their content on total tRNA pool. Since a minimum of 100 ng is required for LC-MS/MS analysis, no extra purification steps, such as gel excision procedure, were applied to these samples.

Table 6 Yield of individual tRNA purified by biotin/streptavidin isolation protocol

tRNA	Amount of individual tRNA isolated from 100 µg of total tRNA pool
$tRNA^{Leu}$ ($cmnm^5UmAA$)	600-700 ng
$tRNA^{Ser}$ (cmo^5UGA)	700-800 ng
$tRNA^{Leu}$ (CmAA)	425-450 ng
$tRNA^{Ser}$ (CGA)	90-225 ng

1. Setting up DNA-NH_2/NHS isolation protocol

Since we had contamination/loss issues with the biotin/streptavidin protocol (DNA leakage, non-reusable magnetic beads, loss of material in repetitive precipitation steps), we decided evaluate the performance of DNA-NH_2/NHS isolation protocol. In brief, the principle is very similar to the biotin/streptavidin protocol (figure 26), but complementary DNA oligonucleotides carry a primary amine at the 5'-end and covalently bind to NHS-activated agarose gel. In an appropriate carbonate buffer at basic pH (9-10), DNA-NH_2 and NHS groups readily react and create a covalent amide bond. This covalent link should prevent DNA oligonucleotide leakage. Moreover, HiTrap agarose columns coupled to specific DNA oligonucleotides can be used repetitively, since the NH_2/NHS covalent link is quite stable. With this technique, 1 mL HiTrap columns are used instead of classical 1.5 mL Eppendorf tubes. It is not an issue when HiTrap columns are used for the purification of proteins at room temperature but for individual tRNA isolation, hybridization with DNA oligonucleotide is done

at 65°C. Moreover, for a better hybridization and reduced aspecific binding, total tRNA pools were recirculating through the column by a peristaltic pump. This closed circuit allows to increase the contact tile and thus the binding efficiency and the yield of the individual tRNA. In addition, with an appropriate binding conditions, other non-target tRNA are not retained on the column by aspecific interactions. Technically, we used an oven capable to accommodate recipient for total tRNA sample, HiTrap 1mL column and a peristaltic pump. Washing step is done with a buffer at lower salt concentration and removes the residual unspecific tRNA. For elution, the column is placed into a water bath at 75°C with a buffer without salt leading to the elution of the individual tRNA from the column. Since the elution volume is substantial (several mL), eluted RNA is precipitated to concentrate it. In order to obtain a pure individual tRNA, sample is then loaded on a denaturing gel and band corresponding to the correct size is excised. This additional step (compared to the biotin/streptavidin method) allows a better purity level but considerably decreases the yield.

The figure 29 (left part) represents the first optimization experiments. Apart from the band corresponding to the target tRNA, we can notice several bands (b1, b2 and b3) corresponding to fragments of a lower size. At this point it was not clear if these fragments correspond to tRNA contaminants (b1 and b2) or oligonucleotide leakage (b3) (in these experiments DNA oligonucleotides are 40 nt in length). Since, NH_2-DNA oligonucleotides are not fluorescein modified, DNA leakage cannot be detected by measuring the fluorescence signal. However, the nature of band was verified by hybridization of each eluted fragment with full-length DNA oligonucleotides with 5'biotin and 3'fluorescein. Duplex formation was assessed by loading the potential RNA/DNA-FL duplex on a native gel. On the right part of the figure 29, we observe a shift for all three fragments (b1, b2, b3) meaning that they correspond to degradation products from the specific tRNA of interest. Hybridization is only partial, since molar ratio between RNA and DNA oligonucleotide was not determined for this verification. The band b3 also hybridizes to the oligo indicating that it is not leaked DNA oligonucleotide from the column. Thus, the flow-through can be used for further tRNA isolations without contamination.

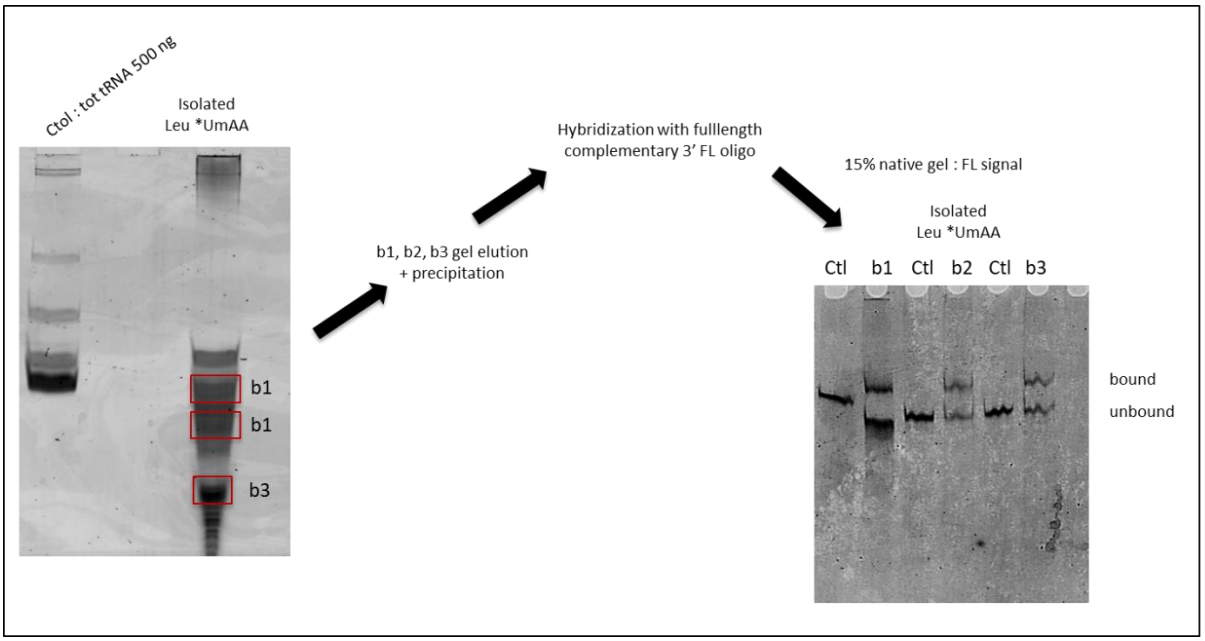

Figure 29 First individual isolated tRNA are degraded

Left part: Isolated $tRNA^{Leu}$ ($cmnm^5UmAA$) from a protocol where buffers contain $MgCl_2$ was loaded on a denaturing gel and signal was measured after gel red staining. Apart from the full-length RNA corresponding to the upper band, there are three other bands with a lower size

Right part: after gel excision, RNA elution and precipitation from the three bands, RNA are hybridized to a full-length oligonucleotide with fluorescein molecule in 3'-end. Potential duplexes are loaded on a native gel. b1, b2 and b3 hybridize to the oligonucleotide and leads to an upper shift (compared to control with oligonucleotides but without any RNA). These fragments are thus only degradation products from the targeted tRNA but don't come from contamination or DNA leakage.

Legends: FL Fluorescein/ Ctol Control

Since shorter fragments are degradation products of the same RNA this leads to a substantial loss of material. This degradation should be reduced or avoided as much as possible. Buffer used for tRNA hybridization and washing contains $MgCl_2$. Although many buffers used for RNA manipulations contain $MgCl_2$, it was demonstrated the Mg2+ ion enhances RNA degradation (366) especially at high temperature (like it is in hybridization, washing and elution steps). Thus, we decided to remove $MgCl_2$ from buffers to avoid tRNA degradation and increase the final yield.

Finally, after several other smaller optimizations such as the determination of the incubation time for tRNA hybridization, temperature and volumes during washing and elution, we obtained almost pure isolated tRNA (figure 30). Here all four tRNA isolated simultaneously from one total tRNA pool (1 mg) are presented. Indeed, it is possible to connect two HiTrap columns together. Moreover, the peristaltic pomp can hold several tubings. Here by pumping in parallel the same total tRNA pool through four HiTrap columns connected in parallel (2x2, figure 31), we isolated four specific tRNA.

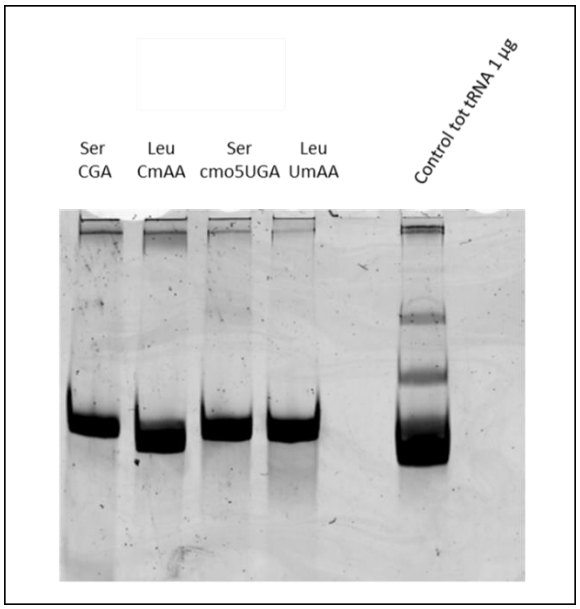

Figure 30 Profile of individual tRNA after final optimizations

From 1 mg of tot tRNA, all four tRNA were isolated in parallel and the whole sample was loaded on a denaturing gel and RNA was detected after gel red staining. The four profile show a specific band corresponding to each isolated tRNA and without RNA degradation.

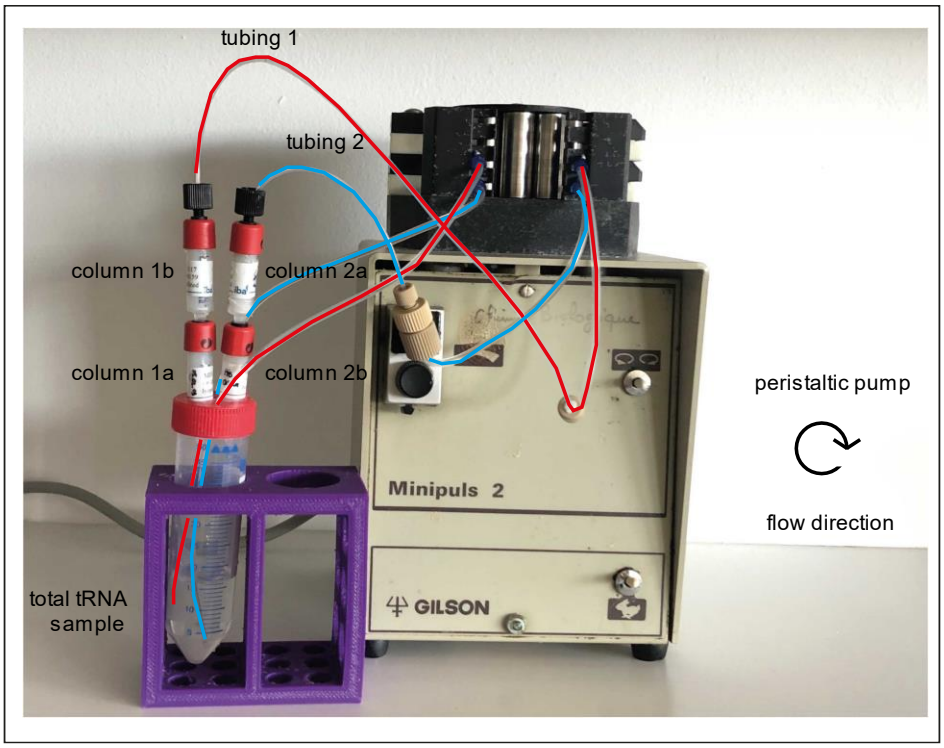

Figure 31 Set up for the parallel isolation of four individual tRNA

Two tubes 1 and 2 (red and blue respectively) are recirculating the same total tRNA sample via a peristaltic pump. For each tubing, two columns (a and b) can be connected.

For total tRNA under control conditions, the yield for the four tRNA is indicated in the table 7. Since there is an additional step of purification by gel and isolation is done in parallel, it is hard to compare these yields with the ones obtained with the biotin/streptavidin method.

Table 7 Individual tRNA yield in NH_2/NHS isolation method

tRNA	**Amount of individual tRNA isolated from 1 mg of total tRNA pool**
tRNA Leu cmnm5UmAA	400-500 ng
tRNA Ser cmo5UGA	250-350 ng
tRNA Leu CmAA	350-700 ng
tRNA Ser CGA	250-400 ng

To conclude on this technique, an important advantage is the possibility to re-use columns coupled with a specific DNA oligonucleotide for many repetitive isolation cycles and thus decreases considerably the cost compared to the streptavidin/biotin method, where new beads and biotinylated DNA oligo are used at every time. In addition, there is no DNA oligonucleotide leakage, no cross-contamination and we were able to isolate four (possible even more) tRNA at the same time. These are the reasons why we decided to use this individual tRNA isolation method for further LC-MS/MS experiment for validation of the RiboMethSeq data.

c. LC-MS/MS validation

With successful isolation of individual tRNA, we proceeded to the digestion of RNA into nucleosides and determined the level of specific 2'O-methylations. Six candidates already showing substantial differences in RiboMethSeq data were measured: $tRNA^{Ser}$ (CGA)-Gm18, $tRNA^{Leu}$ (cmnm^{5}UmAA)-Gm18, $tRNA^{Ser}$ (cmo^{5}UGA)-Gm18 and -Cm32 and $tRNA^{Leu}$ (CmAA)-Gm18 and -Cm34. The figure 32 shows the comparison between MethScores from RiboMethSeq and MS quantification data. Comparison of modification level between control and stress conditions is expressed as % of increase or decrease. For all Gm18 positions MS data validate the increased modification level observed by RiboMethSeq. A significant increase is visible for $tRNA^{Ser}$ (CGA)-Gm18, $tRNA^{Leu}$ (cmnm^{5}UmAA)-Gm18, $tRNA^{Ser}$ (cmo^{5}UGA)-Gm18. Concerning $tRNA^{Leu}$ (CmAA)-Gm18, for both RiboMethSeq and MS results, the effect was weaker but still quite consistent. Since the precision of RiboMethSeq (~5%) is better than for MS quantification (~10%), difference is not statistically significant, but the tendency stays the same. For the position 34 with $tRNA^{Leu}$ (CmAA)-Cm34, we were expecting a strong decrease of the modification level under chloramphenicol stress and a modest decrease for streptomycin. Similar profile is also observed for the MS data. Finally, for $tRNA^{Ser}$

(cmo^{5}UGA)-Cm32, the increase of the modification level was expected from RiboMethSeq data, but MS quantification does not show statistically significant changes. This may be due to the presence of another strong modification at position 34 in the same tRNA and variation of modification level at position 34 may affect RiboMethSeq quantification for position 32. Indeed, MethScore calculations take into account two neighbouring nucleotides, thus including the position 34. Moreover, this tRNA contains i^{6}A37 and this proximal nucleotide may affect 5'- and 3'-end coverage, thus altering MethScore for anticodon loop positions. In it noteworthy that tRNA^{Ser} (cmo^{5}UGA)-Cm32 was the only Nm32 position to be involved in stress response where all the others remained unaffected.

Thus, by LC-MS/MS quantification, we were able to validate the two behaviours observed in RiboMethSeq data, namely the global increase of Gm18 in several tRNA and the decrease of the modification level for position 34 under chloramphenicol and streptomycin stress.

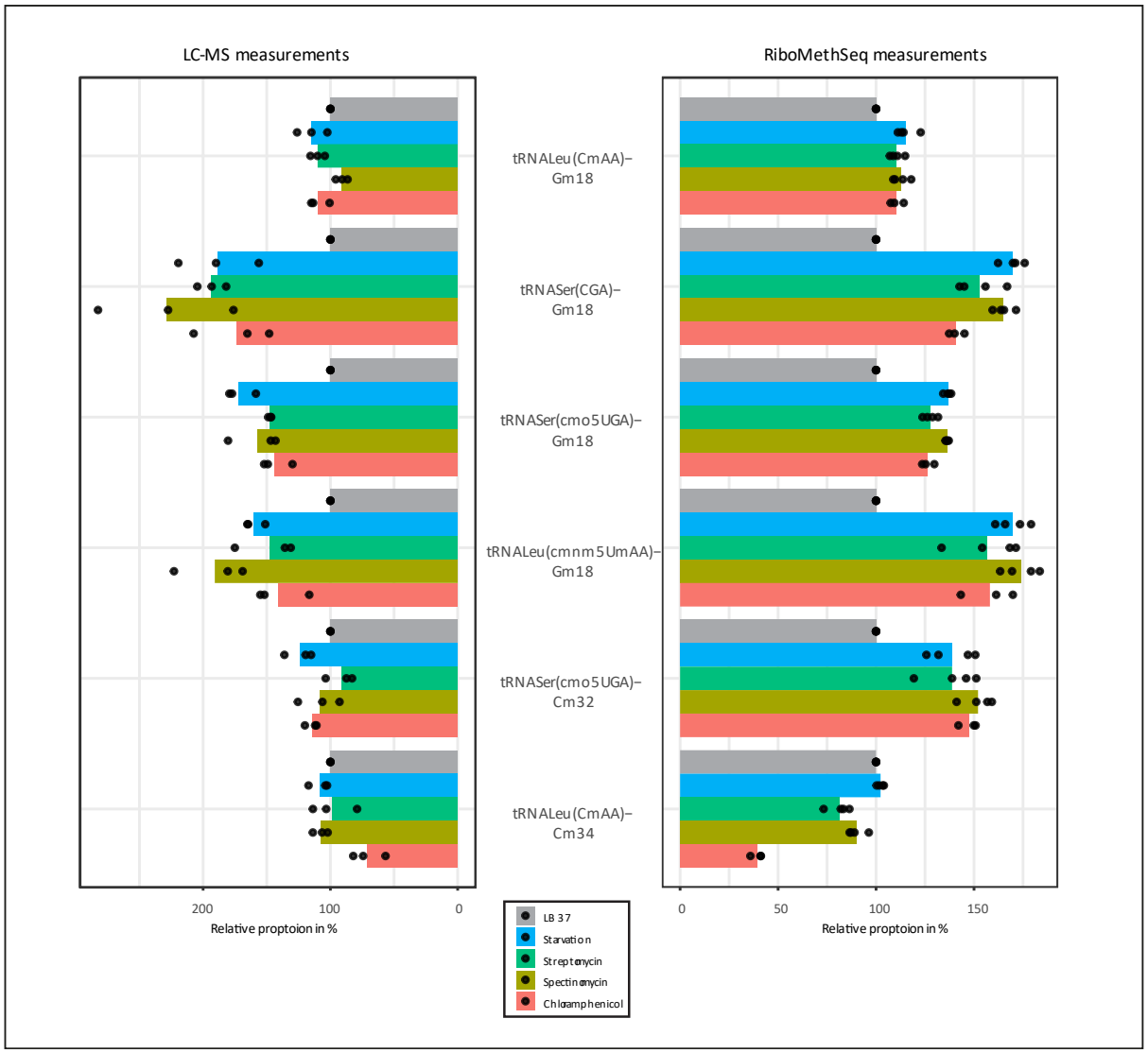

Figure 32 Comparison between RiboMethSeq and LC-MS measurements

The six studied individual tRNA are represented in relative quantification. Data for LC-MS and RiboMethSeq are presented in percentage of increasing or decreasing compared to the control at 100%. Each black dot corresponds to a biological replicate.

III. tRNA distribution

We studied the dynamics of tRNA 2'O-methylation under stress conditions and confirmed that tRNA modifications are involved in stress response. However, we were wondering if the observed increase or decrease correlates to the change in the tRNA proportion in the global tRNA pool. To answer this question, we also measured alterations of tRNA distribution upon stress.

a. Global tRNA sequencing data

tRNA distribution can be deduced directly from RiboMethSeq sequencing data, since all tRNA species are randomly fragmented, fragments are converted to libraries and sequenced. Thus, variation of the tRNA reads count correlates with changes in tRNA pool. However, due to highly biased amplification, the relative molar proportions of different tRNA cannot be defined essentially from these data.

We compared the number of reads for each tRNA in control and under stress conditions. In the figure 33, tRNA counts are first normalized to the total size of the library (tRNA aligned reads) and then to the average value for individual tRNA species. Globally, composition of the tRNA pool remains rather constant, except for $tRNA^{Ile}$ (k^2CAU), ^{Val} (GAC) and ^{Arg} (CCG) which seems to be increased under streptomycin stress. This may be related to their overexpression in response to stress, or by changes in tRNA modification profile, allowing better amplification during library preparation. However, none of these tRNA are known to carry a 2'O-methylation.

In conclusion, stress conditions have a stronger impact on tRNA 2'O-methylations, while only minor changes in tRNA distribution were observed. Moreover, modulation of global tRNA 2'-O-methylation observed for total *E. coli* tRNA by LC-MS/MS measurements, is explained by a change in the modification level in tRNA population and not to the change of the tRNA distribution. Additionally, some tRNA such as $tRNA^{Leu}$ (CmAA) and $tRNA^{Leu}$ ($cmnm^5UmAA$), carry modified nucleotides with an opposite behaviour under stress conditions. Our results show that there is little (if any) correlation between the changes in tRNA 2'-O-modification profile and alteration of tRNA distribution under stress conditions in bacteria.

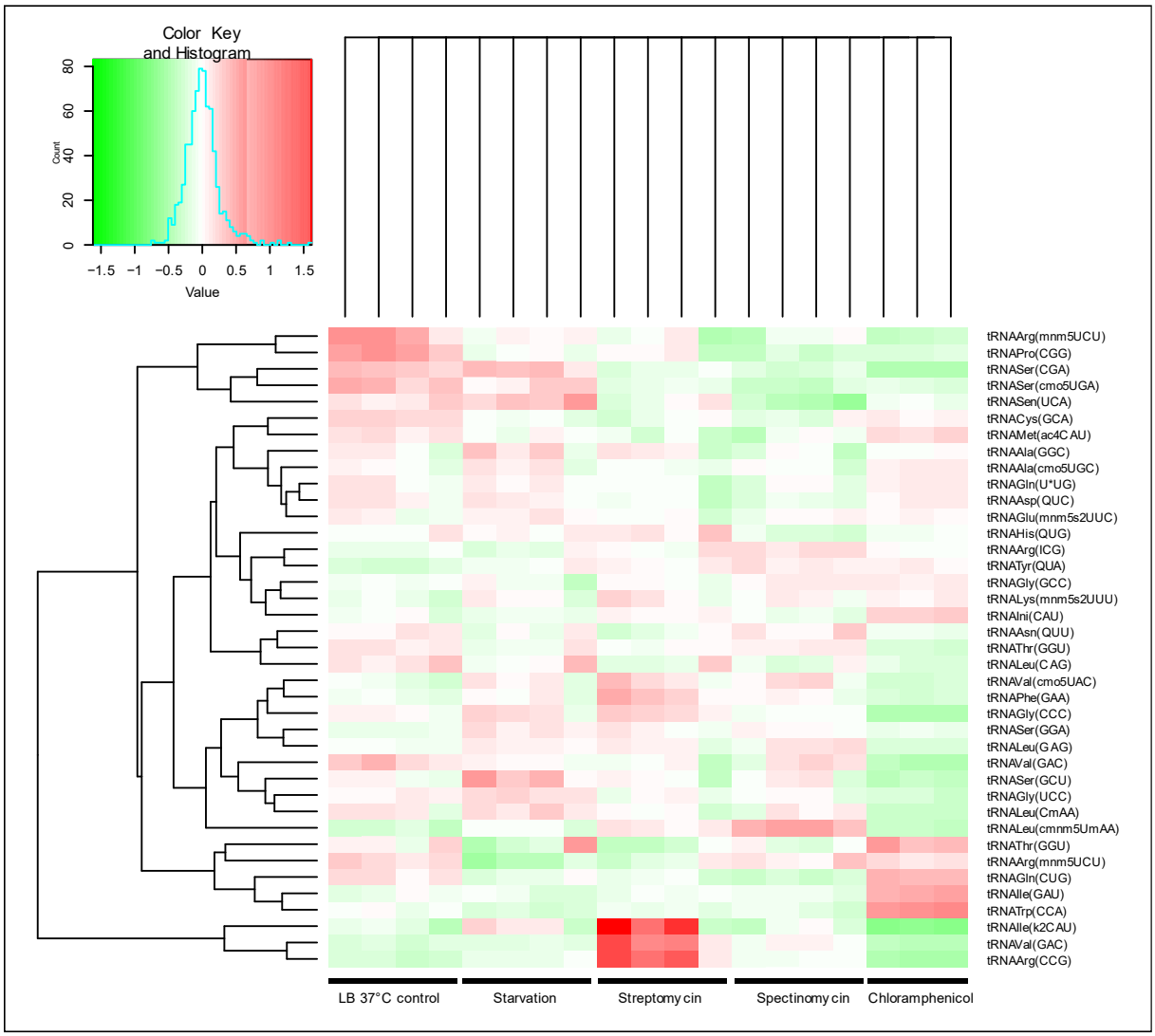

Figure 33 Changes of tRNA proportion under stress conditions

Raw tRNA count were first normalized on the total tRNA counts for each condition. A second normalization was done to obtain average deviation from the median. A value of one corresponds to 100% of increase compared to the average.

b. Analysis of tRNA distribution by microscale thermophoresis (MST)

Since analysis of tRNA composition by deep sequencing is known to be highly biased due to unequal amplification and ligation of different fragments (367), this method provides only some broad indications and relative quantification. Thus, the observed changes in tRNA pool compositions have to be validated by independent approach. For this validation we employed an alternative method that allows precise quantification for molar concentrations of tRNA species: microscale thermophoresis (MST). In typical MST experiment, individual tRNA present in total tRNA sample is hybridized with a full-length complementary DNA oligonucleotide labelled with fluorescein and placed in capillaries. Then an infra-red laser is used to generate a temperature gradient inside the capillaries. MST detects the fluorescence of

the probe and monitors its diffusion due to the temperature gradient (left part figure 34). RNA-DNA duplexes and unbound probes behave differently, either duplexes stay in the middle and free DNA oligo escapes from the spot heated by laser and go to the sides of the capillary, or *vice versa*. For quantification of the given individual tRNA, constant amount of labelled DNA probes are hybridized with an increasing amount of total tRNA. Then, normalized fluorescence signal is plotted against the concentration ligand and results in a sigmoidal curve (right part figure 34) where parameters such as the inflection point (EC_{50}) can be determined. This parameter corresponds to the concentration of total RNA required for 50% of hybridization. If the concentration of the DNA probe is known, the absolute amount of individual tRNA can be determined (see Material and Methods section for more details Chapter II, C, II, d: Thermophoresis experiment).

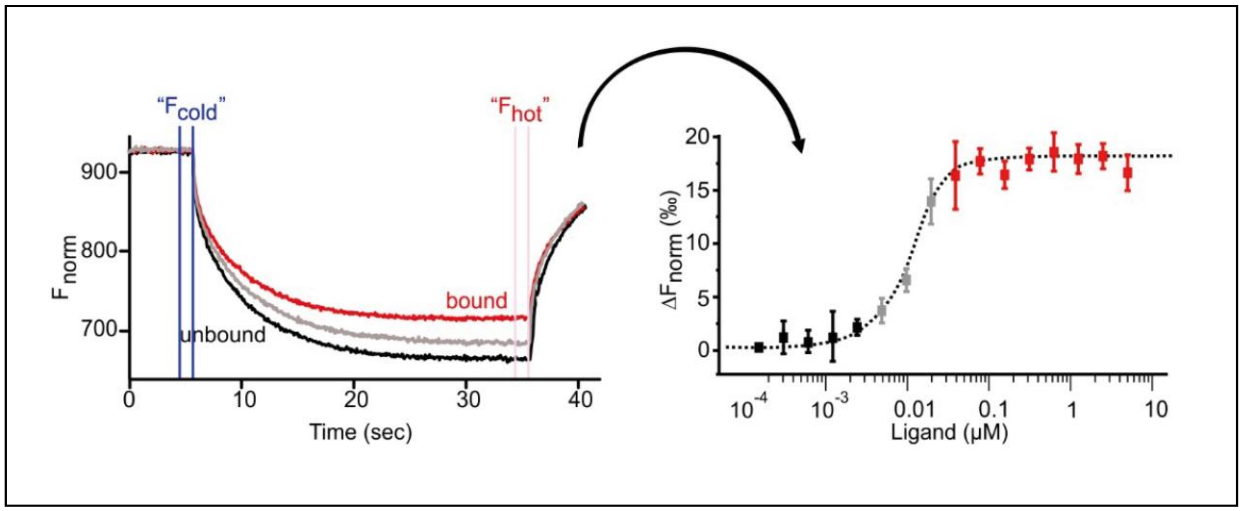

Adapted from Schubert and Längst, AIMS Biophysics. 2015 (368)

Figure 34 Microscale thermophoresis (MST) principle

16 capillaries contain a fluorescent DNA probe interacting with increasing amount of unlabelled ligand. The fluorescence is recorded over time with a gradient temperature performed in parallel via a laser. Three of the 16 traces are represented. Normalized fluorescence signals are plotted against the ligand concentration and give a sigmoidal curve on the left part of the graph. Then binding parameters such as EC_{50} can be calculated (black colour corresponds to unbound probe, grey to partially bound and red to fully bound probes).

1. Global tRNA distribution in *E. coli*

First, we compared two techniques, deep sequencing and MST to measure the global tRNA distribution in *E. coli* strain grown under normal conditions (LB 37°C). Culture, total tRNA isolation and MST experiments were performed by Christina Dal Malgro and Felix Green from Pr Helm's group, while I prepared sequencing libraries from the same samples, the NGS core facility UMS 2008 IBSLor performed sequencing and Pr Yuri Motorin extracted raw tRNA counts data for further analysis. The figure 35 represents the tRNA proportion (% of each

individual tRNA in the total tRNA pool) measured by deep sequencing and by MST. From the first glance, it is clear that correlation is very limited for MST data compared to deep sequencing. Some tRNA are under-represented while other are over-represented, which is expected results since the two methods are different. Moreover, similar results were described in Jacob et al, 2019 (367) for analysis of S. c*erevisiae* total tRNA fractions. There are several reasons for such discrepancies. First, library preparation certainly induces biases in measured tRNA distribution by differential amplification efficiency according to tRNA species (339,369,370). In other words, some tRNA species will be more amplified than other and thus lead to a bias in tRNA distribution. Secondly, modifications present in tRNA are susceptible to block the reverse transcription, limiting representation of these sequences in the sequencing data.

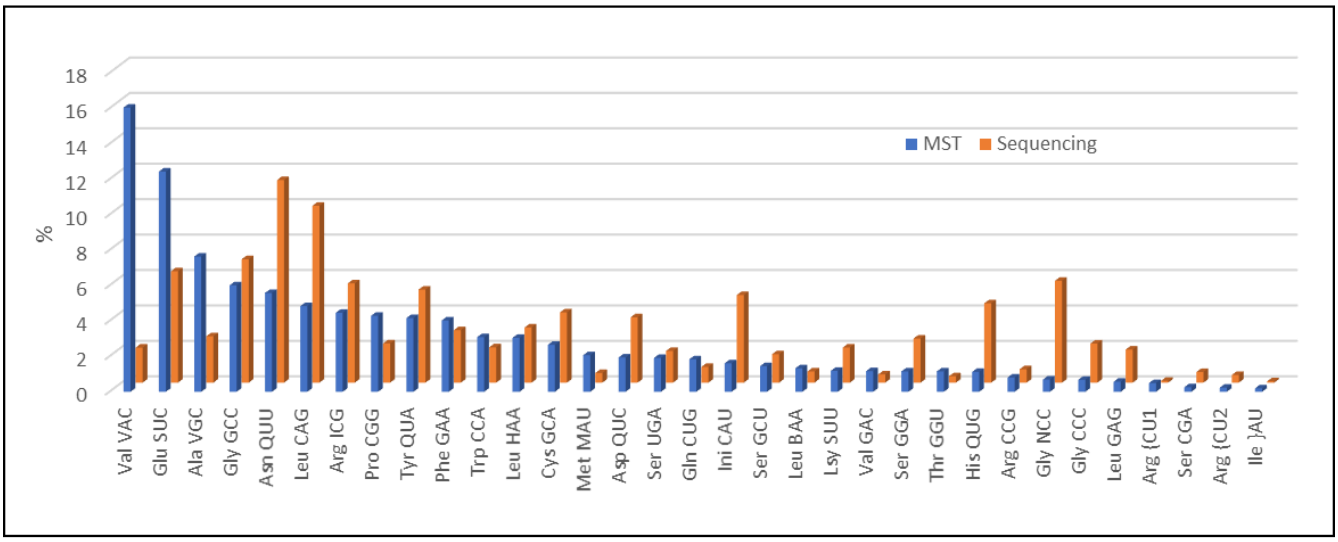

Figure 35 tRNA distribution in E. coli measured by deep sequencing and MST experiments

2. MST validation for tRNA distribution effect under stress conditions

Even if MST and deep sequencing give different results in tRNA quantification, sequencing data can still be used for relative tRNA content quantification under different conditions, since amplification biases are controlled and are the same in all samples for the same tRNA sequence. Therefore, MST can be used for validation of these data even if tRNA distribution is not strongly affected under stress conditions used in our project.

MST measurements were thus performed with the same four fluorescently labelled full-length complementary DNA probes used previously for tRNA isolation in the biotin/streptavidin

protocol. Since a substantial amount of total tRNA fraction are required for MST measurements, comparison was done only for conditions of spectinomycin stress.

First of all, tRNAs showing modulation of their 2'O-methylation level in response to growth stress are not well represented in the total *E. coli* tRNA. While some tRNA can represent until 15% of the pool, these tRNA are only present at 0.22% - 2% under control conditions (table 8). In stress conditions we observe an increase of at least two-fold for $tRNA^{Leu}$ ($cmnm^5UmAA$) and a decrease of ~50% for $tRNA^{Ser}$ (cmo^5UGA) and $tRNA^{Ser}$ (CGA). No change was observed for $tRNA^{Leu}$ (CmAA). Fold change and even absolute level of expression between deep sequencing data and MST experiment are relatively similar. This validates the relative quantification of tRNA in deep sequencing experiment and changes observed under stress conditions.

Table 8 tRNA distribution in Sequencing and MST experiment for four given tRNA

Experiment were performed with three biological triplicates, the average is represented here. The same samples were used for both sequencing and MST experiment.

tRNA	Sequencing			MST		
	control	spectinomycin	Fold change	control	spectinomycin	Fold change
	tRNA %			tRNA %		
Leu $cmnm^5UmAA$	1.9	4.6	2.42	2.05	4.23	2.06
Ser cmo^5UGA	1.9	1.1	0.58	1.63	0.74	0.45
Leu CmAA	0.98	1.1	1.12	0.61	0.69	1.13
Ser CGA	0.22	0.15	0.68	0.42	0.25	0.59

IV. Discussion conclusion

In this project we discovered dynamic *E. coli* tRNA 2'O-methylation as a response to stress growth conditions. Two major behaviour were observed. Half of tRNA Gm18 sites increase in starvation, streptomycin, spectinomycin and chloramphenicol stress conditions, while all 2'O-methylated in the position 34 are decreasing in chloramphenicol and streptomycin stress.

The observed increase of tRNA 2'-O-methylation may be explained either by increased expression of the corresponding RNA: modification enzyme or by the increased "contact" time between the substrate tRNA and enzyme under slow growth conditions. Indeed, in all cases increased tRNA Gm18 methylation was observed in slowly growing cells (starvation, antibiotic stress). However, low growth temperature (20°C) and/or poor medium (M9) do not lead to increased tRNA modification. Thus, the effect is probably related to the increased expression of the corresponding RNA: modification enzyme. Unfortunately, antibodies against bacterial

TrmH, TrmJ or TrmL are not available, so this hypothesis cannot be easily verified by simple Western blotting. Nevertheless, one can envisage to measure levels of mRNAs encoding TrmH, TrmJ and TrmL by RT-qPCR.

In contrast, the decrease of tRNA modification steady-state level can be only explained by accelerated turnover of modified tRNA under stress and their replacement by newly synthetized and poorly modified counterparts.

We observed that different locations of 2'O-methylation in tRNA seem to be modulated by different stress and may be involved in different cell regulation mechanisms. It has been demonstrated that dynamic regulation of tRNA modification at the wobble base (position 34) is involved in the regulation of gene expression. The so-called modification tunable transcripts (MoTTs) may change the codon usage and modulate the efficiency of mRNA decoding. This would lead to a stress reprogramming system leading to the production of proteins required for the stress response. In fact, the mRNA codon usage is not random and depending on the expressed gene, only a subset of synonymous codons may be enriched compared to others. So MoTTs are able to stimulate translation only of certain transcripts which are enriched for specific codons. This will increase translational fidelity, but also allow a faster translation for some codons leading to the production of particular proteins in response to stress. Modifications known to be involved in such regulation are mostly m^5C and mcm^5U residues and the majority of studies was done for eukaryotic species (*S. cerevisiae*) (292,329,330). Nevertheless, no evidences were provided for the same function of ribose. One can imagine that *E. coli* Nm34 have the same function that are already described for MoTTs. It would be of interest to perform ribosome profiling combined to proteomic analysis for our samples in order to identify codon bias in transcripts when they are translated as well as upregulated proteins.

In most of Gram-negative bacteria RNA modification found at the position 18 in D-loop, is exclusively a Gm. It is likely that the primary function for this modification is not stress-related

response, but it can escape from the innate immune system during a host invasion. Indeed, it is now well established that RNA 2'-O-methylations act as immunosuppressors.

In the field of innate immunity, Toll-like receptors (TLR) play a crucial role. They recognize microbial associated molecular patterns (MAMP) and thus activate immune cells. TLR3, 7, 8, 9 and 13 (mouse specific) are known to be activated by different nucleic acids DNA and RNA. Indeed, TLR3 is specific for double stranded RNA, mouse TLR13 for bacterial 23S rRNA and TLR 9 for unmethylated CpG-DNA. Moreover, TLR7 and TLR8 are activated by single stranded RNA of bacterial origin. In humans, TLR7 is expressed only in plasmacytoid dendritic and B cells and induces the production of type I interferon such as IFN-α, whereas TLR8 is found in monocytes, myeloid dendritic cells and regulatory T cells and its activation leads the production of cytokines (371). The innate immune system is able to make a difference between "self" and "non-self" RNA molecules due to specific RNA modifications, spatial restrictions and sequence positions in nucleic acids. Concerning 2'O-methylation, *in vitro* studies showed that their incorporation in *in vitro* RNA transcripts, siRNA or 18S rRNA prevents TLR activation (371,372). In fact, in native RNA, it was demonstrated that Gm18 in bacterial *E. coli* tRNA is responsible for escape from the immune response and that bacterial $tRNA^{Tyr}$ seems to play a major role (267,268). The molecular mechanism of immunosupression is still poorly understood. 2'-O-methylated tRNA is a TLR7 antagonist (373) with a recognition pattern of two nucleotides including Gm18 and its downstream neighbouring nucleotide (374). In addition, it was shown that 2'-O-methylation acts as an inhibitor for TLR7, but not for TLR8 (371). However, other bacterial species that lack Gm18, such as Gram-positive strains (e.g. *S. aureus*) also inhibit TLR7 response. This shows that 2'-O-methylations at other positions in tRNA or rRNA may also have immunosuppression properties (268).

Thus, in perspective of this work, we started a collaboration with Pr. Alexander Dalpke now located at the Institute of Medical Microbiology and Hygiene in Dresden. We were wondering if the increase of Gm18 content during starvation and antibiotic stress response is able to modulate the innate immune system. We hypothesized that stress conditions used in our study may somehow mimic the environment during host invasion (starvation or antibiotics conditions). Under these conditions, the increased Gm18 level could help bacteria to reduce the host immune response during invasion and thus increase the infectivity/pathogenicity.

In order to evaluate immunostimulation properties of total tRNA samples extracted from control and stress condition (chloramphenicol stress was used here) were sent to Pr. A. Dalpke lab for

interferon alpha (IFN-α) production assay with peripheral blood mononuclear cells (PBMC). Unfortunately, the amount of tRNA required for these tests is quite substantial (several µg) and does not allow measurements of immunostimulation properties of individual isolated tRNA. If first data on total tRNA reveal interesting results, additional experiments with scaled-up cultures can be performed in order to get enough tRNA species for measurements.

In our project, we were using *E. coli* DH5α strain commonly used in laboratories for fundamental research. Thanks to the collaboration with Pr. A. Dalpke, we will have the opportunity to analyse also clinical *E. coli* isolates coming from patients. It would be important to perform the same stress experiment pipeline (control, starvation, antibiotics conditions) on these strains in order to know if the same behaviour is also observed for bacteria that already were involved in host invasion. Collection of these clinical isolates disposes strains without any resistance, but also gentamycin resistant strains. Gentamycin is another antibiotic from aminoglycoside group, it binds to 16S rRNA and large sub-unit of the ribosome and interferes with the initiation complex leading to misreading of mRNA (decreases the translation fidelity). Since gentamycin was not initially included in our study design, we first checked if such stress gives the same alterations of the tRNA modification profile. The figure 36 represents the heatmap for MethScores in duplicate of control conditions and duplicate under gentamycin stress. We observed a profile which is similar to previous data obtained for streptomycin stress, namely the increased level of four Gm18 and one Cm32 (position excluded due to bias in RiboMethSeq quantification): $tRNA^{Ser}$ (cmo^5UGA)-Cm32, $tRNA^{Ser}$ (CGA)-Gm18, $tRNA^{Leu}$ ($cmnm^5UmAA$)-Gm18, tRNA Ser (cmo^5UGA)-Gm18, tRNA Gln (CUG)-Gm18. Only for $tRNA^{Leu}$ (CmAA)-Gm18, we don't see a difference, but it was the one with the lowest change in our previous experiments too. For, $tRNA^{Leu}$ ($cmnm^5UmAA$)-Um34 and $tRNA^{Leu}$ (CmAA)-Cm34, there is a slight decrease such as it was observed under streptomycin condition. So, the use of gentamycin stress can be further pursued in collaboration with Pr. A. Dalpke.

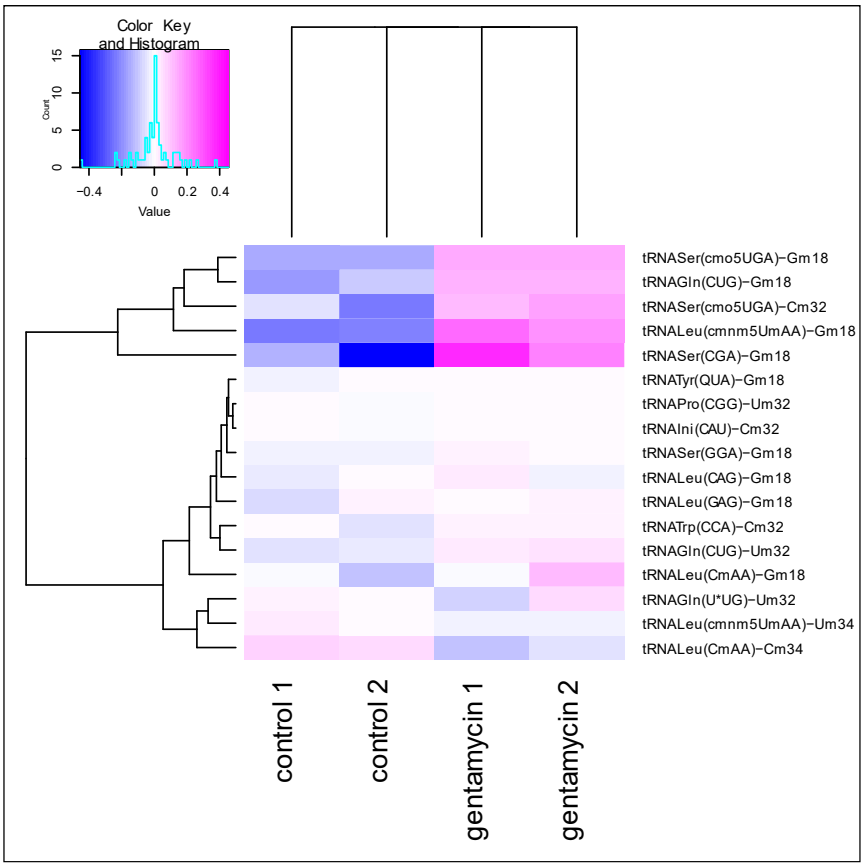

Figure 36 Heatmap for the level of 2'O-methylation in control and gentamycin stress condition

Gentamycin stress was done with the same pipeline as other stress conditions. Concentration was determined by a growth curve in different antibiotics conditions. A concentration of 5µg/ mL was leading to 90% reduction of the growth late, so we used it for gentamycin stress.

In Summary for this chapter, *E. coli* 2'O-methylations are involved in stress response and could play a role either as MoTTs or to reduce innate immune system response to bacterial tRNA. This creates a lot of new possibilities for 2'O-methylations and contributes to the better understanding of complex post-transcriptionally regulation systems.

General discussion

During the three years of my PhD thesis, I had the opportunity to work on diverse projects related to applications of high-throughput sequencing. In particular, the two chapters described in this manuscript show how this technology can be used for different RNA studies. First, I investigated the composition of exRNA population present in human plasma. Here, the goal was to use non-biased technology without the need to guess RNA target, like microarrays or RT-PCR. Using deep sequencing, I was able to determine the global composition of RNA in the whole plasma and in its sub-populations. Secondly, I used deep sequencing in order to measure the level of post-transcriptional modifications in *E. coli* tRNA species. In this case, the goal was not to sequence RNA species, but rather use deep sequencing as a tool, in order to detect and quantify specific RNA modifications, namely 2'O-methylations. I was able to demonstrate how Gm18 in *E. coli* tRNA is important for bacterial stress response.

These two projects show that high-throughput sequencing is a powerful and efficient technology that can be applied for a large subset of purposes. Nevertheless, it is crucial to always pay attention on the experimental biases that go hand in hand with this technology. This is why, in both projects I used a rigorous methodology. In exRNA project, I carefully designed the study in order to avoid as much as possible technical and bioinformatical errors. I spend a lot of time to determine what were the best methods for exRNA isolation and study. However, we had to be aware of the non-visible biases that could interfere in our data. Concerning the second project, I used other complementary techniques (LC-MS/MS, MST) in order to validate our data obtained by deep sequencing. Altogether, I was able to measure the importance of high-throughput sequencing in molecular biology research and especially in the complex and diverse RNA field.

When we talk about extracellular RNA of non-human origin or bacterial tRNA modifications that play a role in host immunomodulation properties, we instinctively think of infectious diseases and pathogenicity. There are three major strategies employed by bacteria, viruses and parasites to fight against either the innate or the acquired immune system (well reviewed in Finlay et McFadden, *Cell*. 2006 (375)).

The first strategy is to hide from recognition by the immune system. Viruses and bacteria can use a camouflage by dysplaing host-derived proteins on their surface/envelop (pretend they are elements of the host) or by producing carbohydrate capsules (to hide their bacterial antigens) respectively. Pathogens also use antigenic variation to fool the acquired immune system: by

modifying their surface antigens, pathogens can re-infect the host without activating the acquired immune cells that don't recognize them. Another way to escape from the innate immune system is to attenuate/inhibit the immune response by preventing the production of cytokines. From this standpoint, microorganisms can attenuate/inhibit TLR activation. As already described in the discussion section of the chapter II of this PhD thesis manuscript, TLR recognize PAMP (pathogens-associated molecular patterns) and therefore generate a cascade of activations leading to the production of NF-KB, interferons and other inflammatory factors and to the release of cytokines outside the cell. Thus, pathogens are able to play with TLR recognition pattern and modulate PAMP. If TLR activation is prevented, therefore downstream pathways leading to the production of cytokines are inhibited. Secondly, microorganisms can directly act and attack/weaken the host immune cells. They are able to secrete virulence molecules with different functions. These immune modulators can paralyse phagocytose phenomenon, avoid phagolysosomal fusion, dysregulate natural killer cells or mediate the production of reactive oxygen species and nitric oxide components. They obviously include a multitude of toxins that directly kill host cells.

Finally, the last strategy is to manipulate the host systems in order to spread themselves in the organism. Pathogens secrete immune modulators that mediate bacterial uptake or reprogram vesicular trafficking to enhance intracellular parasitism. They are also able to manipulate apoptosis, by suppressing apoptotic death of host cells, preferring cytotoxic death and thus neutralizing a variety of host cells.

Both projects I've conducted during my phD thesis enter exactly in this domain of research and contribute to understand strategies employed by bacteria to invade their host. On one side, I've demonstrated that under conditions, partially mimicking infection/treatment for bacterial invasion, bacterial tRNA modification gains higher relative proportion of immunosuppressive Gm18 residues. The consequence is a global decrease of immunostimulation capacity of bacterial RNA and even if RNA contributes only moderately to global immunostimulation by living bacteria (376–379), RNA (and particularly tRNA) are particularly stable in acidic endosomal environment, and such reduced TLR7-driven immunostimulation may contribute to attenuated immune response and thus facilitate establishment of bacterial infection.

On the other side, EV and exosomes in particular, are clearly involved in infection diseases. Indeed, we and others showed that EV contain microbiota's molecular elements (nucleic acids, proteins) (223) but some pathogens like bacteria and viruses (as already described in the

discussion section of the chapter I) use EV to better invade their host. In fact, they play a role in each of the three major strategies described below: hide, attack and/or manipulate. Pathogens enter the cell via the endosomal pathway and affect composition of nacent exosomes by modifying their composition with foreign nucleic acids or proteins. Some are also able to introduce themselves entirely in exosomes. As described above, pathogens need to hide from the immune system and can do it by three different ways. They can be protected inside exosomes and thus they don't trigger the immune system, exosomes can modify pathogen-related substances or exosomes can suppress immune molecules. As examples, hepatitis C and genome of hepatitis A viruses stay in multivesicular body, they are secreted into exosomes and can then infect specific targets (224,228,229). Here, Alix and VPS4b exosomal proteins are involved (380). Moreover, RNA from hepatitis E are found in exosomal fractions into infectious particles without triggering antibodies. To escape their surveillance, particles have to be modified but the specific mechanism is still unknown (381). Interestingly, in Epstein-Barr virus infection, pathogens escape the immune system by sequestering immune effectors like caspase 1 and interleukines into exosomes (382). Finnally, pathogens can then manipulate the EV system to regulate the functions of recipient cells in order induce pathological consequences. For instance, exosomes infected by *S. aureus* contain bacterial pore forming the α-toxin, exosomes will deliver these virulence factors to distant cells in order to kill them (383). Moreover, some viruses, spread viral protein RNA and even miRNA by exosome uptake system in recipient cells in order to regulate their functions such as promoting the apoptosis of cells in interaction with T- and monocytes cells (384,385).

Thus, both projects I've carried out during my PhD thesis enrol completely in the field of infection disease and immunity. In the world where bacteria are more and more resistant to classical antibiotics treatments, the need to develop alternative antimicrobial therapies is critical. This is why, continue to study how pathogens are able to infect their host without triggering the innate or acquired system is very important. We could better understand how they work and determine their weaknesses. This knowledge is essential for potential implementation of new preventive and therapeutic strategies.

Material and Methods

All material and methods concerning exRNA project is described in Galvanin et al, 2019, *Biochimie (*Annexe 1*)* (208). For the second project, total tRNA isolation procedure, library preparation, sequencing and bioinformatics procedure are described in the article Galvanin et al, 2019, *Methods in Molecular Biology* (Annexe 2) (364).

I. Material :

a. Chemicals, reagents, enzymes and ready-to-use buffers

The principal chemical, enzymes and ready-to-use buffers are described in the following table 9.

Table 9 Chemicals, reagents, enzymes and ready-to-use buffers

Product	Manufacturer
10 X TBE buffer	Carl Roth
Acetonitrile	Honeywell
Benzonase® Nuclease	Sigma
Chloramphenicol	Euromedex
Fast AP	Thermo Fisher Scientific
Gel buffer concentrate	Carl Roth
Gel concentrate	Carl Roth
Gel diluent	Carl Roth
Gentamycin	Sigma
InSolution Tetrahydro uridine (THU)	Merck
N,N,N,N'-Tetramethyl ethylenediamine (TEMED)	Carl Roth
Nuclease P1	Sigma
Pentostatine >95%	Sigma
Snake Venom Phosphodiesterase	Worthington Biochemical Corporation
Spectinomycin	Sigma
Streptomycin	Sigma

b. Buffers and mediums

The made buffers and medium used are described in the following table 10

Table 10 Buffers and medium

Product	Composition
1X B&W buffer	5 mM Tris-HCl (pH 7,5), 0.5 mM EDTA, 1 M NaCl
1X PAGE	Na 2 HPO4*12H 2 O 8.1 mM; KH 2 PO4 1.47 mM, NaCl 137 mM; KCl 2.7 mM; pH 7.2-7.4
20X SSC	3M NaCl, 300 mM trisodiumcitrate (pH 7,0)
APS	10% APS (m/v) in Milli-Q water
Buffer A/ blocking buffer	ethanolamine 0.5 M, NaCl 0.5 M, pH 8.3
Buffer B/ wash buffer	0.1 M sodium acetate, 0.5 M NaCl, pH 4 with acetic acid
Chloramphenicol	stock solution 10 mg/mL in ethanol
Gel Elution buffer	NH4oAc 0.5M pH 5.3
Gentamycin	stock solution 10 mg/mL in water
LB medium	Tryptone 10 g/L, Yeast extract 5 g/L, NaCl 10 g/L
Loading dye	90% (v/v) formamide in 1X TBE
M9 medium	Na2HPO4 33.7mM, KH2PO4 22.0 mM, NaCl 8.55 mM, NH4Cl 9.35 mM, glucose 0.4%, MgSO4 1mM, CaCl2 2.3 mM, thiamine 1 µg/mL, FeCl3 1mM, MnCl2 1mM, ZnSO4 1mM, CoCl2 0.2 mM, CuCl2 0.2 mM, NuCl2 0.2 mM, Na2Mo 0.2 mM, Na2Mo 0.2 mM, Na2Se 0.2 mM, H3BO3 0.2 mM
Oligonucleotide Coupling buffer	0.2 M NaHCO3, 0.5 M NaCl pH 8.3
Spectinomycin	stock solution 10 mg/mL in water
Storage buffer/phosphate buffer	50 mM Na2HPO4 pH 7.1, NaN3 0,1%
Streptomycin	stock solution 10 mg/mL in water
tRNA binding buffer	1.2 M NaCl, 30mM Hepes KOH pH 7.4
tRNA elution buffer	1 mM EDTA, 1 mM HEPES
wash buffer	10 mM HEPES, 100 mM NaCl

c. Oligonucleotides

Table 11 Oligonucleotides used for individual tRNA isolation and relative quantifications by MST experiment

Project	Targeted tRNA	Position of interest	Modifications	Length	Sequence
Biotin/ Streptavidin and MST	Leu cmnm^{5}UmAA	Gm18	5' biotin 3' fluorescein	90 nt	AAATGGTACCCGGAGCGGGACTTGAACCCGCACAG CGCGAACGCCGAGGGATTTTAAATCCCTTGTGTCTA CCGATTCCACCATCCGGGC
	Ser cmo^{5}UGA	Gm18 Cm32		91 nt	AAATGGCGGAAGCGCAGAGATTCGAACTCTGGAAC CCTTTCGGGTCGCCGGTTTTCAAGACCGGTGCCTTC AACCGCTCGGCCACACTTCC
	Leu CmAA	Gm18 Cm34		88 nt	AAATGGTGCCGAAGGCCGGACTCGAACCGGCACGT ATTTCTACGGTTGATTTTGAATCAACTGTGTCTACC GATTTCGCCACTTCGGC
	Ser CGA	Gm18		93 nt	AAATGGCGGAGAGAGGGGGATTTGAACCCCCGGTA GAGTTGCCCCTACTCCGGTTTTCGAGACCGGTCCGT TCAGCCGCTCCGGCATCTCTCC
NH_2 NHS	Leu cmnm^{5}UmAA	Gm18	5' hexyl linked primary amine	40 nt	TGGTACCCGGAGCGGGACTTGAACCCGCACAGCGC GAACG
	Ser cmo^{5}UGA	Gm18 Cm32			TGGCGGAAGCGCAGAGATTCGAACTCTGGAACCCT TTCGG
	Leu CmAA	Gm18 Cm34			TGGTGCCGAAGGCCGGACTCGAACCGGCACGTATT TCTAC
	Ser CGA	Gm18			TGGCGGAGAGAGGGGGATTTGAACCCCCGGTAGAG TTGCC

Table 12 Oligonucleotides used for global tRNA distributin determination by MST experiments

Amino acid	Anticodon	Sequence
Cys	GCA	AAA TGG TGG TGG GGG AAG GAT TCG AAC CTT CGA AGT CGA TGA CGG CAG ATT TAC AGT CTG CTC CCT TTG GCC GCT CGG GAA CCC CAC C
Leu	)AA	AAA TGG AGC GGG CGA AGG GAA TCG AAC CCT CGT ATA GAG CTT GGG AAG CTC TCG TTC TAC CAT TGA ACT ACG CCC GC
Phe	GAA	AAA TGG TTG CGG GGG CCG GAT TTG AAC CGA CGA TCT TCG GGT TAT GAG CCC GAC GAG CTA CCA GGC TGC TCC ACC CCG CG
Ser	UGA	AAA TGG TGG GTC GTG CAG GAT TCG AAC CTG CGA CCA ATT GAT TAA AAG TCA ACT GCT CTA CCA ACT GAG CTA ACG ACC C
Trp	CCA	AAA TGG CGG TGA GGC GGG GAT TCG AAC CCC GGA TGC AGC TTT TGA CCG CAT ACT CCC TTA GCA GGG GAG CGC CTT CAG CCT CTC GGC CAC CTC ACC
Tyr	QUA	AAA TGG TGC TGA TAG GCA GAT TCG AAC TGC CGA CCT CAC CCT TAC CAA GGG TGC GCT CTA CCA ACT GAG CTA TAT CAG C
Ala	VGC	AAA T GGT GGG TGA TGA CGG GAT CGA ACC GCC GAC CCC CTC CTT GTA AGG GAG GTG CTC TCC CAG CTG AGC TAA TCA CCC
Arg	ICG	AAA TGG CGG AGA GAG GGG GAT TTG AAC CCC CGG TAG AGT TGC CCC TAC TCC GGT TTT CGA GAC CGG TCC GTT CAG CCG CTC CGG CAT CTC TCC
Arg	CCG	AAA TGG AGG CGC GTT CCG GAG TCG AAC CGG ACT AGA CGG ATT TGC AAT CCG CTA CAT AAC CGC TTT GTT AAC GCG CC
Arg	{CU1	AAA TGG TAC CCG GAG CGG GAC TTG AAC CCG CAC AGC GCG AAC GCC GAG GGA TTT TAA ATC CCT TGT GTC TAC CGA TTC CAC CAT CCG GGC
Arg	{CU2	AAA TGG TGC CCG GAC TCG GAA TCG AAC CAA GGA CAC GGG GAT TTT CAA TCC CCT GCT CTA CCG ACT GAG CTA TCC GGG C
Asn	QUU	AAA TGG CGG AAG CGC AGA GAT TCG AAC TCT GGA ACC CTT TCG GGT CGC CGG TTT TCA AGA CCG GTG CCT TCA ACC GCT CGG CCA CAC TTC C

Asp	QUC	AAA TGG CAG GGG CGG AGA GAC TCG AAC TCC CAA CAC CCG GTT TTG GAG ACC GGT GCT CTA CCA ATT GAA CTA CGC CCC T
Gln	CUG	AAA TGG TGG AGC TAT GCG GGA TCG AAC CGC AGA CCT CCT GCG TGC AAA GCA GGC GCT CTC CCA GCT GAG CTA TAG CCC C
Glu	SUC	AAA TGG TGC ATC CGG GAG GAT TCG AAC CTC CGA CCG CTC GGT TCG TAG CCG AGT ACT CTA TCC AGC TGA GCT ACG GAT GC
Gly	CCC	AAA TGG CGC GCC CGA CAG GAT TCG AAC CTG AGA CCT CTG CCT CCG GAG GGC AGC GCT CTA TCC AGC TGA GCT ACG GGC GC
Gly	GCC	AAA TGG CGC GCC CTG CAG GAT TCG AAC CTG CGG CCC ACG ACT TAG AAG GTC GTT GCT CTA TCC AAC TGA GCT AAG GGC GC
Gly	{CC	AAA TGG TGT CCC CTG CAG GAA TCG AAC CTG CAA TTA GCC CTT AGA AGG GGC TCG TTA TAT CCA TTT AAC TAA GAG GAC
His	QUG	AAA TGG CTC CTC TGA CTG GAC TCG AAC CAG TGA CAT ACG GAT TAA CAG TCC GCC GTT CTA CCG ACT GAA CTA CAG AGG A
Ile	GAU	AAA TGG CGG AAC GGA CGG GAC TCG AAC CCG CGA CCC CCT GCG TGA CAG GCA GGT ATT CTA ACC GAC TGA ACT ACC GCT CC
Ile	}AU	AAA TGG CTG GGG TAC GAG GAT TCG AAC CTC GGA ATG CCG GAA TCA GAA TCC GGT GCC TTA CCG CTT GGC GAT ACC CCA
Ini	CAU	AAA TGG CGT CCC CTA GGG GAT TCG AAC CCC TGT TAC CGC CGT GAA AGG GCG GTG TCC TGG GCC TCT AGA CGA AGG GGA C
Leu	BAA	AAA TGG AGC GGG AAA CGA GAC TCG AAC TCG CGA CCC CGA CCT TGG CAA GGT CGT GCT CTA CCA ACT GAG CTA TTC CCG C
Leu	CAG	AAA TGG AGC GGG CAG CGG GAA TCG AAC CCG CAT CAT CAG CTT GGA AGG CTG AGG TAA TAG CCA TTA TAC GAT GCC CGC

II. Methods:

a. *E. coli* growth: control and stress conditions

For all *E. coli* culture, DH5α was used. A first preculture from a glycerol stock was performed in 10 mL LB overnight at 37°C and at 190 rpm. Then, a second precultured was seeded at 0.05 OD_{600nm} and cultured until 1-2 OD_{600nm}. This is this second preculture that was used for the seeding of control and stress conditions in each batch of experiment.

- Control condition: from the second preculture, *E. coli* is seeded between 0.01-0.05 OD_{600nm} and grown for few hours in LB medium, 37°C, 190 rpm until 0.8-1.2 OD_{600nm}. For growth curves, cells were cultures until the stationary phase and OD_{600nm} was monitored several times.
- Temperature conditions: the same culture parameters than the condition one are used except bacteria were cultured at either 42°C or 20°C.
- Minimal medium condition: the same culture parameters than the condition one are used except bacteria were cultured in minimal medium M9.
- Hypoxia like condition

- protocol A: bacteria were grown in a closed glass bottle instead of an Erlenmeyer in LB medium (the bottle was not full of medium) at 37°C or 20°C, at 190 rpm.
- protocol B: bacteria were grown in 50 mL Falcon tubes full of LB medium and incubated without shaking at either 37°C or 20°C.

For both conditions, cells were harvest when the medium is trouble and corresponds to the expected OD_{600nm}. It is not possible to put back again the culture once we opened it to determine its OD_{600nm}.

- Starvation: Bacteria were grown as the control condition. When the culture reached the expected OD_{600nm}. Cells are harvest in 50 mL Falcon tubes for 5 min at 3,500xg and washed with 5 mL of 1X PBS. After another centrifuge step of 5 min at 3500xg. Pellet is resuspended in the same amount of initial LB medium and incubated for 24h at 37°C, 190 rpm.
- Antibiotics conditions

Antibiotics were prepared from dried powder and resuspend in a final concentration of 1mg/mL in milliQ water for all of them except chloramphenicol that was resuspended in Ethanol. Antibiotics solutions were filtered at 0.22 µm for further sterile use. In sterile condition, solution were aliquoted in 1.5 mL Eppendorf tubes and stocked at -20°C. For the determination of antibiotic concentrations, bacteria were grown with several antibiotic concentrations, the OD_{600nm} was monitored during one day.

- Protocol A: bacteria were seeded between 0.01-0.05 µg/mL in LB medium containing a determined concentration of antibiotics leading to a growth delay of around 30% (1.5 µg/mL for streptomycin and 2.5µg/mL for spectinomycin). Cultures were harvest between 0.8-1.2 OD_{600nm}.
- Protocol B: bacteria were grown as the control condition. When the culture reached the expected OD_{600nm}, antibiotics were added to the medium in the determined final concentration (5 µg/mL for streptomycin, 10 µg/mL for spectinomycin, 5 µg/mL for chloramphenicol and 5 µg/mL for gentamycin) and cells were incubated at 37°C, 190 rpm for 24h.

- Concerning experiments performed in biological quadruplates and triplicates, in this case a huge control culture was reached to the expected OD_{600nm} and then was split for the stress conditions (see figure 21 in the results section chapter II, B, I, d, 1: Study design).

For all conditions, cells were pelleted in 50 mL Falcon tubes at 3,500xg for 5min. Pellet was washed with 5 mL of PBS 1X. After another centrifuge step of 5 min at 3,500g, pellet was directly used for further tot tRNA isolation (without storage at -20°C).

You can find the whole material and methods in Galvanin et al, 2019 (364) for tot tRNA isolation procedure and further experiments for the detection and quantification of 2'O-methylations by high-throughput sequencing.

b. Specific tRNA isolation

1. Biotin/streptavidin method

Before individual tRNA isolation, we determined the amount of total tRNA required for 100% of hybridization with full-length complementary probes (described in table 11). A constant amount of the fluorescently labelled DNA probe (in this case 2 pmol), were hybridized in 1X PBS to increasing amounts of total tRNA (0-12 µg). Samples (total volume of 100 µL) were denaturated 3 min at 90°C and hybridized for 10 min à 65°C. After cooling down to room temperature, the samples were mixed with non-denaturing loading dye (50% (v/v) glycerol, 10% (v/v) 10X TBE buffer) and were analysed by 15% native PAGE. The fluorescence of the DNA probe was detected with a Typhoon 9400 device (excitation: 532 nm, emission filter: 526 SP).

Four individual tRNA were isolated from total tRNA by using the hybridization of a complementary DNA probe. The sequences of all used DNA probes are listed in the table 11. The DNA probe carries a fluorophore (fluorescein) on the 3'-end and a biotin label for separation by immobilization on streptavidin-coated magnetic beads (Dynabeads® MyOneTM) on the 5'-end. 200 pmol of the respective DNA probe were hybridized to previously determined amount of total tRNA in 5X SSC buffer in a total volume of 100 µL and incubated for 3 minutes at 90°C followed by an incubation for 10 minutes at 65°C. After this, samples were cooled down to room temperature. The magnetic beads were prepared: 50 µL of beads were placed on a 1.5 mL Eppendorf tube and placed on the magnetic rack, after removing supernatant and removing the beads from the magnetic rack, beads were washed with the same volume of 1X B&W buffer (5 mM Tris-HCl (pH 7,5), 0.5 mM EDTA, 1 M NaCl) three times. Then, beads were resuspended in 5X SCC buffer. For RNA/DNA binding on the beads, the samples were incubated with the magnetic beads 30 minutes at 25 °C under slight shaking at 650 rpm. After placing the tubes on the magnetic rack and removing of the supernatant (flow through

containing non-targeted tRNA), the beads were washed once in 1X SSC buffer and three times in 0.1X SSC buffer. Finally, the pellet of beads was resuspended in 50 µL MilliQ-H_2O and the RNA was eluted by heating for 3 min at 75 °C and the RNA containing supernatant was removed. Samples were stored in -20°C for further LC-MS/MS experiments.

In order to use again the flow through for other individual tRNA isolation, residual probe need to be removed via DNase I digestion. Because 5X SCC prevent DNase I activity, samples were first precipitated (see the Method section Chapter II, C, II, b, 3: section RNA/DNA precipitation) and resuspended in 44µL. Then 100 U DNase I and 10X DNase I buffer were added to a final concentration of 1X DNase I buffer and incubated for 1 hour at 37 °C. Enzymes and buffer were finally removed by the MEGAclear™ Kit according to manufacturer's instruction. Only the volume of Ethanol during RNA binding step was increased to 675 µL in order to keep RNA lower than 100 nt. Sample could then be used for another individual tRNA isolation.

2. NHS/NH_2 method

For the isolation of individual tRNA with the NHS/NH_2 method, we used the GE Healthcare HiTrap™ NHS-Activated HP Columns (1mL).

We bound four oligonucleotides with a primary amine in 5' (table 11) on the columns according to manufacturer's instruction for the four targeted individual tRNA isolation (Leu cmnm^{5}UmAA, Ser cmo^{5}UGA, Leu CmAA and Ser CGA). Column previously put at RT for 15 min was flushed with 6 mL of cold 1 mM HCl. 100 nmol of lyophilized oligonucleotide was resuspended in 1.2 mL of coupling buffer: 0.2 M NaHCO3, 0.5 M NaCl pH 8.3) and was added to the column. Binding was done during 1-2 hours. The column was washed with 6 mL of buffer A (ethanolamine 0.5 M, NaCl 0.5 M, pH 8.3) and buffer B (0.1 M sodium acetate, 0.5 M NaCl, pH 4). A second wash of buffer A is performed with an incubation time of at least 30 min in order to quench the residual free NHS groups. Then, the column was washed with 6 mL of buffer B, buffer A and buffer B. The column is ready for individual tRNA isolation or can be stored in a neutral phosphate buffer (50 mM Na2HPO4 pH 7.1, NaN3 0.1%).

For individual tRNA isolation, the column is first equilibrated for few minutes at 65°C (in an oven capable of containing a peristaltic pomp and the tubes for total tRNA recirculation). In parallel, total tRNA sample was prepared. 1 mg of RNA was heated 2 min at 70°C in 1 mL of tRNA binding buffer (1.2 M NaCl, 30 mM Hepes KOH ph7,4) and directly put on ice. Then

sample was transferred in a 50 mL Falcon tube containing 14 mL of tRNA binding buffer and was connected to the Hi-trap column. Via a peristaltic pomp, total tRNA sample was recirculated at 65°C for at least 1 hour. Column was washed with 10-15 mL of wash buffer (10 mM Hepes, 100 mM NaCl) at 55°C. Individual tRNA was eluted with 7 mL of elution buffer (1 mM Edta, 1 mM Hepes) after putting both buffer and column in preheated water bath at 75°C for 5 min. Elution fractions were precipitated with isopropanol (see the Method section Chapter II, C, II, b, 3: section RNA/DNA precipitation). Samples resuspended in 20 µL milliQ water were loaded on a 10% denaturing gel (see section). Band of interests were cut, frozen for 30 min in -20°C and eluted with 0.5 M NH4oAc at RT 750 rpm (200 µL) overnight. After shaking, the gel suspension was filtered through centrifugal filters (NanoSeps) and the resulting filtrate was ethanol precipitated as described in the section (Method section Chapter II, C, II, b, 3: section RNA/DNA precipitation).

Before our optimization experiment tRNA binding buffers and wash buffer contained 10 mM $MgCl_2$.

For the determination of individual tRNA contamination or degradation, we did a hybridization assay on native gels described in the section (Chapter II, C, II, b, 4: Gel electrophoresis).

3. RNA/DNA precipitation

Samples were supplemented with 1/10 volume of a 5 M ammonium acetate solution (pH 5.2), 1µL of GlycoBlue^T, 2.5 volumes ice cold pure ethanol (−80 °C) (in the case of biotin/streptavidin method) or 0.4 volume of cold isopropanol (in the case of NHS/NH2 method) were mixed by vortexing and stored overnight at −20 °C. Samples were centrifuged at least 30 min, full speed at -4°C. Pellet was washed with 500 µL of Ethanol 80% and centrifuged again 10 min, at full speed at -4°C. Supernatant was removed and pellet was dried at room temperature for 5 min and then resuspended in the required amount of milliQ water.

4. Gel electrophoresis

- Denaturing:

10% denaturing gels, containing 8 M urea, 50 mL of the respective 12% PAGE pre-mixes (40 (v/v) denaturing gel concentrate, 50% (v/v) gel diluent, 10% (v/v) gel buffer concentrate) were mixed with 50 µL tetramethylethylenediamine solution (TEMED) and 400 µL 10% (m/v) ammonium persulfate (APS). After polymerization, gels were pre-run in 1× TBE (Tris-borate-EDTA) buffer for 30 minutes before RNA samples (mixed 1:1 with denaturing loading dye

containing 90% (v/v) formamide and 10% (v/v) 10× TBE) were loaded. Gels were run at 10−15 W for around an hour.

- Native:

15% native polyacrylamide gels were prepared by mixing 50 mL native PAGE pre-mix (37.5% (v/v) native gel concentrate (40%), 10% (v/v) 10X TBE in H_2O) with 50 µL TEMED solution and 1 mL 10% (m/v) APS. After polymerization and a pre-run in 1X TBE buffer for 30 minutes, samples (mixed 1:1 with native loading dye containing 50% (v/v) glycerol and 10% (v/v) 10X TBE buffer in H_2O) were loaded. Gels were run at 15 W for an hour.

Fluorescein signal was directly visualized on the Typhoon 9400 device. For nucleic acid signal visualization, gels were stirred for 20 minutes in GelRed™ 1X staining solution diluted in 1X TBE and the signal was measured on the Typhoon 9400 device. The parameters for Fluorescein signal detection are: excitation 532 nm, emission filter 526 SP while the one for GelRed™ signal measurement are excitation 532 nm, emission filter 610 BP30.

c. Mass spectrometry

a. Digestion

Total tRNA or individual tRNA samples were digested into nucleosides thanks to an enzyme cocktail. 150-300 ng of RNA were incubated overnight at 37°C in 25 mM NH_4OAc (pH 7.5) with the following enzymes: 10 U of Benzonase nuclease, 2 U of thermosensitive Alkaline Phosphatase (Fast AP), 0.6 U of nuclease P1 (NP1), 0.2 U of snake venom phosphodiesterase (PDE) and 200 ng of Pentostatin (PS) and 500 ng of tetrahydrouridine (THU) which are adenosine and cytidine deaminase inhibitors respectively.

b. LC-MS/MS

40 ng of digested RNA were mixed with 10 ng of ^{13}C *S. cerevisiae* total tRNA digest: internal standard (ISTD) and used for LC-MS/MS measurement in order to quantify the level of 2'O-methylations in the samples. One sample contained only 10 ng of ISTD for subsequent normalization during analyses.

Analysis of the samples was performed with an Agilent 1260 Infinity system with binary pump in combination with an Agilent 6460 triple quadrupole (QQQ) mass spectrometer with an electrospray ion source (ESI).

In the LC-part, a C18 reverse phase HPLC column (Synergi™ 4 µm Fusion-RP 80 Å, LC Column 250 x 2 mm, Phenomenex) was used at a temperature of 35 °C. A rising gradient of 100% LC-MS grade acetonitrile and a 5 mM NH_4OAc buffer (pH 5.3, adjusted with acetic acid) was applied with a flow rate at 0.35 mL/min as described in the figure 37.

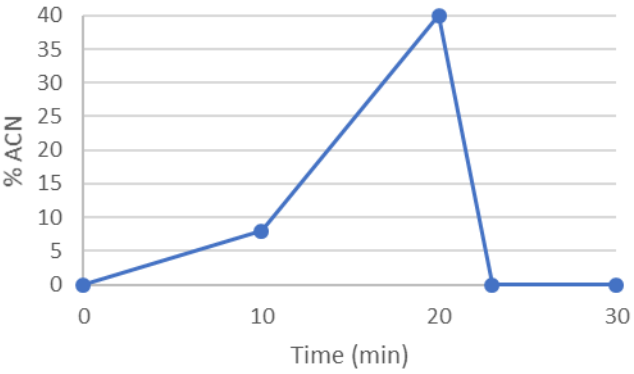

Time (min)	ACN (%)	5 mM NH4OAc (%)
0	0	100
10	8	92
20	40	60
23	0	100
30	0	100

Figure 37 LC gradient

The four main nucleosides were detected photometrically at 254 nm whereas detection of the RNA modifications was conducted via QQQ in the positive ion mode. The parameters of the electrospray ion source (Agilent Jet Stream ESI) are: gas temperature 350°C, gas flow 8 L/min, nebulizer pressure 50 psi, sheath gas temperature 350°C, sheath gas flow 12 L/min, capillary voltage 3,000 V, nozzle voltage 500 V.

For quantification experiments the dMRM mode of the LC-MS/MS was used. Following are the QQQ settings required for adjustment in the table 13.

Table 13 QQQ settings

Modification	Precursor ion (m/z)	Product ion (m/z)	Retention time (min)	Retention time window (min)	Fragmentor voltage (V)	Collision energy (V)	Cell accelerator voltage (V)
Cm	258	112.1	9.3	3	60	9	2
Cm 13C	268	116.1	9.3	3	60	9	2
Gm	298	152	12.4	3	72	5	2
Gm 13C	309	157	12.4	3	72	5	2
Um	259	113	11.3	2	66	5	2
Um 13C	269	117	11.3	2	66	5	2
Pseudouridine	245	209	3.8	2	81	5	2
Pseudouridine 13C	254	218	3.8	2	81	5	2

Subsequent analysis of the peaks with predefined m/z values was performed with the Agilent MassHunter Software, Qualitative Analysis (V. 5.0.519.0). Extraction of ion chromatograms allowed integration of respective peaks, providing values for the area under the curve. In order to normalize these values, the following calculation was performed:

$x = \frac{dMRM(12C) \div dMRM(13C)}{UV(A) - UV(A)ISTD}$. dMRM (^{12}C) or (^{13}C) correspond to values for the area under the curve for ^{12}C (Sample) and ^{13}C molecules (ISTD), UV (A) and UV(A) ISTD corresponds to the peak area of Adenosine in the UV chromatogram of the analysed sample and alone ISTD sample respectively. For comparison between control and stress conditions, control values were reported to 100 % and stress values were subjected to this calculation:

$y = \left(\frac{x\,(stress)}{x\,(associated\ control) - 1}\right) \times 100$ where x corresponds to previously calculated values.

d. Thermophoresis experiment

To determine the tRNA distribution, MicroScale Thermophproesis (MST) experiments were performed. Increasing total tRNA samples were hybridized with a constant amount of 5'Fluorescein labelled probes (as described in the table 14) in 1X PBS and 0.1% PEG. Sequences of probes are reported in tables 11 and 12. Samples were denaturated 3 min at 90°C and hybridized for 10 min at 65°C. Measurement was performed on a MonolithTM NT.115 instrument (NanoTemper Technologies) using Monolith NT.115 Capillaries where samples where added. Experiments were performed at 25°C with the blue laser. MST setting were: LED power 60% (the power of the measuring laser), MST Power 40% (the power of the infrared laser heating the sample), Fluorescence before active laser 5s, MST on 45s (the time the infrared laser was active), Fluorescence after active laser 15s and Delay 25s (the time between measurements).

Table 14 Parameters for the preparation of samples for MST experiment

tRNA	Probe amount (pmol)	Tot tRNA amount (pmol)
All individual tRNA in DH5α strain for global tRNA distribution experiment	0.5	0.004-20
Leu cmnm^{5}UmAA	0.4	0.008-4
Ser cmo^{5}UGA	0.4	0.008-4
Leu CmAA	0.2	0.008-4
Ser CGA	0.1	0.008 -10

MST measurements were analysed using the NT analysis software in the "thermophoresis" setting. Parameters for cold and hot areas were defined as follow: cold (start: 5.8 s, length: 1.1 s) and hot (start: 48.03 s, length: 1.91 s). Normalized fluorescence ratios (hot/cold x1000, F_{Norm}) were exported and plotted versus the $\log_{10}$ of the respective concentration using the GraphPad Prism 7.01 software for each titration experiment. Binding curves were obtained from the data points using a dose-response fit with variable slope. To determine the percentage of proportion of each individual tRNA, we used the following equation (c_{probe} probe concentration, *vol* sample volume, $_{EC50}$ concentration for 50% of hybridization).

$$\%\ \boldsymbol{target\ tRNA} = \frac{\boldsymbol{c_{probe} * vol}}{\boldsymbol{EC_{50} * 2 * vol}} * \mathbf{100} = \frac{\boldsymbol{n_{probe}}}{\boldsymbol{n_{total\ tRNA}}} * \mathbf{100} = \frac{\boldsymbol{n_{target}}}{\boldsymbol{n_{total\ tRNA}}} * \mathbf{100}$$

Annexe 1

ARTICLE IN PRESS

Biochimie xxx (xxxx) xxx

Contents lists available at ScienceDirect

Biochimie

journal homepage: www.elsevier.com/locate/biochi

Research paper

Diversity and heterogeneity of extracellular RNA in human plasma

Adeline Galvanin [a], Gabriel Dostert [a], Lilia Ayadi [a, b], Virginie Marchand [b], Émilie Velot [a], Yuri Motorin [a, b, *]

[a] UMR7365 IMoPA CNRS-Lorraine University, Biopôle, 9 avenue de la forêt de haye, 54505, Vandoeuvre-les-Nancy, France
[b] UMS2008 IBSLor CNRS-INSERM-Lorraine University, Biopôle, 9 avenue de la forêt de haye, 54505, Vandoeuvre-les-Nancy, France

ARTICLE INFO

Article history:
Received 31 January 2019
Accepted 14 May 2019
Available online xxx

Keywords:
Extracellular RNAs (exRNAs)
Exogenous RNA
Deep sequencing
Extracellular vesicles
Human plasma

ABSTRACT

Extracellular RNAs (exRNAs) are secreted by nearly all cell types and are now known to play multiple physiological roles. In humans, exRNA populations are found in nearly any physiological liquid and are attracting growing interest as a potential source for biomarker discovery. Human plasma, a readily available sample for biomedical analysis, reported to contain various subpopulations of exRNA, some of which are most likely components of plasma ribonucleoproteins (RNPs), while others are encapsulated into extracellular vesicles (EVs) of different size, origin and composition. This variation explains the extreme complexity of the human exRNA fraction in plasma. In this work, we aimed to characterize exRNA species from blood samples of healthy human donors to achieve the most comprehensive overview of the species, sizes and origins of the exRNA present in plasma fractions. Unbiased analysis of exRNA composition was performed with prefractionation of plasma exRNA followed by library preparation, sequencing and bioinformatics analysis. Our results demonstrate that, in addition to "mature", adaptor ligation-competent RNA species (5′-P/3′-OH), human plasma contains a substantial proportion of degraded RNA fragments (5′-OH/3′-P or cycloP), which can be made competent for ligation using appropriate treatments. These degraded RNAs represent the major fraction in the overall population and mostly correspond to rRNA, in contrast to mature products, which mostly contain miRNAs and hY4 RNA fragments. Precipitation polyethylene glycol (PEG)-based kits for EV isolation yield a fraction that is highly contaminated by large RNPs and by RNA loosely bound to EVs. Purer EV preparations are obtained by using proteinase K and RNase A treatment, as well as by size-exclusion chromatography (SEC). These samples have rather distinct RNA compositions compared to PEG-precipitated EV preparations and contain a substantial proportion of exRNA of non-human origin, arising from human skin and gut microbiota, including viral microbiota. These exogenous exRNAs represent up to 75–80% of total RNA reads in highly purified extracellular vesicles, paving the way for biomedical exploitation of these non-human biomarkers.

1. Introduction

1.1. Extracellular RNA origins

In addition to intracellular RNAs, it is now well established that a multitude of RNAs also circulates outside of cells (extracellular RNAs, exRNA) [1,2]. These species are secreted by various cells via different mechanisms that are not yet fully understood [3,4]. In multicellular organisms, exRNAs are present in almost every biological fluid (urine, milk, saliva …), the most studied of which is certainly blood [5–7]. To be stable in such an unfavorable extracellular environment rich in ribonucleases (RNases), circulating RNAs require protection from nucleolytic degradation. This

Abbreviations: exRNAs, Extracellular RNAs; EVs, extracellular vesicles; SEC, size-exclusion chromatography; RNPs, ribonucleoproteins; PEG, polyethylene glycol; RNases, ribonucleases; LDL and HDL, low- and high-density lipoproteins; MVEs/MVBs, multivesicular endosomes/multivesicular bodies; ESCRT, endosomal sorting complexes required for transport; PES, polyethersulfone; PBS, phosphate-buffered saline; NTA, NanoParticle Tracking Analysis; PNK, T4 polynucleotide kinase; NEB, New England Biolabs; MN, Macherey-Nagel; SSU/LSU, small/large subunit.

* Corresponding author. UMR7365 IMoPA CNRS-Lorraine University, BioPôle, 9 avenue de la forêt de haye, 54505, Vandoeuvre-les-Nancy, France.
E-mail address: Yuri.Motorin@univ-lorraine.fr (Y. Motorin).

https://doi.org/10.1016/j.biochi.2019.05.011
0300-9084/

Please cite this article as: A. Galvanin et al., Diversity and heterogeneity of extracellular RNA in human plasma, Biochimie, https://doi.org/10.1016/j.biochi.2019.05.011

protection can be ensured in two different ways.

On one hand, some RNAs, especially miRNAs, are in a "soluble state" and are included in ribonucleoprotein (RNP) complexes containing both ribonucleic acids and associated proteins [8,9], or, more rarely, as a part of particles, such as low- and high-density lipoproteins (LDL and HDL) [10] or exomeres [11].

On the other hand, RNAs are also found in particles released from the cell, termed extracellular vesicles (EVs) [12–15]. These vesicles are delimited by a lipid bilayer membrane and cannot replicate. There are evolving recommendations to characterize their subtypes, particularly in complex biological fluids. To date, there is no well-established consensus on specific markers of EV subtypes [16,17]. Nevertheless, three major types of EVs have been described according to their size and biogenesis: apoptotic bodies [18–20], microvesicles (or budding/shedding vesicles) [21–23] and exosomes [24–26]. Apoptotic bodies are 1–5 μm vesicles that arise from apoptotic cells through invagination. They are composed predominantly of fragmented DNA and histones. Microvesicles, from 100 nm to ~1 μm in size, are formed by budding of the plasma membrane, and their contents depend on where in the cell budding occurs. Their membrane composition is similar to the parental cell [23]. Microvesicles are enriched in phosphatidylserine, lipid rafts, cell lineage markers and cell surface receptors [23,27,28]. The third type of EVs, called exosomes, are particles of 50–150 nm in size [29] originating from the classical endocytic pathway (see reviews [25,30] for details on exosomes biogenesis and composition). Endocytosis is commonly mediated via clathrin-coated vesicles after which endocytic vesicles progress from early to multivesicular endosomes (MVEs, also called multivesicular bodies, MVBs). MVEs often fuse with lysosomes for degradation but can also join the plasma membrane, thereby releasing exosomes to the extracellular space [29]. Their fate depends on the MVE composition. MVEs rich in cholesterol and poor in lysobisphophatidic acid are secreted as exosomes, while when the proportion of cholesterol to lysobisphophatidic acid is inverted, they are directed to the lysosomal pathway. Most future exosomes follow a secretory pathway involving the endosomal sorting complexes required for transport (ESCRT). Members of ESCRT, such as proteins Alix or TSG101, are considered internal exosomal markers. Moreover, transmembrane tetraspanin proteins (e.g., CD9, CD63 and CD81) are highly enriched in exosomal membranes and serve as major external exosome markers [29] (see review [31] for details on tetraspanins).

Considering these multiple secretory pathways, exRNA composition is extremely diverse and heterogeneous [18,32]. Depending on the origin of biological samples and, even more importantly, on the experimental approaches used for characterization of exRNA, the results of different studies are barely comparable. This is an important issue, since exRNAs are attractive biomarkers for pathology and disease, with growing applications in diagnostics and prognostics [33–37]. Indeed, highlighting new biomarkers from populations present in the circulating blood could improve diagnostic methodology by allowing use of liquid biopsies instead of classical invasive biopsy types.

1.2. Extraction of exRNA from human blood

1.2.1. Choosing between serum and plasma

Analysis of human blood is of great interest for clinical diagnostics, and numerous standard treatment protocols are available. Most common pretreatments consist of preparation of plasma or serum fractions from blood. Plasma is obtained by centrifugation in the presence of anticoagulants, while serum is prepared by centrifugation of coagulated samples. Technically, working with serum is easier, but it is known that platelets release many EVs containing miRNAs in response to coagulation [38], and this considerably affects the composition of exRNAs originally present in circulating blood. For this reason, plasma is the preferred source when studying exRNAs as potential biomarkers [39].

However, some popular anticoagulants, such as heparin and EDTA, are not compatible with downstream applications (e.g., polymerase chain reaction, PCR) and are generally replaced with citrate or acid citrate dextrose [40–42]. In addition, special care should be taken during these initial centrifugation steps to prevent release of platelet-derived EVs [41].

1.2.2. Extraction of exRNA from EVs and RNPs

Extracellular RNAs present in whole plasma, by themselves or in its subpopulations (EVs or RNPs), have to be extracted for further analysis. Classical phenol/chloroform or TRIzol extractions are not efficient enough for these types of samples [43]. In fact, the yield is rather low, and small RNAs (<70 nt), which represent the majority of exRNAs [44], are generally lost [45–47]. Thus, column-based RNA extraction kits, such as the Nucleospin® miRNA (Macherey-Nagel) or the miRNeasy Micro kit from Qiagen, are generally used.

1.3. Characterization of human exRNAs in plasma

1.3.1. Fractionation of human plasma to obtain exRNA subpopulations

Human plasma is rather viscous and contains a high concentration of soluble proteins, mostly albumin and immunoglobulins but also lipoproteins and lipoprotein particles: HDL, LDL and chylomicrons. This complex composition should be taken into account for fractionation.

Among all subpopulations of exRNA present in plasma, the exosomal (or generally, EV) fraction is the best studied because these vesicles have a specific biogenesis, perform known biological functions and have been demonstrated to be involved in several diseases [29,48–50]. For analysis of EV-derived exRNA, cell cultures in conditioned media are generally used. From these samples, EVs are purified using relatively standardized techniques, mostly differential centrifugation steps, followed by ultracentrifugation to pellet submicrometric particles [51]. However, compared to complex and viscous plasma, conditioned media has a simple and controlled composition. Thus, these classical fractionation methods yield poor results with plasma, since protein complexes, lipoproteins and RNPs also sediment during ultracentrifugation [8,52].

Improvements can be obtained by the use of density gradient/cushion centrifugation [4], where particles are separated by their floating density allowing separation of soluble protein aggregates from EV. However, these methods are very laborious and require specific equipment and reagents [53,54].

Apart from "gold standard" ultracentrifugation protocols, many other methods for EV purification are commercially available. These methods are either based on the use of "precipitation agents" of unknown composition (Exoquick™ Exosome precipitation solution, System Biosciences, Total Exosome Isolation Reagent, Invitrogen, miRCURY™ Exosome Isolation Kit, Exiqon) or on immunoaffinity selection of EVs containing specific protein markers (usually membrane tetraspanins CD9, CD63 and CD81). However, none of these methods offers sufficient purity of obtained EVs, which are still heavily contaminated by plasma proteins [55]. Immunoaffinity-based methods [55–57] avoid important contamination by plasma proteins and non-EV exRNA but could potentially exclude important EV populations without specific membrane markers, since specific antibodies are used for the selection step [39].

Finally, alternative techniques based on size-exclusion chromatography (SEC, qEV column, Izon) have been developed. These methods avoid protein aggregates and provide EV fractions free of

Please cite this article as: A. Galvanin et al., Diversity and heterogeneity of extracellular RNA in human plasma, Biochimie, https://doi.org/10.1016/j.biochi.2019.05.011

protein contamination. Several comparative studies concluded that SEC is the best method for EV isolation from plasma [58–60] since only a few HDL particles were found in the size range of EVs [61]. Moreover, it is possible to obtain EV and non-EV fractions (mostly RNPs) in parallel.

Other protocols for EV purification, such as alternating current electrokinetic microarray chips, are certainly promising but require sophisticated and specific equipment [62].

In any case, for each method, it is crucial to perform either physical or biological validation after isolation/enrichment of appropriate exRNA subpopulations. Size distribution and concentration of nanoparticles are determined by Nanoparticle Tracking Analysis using a NanoSight [63], while electron microscopy establishes size and morphological characteristics of particles, such as a lipid bilayer [64–66]. One can also cite Dynamic Light Scattering that gives size distribution but does not provide information about particle concentrations [67,68]. For biological validation, immunoblotting targeting specific biomarkers, such as TSG101 (46 kDa), Alix (96 kDa) or tetraspanins CD63 (26 kDa), CD9 (26 kDa) and CD81 (26 kDa) for exosomes are a standard procedure for EVs secreted by cells in culture [69,70]. All these techniques are used routinely for EVs derived from specific cells grown in culture. However, in complex biological fluids containing a huge proportion of proteins and lipids, validation of EV preparations may present a true challenge.

1.3.2. Characterization of extracellular RNAs in plasma

Initial studies on the composition of exRNA from extracellular vesicles showed the presence of miRNA and more than a thousand different mRNAs [71]. These mRNAs even seem to be functional because after transfer of mouse extravesicular RNAs into human mast cells, new mouse proteins were found to be produced in the recipient cells, indicating that transferred exosomal mRNAs can be translated after entering another cell. In this study, authors used miRNA and mRNA specific microarrays for exRNA characterization. Indeed, the first methods used for RNA characterization were mostly real-time quantitative RT-qPCR [9,72,73] or hybridization-based assays [9,74]. However, these methods require the design of specific oligonucleotides to known targets. Thus, it is not possible to determine the presence of unexpected RNA transcripts. Currently, high-throughput sequencing overcomes this issue by sequencing and identifying all RNAs present in a given sample. In the last decade, more than a dozen papers have described exRNA content from plasma/serum and/or respective extracellular vesicles [5,32,34,35,75–81]. Using RNA sequencing, almost all known RNA species identified have been found in blood and extracellular vesicles: mRNA, rRNA, tRNA, miRNA, piRNA, snoRNA, vault RNA, Y RNA, lncRNA, etc. However, the reported proportion of different RNA varies dramatically from one study to another (Table 1). For instance, protein coding RNA and miRNA are described at 24.5% and 8.8% in one study, respectively [79], while another study with a similar design reported a proportion of 20% and 42%, respectively [34]. Moreover, the proportion of rRNA was reported to be low (<10%) in one study [78], while the same rRNA was found to be a major species at ~50% in another study [35]. These discrepancies most likely reflect extreme heterogeneity in sample preparation and in the techniques used to isolate and characterize extracellular vesicle fractions [82]. Distinctions may also arise from the methods used in library preparation for sequencing, as well as from the bioinformatics pipeline used for data analysis and interpretation (discussed in Ref. [83]).

Globally, it is a significant challenge to characterize exRNA content when plasma is used as source [84]. It is therefore critical to carefully design the study and to be aware of possible contamination issues, which may affect sample composition.

In this work, we approached the exhaustive characterization of exRNA from healthy human plasma samples using a combination of extraction/characterization approaches and deep sequencing, followed by extensive bioinformatics analysis. Our results demonstrate that the extreme heterogeneity of human plasma exRNA depends on the purity of isolated extracellular vesicles. Extracellular RNA contains various types of both mature and degraded RNAs, also unexpectedly including high proportions of foreign (non-human) RNAs derived from the human microbiota (bacteria, fungi and viruses). Our data show that, compared to total human plasma, highly purified human EVs contain a substantial fraction of exogenous RNAs, likely reflecting the past and current state of individual microbiota composition.

2. Material and methods

2.1. Collection of human plasma samples

Plasma samples used in this study were from healthy men blood donors. They agreed to give their blood for biological research at the French Blood Transfusion Institution. Blood was collected in a pocket containing sodium citrate as anticoagulant and was immediately centrifuged for 15 min at 2,000×*g* at room temperature (RT). In order to remove cellular debris, the supernatant corresponding to plasma was centrifuged again for 10 min at 1,500×*g* at RT. Supernatant was finally centrifuged for 15 min at 16,000×*g* at RT. Finally, the resulting supernatant was filtered through a 0.22 μm polyethersulfone (PES) membrane filter to obtain "pre-treated" plasma.

2.2. Plasma fractionation

2.2.1. Ultracentrifugation

1 mL of pre-treated plasma was centrifuged for 2 h at 120,000×*g* at 4 °C in high-speed ultracentrifuge (Thermo Scientific Sorval MX120) with S45A rotor. Pellet was resuspended in 400 μL of RNase-free water by rotation head-over-tail for 1–2 h at 4 °C.

2.2.2. Precipitation-based kits

Four commercially available kits based on exosome precipitation were used following the manufacturer's instructions: miRCURY™ Exosome Isolation Kit – Serum and plasma (Exiqon), Total Exosome Isolation (Invitrogen), Exosome Precipitation Solution (Serum/Plasma) (Macherey-Nagel) and ExoQuick™ Exosome Precipitation Solution (System Bioscience). Briefly, according to the manufacturer's guidelines, pre-cleared plasma (400–1000 μL) was mixed with an appropriate volume of precipitation buffer. After a vortexing step and indicated incubation time at RT, extracellular vesicles were pelleted by centrifugation and resuspended in RNase-free water or phosphate-buffered saline (PBS) by rotation head-over-tail 1–2 h at 4 °C. The kit from Exiqon provides an optional depletion of fibrinogen by thrombin treatment before EV isolation.

2.2.3. Proteinase K/RNase A treatment

EV fraction enriched from 400 μL of plasma using miRCURY™ Exosome Isolation Kit – Serum and plasma (Exiqon) was incubated with 20 μg of proteinase K in 100 mM Tris-HCl pH 7.6, for 2 h at 30 °C. Proteinase K was inactivated by heating samples for 15 min at 70 °C. Then, samples were treated with RNase A at 10 μg/mL for 15 min at RT and then stored a – 20 °C.

2.2.4. Size-exclusion chromatography (SEC)

EV fraction enriched from 500 μL of plasma using miRCURY™ Exosome Isolation Kit – Serum and plasma (Exiqon) was used for EV purification by SEC using the qEV column from Izon. This

Please cite this article as: A. Galvanin et al., Diversity and heterogeneity of extracellular RNA in human plasma, Biochimie, https://doi.org/10.1016/j.biochi.2019.05.011

Table 1
Published studies of human blood exRNA characterization. Twelve studies on human blood/plasma exRNA characterization were compared by different parameters: type of sample and treatment, RNA extraction method, RNA sequencing and analysis method.

Sample type	Blood treatment	RNA extraction methods	RNA seq methods	Studied RNA	Majors species found	Comments/Potential issues	Reference
Exosomes from plasma	Exoquick (System Biosciences) +/− RNase A treatment	miRNeasy micro kit (Qiagen)	Illumina sequencing (NEBNext® Multiplex Small RNA Library Prep Set for Illumina and NEXTflex) - RNA sequencing kit (Bioo Scientific) - TruSeq Small RNA sample preparation kit (Illumina) Size selection of the libraries 140–160 bp	miRNA, rRNA, lncRNA, DNA,tRNA, miscRNA, piRNA, mRNA, snRNA, snoRNA, other	miRNA, rRNA	Kit based on precipitation includes a lot of soluble extracellular RNA RNA from RNP or lipoproteins that are not sensitive to RNase A	Huang et al., 2013 [78]
Exosomes from serum	Total exosome isolation (from serum) reagent (Invitrogen)	Total exosome RNA and protein isolation kit (Invitrogen)	Ion proton system (Ion Total RNA-Seq Kit v2 [Thermofischer])	miRNA, tRNA, rRNA, mRNA, snRNA, scaRNA, snoRNA, piRNA	miRNA, mRNA, tRNA	Kit based on precipitation includes a lot of soluble extracellular RNA	Li et al., 2014 [35]
Plasma	N.A.	miRCURY RNA Isolation Kit-biofluids (Exiqon)	Ion proton system (Ion Total RNAseq kit v2 [Thermofischer])	rRNA removal miRNA, tRNA, snoRNA, piRNA, and other RNA RFam database	miRNA, piRNA, snoRNA		Freedman et al., 2016 [76]
Exosomes from plasma	Exoquick (System Bioscience) + RNase A treatment	miRNeasy micro kit (Qiagen)	Illumina sequencing (NEBNext® Multiplex Small RNA Library Prep Set for Illumina) Size selection of the libraries 140–160 bp	miRNA, piRNA, siRNA, lncRNA, mRNA, pseudogenes, antisense RNA, rRNA, snRNA, snoRNA, misc RNA other transcribed RNA, FLJ human cDNA and predicted RNA	miRNA, piRNA	Kit based on precipitation includes a lot of soluble extracellular RNA. RNA from RNP or lipoproteins are not sensitive to RNase A	Yuan et al., 2016 [34]
Serum	N.A.	>Circulating Nucleic Acid Kit (Qiagen). TRIzol LS Reagent, miRNeasy Serum/Plasma kit (Qiagen), QiaSymphony RNA extraction kit (Qiagen), miRCURY RNA Isolation Kit-biofluids (Exiqon)	Illumina sequencing (TruSeq Small RNA sample preparation kit) Size selection of the libraries 5–40 bp	miRNAs, isomiRs, tDRs and osRNAs	osRNAs, tDRs, miRNA (including isomiR)	Serum: includes RNA from platelets secretion: affects the composition of exRNA originally present in circulating blood	Guo et al., 2017 [75]
EV from plasma	Differential centrifugation, ultracentrifugation	Total RNA purification kit (Norgen Biotek) RNA fragmentation by RNase III	Ion proton system (Ion Total RNA-Seq Kit v2 [Thermofisher])	rRNA removal pseudogenes, mRNA, lncRNA, miRNA, tRNA, misc RNA, other	mRNA	Ultracentrifugation of viscous plasma sample can co-pellet soluble extracellular RNA	Amorim et al., 2017 [79]
Whole platelet poor plasma, 16,000×g vesicles, 160,000×g vesicles and particles depleted in plasma	Differential centrifugation procedure	TRIzol reagent (Life Technologies) dephosphorylation/ phosphorylation treatment size selection on a gel for RNA > 19 nt	SOLiD sequencing (SOLiD total RNA-Seq kit [Life Technologies])	Mitochondrial RNA, human genomic repeat consensus sequences, tRNA, rRNA, snRNA, small cytoplasmic RNA	rRNA, mRNA, mitochondrial RNA (for plasma and 16,000×g vesicles only)	Ultracentrifugation of viscous plasma sample can co-pellet soluble extracellular RNA	Savelyeva et al., 2017 [32]
Plasma	N.A.	mirVana miRNA Isolation kit (Thermofisher)	Illumina sequencing (TruSeq Small RNA sample preparation kit) Gel purification: removal of dimers	rRNA, miRNA, tRNA, piRNA, RNA from ENSEMBL75 database, non-human RNA	Y RNA, miRNA		Yeri et al., 2017 [5]

Plasma	+/- Proteinase K treatment	miRCURY RNA Isolation Kit-biofluids (Exiqon)	Illumina sequencing (NEBNext® Multiplex Small RNA Library Prep Set for Illumina) Size selection of the libraries: RNA of 21–40 nt	rRNA, miRNA, tRNA, snoRNA, piRNA	rRNA, miRNA, tRNA		Danielson et al., 2017 [81]
Plasma and serum	Detergent and Proteinase K treatment	Customized phenol/chloroform procedure	Illumina sequencing (personalized library preparation including RNA size selection)	miRNA, rRNA, tRNA, small cytoplasmic RNA, other cytoplasmic RNA, mRNA	Plasma: miRNA, mRNA, rRNA Serum: miRNA, scRNA, rRNA		Max et al., 2018 [77]

Abbreviations: isomiRs–micro RNA isoforms, lncRNA – long non-coding RNA, miRNA – micro RNA, miscRNA – miscellaneous RNA, mRNA – messenger RNA, osRNAs – other miscellaneous RNA, piRNA – piwi RNA, rRNA – ribosomal RNA, siRNA – small interfering RNA, snoRNA – small nucleolar RNA, snRNA – small nuclear RNA, tDRs – transfer-derived small RNA, tRNA – transfer RNA.

column allows the isolation of vesicles >70 nm in size. Briefly, after column equilibration with 1x PBS, EV from 500 μL of pre-treated plasma were loaded and then eluted with the same buffer. 500 μL fractions were collected. Fractions 7–9 contain EV with a size corresponding to exosomes.

2.3. NanoSight

Particle size distribution and concentration of plasma treated with kits based on precipitation was determined by the NanoSight® LM10 instrument (Malvern). A dedicated software called Nano-Particle Tracking Analysis (NTA) analyzes videos captured giving a particle size distribution and particle count based upon tracking of each particle's Brownian motion. About 1 mL of sample solution diluted from 1/20th to 1/4,000th is injected into a chamber, which is placed under an objective coupled with a camera. The movement of the particles are recorded during 60–90 s in order to follow their respective shift to determine their size and their concentration in the sample.

2.4. Extracellular RNA extraction

RNA were isolated by Nucleospin® miRNA (Macherey-Nagel) for whole plasma exRNA and RNA from EV isolated by precipitation kits. Concerning EV isolated by proteinase K/RNase A treatment and SEC, miRNeasy Micro kit from Qiagen was used. Both kits were found to give the best exRNA yield (1–5 ng of exRNA/mL of plasma) and were used following manufacturer's instructions. Both these kits are based on the same principle and include miRNA and small RNA fractions, without excluding large RNAs which may be present.

2.5. Dephosphorylation/phosphorylation treatment

Isolated RNA were 3′-end dephosphorylated using 5 U of Antarctic phosphatase (New England Biolabs) for 30 min at 37 °C. After the inactivation of the phosphatase for 5 min at 70 °C, RNA were phosphorylated at the 5′-end using 20 U of T4 polynucleotide kinase (PNK) and 1 mM ATP for 1 h at 37 °C. RNA were cleaned up from the enzymatic reactions by RNeasy MinElute Cleanup Kit (Qiagen) according to the manufacturer's recommendations, except that the volume of 96% ethanol was increased to 675 μL for small RNA binding.

2.6. Library preparation

Libraries were prepared following the manufacturer's instructions using the NEBNext® Multiplex Small RNA Library Prep Set for Illumina (NEB). Libraries were cleaned up by GeneJET PCR Purification Kit (Thermo Fisher Scientific). Libraries containing a high proportion of dimers were further purified by an automated agarose gel electrophoresis (Pippin Prep™ 3% agarose gel, Sage Science). The library of interest was specifically eluted in 40 μL by a size selection range between 110 and 300 bp to exclude adaptor dimers. Purified libraries were then concentrated by a Concentrator Plus (Eppendorf). Each library was quantified by Qubit® dsDNA HS Assay Kit (Thermo Fisher Scientific) and the quality was checked on capillary electrophoresis using a HS DNA chip (Agilent).

2.7. Sequencing

Sequencing of Illumina-type libraries was performed either on MiSeq (Illumina) in PE 2 × 75 nt mode to get paired-end information, or on HiSeq1000 (Illumina) in single-read SR50 mode.

Please cite this article as: A. Galvanin et al., Diversity and heterogeneity of extracellular RNA in human plasma, Biochimie, https://doi.org/10.1016/j.biochi.2019.05.011

2.8. Bioinformatics

Initial trimming of raw fastq files was performed by Trimmomatic, v0.32 [85], using the following parameters: first trimming with TruSeq3-SE.fa:2:30:10 LEADING:30 TRAILING:30 SLIDINGWINDOW:4:15 MINLEN:1 AVGQUAL:30 to get distribution of all reads in population, followed by TruSeq3-SE.fa:2:30:7 LEADING:30 TRAILING:30 SLIDINGWINDOW:4:15 MINLEN:10 AVGQUAL:30 for reads used in downstream analysis. The following reference sequences were used for analysis: human 45S pre-rRNA sequence (accession number NR_046235), human genome build hg19 from UCSC, reference sequences for SSU and LSU rRNAs from SILVA database (https://www.arb-silva.de/), release 132, non-redundant SSU_Nr99 sequences and whole LSU collection. Viral/phage reference sequences from NCBI (v68 nov 03 2014, 5794 sequences). Alignment was performed using bowtie 2 in –local (soft trimming) mode and following parameters: D 15 –R 2 –N 1 -L 10 -i S,1,1.15.

3. Results

3.1. Study design

In this study, we used deep sequencing for the exhaustive characterization of exRNA subpopulations in human blood from healthy subjects. Five plasma samples were used (Plasma #1 to Plasma #5) to evaluate the biological diversity among samples. The composition of plasma exRNA is expected to be extremely complex, since these species have diverse origins, secretory pathways and are included within lipid particles of different sizes, as well as in "soluble" RNP complexes. To achieve separation of these subpopulations, different methods for plasma fractionation were used, including precipitation-based commercial kits, size-exclusion chromatography (SEC) and ultracentrifugation methods. In addition, conversion of exRNAs into a sequencing library allows discrimination between "true" maturation products (RNAs having 5′-P/3′-OH extremities) and RNA degradation fragments arising from chemical and enzymatic pathways (5′-OH, 3′-P or cyclophosphate at their extremities).

Since exRNA species are mostly small RNAs or fragments (<70 nts), small RNA sequencing kits are the most appropriate for their conversion into a sequencing library. Here, we used the NEBNext® Multiplex Small RNA Library Prep Set for Illumina (NEB).

In brief, human plasma samples were either directly used to extract exRNA species or first fractionated by precipitation, ultracentrifugation, and/or size-exclusion chromatography and proteinase K/RNase A treatment (Fig. 1) to obtain exRNAs included within vesicles. RNAs were extracted and subjected to Illumina deep-sequencing either directly or after preliminary conversion to ligation-compatible extremities with alkaline phosphatase/T4 polynucleotide kinase treatment (deP/P-treatment). Resulting libraries were sequenced in paired-end or single read modes on MiSeq and HiSeq1000 Illumina sequencers. Subsequent bioinformatics analysis aimed to identify, as much as possible, RNA species present in human plasma.

We applied the following strategy for exRNA mapping and identification:

- local (soft-trimming alignment mode): alignment to the most abundant human rRNA species to sort out reads mapping to these RNAs
- local alignment mode to hg19 human reference genome
- non-mapped to hg19 reads were further aligned to collection of SSU/LSU rRNA sequences from the SILVA database [86] to identify the most represented RNA species from the human microbiota
- finally, to gain insights into the eventual presence of RNAs arising from viral/phage microbiota, non-identified reads were aligned to a virus/phage database. Complete alignment statistics for all studied samples are shown in Table S1.

Overall, this bioinformatics pipeline allowed identification of >80% of all RNA reads present in human plasma samples, except for highly purified extracellular vesicles, where identification was slightly lower due to an important proportion of bacterial reads comprising from 60% to 80% of the population.

3.2. Deep sequencing analysis of exRNAs from pretreated human plasma

First, the total population of human plasma exRNAs was extracted and globally characterized. Bioanalyzer traces show an RNA peak of approximately 80–120 nt in size (Fig. 2A), with the average yield of approximately 8.5 ng RNA/ml of plasma. Extracted exRNA were converted into a library by adaptor ligation at extremities with and without the preliminary deP/P-treatment step (Fig. 2B) and sequenced (Table S1). Inspection of fragment sizes for exRNA extracted from two independent plasma samples (P #1 and P #2) showed a striking difference depending on the applied preliminary treatment. As anticipated, direct ligation of exRNA yielded two major peaks at 21 nt and 33 nt in length (Fig. 2C), presumably corresponding to miRNA fractions and hY4 RNA fragments, respectively. These species were previously reported to be highly abundant in human plasma samples. In contrast, very different profiles were observed for total RNA fractions captured after 3′-deP/5′-P treatment. These samples showed a broad peak of small fragment sizes (12–15 nts) and a substantial proportion of longer (>50 nts) fragments. Even if the proportion of "mature" and degraded RNA fragments is impossible to evaluate using this approach, the yield of sequencing libraries clearly indicates a large domination of degradation products in the exRNA population. Size distribution showed very similar results for RNA fragments in total library preparations (Fig. 2C), fragments aligned to human hg19 genome (Fig. 2D) or reads unmapped for hg19 (Fig. 2E).

The majority of exRNA fragments successfully mapped to the human hg19 genome, but human rRNA–derived fragments were highly abundant in the degraded fraction at the expense of miRNAs and hY4 fragment RNAs compared to mature RNA sequences (Fig. 2DF).

3.3. Fractionation of EVs and "free" exRNAs from human plasma

In general, exRNA fractions are composed of two major subpopulations, those that are most likely included in stable RNPs and those that are encapsulated within EVs of different origins, primarily submicrometric particles. These fractions can be separated using physical methods, such as ultracentrifugation (or gradient ultracentrifugation), but many commercially available kits propose isolation of EVs without this long and laborious step. For clinical exRNA analysis, we first compared the yield and composition of exRNA fractions isolated by ultracentrifugation and precipitation-based kits.

Ultracentrifugation at 120,000×*g* yielded moderate EV levels of ~100 nm in the pellet (Fig. 3A) and thus, a rather low yield of associated exRNAs (Fig. 3B). Indeed, the majority of plasma exRNA remained in the supernatant after ultracentrifugation (named S100), corresponding to the "RNP" fraction. Global profiles of fragment sizes were extremely similar to those previously observed for total plasma (P #2), S100 supernatant and EV fraction for both

Please cite this article as: A. Galvanin et al., Diversity and heterogeneity of extracellular RNA in human plasma, Biochimie, https://doi.org/10.1016/j.biochi.2019.05.011

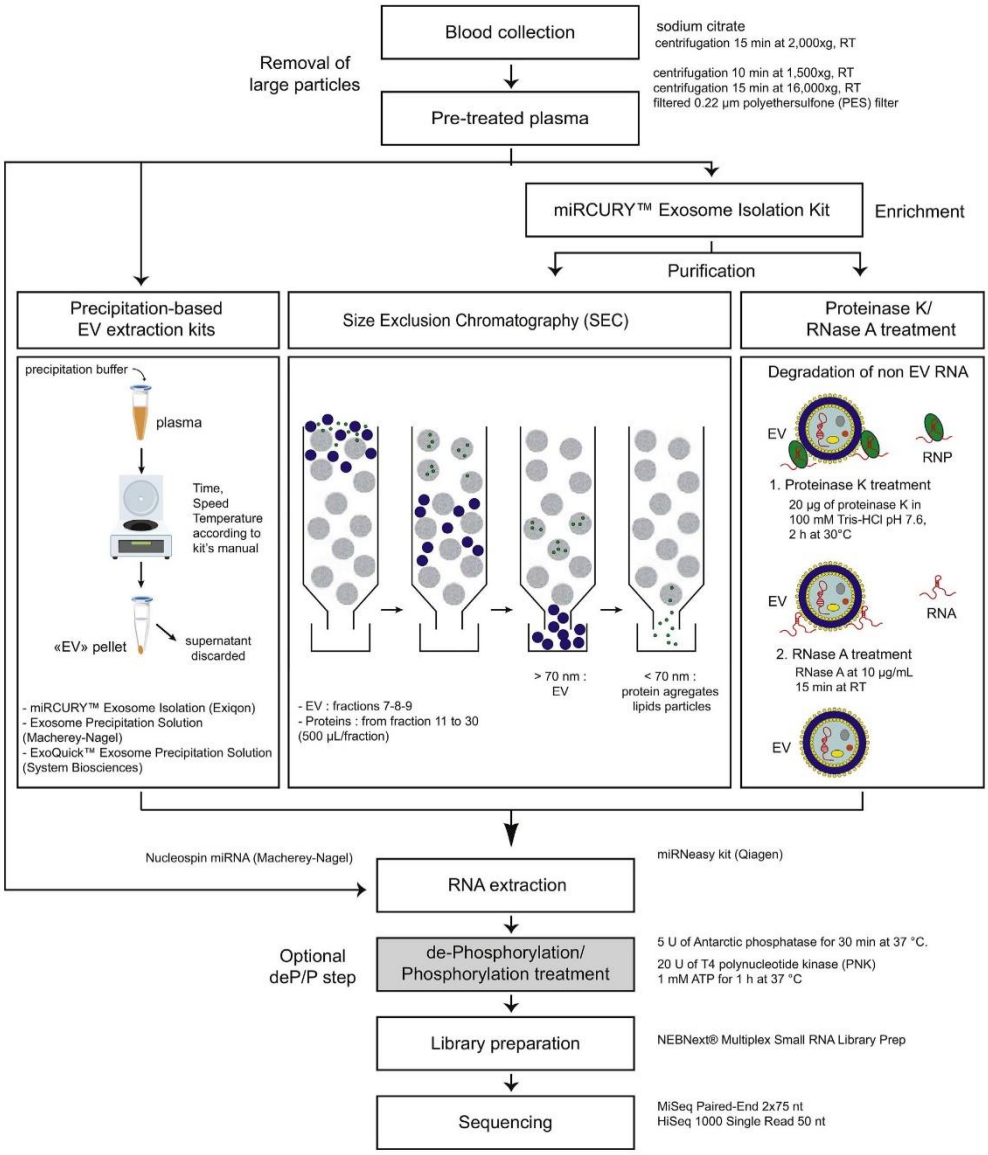

Fig. 1. Flow-chart for exRNA extraction and characterization. After removal of large particles, plasma samples are used for enrichment/purification of EVs using precipitation-based kits, size-exclusion chromatography (SEC) procedures (qEV, Izon) or combined proteinase K and RNase A treatment. In SEC, nanoscale EVs are separated from smaller protein contaminants and eluted in different fractions, while combined proteinase K and RNase A treatment removes RNAs associated with RNPs and external shells of EVs. Only internal exRNAs inside of EV are still protected by the lipid bilayer. Then, enriched or purified samples were submitted for RNA extraction, dephosphorylation/phosphorylation treatment (deP/P), library preparation and RNA sequencing.

mature and degraded RNA (Fig. 3C). Mapping to hg19 reads demonstrated a similar trend, indicating that there is no global selection of specific RNAs into EVs (Fig. 3DE). Very similar results were obtained for another independent plasma sample (P #3, Supplementary Fig. S1).

As anticipated, precipitation-based kits provided enriched fractions containing submicrometric EVs [87–89] with a slightly different size, ~80 nm, but with a higher fractionation yield

Please cite this article as: A. Galvanin et al., Diversity and heterogeneity of extracellular RNA in human plasma, Biochimie, https://doi.org/10.1016/j.biochi.2019.05.011

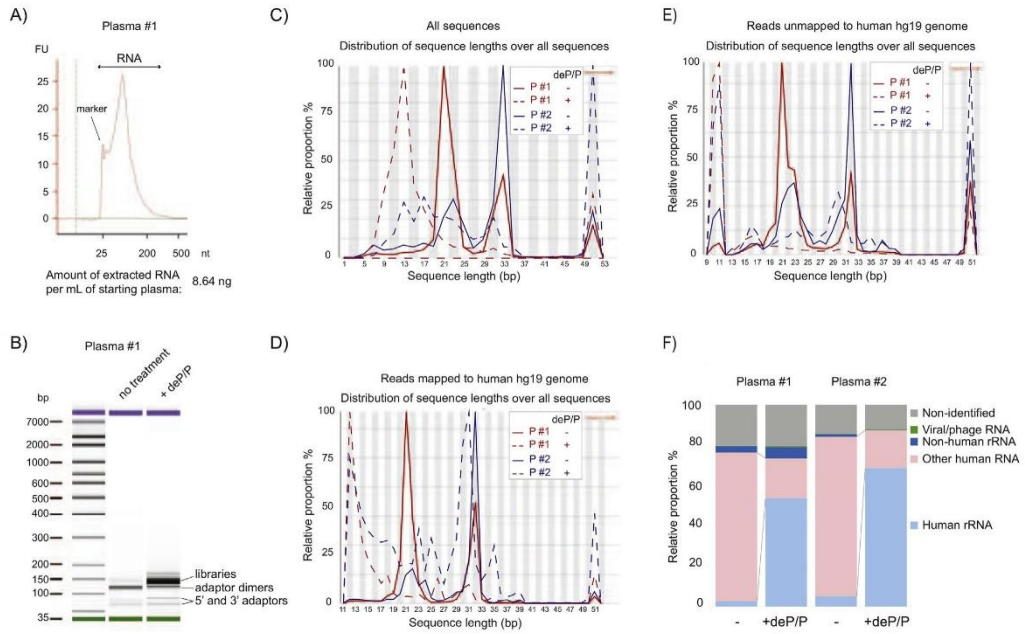

Fig. 2. Characterization of exRNA from human plasma. A – Agilent Bioanalyzer profile of exRNA extracted from human plasma on PicoRNA6000 Chip. B – Agilent Bioanalyzer analysis on High Sensitivity DNA Chip of library preparations with and without (no treatment) preliminary deP/P treatment. Bands corresponding to primer adapters and primer dimers are indicated. C – Size distribution of RNA fragments observed in total library preparations (solid line – untreated samples, dashed line – RNAs treated by deP/P) from whole plasma for two samples (P #1 and P #2). D – Size distribution of fragments aligned to the human hg19 genome. The same line style and samples are used as in panel C. E – Size distribution for reads unmapped to hg19. F – Proportions of human rRNA, other human RNAs, non-human rRNAs and unidentified fragments in exRNA from Plasma #1 and Plasma #2 samples. Proportions are shown for untreated exRNA samples (–) and after preliminary deP/P treatment (deP/P).

compared to the ultracentrifugation approach used for P #2 (Fig. 4A). We have chosen several of them, giving the best EV yield for further characterization (Exosome Isolation kit (Exiqon), ExoQuick™ Exosome precipitation solution (System Biosciences) and Exosome Precipitation solution (Serum/Plasma) from Macherey Nagel (MN)) (Fig. 4B).

Protein composition analysis of the enriched fractions demonstrated a very high concentration of major plasma proteins (mostly serum albumin and immunoglobulins), which certainly coprecipitate together with EVs (Supplement Figure S2AB). Indeed, it has been demonstrated that after ultracentrifugation and precipitation-based kits, the EV fraction is contaminated by protein aggregates that give similar signals by nanoparticle tracking analysis [90]. Thus, plasma fractionation by ultracentrifugation or precipitation-based kits certainly enriches certain EV population(s) but does not provide high EV purity.

exRNA extracted from kit-precipitated EVs follow the same general trend: a minor mature fraction shows 21–22 nt and 31–33 nt peaks, while the degraded population is highly heterogeneous and spans from 9 to 10 nt to >50 nt (Fig. 4C). As in the case of ultracentrifugation-derived EVs, mapping to different reference sequences shows a relatively low human rRNA proportion in mature products, while this proportion becomes substantial in the degraded RNA population (Fig. 4D). Globally, the profile of mapped reads shows that the MN kit gives the best match to EVs prepared by ultracentrifugation. Interestingly, different kits result in variable levels of contamination with non-human rRNA, a parameter that may be used as criteria for their use in different applications (for example, analysis of human or non-human RNAs) (Supplementary Fig. S3).

3.4. Analysis of exRNA in highly purified EVs

To gain better insights into the composition of exRNAs present in the inner compartment of plasma EV particles, we decided to apply a combined purification protocol consisting of initial enrichment of EVs using the miRCURY™ Exosome Isolation kit, followed by their purification using either SEC (qEV column, Izon) or consecutive proteinase K and RNase A treatments (Fig. 1). The last technique is supposed to remove loosely bound exRNAs from RNPs and EV outer shells, while internal RNAs in EVs are protected by the lipid bilayer [91] (Supplementary Fig. S2C).

The yield of exRNAs extracted from these highly purified EVs was relatively low (Fig. 5A). Indeed, the major fraction of exRNAs seems to be bound at the exterior shell of these particles or coprecipitated RNPs. Due to the low yield of exRNA, the analysis was performed using a preliminary deP/P-treatment. A profile of obtained libraries is shown in Fig. 5B.

In contrast to kit-precipitated EVs, highly purified lipid particles have very different fragment size profiles, with rather broad and flat distribution between 10 and 40 nts without any characteristic peaks (Fig. 5C). Of note, the proportion of >50 nt fragments is relatively high compared to all other samples studied.

Alignment to human genome sequences showed that only very short reads were successively mapped, while only a minor proportion of long sequences were aligned (Fig. 5D). Analysis of RNA

Please cite this article as: A. Galvanin et al., Diversity and heterogeneity of extracellular RNA in human plasma, Biochimie, https://doi.org/10.1016/j.biochi.2019.05.011

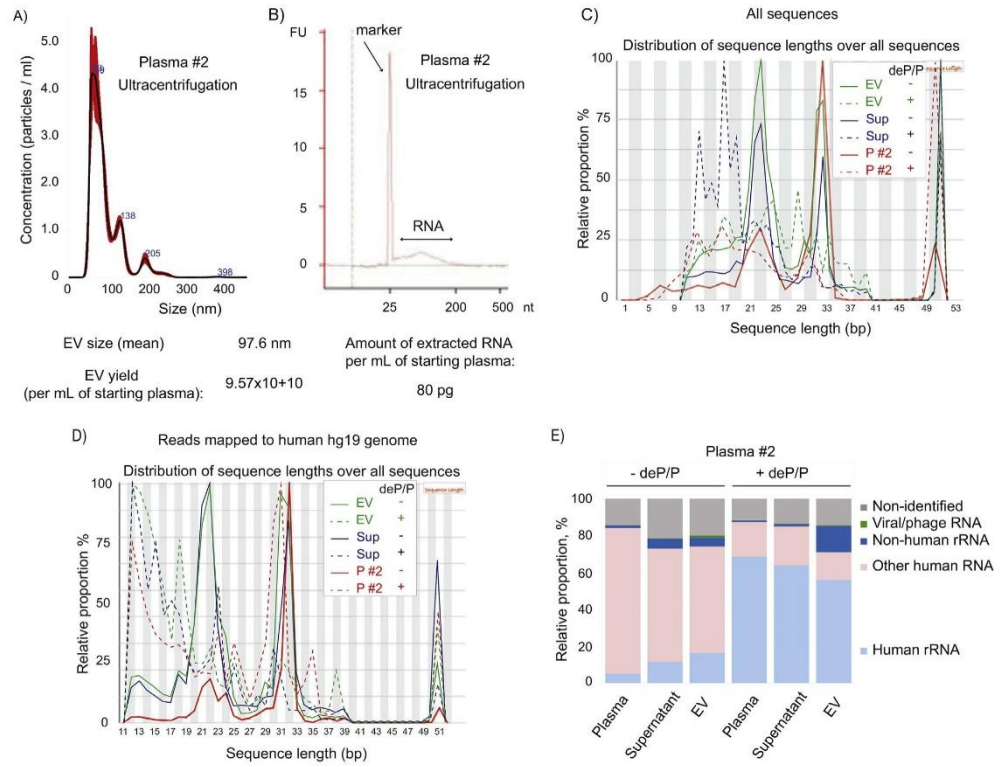

Fig. 3. Characterization of exRNA in EVs obtained by ultracentrifugation. A – NanoSight Nanoparticle Tracking Analysis (NTA) profile for EV fraction obtained by ultracentrifugation. B – Agilent Bioanalyzer profile of exRNAs extracted from ultracentrifugation-derived EVs on PicoRNA6000 Chip. C – Size distribution of RNA fragments observed in total library preparations from whole plasma, plasma (P #2), plasma RNA remaining in the supernatant after ultracentrifugation (S100) and RNA extracted from extracellular vesicle (EV) fraction after ultracentrifugation (solid line – untreated samples, dashed line – RNAs treated by deP/P). D – Size distribution of fragments aligned to the human hg19 genome. The same line style and samples are used as in panel C. E – Proportions of human rRNA, other human RNAs, non-human rRNAs and unidentified fragments in exRNA samples from P #2, S100 supernatant and EV fractions. Proportions are shown for untreated exRNA samples (–) and after preliminary deP/P treatment (deP/P).

populations revealed that human RNA (<20% of total) is mostly represented by rRNA, while major proportions map to non-human rRNA sequences, and almost 40% cannot be identified (Fig. 5E, see also below). These data demonstrate that highly purified EV fractions primarily contain non-human RNAs, and their composition is radically different from those obtained by ultracentrifugation or precipitation.

3.5. Non-human RNAs in plasma exRNA

As clearly seen in Figs. 2F and 3E, different subpopulations of exRNA from human plasma contain nonnegligible proportions of non-human RNA. While this proportion is quite minor (12–20%) in total exRNA from plasma, it becomes substantial in enriched EV preparations and even predominant in highly purified EVs.

Analysis of such non-human RNA species is not straightforward, since the human microbiota genome may represent 300-fold the size of the human genome. However, we speculated that the major portion of these exRNAs comes from bacterial and eukaryotic microbiota rRNA sequences. For identification of such species, we used the SILVA database, containing millions of known rRNA sequences. Alignment was made to a nonredundant version of the SILVA database, including 695,171 sequences of Small SubUnit (SSU) and 198,843 sequences of Large SubUnit (LSU) rRNA species. Approximately 40–50% of non-human RNA reads were successfully aligned to this reduced version of the SILVA rRNA database, indicating that indeed, non-human RNA species are mostly represented by bacterial and eukaryotic rRNAs from the microbiota and even food (various fish species, rice, baker's yeasts). Composition of the bacterial rRNA population was relatively similar in different plasma samples, likely reflecting the composition of the human microbiota. The most frequent species identified were from the Proteobacteria phylum, class Gammaproteobacteria, followed by Bacteroidetes and Firmicutes. More precise identification of bacterial species was not performed, since short rRNA fragments may map to multiple closely related species.

We also attempted alignment of the remaining unidentified sequences to viral/phage RNA/DNA databases to gain insight into potential viral microbiota. Only a very minor proportion of reads was aligned to these reference sequences, but the extraction of uniquely aligned reads allowed for the partial identification of viral/phage species present in samples. Reads mapping to both human

Please cite this article as: A. Galvanin et al., Diversity and heterogeneity of extracellular RNA in human plasma, Biochimie, https://doi.org/10.1016/j.biochi.2019.05.011

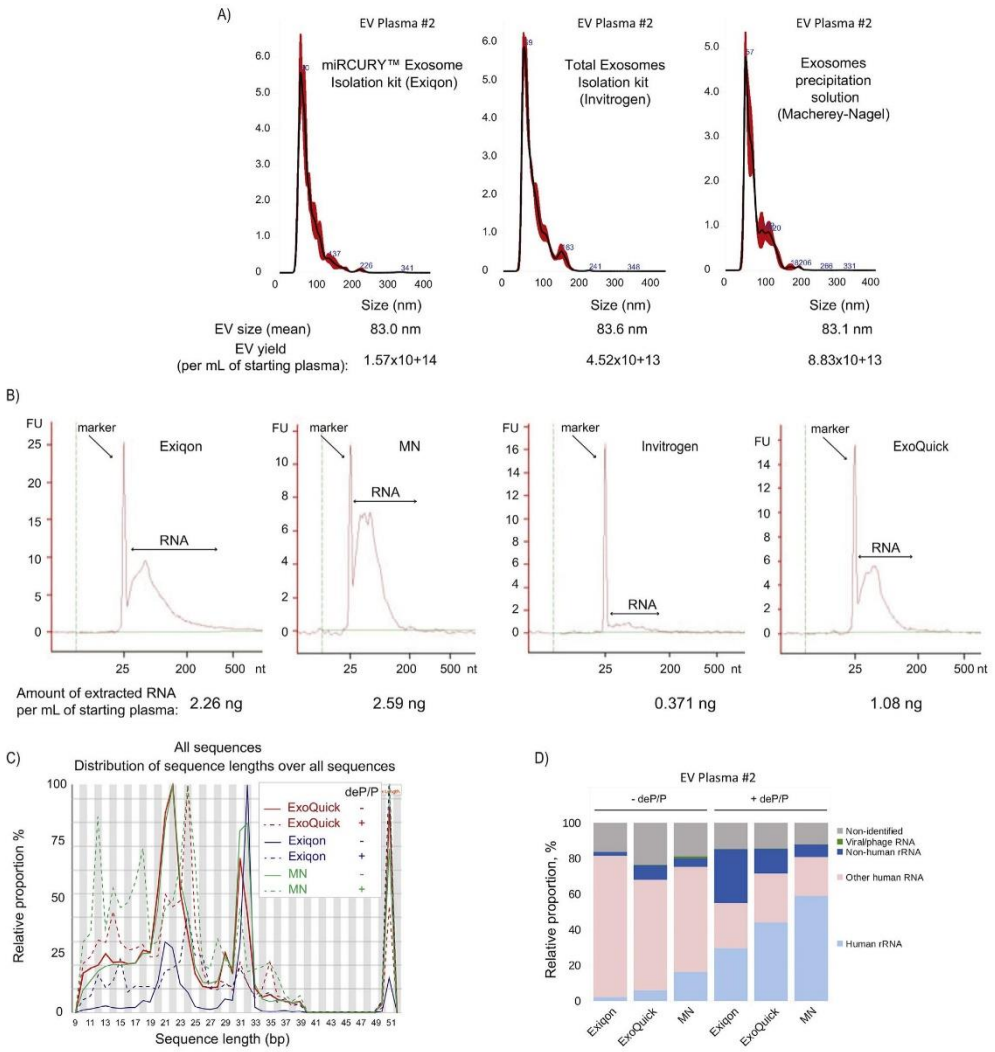

Fig. 4. Characterization of exRNAs extracted from EVs prepared using precipitation-based plasma fractionation kits. A – NanoSight Nanoparticle Tracking Analysis (NTA) profile for EV fractions obtained from Plasma #2 by miRCURY Exiqon kit, Total Exosomes isolation kit (Invitrogen) and Exosome precipitation solution (Macherey-Nagel). B – Agilent Bioanalyzer profile of exRNA extracted from precipitation-derived EVs on PicoRNA6000 Chip. C – Size distribution of RNA fragments observed in total library preparations from EVs isolated by ExoQuick™ Exosome precipitation solution (System Biosciences) and Exiqon and Macherey-Nagel kits (solid line – untreated samples, dashed line – RNAs treated by deP/P). D – Proportions of human rRNA, other human RNAs, non-human rRNAs and unidentified fragments in EV-associated exRNA samples prepared by the same kits as in panel C. Proportions are shown for untreated exRNA samples (–) and after preliminary deP/P treatment (deP/P).

viruses and phages to commensal bacteria were detected, the most frequent of which were Pandoravirus and Herpesvirus. Interestingly, total plasma exRNA was relatively enriched in human viral sequences, while highly purified EVs (SEC column and RNAse A/Proteinase K treatment) contained primarily species mapping to bacterial phages.

Inspection of selected remaining sequences nonmatching to any reference sequences demonstrated either the absence of similarity with any sequence present in actual release of nr/nt NCBI nucleotide collection or indicated bacterial 23S rRNA origin, since reference 23S rRNA list for bacteria is still incomplete in the SILVA database.

4. Discussion

In this study, we demonstrate the complexity of plasma exRNA

Please cite this article as: A. Galvanin et al., Diversity and heterogeneity of extracellular RNA in human plasma, Biochimie, https://doi.org/10.1016/j.biochi.2019.05.011

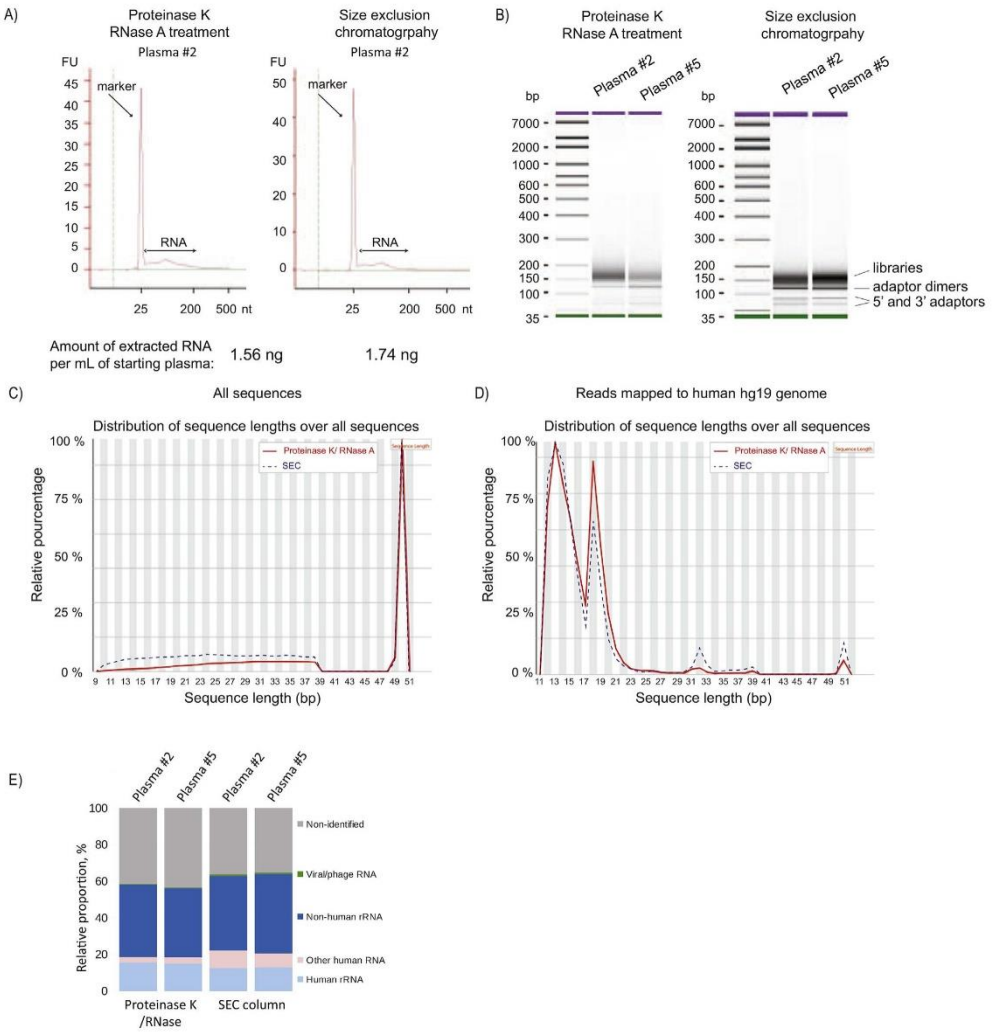

Fig. 5. Characterization of exRNAs from highly purified EVs obtained by size-exclusion chromatography and successive Proteinase K/RNase A treatments. A – Agilent Bioanalyzer profile of exRNAs extracted from highly purified EVs on PicoRNA6000 Chip. B – Agilent Bioanalyzer analysis on High Sensitivity DNA Chip of library preparations for exRNAs from 2 independent plasma samples (Plasma #2 and Plasma #5) obtained by Proteinase K/RNase A treatment and SEC. C – Size distribution of all RNA fragments observed in total library preparations from these 2 samples. D – Size distribution of RNA fragments aligned to human hg19 genome. E – Proportions of human rRNA, other human RNAs, non-human rRNAs, and unidentified fragments in highly purified EVs for the 2 samples (Plasma #2 and Plasma #5).

analysis. This is due to the extreme diversity of exRNA subpopulations and the presence of other molecular components in such a very complex biological fluid. In addition, there are no commonly accepted or standardized methods for sample preparation, analysis and validation, leading to global confusion in the literature. Comparison of exRNA studies is compromised due to numerous biological and technical biases. For example, several studies that published data on exRNA from EVs reported huge differences in the composition of exRNA fractions (proportions of rRNA, miRNA and so on) [34,35,78,79,92] (see Table 1). For instance, analysis of human miRNAs, which are widely employed for biomarker discovery, may be highly biased, depending on the purification procedures used. The RNA content of the exosomes isolated by centrifugation was shown to be very similar to the RNA composition of the human plasma, demonstrating that inappropriate EV purification methods yield preparations highly contaminated with nonexosomal RNA [93]. In addition, several comparative studies highlighted strong differences in exosomal RNA content when extracellular vesicles were isolated from the same biological sample using different methods [58,88,94,95]. Not only global

Please cite this article as: A. Galvanin et al., Diversity and heterogeneity of extracellular RNA in human plasma, Biochimie, https://doi.org/10.1016/j.biochi.2019.05.011

miRNA content was found to be different [94], but the level of individual miRNAs, such as mir let-7-d, miR-25, miR-127–3p, mir-16 and mir-451, were also distinct [94,95]. Such differences in exosomal RNA content were described for plasma-derived exosomes, and, surprisingly, also for cell-derived exosomes obtained from rather well characterized cell culture media [88]. This demonstrates that biases related to exosome purification methods may be important and may lead to lower quality results, even when the biological source is not a complex biofluid like plasma. In this study comparing ultracentrifugation, density gradient protocol and a precipitation-based kit [58], only 40% of miRNAs were common between the three methods. Moreover, mass spectrometry analyses indicate that precipitation methods lead to contamination with PEG and serum proteins [96]. Taken together, this shows the necessity of creating an optimized pipeline for exRNA characterization by limiting biases as much as possible. In our work, we designed each step to balance advantages and drawbacks identified for each procedure, but it is also important to consider the remaining known and unknown issues.

We demonstrate that "mature" and "degraded" populations of exRNAs are quite different in composition and relative proportion in plasma. Thus, depending on the project's objectives, one or another fraction may (or have to) be analyzed separately. Popular methods of EV isolation by ultracentrifugation and various precipitation reagents do not obtain pure EV fractions, and lipid particles are still highly contaminated with RNA-containing RNPs. These enriched EV fractions seem to be similar to a global composition of human exRNA from whole plasma. However, EV isolation methods based on SEC and proteinase K/RNase A treatment result in quite distinct exRNA composition associated with highly purified vesicles, which mostly contain degraded fragments of non-human exRNA.

Exhaustive bioinformatics analysis of exRNA by deep sequencing is also not straightforward. First, the average size of exRNA fragments is rather small, and the proportion of very short reads <15 nt is substantial. These fragments are difficult to identify unambiguously, since they may perfectly map to various reference sequences. In this work, we used alignment to human rRNA as a first step, expecting that such fragments may be highly abundant, which is indeed the case for degraded exRNA populations. The second alignment step attributes all additional human genome related sequences. While direct alignment of RNA-derived reads to genomic sequences seems inappropriate due to the potential absence of intronic regions, the soft-trimming alignment mode used here generally provides correct mapping, even for reads split between two exons.

Third, exRNA fractions in human plasma are highly contaminated by exRNAs of non-human origin, arising from the commensal bacterial/fungal/viral microbiota present in the human body [97,98]. It is anticipated that these non-human RNAs represent primarily highly abundant RNAs from different bacterial and eukaryotic species (rRNA, tRNAs), but no exhaustive analysis of this highly variable population has been performed. In addition, this potential microbiota's metagenome is approximately 300-fold the size of the human genome, and the small size of exRNA fragments does not allow unambiguous sequence alignment, making annotation and analysis extremely complex. In addition, due to numerous posttranscriptional events of RNA maturation and degradation (mostly polyA and/or polyU 3′-addition), exRNA reads may not directly align to reference genomic sequences unless soft-trimming (local) alignment mode is used.

5. Conclusions

The results of this study show that human exRNA in human plasma exists mostly in a "free" but RNP-associated form, which protects the RNA from nuclease degradation. Ultracentrifugation and precipitation-based strategies allow partial enrichment of EV fractions; however, these preparations remain highly contaminated by associated RNPs from the "free" population. The major portion of the "free/RNP-associated" exRNAs are human RNAs, with rRNA being the most prominent constituent. Precipitation-based kits provide little enrichment of EVs, since RNA composition is rather similar for whole plasma and precipitated vesicles.

When alternative protocols based on SEC or proteinase K/RNase treatment were used, the composition of EV-associated exRNAs was revealed to be entirely different, both in size distribution and in composition. Over 80% of exRNAs in these EVs was non-human RNA, representing mostly bacterial rRNA from the human microbiota.

Mature human exRNAs (with 5′-P and 3′-OH extremities such as miRNA and hY4 RNA) are enriched in the "free" population and are still present in EVs obtained using precipitation protocols due to their association and/or coprecipitation. This fraction is minor in the plasma, and the majority of exRNA has "degradation"-type extremities (5′-OH and 3′-P or cyclophosphate). This population is more diverse, and human RNA is mostly represented by rRNA, in addition to non-human (microbiota) rRNAs.

Thus, for the analysis of human mature RNAs, such as miRNA species, the extraction of whole human plasma is recommended, while for more detailed analysis of exRNA issuing from the microbiota, preparation of highly purified EVs should be considered.

Contributors

EV and YM conceived the study, AG and GD performed isolation and characterizations of EVs, AG, LA and VM prepared libraries and performed their sequencing, AG and YM analyzed the data and wrote the manuscript.

Declaration of interests

The authors declare that they have no known competing financial interests or personal relationships that could have appeared to influence the work reported in this paper.

Acknowledgements

This work was co-funded by grant from Lorraine University and from European Union in the framework of FEDER-FSE program "Lorraine et Massif des Vosges 2014–2020". The authors wish to thank Dr. Valérie Jouan-Hureaux (UMR7039 CRAN CNRS-Lorraine University, Vandœuvre-lès-Nancy, France) for performing NTA.

Appendix A. Supplementary data

Supplementary data to this article can be found online at https://doi.org/10.1016/j.biochi.2019.05.011.

References

[1] S. Mohr, C.-C. Liew, The peripheral-blood transcriptome: new insights into disease and risk assessment, Trends Mol. Med. 13 (2007) 422–432, https://doi.org/10.1016/j.molmed.2007.08.003.
[2] C.C. Smith, N.H. Maverakis, W.W. Ackermann, Characterization of extracellular particles released from continuous cell cultures derived from human leukemia, Proc. Soc. Exp. Biol. Med. 152 (1976) 645–650.
[3] N. Sadik, L. Cruz, A. Gurtner, R.S. Rodosthenous, S.A. Dusoswa, O. Ziegler, T.S. Van Solinge, Z. Wei, A.M. Salvador-Garicano, B. Gyorgy, M. Broekman, L. Balaj, Extracellular RNAs: a new awareness of old perspectives, Methods Mol. Biol. 1740 (2018) 1–15, https://doi.org/10.1007/978-1-4939-7652-2_1.

Please cite this article as: A. Galvanin et al., Diversity and heterogeneity of extracellular RNA in human plasma, Biochimie, https://doi.org/10.1016/j.biochi.2019.05.011

[4] K. Li, R.S. Rodosthenous, F. Kashanchi, T. Gingeras, S.J. Gould, L.S. Kuo, P. Kurre, H. Lee, J.N. Leonard, H. Liu, T.B. Lombo, S. Momma, J.P. Nolan, M.J. Ochocinska, D.M. Pegtel, Y. Sadovsky, F. Sánchez-Madrid, K.M. Valdes, K.C. Vickers, A.M. Weaver, K.W. Witwer, Y. Zeng, S. Das, R.L. Raffai, T.K. Howcroft, Advances, challenges, and opportunities in extracellular RNA biology: insights from the NIH exRNA Strategic Workshop, JCI Insight 3 (2018), https://doi.org/10.1172/jci.insight.98942.

[5] A. Yeri, A. Courtright, R. Reiman, E. Carlson, T. Beecroft, A. Janss, A. Siniard, R. Richholt, C. Balak, J. Rozowsky, R. Kitchen, E. Hutchins, J. Winarta, R. McCoy, M. Anastasi, S. Kim, M. Huentelman, K. Van Keuren-Jensen, Total extracellular small RNA profiles from plasma, saliva, and urine of healthy subjects, Sci. Rep. 7 (2017) 44061, https://doi.org/10.1038/srep44061.

[6] A.J. Griswold, J. Perez, K. Nuytemans, T.A. Strong, L. Wang, D.D. Vance, H. Ennis, M.K. Smith, T.M. Best, J.M. Vance, M.A. Pericak-Vance, L.D. Kaplan, Transcriptomic analysis of synovial extracellular RNA following knee trauma: a pilot study, J. Orthop. Res. 36 (2018) 1659–1665, https://doi.org/10.1002/jor.23802.

[7] C. Lässer, V. Seyed Alikhani, K. Ekström, M. Eldh, P. Torregrosa Paredes, A. Bossios, M. Sjöstrand, S. Gabrielsson, J. Lötvall, H. Valadi, Human saliva, plasma and breast milk exosomes contain RNA: uptake by macrophages, J. Transl. Med. 9 (2011) 9, https://doi.org/10.1186/1479-5876-9-9.

[8] J.D. Arroyo, J.R. Chevillet, E.M. Kroh, I.K. Ruf, C.C. Pritchard, D.F. Gibson, P.S. Mitchell, C.F. Bennett, E.L. Pogosova-Agadjanyan, D.L. Stirewalt, J.F. Tait, M. Tewari, Argonaute2 complexes carry a population of circulating microRNAs independent of vesicles in human plasma, Proc. Natl. Acad. Sci. U. S. A. 108 (2011) 5003–5008, https://doi.org/10.1073/pnas.1019055108.

[9] A. Turchinovich, L. Weiz, A. Langheinz, B. Burwinkel, Characterization of extracellular circulating microRNA, Nucleic Acids Res. 39 (2011) 7223–7233, https://doi.org/10.1093/nar/gkr254.

[10] K.C. Vickers, B.T. Palmisano, B.M. Shoucri, R.D. Shamburek, A.T. Remaley, MicroRNAs are transported in plasma and delivered to recipient cells by high-density lipoproteins, Nat. Cell Biol. 13 (2011) 423–433, https://doi.org/10.1038/ncb2210.

[11] H. Zhang, D. Freitas, H.S. Kim, K. Fabijanic, Z. Li, H. Chen, M.T. Mark, H. Molina, A.B. Martin, L. Bojmar, J. Fang, S. Rampersaud, A. Hoshino, I. Matei, C.M. Kenific, M. Nakajima, A.P. Mutvei, P. Sansone, W. Buehring, H. Wang, J.P. Jimenez, L. Cohen-Gould, N. Paknejad, M. Brendel, K. Manova-Todorova, A. Magalhães, J.A. Ferreira, H. Osório, A.M. Silva, A. Massey, J.R. Cubillos-Ruiz, G. Galletti, P. Giannakakou, A.M. Cuervo, J. Blenis, R. Schwartz, M.S. Brady, H. Peinado, J. Bromberg, H. Matsui, C.A. Reis, D. Lyden, Identification of distinct nanoparticles and subsets of extracellular vesicles by asymmetric flow field-flow fractionation, Nat. Cell Biol. 20 (2018) 332–343, https://doi.org/10.1038/s41556-018-0040-4.

[12] B. György, T.G. Szabó, M. Pásztói, Z. Pál, P. Misják, B. Aradi, V. László, É. Pállinger, E. Pap, Á. Kittel, G. Nagy, A. Falus, E.I. Buzás, Membrane vesicles, current state-of-the-art: emerging role of extracellular vesicles, Cell. Mol. Life Sci. 68 (2011) 2667–2688, https://doi.org/10.1007/s00018-011-0689-3.

[13] F. Momen-Heravi, S.J. Getting, S.A. Moschos, Extracellular vesicles and their nucleic acids for biomarker discovery, Pharmacol. Ther. 192 (2018) 170–187, https://doi.org/10.1016/j.pharmthera.2018.08.002.

[14] D.W. Greening, R.J. Simpson, Understanding extracellular vesicle diversity - current status, Expert Rev. Proteomics 15 (2018) 887–910, https://doi.org/10.1080/14789450.2018.1537788.

[15] M.P. Zaborowski, L. Balaj, X.O. Breakefield, C.P. Lai, Extracellular vesicles: composition, biological relevance, and methods of study, Bioscience 65 (2015) 783–797, https://doi.org/10.1093/biosci/biv084.

[16] C. Théry, K.W. Witwer, E. Aikawa, M.J. Alcaraz, J.D. Anderson, R. Andriantsitohaina, A. Antoniou, T. Arab, F. Archer, G.K. Atkin-Smith, D.C. Ayre, J.-M. Bach, D. Bachurski, H. Baharvand, L. Balaj, S. Baldacchino, N.N. Bauer, A.A. Baxter, M. Bebawy, C. Beckham, A. Bedina Zavec, A. Benmoussa, A.C. Berardi, P. Bergese, E. Bielska, C. Blenkiron, S. Bobis-Wozowicz, E. Boilard, W. Boireau, A. Bongiovanni, F.E. Borràs, S. Bosch, C.M. Boulanger, X. Breakefield, A.M. Breglio, M.Á. Brennan, D.R. Brigstock, A. Brisson, M.L. Broekman, J.F. Bromberg, P. Bryl-Górecka, S. Buch, A.H. Buck, D. Burger, S. Busatto, D. Buschmann, B. Bussolati, E.I. Buzás, J.B. Byrd, G. Camussi, D.R. Carter, S. Caruso, L.W. Chamley, Y.-T. Chang, C. Chen, S. Chen, L. Cheng, A.R. Chin, A. Clayton, S.P. Clerici, A. Cocks, E. Cocucci, R.J. Coffey, A. Cordeiro-da-Silva, Y. Couch, F.A. Coumans, B. Coyle, R. Crescitelli, M.F. Criado, C. D'Souza-Schorey, S. Das, A. Datta Chaudhuri, P. de Candia, E.F. De Santana, O. De Wever, H.A. Del Portillo, T. Demaret, S. Deville, A. Devitt, B. Dhondt, D. Di Vizio, L.C. Dieterich, V. Dolo, A.P. Dominguez Rubio, M. Dominici, M.R. Dourado, T.A. Driedonks, F.V. Duarte, H.M. Duncan, R.M. Eichenberger, K. Ekström, S. El Andaloussi, C. Elie-Caille, U. Erdbrügger, J.M. Falcón-Pérez, F. Fatima, J.E. Fish, M. Flores-Bellver, A. Försönits, A. Frelet-Barrand, F. Fricke, G. Fuhrmann, S. Gabrielsson, A. Gámez-Valero, C. Gardiner, K. Gärtner, R. Gaudin, Y.S. Gho, B. Giebel, C. Gilbert, M. Gimona, I. Giusti, D.C. Goberdhan, A. Görgens, S.M. Gorski, D.W. Greening, J.C. Gross, A. Gualerzi, G.N. Gupta, D. Gustafson, A. Handberg, R.A. Haraszti, P. Harrison, H. Hegyesi, A. Hendrix, A.F. Hill, F.H. Hochberg, K.F. Hoffmann, B. Holder, H. Holthofer, B. Hosseinkhani, G. Hu, Y. Huang, V. Huber, S. Hunt, A.G.-E. Ibrahim, T. Ikezu, J.M. Inal, M. Isin, A. Ivanova, H.K. Jackson, S. Jacobsen, S.M. Jay, M. Jayachandran, G. Jenster, L. Jiang, S.M. Johnson, J.C. Jones, A. Jong, T. Jovanovic-Talisman, S. Jung, R. Kalluri, S.-I. Kano, S. Kaur, Y. Kawamura, E.T. Keller, D. Khamari, E. Khomyakova, A. Khvorova, P. Kierulf, K.P. Kim, T. Kislinger, M. Klingeborn, D.J. Klinke, M. Kornek, M.M. Kosanović, Á.F. Kovács, E.-M. Krämer-Albers, S. Krasemann, M. Krause, I.V. Kurochkin, G.D. Kusuma, S. Kuypers, S. Laitinen, S.M. Langevin, L.R. Languino, J. Lannigan, C. Lässer, L.C. Laurent, G. Lavieu, E. Lázaro-Ibáñez, S. Le Lay, M.-S. Lee, Y.X.F. Lee, D.S. Lemos, M. Lenassi, A. Leszczynska, I.T. Li, K. Liao, S.F. Libregts, E. Ligeti, R. Lim, S.K. Lim, A. Linē, K. Linnemannstöns, A. Llorente, C.A. Lombard, M.J. Lorenowicz, Á.M. Lörincz, J. Lötvall, J. Lovett, M.C. Lowry, X. Loyer, Q. Lu, B. Lukomska, T.R. Lunavat, S.L. Maas, H. Malhi, A. Marcilla, J. Mariani, J. Mariscal, E.S. Martens-Uzunova, L. Martin-Jaular, M.C. Martinez, V.R. Martins, M. Mathieu, S. Mathivanan, M. Maugeri, L.K. McGinnis, M.J. McVey, D.G. Meckes, K.L. Meehan, I. Mertens, V.R. Minciacchi, A. Möller, M. Møller Jørgensen, A. Morales-Kastresana, J. Morhayim, F. Mullier, M. Muraca, L. Musante, V. Mussack, D.C. Muth, K.H. Myburgh, T. Najrana, M. Nawaz, I. Nazarenko, P. Nejsum, C. Neri, T. Neri, R. Nieuwland, L. Nimrichter, J.P. Nolan, E.N. Nolte-'t Hoen, N. Noren Hooten, L. O'Driscoll, T. O'Grady, A. O'Loghlen, T. Ochiya, M. Olivier, A. Ortiz, L.A. Ortiz, X. Osteikoetxea, O. Østergaard, M. Ostrowski, J. Park, D.M. Pegtel, H. Peinado, F. Perut, M.W. Pfaffl, D.G. Phinney, B.C. Pieters, R.C. Pink, D.S. Pisetsky, E. Pogge von Strandmann, I. Polakovicova, I.K. Poon, B.H. Powell, I. Prada, L. Pulliam, P. Quesenberry, A. Radeghieri, R.L. Raffai, S. Raimondo, J. Rak, M.I. Ramirez, G. Raposo, M.S. Rayyan, N. Regev-Rudzki, F.L. Ricklefs, P.D. Robbins, D.D. Roberts, S.C. Rodrigues, E. Rohde, S. Rome, K.M. Rouschop, A. Rughetti, A.E. Russell, P. Saá, S. Sahoo, E. Salas-Huenuleo, C. Sánchez, J.A. Saugstad, M.J. Saul, R.M. Schiffelers, R. Schneider, T.H. Schøyen, A. Scott, E. Shahaj, S. Sharma, O. Shatnyeva, F. Shekari, G.V. Shelke, A.K. Shetty, K. Shiba, P.R.-M. Siljander, A.M. Silva, A. Skowronek, O.L. Snyder, R.P. Soares, B.W. Sódar, C. Soekmadji, J. Sotillo, P.D. Stahl, W. Stoorvogel, S.L. Stott, E.F. Strasser, S. Swift, H. Tahara, M. Tewari, K. Timms, S. Tiwari, R. Tixeira, M. Tkach, W.S. Toh, R. Tomasini, A.C. Torrecilhas, J.P. Tosar, V. Toxavidis, L. Urbanelli, P. Vader, B.W. van Balkom, S.G. van der Grein, J. Van Deun, M.J. van Herwijnen, K. Van Keuren-Jensen, G. van Niel, M.E. van Royen, A.J. van Wijnen, M.H. Vasconcelos, I.J. Vechetti, T.D. Veit, L.J. Vella, É. Velot, F.J. Verweij, B. Vestad, J.L. Viñas, T. Visnovitz, K.V. Vukman, J. Wahlgren, D.C. Watson, M.H. Wauben, A. Weaver, J.P. Webber, V. Weber, A.M. Wehman, D.J. Weiss, J.A. Welsh, S. Wendt, A.M. Wheelock, Z. Wiener, L. Witte, J. Wolfram, A. Xagorari, P. Xander, J. Xu, X. Yan, M. Yáñez-Mó, H. Yin, Y. Yuana, V. Zappulli, J. Zarubova, V. Žėkas, J.-Y. Zhang, Z. Zhao, L. Zheng, A.R. Zheutlin, A.M. Zickler, P. Zimmermann, A.M. Zivkovic, D. Zocco, E.K. Zuba-Surma, Minimal information for studies of extracellular vesicles 2018 (MISEV2018): a position statement of the International Society for Extracellular Vesicles and update of the MISEV2014 guidelines, J. Extracell. Vesicles 7 (2018) 1535750, https://doi.org/10.1080/20013078.2018.1535750.

[17] G. Dostert, B. Mesure, P. Menu, É. Velot, How do mesenchymal stem cells influence or are influenced by microenvironment through extracellular vesicles communication? Front Cell Dev Biol 5 (2017) 6, https://doi.org/10.3389/fcell.2017.00006.

[18] R. Crescitelli, C. Lässer, T.G. Szabó, A. Kittel, M. Eldh, I. Dianzani, E.I. Buzás, J. Lötvall, Distinct RNA profiles in subpopulations of extracellular vesicles: apoptotic bodies, microvesicles and exosomes, J. Extracell. Vesicles 2 (2013), https://doi.org/10.3402/jev.v2i0.20677.

[19] A. Saraste, K. Pulkki, Morphologic and biochemical hallmarks of apoptosis, Cardiovasc. Res. 45 (2000) 528–537.

[20] M. Hristov, W. Erl, S. Linder, P.C. Weber, Apoptotic bodies from endothelial cells enhance the number and initiate the differentiation of human endothelial progenitor cells in vitro, Blood 104 (2004) 2761–2766, https://doi.org/10.1182/blood-2003-10-3614.

[21] K. Al-Nedawi, B. Meehan, J. Rak, Microvesicles: messengers and mediators of tumor progression, Cell Cycle 8 (2009) 2014–2018, https://doi.org/10.4161/cc.8.13.8988.

[22] P.A. Holme, N.O. Solum, F. Brosstad, M. Røger, M. Abdelnoor, Demonstration of platelet-derived microvesicles in blood from patients with activated coagulation and fibrinolysis using a filtration technique and western blotting, Thromb. Haemostasis 72 (1994) 666–671.

[23] E. Cocucci, G. Racchetti, J. Meldolesi, Shedding microvesicles: artefacts no more, Trends Cell Biol. 19 (2009) 43–51, https://doi.org/10.1016/j.tcb.2008.11.003.

[24] G. van Niel, G. D'Angelo, G. Raposo, Shedding light on the cell biology of extracellular vesicles, Nat. Rev. Mol. Cell Biol. 19 (2018) 213–228, https://doi.org/10.1038/nrm.2017.125.

[25] M. Colombo, G. Raposo, C. Théry, Biogenesis, secretion, and intercellular interactions of exosomes and other extracellular vesicles, Annu. Rev. Cell Dev. Biol. 30 (2014) 255–289, https://doi.org/10.1146/annurev-cellbio-101512-122326.

[26] L. Blanc, M. Vidal, New insights into the function of Rab GTPases in the context of exosomal secretion, Small GTPases 9 (2018) 95–106, https://doi.org/10.1080/21541248.2016.1264352.

[27] E. Turola, R. Furlan, F. Bianco, M. Matteoli, C. Verderio, Microglial microvesicle secretion and intercellular signaling, Front. Physiol. 3 (2012) 149, https://doi.org/10.3389/fphys.2012.00149.

[28] C. D'Souza-Schorey, J.W. Clancy, Tumor-derived microvesicles: shedding light on novel microenvironment modulators and prospective cancer biomarkers, Genes Dev. 26 (2012) 1287–1299, https://doi.org/10.1101/gad.192351.112.

[29] G. Raposo, W. Stoorvogel, Extracellular vesicles: exosomes, microvesicles, and friends, J. Cell Biol. 200 (2013) 373–383, https://doi.org/10.1083/jcb.201211138.

[30] N.P. Hessvik, A. Llorente, Current knowledge on exosome biogenesis and

Please cite this article as: A. Galvanin et al., Diversity and heterogeneity of extracellular RNA in human plasma, Biochimie, https://doi.org/10.1016/j.biochi.2019.05.011

release, Cell. Mol. Life Sci. 75 (2018) 193–208, https://doi.org/10.1007/s00018-017-2595-9.
[31] Z. Andreu, M. Yáñez-Mó, Tetraspanins in extracellular vesicle formation and function, Front. Immunol. 5 (2014) 442, https://doi.org/10.3389/fimmu.2014.00442.
[32] A.V. Savelyeva, E.V. Kuligina, D.N. Bariakin, V.V. Kozlov, E.I. Ryabchikova, V.A. Richter, D.V. Semenov, Variety of RNAs in peripheral blood cells, plasma, and plasma fractions, BioMed Res. Int. 2017 (2017), https://doi.org/10.1155/2017/7404912.
[33] R.C. Rennert, F.H. Hochberg, B.S. Carter, ExRNA in biofluids as biomarkers for brain tumors, Cell. Mol. Neurobiol. 36 (2016) 353–360, https://doi.org/10.1007/s10571-015-0284-5.
[34] T. Yuan, X. Huang, M. Woodcock, M. Du, R. Dittmar, Y. Wang, S. Tsai, M. Kohli, L. Boardman, T. Patel, L. Wang, Plasma extracellular RNA profiles in healthy and cancer patients, Sci. Rep. 6 (2016) 19413, https://doi.org/10.1038/srep19413.
[35] M. Li, E. Zeringer, T. Barta, J. Schageman, A. Cheng, A.V. Vlassov, Analysis of the RNA content of the exosomes derived from blood serum and urine and its potential as biomarkers, Philos. Trans. R. Soc. Lond. B Biol. Sci. 369 (2014), https://doi.org/10.1098/rstb.2013.0502.
[36] M. He, Y. Zeng, Microfluidic exosome analysis toward liquid biopsy for cancer, J. Lab. Autom. 21 (2016) 599–608, https://doi.org/10.1177/2211068216651035.
[37] V.R. Minciacchi, A. Zijlstra, M.A. Rubin, D. Di Vizio, Extracellular vesicles for liquid biopsy in prostate cancer: where are we and where are we headed? Prostate Cancer Prostatic Dis. 20 (2017) 251–258, https://doi.org/10.1038/pcan.2017.7.
[38] A.J. Mitchell, W.D. Gray, S.S. Hayek, Y.-A. Ko, S. Thomas, K. Rooney, M. Awad, J.D. Roback, A. Quyyumi, C.D. Searles, Platelets confound the measurement of extracellular miRNA in archived plasma, Sci. Rep. 6 (2016) 32651, https://doi.org/10.1038/srep32651.
[39] B. Mateescu, E.J.K. Kowal, B.W.M. van Balkom, S. Bartel, S.N. Bhattacharyya, E.I. Buzás, A.H. Buck, P. de Candia, F.W.N. Chow, S. Das, T.A.P. Driedonks, L. Fernández-Messina, F. Haderk, A.F. Hill, J.C. Jones, K.R.V. Keuren-Jensen, C.P. Lai, C. Lässer, I. di Liegro, T.R. Lunavat, M.J. Lorenowicz, S.L.N. Maas, I. Mäger, M. Mittelbrunn, S. Momma, K. Mukherjee, M. Nawaz, D.M. Pegtel, M.W. Pfaffl, R.M. Schiffelers, H. Tahara, C. Théry, J.P. Tosar, M.H.M. Wauben, K.W. Witwer, E.N.M.N.-'t Hoen, Obstacles and opportunities in the functional analysis of extracellular vesicle RNA — an ISEV position paper, J. Extracell. Vesicles 6 (2017) 1286095, https://doi.org/10.1080/20013078.2017.1286095.
[40] E. Beutler, T. Gelbart, W. Kuhl, Interference of heparin with the polymerase chain reaction, Biotechniques 9 (1990) 166.
[41] R. Lacroix, C. Judicone, M. Mooberry, M. Boucekine, N.S. Key, F. Dignat-George, The ISTH SSC Workshop, Standardization of pre-analytical variables in plasma microparticle determination: results of the International Society on Thrombosis and Haemostasis SSC Collaborative workshop, J. Thromb. Haemost. (2013), https://doi.org/10.1111/jth.12207.
[42] M. Yokota, N. Tatsumi, O. Nathalang, T. Yamada, I. Tsuda, Effects of heparin on polymerase chain reaction for blood white cells, J. Clin. Lab. Anal. 13 (1999) 133–140, https://doi.org/10.1002/(SICI)1098-2825(1999)13:3<133::AID-JCLA8>3.0.CO;2-0.
[43] M. Eldh, J. Lötvall, C. Malmhäll, K. Ekström, Importance of RNA isolation methods for analysis of exosomal RNA: evaluation of different methods, Mol. Immunol. 50 (2012) 278–286, https://doi.org/10.1016/j.molimm.2012.02.001.
[44] A.M. Hoy, A.H. Buck, Extracellular small RNAs: what, where, why?: Figure 1, Biochem. Soc. Trans. 40 (2012) 886–890, https://doi.org/10.1042/BST20120019.
[45] A. Etheridge, K. Wang, D. Baxter, D. Galas, Preparation of small RNA NGS libraries from biofluids, Methods Mol. Biol. 1740 (2018) 163–175, https://doi.org/10.1007/978-1-4939-7652-2_13.
[46] C. Soekmadji, A.F. Hill, M.H. Wauben, E.I. Buzás, D. Di Vizio, C. Gardiner, J. Lötvall, S. Sahoo, K.W. Witwer, Towards mechanisms and standardization in extracellular vesicle and extracellular RNA studies: results of a worldwide survey, J. Extracell. Vesicles 7 (2018) 1535745, https://doi.org/10.1080/20013078.2018.1535745.
[47] J. Small, S. Roy, R. Alexander, L. Balaj, Overview of protocols for studying extracellular RNA and extracellular vesicles, Methods Mol. Biol. 1740 (2018) 17–21, https://doi.org/10.1007/978-1-4939-7652-2_2.
[48] J. De Toro, L. Herschlik, C. Waldner, C. Mongini, Emerging roles of exosomes in normal and pathological conditions: new insights for diagnosis and therapeutic applications, Front. Immunol. 6 (2015), https://doi.org/10.3389/fimmu.2015.00203.
[49] C.V. Harding, J.E. Heuser, P.D. Stahl, Exosomes: looking back three decades and into the future, J. Cell Biol. 200 (2013) 367–371, https://doi.org/10.1083/jcb.201212113.
[50] D.D. Taylor, C. Gercel-Taylor, The origin, function, and diagnostic potential of RNA within extracellular vesicles present in human biological fluids, Front. Genet. 4 (2013), https://doi.org/10.3389/fgene.2013.00142.
[51] C. Théry, S. Amigorena, G. Raposo, A. Clayton, Isolation and characterization of exosomes from cell culture supernatants and biological fluids, Curr Protoc Cell Biol. Chapter 3 (2006), https://doi.org/10.1002/0471143030.cb0322s30. Unit 3.22.
[52] H.M. Colhoun, J.D. Otvos, M.B. Rubens, M.R. Taskinen, S.R. Underwood, J.H. Fuller, Lipoprotein subclasses and particle sizes and their relationship with coronary artery calcification in men and women with and without type 1 diabetes, Diabetes 51 (2002) 1949–1956.
[53] R.P. Alexander, N.-T. Chiou, K.M. Ansel, Improved Exosome Isolation by Sucrose Gradient Fractionation of Ultracentrifuged Crude Exosome Pellets, Protocol Exchange, 2016, https://doi.org/10.1038/protex.2016.057.
[54] K. Li, D.K. Wong, K.Y. Hong, R.L. Raffai, Cushioned-density gradient ultracentrifugation (C-DGUC): a refined and high performance method for the isolation, characterization, and use of exosomes, Methods Mol. Biol. 1740 (2018) 69–83, https://doi.org/10.1007/978-1-4939-7652-2_7.
[55] S.I. Brett, F. Lucien, C. Guo, K.C. Williams, Y. Kim, P.N. Durfee, C.J. Brinker, J.I. Chin, J. Yang, H.S. Leong, Immunoaffinity based methods are superior to kits for purification of prostate derived extracellular vesicles from plasma samples, Prostate 77 (2017) 1335–1343, https://doi.org/10.1002/pros.23393.
[56] P. Sharma, S. Ludwig, L. Muller, C.S. Hong, J.M. Kirkwood, S. Ferrone, T.L. Whiteside, Immunoaffinity-based isolation of melanoma cell-derived exosomes from plasma of patients with melanoma, J. Extracell. Vesicles 7 (2018) 1435138, https://doi.org/10.1080/20013078.2018.1435138.
[57] D. Zocco, N. Zarovni, Extraction and analysis of extracellular vesicle-associated miRNAs following antibody-based extracellular vesicle capture from plasma samples, Methods Mol. Biol. 1660 (2017) 269–285, https://doi.org/10.1007/978-1-4939-7253-1_22.
[58] J. Van Deun, P. Mestdagh, R. Sormunen, V. Cocquyt, K. Vermaelen, J. Vandesompele, M. Bracke, O. De Wever, A. Hendrix, The impact of disparate isolation methods for extracellular vesicles on downstream RNA profiling, J. Extracell. Vesicles 3 (2014), https://doi.org/10.3402/jev.v3.24858.
[59] Z. Andreu, E. Rivas, A. Sanguino-Pascual, A. Lamana, M. Marazuela, I. González-Alvaro, F. Sánchez-Madrid, H. de la Fuente, M. Yáñez-Mó, Comparative analysis of EV isolation procedures for miRNAs detection in serum samples, J. Extracell. Vesicles 5 (2016), https://doi.org/10.3402/jev.v5.31655.
[60] R. Stranska, L. Gysbrechts, J. Wouters, P. Vermeersch, K. Bloch, D. Dierickx, G. Andrei, R. Snoeck, Comparison of membrane affinity-based method with size-exclusion chromatography for isolation of exosome-like vesicles from human plasma, J. Transl. Med. 16 (2018) 1, https://doi.org/10.1186/s12967-017-1374-6.
[61] A.N. Böing, E. van der Pol, A.E. Grootemaat, F.A.W. Coumans, A. Sturk, R. Nieuwland, Single-step isolation of extracellular vesicles by size-exclusion chromatography, J. Extracell. Vesicles 3 (2014), https://doi.org/10.3402/jev.v3.23430.
[62] S.D. Ibsen, J. Wright, J.M. Lewis, S. Kim, S.-Y. Ko, J. Ong, S. Manouchehri, A. Vyas, J. Akers, C.C. Chen, B.S. Carter, S.C. Esener, M.J. Heller, Rapid isolation and detection of exosomes and associated biomarkers from plasma, ACS Nano 11 (2017) 6641–6651, https://doi.org/10.1021/acsnano.7b00549.
[63] B. Vestad, A. Llorente, A. Neurauter, S. Phuyal, B. Kierulf, P. Kierulf, T. Skotland, K. Sandvig, K.B.F. Haug, R. Øvstebø, Size and concentration analyses of extracellular vesicles by nanoparticle tracking analysis: a variation study, J. Extracell. Vesicles 6 (2017) 1344087, https://doi.org/10.1080/20013078.2017.1344087.
[64] L. Reimer, Transmission Electron Microscopy: Physics of Image Formation and Microanalysis, Springer-Verlag, Berlin Heidelberg, 1984. //www.springer.com/la/book/9783662135532. (Accessed 29 January 2019).
[65] M. Adrian, J. Dubochet, J. Lepault, A.W. McDowall, Cryo-electron microscopy of viruses, Nature 308 (1984) 32–36.
[66] Y. Wu, W. Deng, D.J. Klinke, Exosomes: improved methods to characterize their morphology, RNA content, and surface protein biomarkers, Analyst 140 (2015) 6631–6642, https://doi.org/10.1039/c5an00688k.
[67] A.S. Lawrie, A. Albanyan, R.A. Cardigan, I.J. Mackie, P. Harrison, Microparticle sizing by dynamic light scattering in fresh-frozen plasma, Vox Sang. 96 (2009) 206–212, https://doi.org/10.1111/j.1423-0410.2008.01151.x.
[68] C. Gercel-Taylor, S. Atay, R.H. Tullis, M. Kesimer, D.D. Taylor, Nanoparticle analysis of circulating cell-derived vesicles in ovarian cancer patients, Anal. Biochem. 428 (2012) 44–53, https://doi.org/10.1016/j.ab.2012.06.004.
[69] E.J.K. Kowal, D. Ter-Ovanesyan, A. Regev, G.M. Church, Extracellular vesicle isolation and analysis by western blotting, Methods Mol. Biol. 1660 (2017) 143–152, https://doi.org/10.1007/978-1-4939-7253-1_12.
[70] C. Gardiner, D. Di Vizio, S. Sahoo, C. Théry, K.W. Witwer, M. Wauben, A.F. Hill, Techniques used for the isolation and characterization of extracellular vesicles: results of a worldwide survey, J. Extracell. Vesicles 5 (2016) 32945, https://doi.org/10.3402/jev.v5.32945.
[71] H. Valadi, K. Ekström, A. Bossios, M. Sjöstrand, J.J. Lee, J.O. Lötvall, Exosome-mediated transfer of mRNAs and microRNAs is a novel mechanism of genetic exchange between cells, Nat. Cell Biol. 9 (2007) 654–659, https://doi.org/10.1038/ncb1596.
[72] N.J. Park, H. Zhou, D. Elashoff, B.S. Henson, D.A. Kastratovic, E. Abemayor, D.T. Wong, Salivary microRNA: discovery, characterization, and clinical utility for oral cancer detection, Clin. Cancer Res. 15 (2009) 5473–5477, https://doi.org/10.1158/1078-0432.CCR-09-0736.
[73] M. Hanke, K. Hoefig, H. Merz, A.C. Feller, I. Kausch, D. Jocham, J.M. Warnecke, G. Sczakiel, A robust methodology to study urine microRNA as tumor marker: microRNA-126 and microRNA-182 are related to urinary bladder cancer, Urol. Oncol. 28 (2010) 655–661, https://doi.org/10.1016/j.urolonc.2009.01.027.
[74] D. Zubakov, A.W.M. Boersma, Y. Choi, P.F. van Kuijk, E.A.C. Wiemer, M. Kayser, MicroRNA markers for forensic body fluid identification obtained from microarray screening and quantitative RT-PCR confirmation, Int. J. Leg. Med. 124 (2010) 217–226, https://doi.org/10.1007/s00414-009-0402-3.
[75] Y. Guo, K. Vickers, Y. Xiong, S. Zhao, Q. Sheng, P. Zhang, W. Zhou, C.R. Flynn, Comprehensive evaluation of extracellular small RNA isolation methods from serum in high throughput sequencing, BMC Genomics 18 (2017), https://doi.org/10.1186/s12864-016-3470-z.

Please cite this article as: A. Galvanin et al., Diversity and heterogeneity of extracellular RNA in human plasma, Biochimie, https://doi.org/10.1016/j.biochi.2019.05.011

[76] J.E. Freedman, M. Gerstein, E. Mick, J. Rozowsky, D. Levy, R. Kitchen, S. Das, R. Shah, K. Danielson, L. Beaulieu, F.C.P. Navarro, Y. Wang, T.R. Galeev, A. Holman, R.Y. Kwong, V. Murthy, S.E. Tanriverdi, M. Koupenova-Zamor, E. Mikhalev, K. Tanriverdi, Diverse human extracellular RNAs are widely detected in human plasma, Nat. Commun. 7 (2016) 11106, https://doi.org/10.1038/ncomms11106.

[77] K.E.A. Max, K. Bertram, K.M. Akat, K.A. Bogardus, J. Li, P. Morozov, I.Z. Ben-Dov, X. Li, Z.R. Weiss, A. Azizian, A. Sopeyin, T.G. Diacovo, C. Adamidi, Z. Williams, T. Tuschl, Human plasma and serum extracellular small RNA reference profiles and their clinical utility, Proc. Natl. Acad. Sci. U. S. A. 115 (2018) E5334–E5343, https://doi.org/10.1073/pnas.1714397115.

[78] X. Huang, T. Yuan, M. Tschannen, Z. Sun, H. Jacob, M. Du, M. Liang, R.L. Dittmar, Y. Liu, M. Liang, M. Kohli, S.N. Thibodeau, L. Boardman, L. Wang, Characterization of human plasma-derived exosomal RNAs by deep sequencing, BMC Genomics 14 (2013) 319, https://doi.org/10.1186/1471-2164-14-319.

[79] M.G. Amorim, R. Valieris, R.D. Drummond, M.P. Pizzi, V.M. Freitas, R. Sinigaglia-Coimbra, G.A. Calin, R. Pasqualini, W. Arap, I.T. Silva, E. Dias-Neto, D.N. Nunes, A total transcriptome profiling method for plasma-derived extracellular vesicles: applications for liquid biopsies, Sci. Rep. 7 (2017), https://doi.org/10.1038/s41598-017-14264-5.

[80] S.U. Umu, H. Langseth, C. Bucher-Johannessen, B. Fromm, A. Keller, E. Meese, M. Lauritzen, M. Leithaug, R. Lyle, T.B. Rounge, A comprehensive profile of circulating RNAs in human serum, RNA Biol. 15 (2018) 242–250, https://doi.org/10.1080/15476286.2017.1403003.

[81] K.M. Danielson, R. Rubio, F. Abderazzaq, S. Das, Y.E. Wang, High throughput sequencing of extracellular RNA from human plasma, PLoS One 12 (2017), https://doi.org/10.1371/journal.pone.0164644 e0164644.

[82] H.H. Cheng, H.S. Yi, Y. Kim, E.M. Kroh, J.W. Chien, K.D. Eaton, M.T. Goodman, J.F. Tait, M. Tewari, C.C. Pritchard, Plasma processing conditions substantially influence circulating microRNA biomarker levels, PLoS One 8 (2013), https://doi.org/10.1371/journal.pone.0064795 e64795.

[83] J.P. Tosar, A. Cayota, E. Eitan, M.K. Halushka, K.W. Witwer, Ribonucleic artefacts: are some extracellular RNA discoveries driven by cell culture medium components? J. Extracell. Vesicles 6 (2017) 1272832, https://doi.org/10.1080/20013078.2016.1272832.

[84] A.M. Ainsztein, P.J. Brooks, V.G. Dugan, A. Ganguly, M. Guo, T.K. Howcroft, C.A. Kelley, L.S. Kuo, P.A. Labosky, R. Lenzi, G.A. McKie, S. Mohla, D. Procaccini, M. Reilly, J.S. Satterlee, P.R. Srinivas, E.S. Church, M. Sutherland, D.A. Tagle, J.M. Tucker, S. Venkatachalam, The NIH extracellular RNA communication consortium, J. Extracell. Vesicles 4 (2015) 27493.

[85] A.M. Bolger, M. Lohse, B. Usadel, Trimmomatic: a flexible trimmer for Illumina sequence data, Bioinformatics 30 (2014) 2114–2120, https://doi.org/10.1093/bioinformatics/btu170.

[86] C. Quast, E. Pruesse, P. Yilmaz, J. Gerken, T. Schweer, P. Yarza, J. Peplies, F.O. Glöckner, The SILVA ribosomal RNA gene database project: improved data processing and web-based tools, Nucleic Acids Res. 41 (2013) D590–D596, https://doi.org/10.1093/nar/gks1219.

[87] B. György, K. Módos, É. Pállinger, K. Pálóczi, M. Pásztói, P. Misják, M.A. Deli, A. Sipos, A. Szalai, I. Voszka, A. Polgár, K. Tóth, M. Csete, G. Nagy, S. Gay, A. Falus, A. Kittel, E.I. Buzás, Detection and isolation of cell-derived microparticles are compromised by protein complexes resulting from shared biophysical parameters, Blood 117 (2011) e39–e48, https://doi.org/10.1182/blood-2010-09-307595.

[88] Y.-T. Tang, Y.-Y. Huang, L. Zheng, S.-H. Qin, X.-P. Xu, T.-X. An, Y. Xu, Y.-S. Wu, X.-M. Hu, B.-H. Ping, Q. Wang, Comparison of isolation methods of exosomes and exosomal RNA from cell culture medium and serum, Int. J. Mol. Med. 40 (2017) 834–844, https://doi.org/10.3892/ijmm.2017.3080.

[89] A.E. Grigor'eva, N.S. Dyrkheeva, O.E. Bryzgunova, S.N. Tamkovich, B.P. Chelobanov, E.I. Ryabchikova, [Contamination of exosome preparations, isolated from biological fluids], Biomed Khim 63 (2017) 91–96, https://doi.org/10.18097/PBMC20176301 91.

[90] V. Filipe, A. Hawe, W. Jiskoot, Critical evaluation of Nanoparticle Tracking Analysis (NTA) by NanoSight for the measurement of nanoparticles and protein aggregates, Pharm. Res. (N. Y.) 27 (2010) 796–810, https://doi.org/10.1007/s11095-010-0073-2.

[91] F. Royo, K. Schlangen, L. Palomo, E. Gonzalez, J. Conde-Vancells, A. Berisa, A.M. Aransay, J.M. Falcon-Perez, Transcriptome of extracellular vesicles released by hepatocytes, PLoS One 8 (2013), https://doi.org/10.1371/journal.pone.0068693 e68693.

[92] F.A. San Lucas, K. Allenson, V. Bernard, J. Castillo, D.U. Kim, K. Ellis, E.A. Ehli, G.E. Davies, J.L. Petersen, D. Li, R. Wolff, M. Katz, G. Varadhachary, I. Wistuba, A. Maitra, H. Alvarez, Minimally invasive genomic and transcriptomic profiling of visceral cancers by next-generation sequencing of circulating exosomes, Ann. Oncol. 27 (2016) 635–641, https://doi.org/10.1093/annonc/mdv604.

[93] D. Khare, N. Goldschmidt, A. Bardugo, D. Gur-Wahnon, I.Z. Ben-Dov, B. Avni, Plasma microRNA profiling: exploring better biomarkers for lymphoma surveillance, PLoS One 12 (2017), https://doi.org/10.1371/journal.pone.0187722.

[94] M. Ding, C. Wang, X. Lu, C. Zhang, Z. Zhou, X. Chen, C.-Y. Zhang, K. Zen, C. Zhang, Comparison of commercial exosome isolation kits for circulating exosomal microRNA profiling, Anal. Bioanal. Chem. 410 (2018) 3805–3814, https://doi.org/10.1007/s00216-018-1052-4.

[95] I. Helwa, J. Cai, M.D. Drewry, A. Zimmerman, M.B. Dinkins, M.L. Khaled, M. Seremwe, W.M. Dismuke, E. Bieberich, W.D. Stamer, M.W. Hamrick, Y. Liu, A comparative study of serum exosome isolation using differential ultracentrifugation and three commercial reagents, PLoS One 12 (2017), https://doi.org/10.1371/journal.pone.0170628.

[96] G.K. Patel, M.A. Khan, H. Zubair, S.K. Srivastava, M. Khushman, S. Singh, A.P. Singh, Comparative analysis of exosome isolation methods using culture supernatant for optimum yield, purity and downstream applications, Sci. Rep. 9 (2019), https://doi.org/10.1038/s41598-019-41800-2.

[97] M.W. Carroll, S. Haldenby, N.Y. Rickett, B. Pályi, I. Garcia-Dorival, X. Liu, G. Barker, J.A. Bore, F.R. Koundouno, E.D. Williamson, T.R. Laws, R. Kerber, D. Sissoko, N. Magyar, A. Di Caro, M. Biava, T.E. Fletcher, A. Sprecher, L.F.P. Ng, L. Rénia, N. Magassouba, S. Günther, R. Wölfel, K. Stoecker, D.A. Matthews, J.A. Hiscox, Deep sequencing of RNA from blood and oral swab samples reveals the presence of nucleic acid from a number of pathogens in patients with acute ebola virus disease and is consistent with bacterial translocation across the gut, mSphere 2 (2017), https://doi.org/10.1128/mSphereDirect.00325-17.

[98] A. Heintz-Buschart, D. Yusuf, A. Kaysen, A. Etheridge, J.V. Fritz, P. May, C. de Beaufort, B.B. Upadhyaya, A. Ghosal, D.J. Galas, P. Wilmes, Small RNA profiling of low biomass samples: identification and removal of contaminants, BMC Biol. 16 (2018) 52, https://doi.org/10.1186/s12915-018-0522-7.

Please cite this article as: A. Galvanin et al., Diversity and heterogeneity of extracellular RNA in human plasma, Biochimie, https://doi.org/10.1016/j.biochi.2019.05.011

Annexe 2

Chapter 21

Mapping and Quantification of tRNA 2′-*O*-Methylation by RiboMethSeq

Adeline Galvanin, Lilia Ayadi, Mark Helm, Yuri Motorin, and Virginie Marchand

Abstract

Current development of epitranscriptomics field requires efficient experimental protocols for precise mapping and quantification of various modified nucleotides in RNA. Despite important advances in the field during the last 10 years, this task is still extremely laborious and time-consuming, even when high-throughput analytical approaches are employed. Moreover, only a very limited subset of RNA modifications can be detected and only rarely be quantified by these powerful techniques. In the past, we developed and successfully applied alkaline fragmentation-based RiboMethSeq approach for mapping and precise quantification of multiple 2′-*O*-methylation residues in ribosomal RNA. Here we describe a RiboMethSeq protocol adapted for the analysis of bacterial and eukaryotic tRNA species, which also contain 2′-*O*-methylations at functionally important RNA regions.

Key words 2′-*O*-Methylation, High-throughput sequencing, tRNA modification, Ribose methylation, Alkaline fragmentation

1 Introduction

Following transcription, nascent cellular RNAs undergo complex posttranscriptional maturation, which includes a multitude of chemical modifications altering parental nucleotides in RNA chain. One of the most frequent RNA modification is the addition of a methyl group occurring on a nucleobase or on the 2′-OH of the ribose [1–4]. The major current challenge in the epitranscriptomics field is a careful mapping of different RNA modifications, as well as precise quantification of the modification rate for every given site. Taking into account that methylated nucleotides are found in almost every studied RNA species, and their presence allows fine modulation (tuning) of RNA properties in different cellular processes [5–8], it is essential to develop appropriate high-throughput analysis techniques. Previous studies were only focused on individual modification sites and thus experiments were

Narendra Wajapeyee and Romi Gupta (eds.), *Epitranscriptomics: Methods and Protocols*, Methods in Molecular Biology, vol. 1870, https://doi.org/10.1007/978-1-4939-8808-2_21,

tedious and time consuming [9–13]. Recently we developed the RiboMethSeq protocol for mapping 2′-*O*-methylation sites by alkaline hydrolysis coupled to Illumina next generation sequencing [14, 15]. Ribose methylation protects the 3′-adjacent phosphodiester bond from cleavage at alkaline conditions, while all other phosphodiester bonds in RNA remain sensitive to alkaline hydrolysis, creating a more or less regular cleavage profile. Thus, an important protection observed at a given phosphodiester bond is an indication for the presence of a 2′-*O*-methylation at the 5′-adjacent nucleotide.

Together with ribosomal RNA (rRNA), one of the best-known RNA species are the transfer RNA (tRNA), whose properties and functions have now been studied for decades. However, due to tRNA small size, their rather stable secondary (2D) and tertiary (3D) structures as well as an important proportion of other modified nucleotides, the RiboMethSeq protocol had to be considerably amended for tRNA analysis [16]. Moreover, tRNAs represent only 10–15% of total RNA contrary to at least 80% for rRNA. Thus, it is crucially important to enrich tRNA population before library preparation in order to avoid parasitic rRNA sequencing leading to a decrease in the reading depth (coverage) for target species.

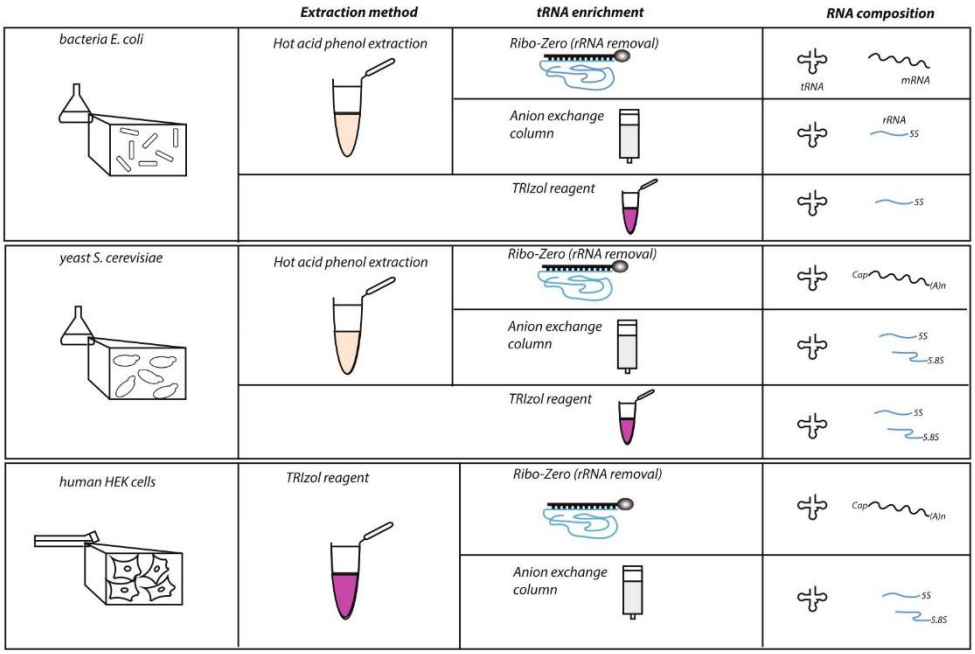

Fig. 1 Overview of tRNA enrichment procedure from bacterial, yeast, and human total RNA. The flow chart depicts the different total RNA extraction techniques and tRNA enrichment protocols used for bacteria, yeast, and human

Here we describe an experimental procedure for mapping and quantification of tRNA 2′-*O*-methylated residues by Illumina RiboMethSeq protocol. Previously reported bacterial and yeast tRNA 2′-*O*-methylation sites can be detected and quantified. We also performed comparative analysis of several popular small RNA purification procedures used for tRNA enrichment (Fig. 1). Bias-free tRNA isolation can be achieved by anion exchange chromatography (Macherey Nagel) or rRNA removal by Ribo-Zero kits (Illumina) (Figs. 2 and 3). Unexpectedly, tRNA enrichment for bacteria can also be achieved by TRIzol™ -based cell lysis protocol.

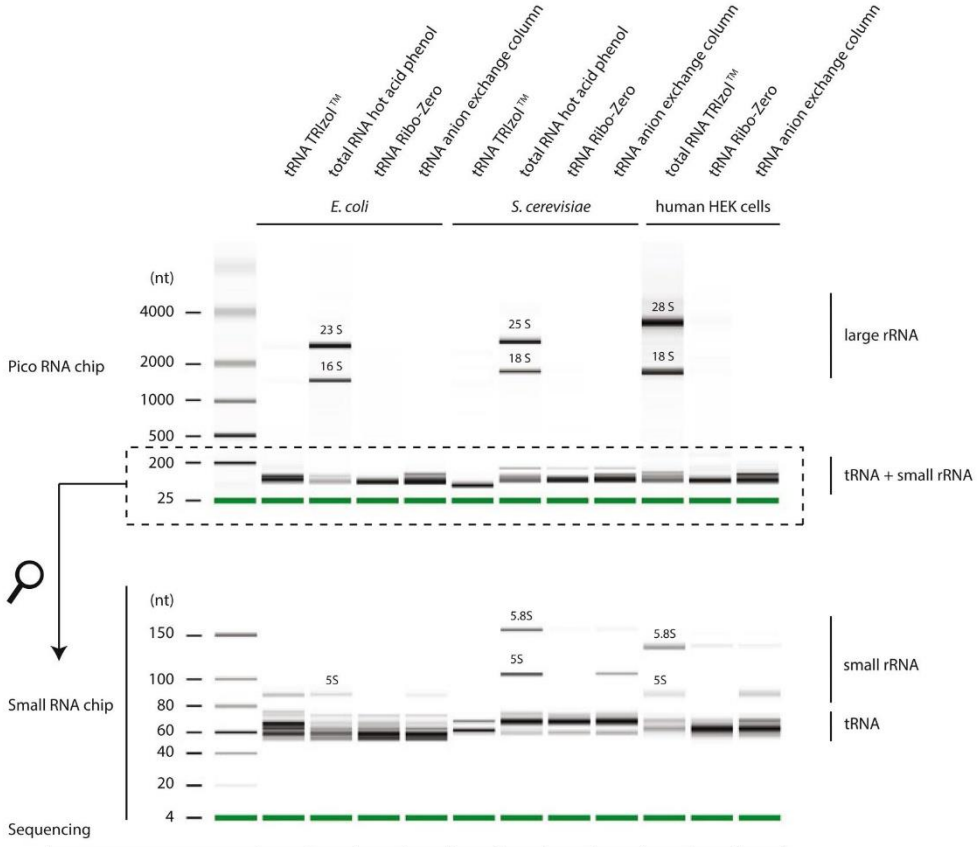

% of reads aligned for tRNA	40.4	6.1	52.6	48.2	50.7	7.8	41.0	25.3	3.5	17.8	16.3
% of reads aligned for rRNA	40.7	84.3	5.4	35.1	38.5	83.5	29.4	63.9	85.1	19.9	48.7

Fig. 2 Capillary electrophoresis profiles of total RNA and tRNA fractions obtained by different extraction methods for bacteria, yeast, and human. Top panel—Pico RNA chip (separation range 25–5000 nt), bottom panel—Small RNA chip (separation range 4–200 nt). Appropriate RNA ladder is loaded at the first lane. Migration positions for rRNAs and tRNAs are indicated at the right. The table at the bottom shows the % of total reads aligned to tRNA and to rRNA

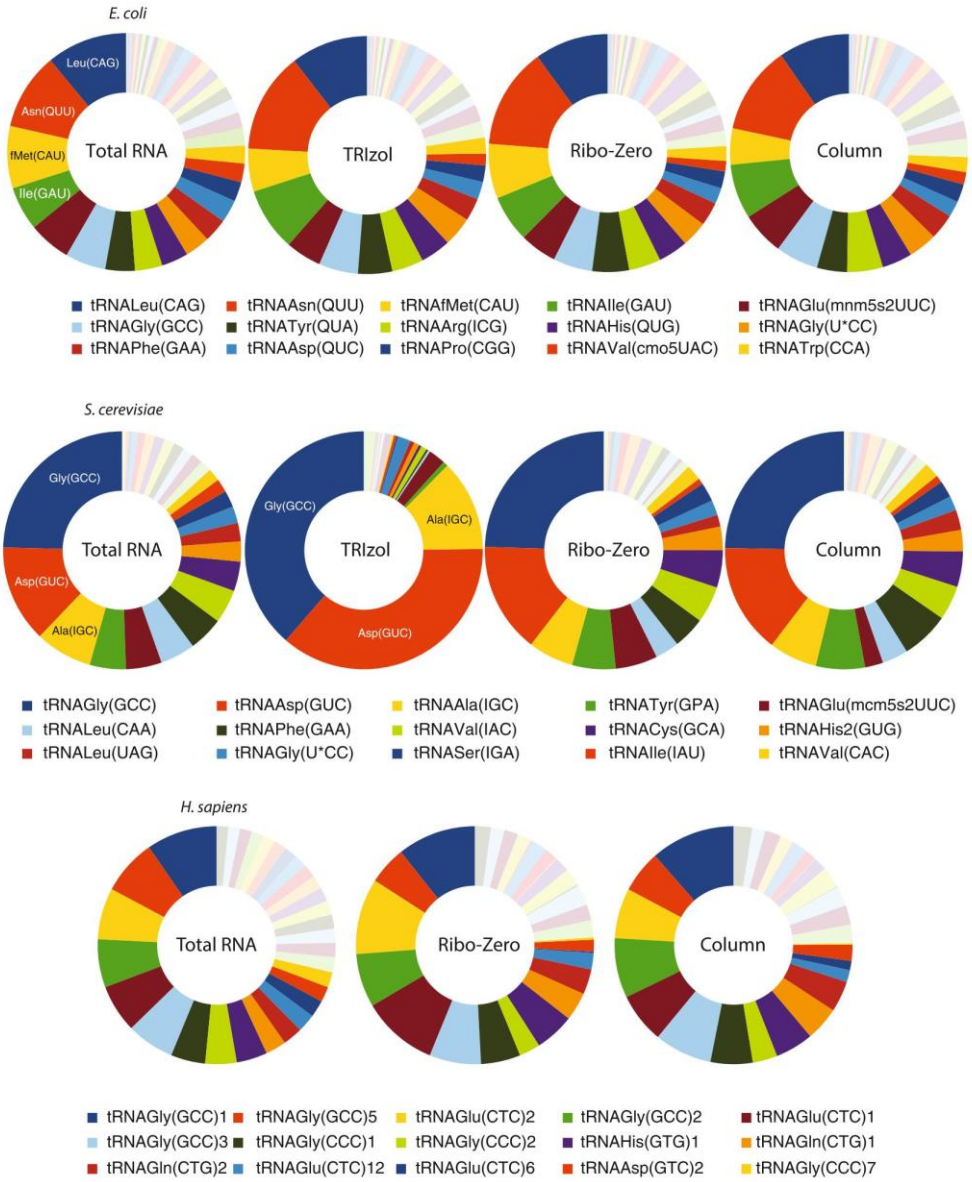

Fig. 3 Observed biases with the different tRNA enrichment techniques. Analysis of tRNA fractions composition for *E. coli*, *S. cerevisiae*, and *H. sapiens*. Proportion of sequencing reads mapped to different tRNA species in total RNA fraction (hot acid phenol extraction), in tRNAs extracted by TRIzol™, by Ribo-Zero rRNA removal kit and by AXR 80 anion-exchange column. Identity of the 15 most abundant tRNA species is shown at the bottom. Other less abundant tRNA species are shaded. For human HEK cells, total RNA fraction was extracted with TRIzol™ protocol, only the 30 most abundant tRNA species are shown

However, TRIzol™ -based RNA extraction protocol is restricted to bacteria, since our results show a strong bias in tRNA composition of small RNA fraction obtained from yeast cells (Fig. 3).

2 Materials

Prepare all solutions using RNase-free water. Wear gloves to prevent degradation of RNA samples by RNases.

2.1 Total RNA Extraction

2.1.1 Yeast and Bacteria Total RNA Extraction by Hot Acid Phenol

1. Yeast or bacteria cell culture (10 mL of culture grown to an OD600 of 0.7–2).
2. RNase-free 1.5 mL microcentrifuge tubes.
3. RNase-free water.
4. AE buffer: 50 mM NaOAc in water, pH 5.2, 10 mM EDTA.
5. 10% (w/v) SDS.
6. Acid phenol, pH 4.5.
7. Phenol:Chloroform:Isoamyl alcohol mix (25:24:1, v/v).
8. Chloroform.
9. 3 M NaOAc in water, pH 5.2.
10. 96% Ethanol.
11. 80% Ethanol.
12. Dry ice.
13. Refrigerated tabletop centrifuge.
14. Water bath or heating block set to 65 °C.
15. UV-spectrophotometer.

2.1.2 Human Total RNA Extraction by TRIzol™

1. Human HEK cells (8–10 × 10^6 cells grown to 90–100% confluence in a cell culture Petri dish).
2. 10× PBS pH 7.4 (Gibco).
3. RNase-free 1.5 mL microcentrifuge tubes.
4. RNase-free water.
5. TRIzol™ reagent.
6. Chloroform.
7. Refrigerated tabletop centrifuge.
8. Isopropanol.
9. 15 mg/mL GlycoBlue coprecipitant (e.g., Ambion).
10. 75% Ethanol.

2.2 tRNA Purification/ Enrichment

2.2.1 tRNA Enrichment by Column Chromatography

1. NucleoBond® RNA/DNA kit containing AXR 80 anion exchange columns and buffers (Macherey-Nagel) (*see* **Note 1**).
2. RNase-free 1.5 mL microcentrifuge tubes.
3. RNase-free 5 mL microcentrifuge tubes.
4. Isopropanol.
5. 15 mg/mL GlycoBlue coprecipitant (e.g., Ambion).
6. Refrigerated tabletop centrifuge.
7. 80% Ethanol.
8. RNase-free water.

2.2.2 tRNA Enrichment by rRNA Depletion

1. Ribo-Zero rRNA removal kits: Human/Mouse/Rat or Yeast or Gram-negative Bacteria (Illumina).
2. RNase-free 1.5 mL microcentrifuge tubes.
3. Magnetic stand.
4. RNase-free water.
5. RNase-free 0.2 mL PCR tubes.
6. Heating block or thermal cycler.
7. 3 M NaOAc in water, pH 5.2.
8. 15 mg/mL GlycoBlue coprecipitant (e.g., Ambion).
9. 96% Ethanol.
10. 80% Ethanol.
11. Refrigerated tabletop centrifuge.

2.2.3 tRNA Enrichment by Selective TRIzol™ Extraction (Only Recommended for Bacteria)

1. Bacteria (DH5α) culture (10 mL of culture grown to exponential phase to an OD_{600} of 0.7–2).
2. RNase-free 50 mL Falcon tubes.
3. 10× PBS pH 7.4 (Gibco).
4. RNase-free 1.5 mL microcentrifuge tubes.
5. TRIzol™ reagent.
6. Chloroform.
7. Refrigerated tabletop centrifuge.
8. Isopropanol.
9. 15 mg/mL GlycoBlue coprecipitant (e.g., Ambion).
10. 75% Ethanol.
11. RNase-free water.

2.3 RNA Quantification and tRNA Quality Control

2.3.1 RNA Quantification

1. UV-visible spectrophotometer for small volumes: any kind of UV-visible spectrophotometer allowing measurements of 1 µL samples. We use NanoDrop™ 2000.
2. RNase-free 1.5 mL microcentrifuge tubes.
3. RNase-free water.

2.3.2 tRNA Quality Assessment

1. Agilent 2100 Bioanalyzer or 2200 TapeStation (Agilent Technologies) or Experion (BioRad) or LabChip GX (Caliper). We use an Agilent 2100 Bioanalyzer.
2. Agilent RNA 6000 Pico kit (quantitative range 50–5000 pg/µL) (*see* **Note 2**).
3. Chip priming station (Agilent Technologies).
4. RNase-free 1.5 mL microcentrifuge tubes.
5. RNase-free water.

2.4 Alkaline Hydrolysis and tRNA Fragmentation Quality Control

2.4.1 Alkaline Hydrolysis

1. Sodium bicarbonate buffer: 100 mM, pH 9.2.
2. RNase-free water.
3. Individual RNase-free 0.2 mL PCR tubes.
4. PCR Thermal cycler (we use Agilent SureCycler 8000).
5. RNase-free 1.5 mL microcentrifuge tubes.
6. 96% Ethanol.
7. 15 mg/mL GlycoBlue™ coprecipitant (e.g., Ambion). To homogenize.
8. 3M NaOAc in water, pH5.2. To homogenize.
9. Dewar containing liquid nitrogen.

2.4.2 tRNA Fragmentation Quality Control

1. Agilent 2100 Bioanalyzer (Agilent Technologies).
2. Agilent RNA 6000 Pico kit (quantitative range 50–5000 pg/µL) (*see* **Note 2**).
3. Chip priming station (Agilent Technologies).
4. RNase-free 1.5 mL microcentrifuge tubes.

2.5 End-Repair

1. RNase-free water.
2. Antarctic Phosphatase: 5 U/µL (New England Biolabs).
3. T4 PNK: 10 U/µL (New England Biolabs).
4. RiboLock RNase Inhibitor: 40 U/µL.
5. ATP: 100 mM.
6. RNase-free 0.2 mL PCR tubes, strips of 8.
7. Flat PCR Caps, strips of 8.
8. PCR thermal cycler (we use Agilent SureCycler 8000).

2.6 RNA Purification

1. RNeasy MinElute Cleanup kit.
2. 96% Ethanol.
3. 80% Ethanol.

2.7 Library Preparation Using NEBNext® Multiplex Small RNA Library Prep Set for Illumina®

1. NEBNext® Multiplex Small RNA Library Prep Set for Illumina® (set 1 or 2, New England Biolabs) (*see* **Note 3**).
2. Individual 0.2 mL PCR tubes.
3. RNase-free 0.2 mL PCR tubes, strips of 8.
4. Flat PCR Caps, strips of 8.
5. Thermal cycler.

2.8 Library Purification Using GeneJET PCR Purification Kit

1. GeneJET PCR Purification kit or equivalent.
2. RNase-free 1.5 mL microcentrifuge tubes.
3. RNase-free 1.5 mL DNA low-binding tubes.

2.9 Library Quantification and Quality Assessment

2.9.1 Library Quantification

1. Any kind of fluorometer able to quantify DNA library with high sensitivity (e.g., Qubit® 2.0 fluorometer).
2. Qubit® dsDNA HS Assay kit (0.2–100 ng).
3. Thin-walled polypropylene tubes of 500 μL compatible with the fluorometer (e.g., Qubit® Assay Tube or Axygen® PCR-05-C tubes).

2.9.2 Library Quality Assessment

1. Agilent 2100 Bioanalyzer (Agilent Technologies).
2. Agilent HS DNA kit (quantitative range 5–500 pg/μL).
3. Chip priming station (Agilent Technologies).
4. RNase-free 1.5 mL microcentrifuge tubes.

2.10 Library Sequencing

1. Any kind of Illumina sequencers (starting from Miseq to Hiseq).
2. Any appropriate sequencing kit for a single read length of 35–50 nt.

2.11 Bioinformatic Analysis

1. Unix (Linux) server (we are using Illumina Compute Dell server).
2. Adapter trimming software Trimmomatic (current version 0.36 http://www.usadellab.org/cms/?page=trimmomatic).
3. Alignment software Bowtie 2.0 (current version 2.2.9 http://bowtie-bio.sourceforge.net/bowtie2/index.shtml).
4. R environment ver 3.3.3 for calculations of RiboMethSeq scores and data analysis.

3 Methods

3.1 Total RNA Extraction

3.1.1 Yeast and Bacteria Total RNA Extraction by Hot Acid Phenol

The following protocol for yeast/bacteria total RNA isolation using hot acid phenol is adapted from [17].

1. Transfer yeast/bacteria cell culture in 1.5 mL microcentrifuge tubes and pellet cells by centrifugation at 1200 × *g* for 5 min at room temperature. Discard the supernatant.
2. Resuspend cells in 1 mL of RNase-free water. Centrifuge for 1 min at full speed at room temperature. Discard the supernatant.
3. Resuspend the cell pellet in 400 μL of AE buffer.
4. Add 40 μL of 10% SDS and vortex until the pellet is completely resuspended.
5. Add 440 μL of acid phenol. Vortex.
6. Incubate for 4 min at 65 °C and then cool rapidly the mixture on dry ice for 2–3 min.
7. Centrifuge the samples for 10 min at full speed at room temperature. Transfer carefully the aqueous (upper) phase to a new 1.5 mL microcentrifuge tube.
8. Add 420 μL of phenol:chloroform:IAA, vortex, and centrifuge for 10 min at full speed at room temperature.
9. Transfer the aqueous phase to a new 1.5 mL centrifuge tube. Add 400 μL of chloroform. Vortex and centrifuge at full speed at room temperature for 10 min.
10. Transfer the aqueous phase to a new 1.5 mL centrifuge tube. Add 40 μL of 3 M NaOAc and 1 mL of 96% ethanol. Place at −80 °C for at least 30 min.
11. Centrifuge for 30 min at full speed at 4 °C.
12. Discard the supernatant and wash pellet with 500 μL of 80% ethanol.
13. Centrifuge for 5 min at full speed at 4 °C.
14. Discard the supernatant, centrifuge again your samples for a short spin.
15. Remove any liquid left.
16. Incubate samples with open lid for 2 min at 37 °C or 5 min at room temperature.
17. Resuspend the pellet with 10 μL of RNase-free water and pool your samples.
18. Quantify yeast or bacteria total RNA samples by measuring A_{260nm} using a UV-spectrophotometer (see **Note 4**) (*see* Subheading 3.3.1). Check the quality of your samples by using the Agilent 2100 Bioanalyzer (*see* Subheading 3.3.2).

3.1.2 Human HEK Total RNA Extraction by TRIzol™

Total RNA was isolated using TRIzol™ following the manufacturer's instructions.

1. HEK cells grown in a cell culture Petri dish are washed with 1.5 mL 1× PBS.
2. After PBS removal, add 1 mL of TRIzol™ directly to the culture dish to lyse the cells, scrap the cells, and pipet the lysate up and down several times to homogenize.
3. Incubate for 5 min at room temperature to get complete RNP dissociation.
4. Add 200 µL chloroform, vortex, and incubate for 2–3 min at room temperature.
5. Centrifuge for 15 min at 12,000 × *g* at RT.
6. Transfer the aqueous phase containing RNA in a new 1.5 mL microcentrifuge tube and add 500 µL of isopropanol and 1 µL of Glycoblue™, mix by inverting the tube up and down several times.
7. Incubate for 10 min at room temperature.
8. Centrifuge for 10 min at 12,000 × *g* at 4 °C.
9. Discard the supernatant and wash pellet with 1 mL of 75% ethanol.
10. Centrifuge for 5 min at 7500 × *g* at 4 °C.
11. Discard the supernatant, centrifuge again for a short spin.
12. Remove any liquid left.
13. Incubate with open lid for 2 min at 37 °C or 5 min at room temperature.
14. Resuspend the pellet with 50 µL of RNase-free water.
15. Quantify human total RNA samples by measuring A_{260nm} using a UV-spectrophotometer (see Subheading 3.3.1). Check the quality of your samples by using the Agilent 2100 Bioanalyzer (see Subheading 3.3.2).

3.2 tRNA Purification/ Enrichment

2–30 µg of total RNA extracted either with hot acid phenol (*see* Subheading 3.1.1) or with TRIzol™ (*see* Subheading 3.1.2) are used as a starting point for tRNA enrichment. The protocol used for tRNA enrichment by column is according to the manufacturer's instructions (Macherey-Nagel).

3.2.1 tRNA Enrichment by Column Chromatography

1. Adjust the volume of total RNA to 100 µL with RNase-free water (*see* **Note 5**).
2. Add 5 mL of buffer R0 and mix carefully.
3. Equilibrate the AXR 80 column with 1.5 mL of R1 buffer.
4. Transfer your sample to the AXR 80 column.

5. Wash the column four times with 1.5 mL of R1 buffer.
6. Add 2.5 mL of R2 buffer to the column and collect the eluate in a 5 mL tube.
7. Add 2.5 mL of isopropanol and 1 μL of Glycoblue™ to the elution fraction.
8. Incubate for 15 min on ice.
9. Centrifuge for 25 min at 10,000 × *g* at 4 °C.
10. Discard the supernatant and wash the pellet with 2 mL of 80% ethanol for 5 min at 10,000 × *g* at 4 °C.
11. Discard the supernatant and centrifuge again your samples for a short spin.
12. Remove any liquid left.
13. Incubate your sample with open lid for 2 min at 37 °C or 5 min at room temperature.
14. Resuspend the pellet with 50 μL of RNase-free water.
15. Quantify tRNA samples by measuring A_{260nm} using a UV-spectrophotometer (*see* Subheading 3.3.1). Check the quality of your tRNA preparation by using the Agilent 2100 Bioanalyzer (*see* Subheading 3.3.2).

3.2.2 tRNA Enrichment by rRNA Depletion

2.5–5 μg of total RNA extracted either with hot acid phenol (*see* Subheading 3.1.1) or with TRIzol™ (*see* Subheading 3.1.2) are used as a starting point for rRNA removal. For each species (human, yeast, or bacteria) use the appropriate kits/buffers.

1. For each sample, dispense 225 μL of magnetic beads in a 1.5 mL microcentrifuge tube.
2. Place on a magnetic stand, with cap open, and wait until the liquid is clear (around 1 min).
3. Remove and discard the supernatant.
4. Wash beads twice by adding 225 μL of RNase-free water and vortex to resuspend.
5. Place on a magnetic stand, with cap open, and wait until the liquid is clear.
6. Remove and discard all supernatant.
7. Remove from the magnetic stand.
8. Add 65 μL of magnetic bead resuspension solution, vortex to resuspend. Set aside at room temperature.
9. In a 0.2 mL microcentrifuge tube, add 4 μL of Ribo-Zero Reaction Buffer, 26 μL of RNA sample diluted in RNase-free water, and 10 μL of Ribo-Zero Removal Solution (*see* **Note 6**). Mix by pipetting up and down.
10. Place on the preheated heating block or thermal cycler at 68 °C and incubate for 10 min.

11. Remove from heat, and then centrifuge briefly.
12. Incubate at room temperature for 5 min.
13. Add 40 µL RNA sample to a 1.5 mL tube containing 65 µL washed magnetic beads. Immediately pipette to mix.
14. Vortex for 10 s.
15. Incubate at room temperature for 5 min.
16. Place on the preheated heating block at 50 °C and incubate for 5 min.
17. Immediately place on a magnetic stand, with cap open, and wait until the liquid is clear.
18. Transfer 85–90 µL of supernatant containing rRNA-depleted RNA to a fresh 1.5 mL microcentrifuge tube.
19. Add RNase-free water to bring the volume to 180 µL.
20. Add 18 µL of NaOAc, 1 µL of Glycoblue™, and 600 µL of 96% ethanol. Mix by inverting the tube up and down several times.
21. Place at −80 °C for 30 min.
22. Centrifuge for 30 min at full speed at 4 °C.
23. Discard the supernatant and wash the pellet with 500 µL of 80% ethanol.
24. Centrifuge for 5 min at full speed at 4 °C.
25. Remove any liquid left.
26. Incubate samples with open lid for 2 min at 37 °C or 5 min at room temperature.
27. Resuspend the pellet with 10 µL of RNase-free water.
28. Quantify RNA samples by measuring A_{260nm} using a UV-spectrophotometer (*see* Subheading 3.3.1). Check the quality of your samples by using the Agilent 2100 Bioanalyzer (*see* Subheading 3.3.2).

3.2.3 tRNA Enrichment by Selective TRIzol™ Extraction (Only Recommended for Bacteria)

1. Transfer 10 mL of bacteria culture in a 50 mL Falcon tube.
2. Pellet cells by centrifugation at 4500 × *g* for 5 min at room temperature.
3. Resuspend the pellet with 5 mL 1× PBS and centrifuge at 4500 × *g* for 5 min at room temperature.
4. The pellet is quickly resuspended in 3 mL of TRIzol™.
5. Separate in 3× 1.5 mL ultracentrifuge tubes.
6. Incubate for 5 min to get complete RNP dissociation.
7. Centrifuge at 12,000 × *g* for 5 min at RT and transfert the supernatant to a clean 1.5 ml ultracentrifuge tube.
8. Add 200 µL chloroform, vortex, and incubate for 2–3 min at RT.

9. Centrifuge for 15 min at 12,000 × *g* at RT.
10. Transfer the aqueous phase containing RNA in a new 1.5 mL microcentrifuge tube and add 500 µL of isopropanol and 1 µL of Glycoblue™, mix well.
11. Incubate for 10 min at room temperature.
12. Centrifuge for 10 min at 12,000 × *g* at 4 °C.
13. Discard the supernatant and wash pellet with 1 mL of 75% ethanol.
14. Centrifuge for 5 min at 7500 × *g* at 4 °C.
15. Discard the supernatant, centrifuge again your samples for a short spin.
16. Remove any liquid left.
17. Incubate samples with open lid for 2 min at 37 °C or 5 min at room temperature.
18. Resuspend the pellet with 50 µL of RNase-free water.
19. Quantify RNA samples by measuring A_{260nm} using a UV-spectrophotometer (*see* Subheading 3.3.1). Check the quality of your samples by using the Agilent 2100 Bioanalyzer (*see* Subheading 3.3.2).

3.3 RNA Quantification and tRNA Quality Control

Carry out all procedures at room temperature.

3.3.1 RNA Quantification

1. On a Nanodrop 2000 start screen, select the "Nucleic Acid" application.
2. After the wavelength verification test, select the type of sample to measure, in this case "RNA."
3. Prepare the blank: the buffer/solution used for sample resuspension but without any trace of RNA (e.g., RNase-free water).
4. Load 1 µL of the blank solution to the bottom pedestal, lower the arm, and click on the "Blank" button.
5. Wipe the upper and lower pedestal using a dry wipe and load 1 µL of one of your samples of interest to the bottom pedestal, lower the arm, and click "Measure."
6. Analyze the data obtained for your different RNA samples. For "pure" RNAs, the ratio A260/A280 should be 2, the ratio A260/A230 should be in the range of 1.8–2.2 (*see* **Notes 7** and **8**).

3.3.2 tRNA Quality Assessment

1. Before starting the experiments, equilibrate all solutions of the kit at room temperature for at least 30 min in the dark. Vortex them and spin them down before use.
2. Transfer 550 µL of gel matrix (red cap vial) into a spin filter provided in the kit.

3. Centrifuge for 10 min at 1500 × *g* at room temperature.
4. Prepare 65 µL aliquots of the gel and store them at 4 °C for a maximum of 1 month.
5. Prepare the gel-dye mix by mixing 1 µL of RNA dye concentrate to a gel aliquot.
6. Centrifuge for 10 min at 13,000 × *g* at room temperature.
7. Dilute your RNA samples quantified on Nanodrop to 3–5 ng/µL with RNase-free water to be within the optimal range concentration of the assay.
8. Add 1 µL of your diluted RNA samples to 11 different 1.5 mL tubes already containing 5 µL of RNA marker (green cap vial) (*see* **Note 9**). Mix by pipetting up and down.
9. Mix 1 µL of the ladder (*see* **Note 10**) with 5 µL of RNA marker (green cap vial). Mix by pipetting up and down.
10. Prepare the chip priming station. Adjust the syringe clip to the highest top position.
11. Load 9 µL of the gel-dye mix in the well marked with a "G" surrounded by a black circle.
12. Close the chip priming station properly and press the plunger of the syringe until it is held by the clip.
13. Wait for 30 s and then release the clip.
14. Wait for 5 s until the plunger stops and pull it slowly back to the 1 mL position of the syringe.
15. Open the chip priming station and load 9 µL of the gel-dye mix in the two other wells marked "G."
16. Load 9 µL of the conditioning solution (white cap vial) in the well marked "CS."
17. Load 6 µL of the diluted ladder in the well marked with a ladder.
18. Load 6 µL of the diluted RNA samples in the wells marked 1–11.
19. Inspect the chip and make sure that no liquid spill is present on the edges of the wells.
20. Insert the chip in the Agilent 2100 Bioanalyzer and close the lid (*see* **Note 11**).
21. Select the following assay "Eukaryote Total RNA Pico series II" in the 2100 expert software screen.
22. Press "Start" to begin the chip to run (*see* **Note 12**).
23. After the run, immediately remove the chip and clean the electrodes with the electrode cleaner filled with 350 µL of RNase-free water.
24. Analyze the results of the chip (Fig. 2).

3.4 Alkaline Hydrolysis and tRNA Fragmentation Quality Control

3.4.1 Alkaline Hydrolysis

1. Prepare one 1.5 mL tube per sample to be analyzed ("precipitation tube") containing 10 μL of NaOAc, 1 μL of Glycoblue™, and 1 mL of 96% ethanol for subsequent precipitation of the sample (store at −20 °C until further use).
2. Dilute your RNA samples to a concentration of 10 ng/μL with RNase-free water.
3. To individual PCR tubes, add 10 μL of each of your diluted RNA samples (*see* **Note 13**), keep on ice until further use.
4. Add 10 μL of bicarbonate buffer and mix by pipetting up and down.
5. Incubate in a thermal cycler preheated at 95 °C. Start a timer and incubate for 8–14 min (*see* **Note 14**).
6. Proceed with the next sample every 30 s.
7. Stop each reaction after the required time at 95 °C by spinning down the PCR microtube and add the whole sample into the corresponding 1.5 mL precipitation tube from **step 1**.
8. Mix by inverting the tube several times and throw it into liquid nitrogen.
9. Recover it from the liquid nitrogen and centrifuge your samples for 30 min at 4 °C at full speed in a microcentrifuge.
10. Take out the supernatant and make sure not to loose the pellet.
11. Wash with 600 μL of 80% ethanol.
12. Centrifuge your samples for 10 min at 4 °C at full speed.
13. Take out the supernatant.
14. Centrifuge your samples for a short spin.
15. Remove any liquid left.
16. Incubate your samples with open lid for 2 min at 37 °C or 5 min at room temperature.
17. Resuspend the pellet with 20 μL of RNase-free water.

3.4.2 tRNA Fragmentation Quality Control

1. Prepare your samples by mixing 5 μL of RNA marker (green cap vial) with 1 μL of your fragmented RNA samples.
2. With the rest of gel-dye mix, load 9 μL in the well marked "G" surrounded with a black circle and proceed as described in section "tRNA quality control" from **steps 12** to **23** from Subheading 3.3.2.
3. Analyze the results obtained.

3.5 End-Repair

1. Combine 16 μL of your treated RNA samples in a PCR tube with 2 μL of phosphatase buffer, 1 μL of RiboLock RNase Inhibitor, and 1 μL of Antarctic Phosphatase.
2. Mix by pipetting up and down.

3. Incubate the PCR tubes for 30 min at 37 °C and then for 5 min at 70 °C (to inactivate the phosphatase) and store for indefinite hold at 4 °C in a thermal cycler.
4. Add the following components to the previous mix: 21.5 μL of RNase-free water, 5 μL of PNK buffer, 0.5 μL of ATP, 1 μL of RiboLock RNase Inhibitor, 2 μL of PNK enzyme.
5. Incubate in a thermal cycler for 1 h at 37 °C and immediately proceed to the next step.

3.6 RNA Purification

All the reagents except ethanol used for RNA purification are part of RNeasy MinElute Cleanup kit. Carry out all procedures at room temperature.

1. Transfer the sample to a new 1.5 mL tube and add 50 μL of RNase-free water to adjust the final volume to 100 μL.
2. Add 350 μL of RLT buffer, mix by vortexing.
3. Add 675 μL of 96% ethanol and mix by inverting the tube up and down (*see* **Note 15**).
4. Transfer 700 μL of the sample to an RNeasy MinElute spin column (stored at 4 °C until use). Centrifuge for 30 s at 8000 × *g*.
5. Repeat the **step 4** with the rest of the sample. Then, add 500 μL of RPE buffer to the column. Centrifuge for 30 s at 8000 × *g*.
6. Discard the flowthrough. Add 750 μL of 80% ethanol. Centrifuge for 2 min at 8000 × *g*.
7. Transfer the column to a new collection tube and centrifuge at full speed for 5 min with the lid open.
8. Transfer the column to a new 1.5 mL tube (provided with the kit). Add 10 μL of RNase- free water in the center of the column filter. Wait for 1 min.
9. Centrifuge at full speed for 1 min to elute. The recovered volume is about 9 μL.

3.7 Library Preparation Using NEBNext® Multiplex Small RNA Library Prep Set for Illumina®

1. Mix 6 μL of RNA sample with 1 μL of 3′SR adaptor (green cap vial) in a PCR tube.
2. Incubate for 2 min at 70 °C in a preheated thermal cycler. Transfer immediately to ice.
3. Add 10 μL of 3′ Ligation Buffer (green cap vial) and 3 μL of 3′ Ligation Enzyme (green cap vial).
4. Incubate for 1 h at 25 °C in a thermal cycler.
5. Add 4.5 μL of RNase-free water and 1 μL of SR RT primer (pink cap vial).

6. Incubate for 5 min at 75 °C, 15 min at 37 °C, and 15 min at 25 °C.
7. Within the last 15 min of incubation, add 1.1*n (n = number of samples) μL of the 5′ SR adaptor (yellow cap vial) in an individual PCR tube (previously resuspended in 120 μL of RNase-free water and stored at −80 °C).
8. Denature the 5′SR adaptor in a thermal cycler for 2 min at 70 °C and immediately place the tube on ice (*see* **Note 16**).
9. Add 1 μL of 5′SR adaptor (previously denatured), 1 μL of 5′ Ligation Reaction Buffer (yellow cap vial), and 2.5 μL of Ligase Enzyme Mix (yellow cap vial).
10. Incubate for 1 h at 25 °C in a thermal cycler.
11. Add the following components to the adaptor ligated RNA mix from the previous step: 8 μL of First strand synthesis reaction buffer (red cap vial), 1 μL of Murine RNase inhibitor (red cap vial), 1 μL of ProtoScript II reverse transcriptase (red cap vial) and mix well by pipetting up and down.
12. Incubate for 1 h at 50 °C.
13. Immediately proceed to PCR amplification (*see* **Note 17**). Add the following components to the RT reaction mix from the previous step: 50 μL of LongAmp Taq Master Mix (blue cap vial), 2.5 μL of SR primer (blue cap vial), 2.5 μL of index primer (*see* **Note 18**), and 5 μL of RNase-free water. Mix well.
14. Perform the following PCR cycling conditions: 1 cycle of initial denaturation for 30 s at 94 °C, 12–15 cycles of denaturation 15 s at 94 °C, annealing 30 s at 62 °C, extension 15 s at 70 °C, 1 cycle of final extension for 5 min at 70 °C and store at 4 °C for indefinite hold.

3.8 Purification of the Library Using GeneJET PCR Purification Kit

Carry out all procedures at room temperature.

1. Transfer the PCR mix to a 1.5 mL tube, and add 100 μL of binding buffer. Mix thoroughly.
2. Transfer the solution to the purification column. Centrifuge at full speed for 30 s. Discard the flowthrough.
3. Add 700 μL of wash buffer to the column and centrifuge at full speed for 30 s. Discard the flowthrough.
4. Centrifuge the empty column for 1 additional min.
5. Transfer the column to a clean 1.5 mL DNA low-binding tube. Add 30 μL of Elution buffer to the center of the column membrane and centrifuge at full speed for 1 min.
6. Store the purified library at −20 °C until further use.

3.9 Library Quantification and Quality Assessment

3.9.1 Library Quantification

1. Before starting the experiments, incubate all solutions of the Qubit dsDNA HS assay kit at room temperature for at least 30 min. The kit provides the concentrated assay reagent, dilution buffer, and pre-diluted standards.
2. Prepare the dye working solution by diluting the concentrated assay reagent 1:200 in dilution buffer. Prepare 200 μL of working solution for each sample and two additional standards.
3. Prepare the two standards annotated "C" and "D" by mixing 10 μL of standard with 190 μL of working solution.
4. Add working solution to 1 μL of library sample to obtain 200 μL in total.
5. Vortex the tubes for 2 s and incubate them for 2 min at room temperature.
6. Insert the tubes into the Qubit® 2.0 Fluorometer and proceed with measurements: on the home screen of the Qubit® 2.0 Fluorometer, choose the type of assay (e.g., "HS DNA") for which you want to perform a new calibration.
7. Press "Yes" to read new standards.
8. When indicated, insert the standard tube and press "Read." Standard #1 and #2 correspond to standards "C" and "D," respectively.
9. Once the calibration is done, insert each sample and press "Read" to make the measurements. Check that the value of your samples is within the assay's range, and press "Calculate Stock Conc" (*see* **Note 19**).

3.9.2 Library Quality Assessment

1. Before starting the experiments, incubate all solutions of the Agilent High Sensitivity DNA kit at room temperature for at least 30 min in the dark. Vortex them and spin them down before use.
2. Add 15 μL of High sensitivity DNA dye concentrate (blue cap vial) into a High Sensitivity DNA gel matrix vial (red cap vial) (*see* **Note 20**).
3. Vortex for 10 s and transfer the gel-dye mix to the center of the spin filter.
4. Centrifuge for 10 min at 2240 × *g*.
5. Add 1 μL of each of your library to 11 different tubes of 1.5 mL already containing 5 μL of RNA marker (green cap vial). Mix by pipetting up and down.
6. Mix 1 μL of the ladder (yellow cap vial) with 5 μL of High sensitivity DNA marker (green cap vial). Mix by pipetting up and down.
7. Prepare the chip priming station. Adjust the syringe clip to the lowest top position.

8. Load 9 μL of the gel-dye mix in the well marked with a "G" surrounded by a black circle.
9. Close the chip priming station properly and press the plunger of the syringe until it is held by the clip.
10. Wait for 1 min and then release the clip.
11. Wait for 5 s until the plunger stops and pull it slowly back to the 1 mL position of the syringe.
12. Open the chip priming station and load 9 μL of the gel-dye mix in the 3 other wells marked "G."
13. Load 6 μL of the diluted ladder in the well marked with a ladder.
14. Load 6 μL of the diluted library samples in the wells labeled 1–11.
15. Insert the chip in the Agilent 2100 Bioanalyzer, close the lid, and select the following assay "High Sensitivity DNA" in the 2100 expert software screen.
16. Press "Start" to begin the chip to run.
17. After the run, immediately remove the chip and clean the electrodes with the electrode cleaner filled with 350 μL of RNase-free water.
18. Analyze the results of the chip.

3.10 Library Sequencing

1. For sequencing, libraries are multiplexed and diluted to 6–8 pM final concentration.
2. Recommended sequencing depth or coverage for tRNAs is about 10 mln of reads/sample.
3. Sequencing length may vary from 35 to 50 nt in a single read mode.

3.11 Bioinformatic Analysis

1. Trim adapter sequences of raw reads (FastQ files) using Trimmomatic with the following parameters: java -jar trimmomatic-0.35.jar SE -phred33 input.fq.gz output.fq.gz ILLUMINACLIP:TruSeq3-SE:2:30:7 LEADING:30 TRAILING:30 SLIDINGWINDOW:4:15 AVGQUAL:30 MINLEN:8 (*see* **Notes 21** and **22**).
2. Selection of short reads is done by the following script: gzip -dc <*.gz> | awk 'NR%4==1{a=$0} NR%4==2{b=$0} NR%4==3{c=$0} NR%4==0&&length(b)<40{print a"\n"b"\n"c"\n"$0;}' | gzip > <S*.gz>
3. Align the trimmed reads to the appropriate reference sequence (*E. coli* or yeast tRNA dataset) using bowtie2 with the following parameters: bowtie2 -D 15 -R 2 -N 0

-L 10 -i S,1,1.15 -x <bt2-idx> -U <r> –S. The use of soft trimming is not recommended.

4. Selection of only uniquely mapped reads (single reported alignment position in the reference sequence) in the resulting *.sam file was done using values of the NM and XS fields (grep -E "@|NM:" <*.sam>|grep -v "XS:").
5. Uniquely mapped reads were extracted from the *.sam file by RNA ID and converted to *.bed format using bedtools v2.25.0.
6. Count the 5′- and 3′-ends in the produced *.bed file using Unix awk command: awk '{print $2}' <*.bed> | sort | uniq -c | awk '{print $3,$2,$1,$4}' | sort –n (example for 5′-ends).
7. Make a merge of obtained 5′-ends and 3′-ends counting files using custom R script.
8. Calculate ScoreMean for each position, make a ratio of number of 5′-reads ends between preceding and following position and calculate ScoreMean as a ratio of a drop for a given position compared to the average for 4 neighboring positions (−2/+2).
9. Calculate the RiboMethScore(ScoreC2), use the following formula: $\text{RiboMethScore} = 1 - n_i/(0.5*(\text{SUM}(n_j * W_j)/\text{SUM}(W_j) + \text{SUM}(n_k * W_k)/\text{SUM}(W_k))$, where n_i—5′/3″-end count for a given position, j—varies from $i-2$ to $i-1$, k varies from $i+1$ to $i+2$, Weight parameters are defined as 1.0 for −1/+1 and 0.9 for −2/+2 positions.

4 Notes

1. tRNAs are expected to elute from the column at a KCl salt concentration of 0.45–0.65 M.
2. Since the average size of tRNA is below 200 nts, it may be appropriate to use Agilent Small RNA kit (quantitative range 50–2000 pg/μL) following manufacturer's recommendations.
3. The kit NEBNext® Multiplex Small RNA Library Prep Set for Illumina® (set 1) (NEB, E7300S) includes a set of 12 barcoding primers (numbered 1–12) that will be used for multiplexing reactions during PCR amplification. There is also a version set 2 with primers (numbers 13–24). If you do not need these barcoding primers, you may order a similar kit without the primers and use any other source of barcoding primers (Illumina, Epicentre, NEB).
4. The typical amount obtained with 1 mL of a haploïd wild-type yeast culture (BY4741 or BY4742) or bacteria culture (DH5α) grown to an OD_{600} of 1 is about 15–30 μg.
5. The AXR 80 column has a maximal binding capacity of 80 μg.

6. The recommended RNA input is 2.5–5 μg for 10 μL of Removal solution. Nevertheless, it is possible to start with less RNA input 1–2.5 μg, in this case, use 8 μL of Removal solution and dilute RNA in 28 μL of RNase-free water.
7. If your RNA sample is diluted with RNase-free water instead of 10 mM Tris-EDTA (TE) pH 8.0, the ratio A260/A280 may be below 2.0 due to the lower pH of water [18]. A ratio A260/A280 of 1.8 for samples diluted in RNase-free water is considered "pure" for RNA.
8. If your RNA sample is contaminated by phenol or chaotropic salts (e.g., guanidinium thiocyanate used in TRIzol™ extraction or other protocols), this will result in a ratio A260/A230 below 1.8. Another round of Phenol-Chloroform-Isoamyl Alcohol (PCA) extraction and two successive steps of chloroform extraction followed by ethanol precipitation are in this case recommended before alkaline digestion.
9. In case you are working with less than 11 samples, replace RNA with 1 μL of RNase-free water in the empty wells.
10. The ladder loaded in the Pico RNA chip is provided in a separate package and may be prepared before the experiment: spin down the tube and transfer 10 μL to a RNase-free tube. Heat for 2 min at 70 °C. Cool down on ice and add 90 μL of RNase-free water. Prepare 5 μL aliquots using the Safe-Lock PCR tubes provided in the kit and store them at −70 °C. Before use, thaw one tube and keep it on ice. The ladder is quite stable at −70 °C and may be used for at least 4 months.
11. RNase contamination problems of the Bioanalyzer electrodes are very frequent and will affect the RNA integrity number of your samples. Therefore, if the Agilent 2100 Bioanalyzer is also frequently used to run DNA chips, it is strongly recommended to use a dedicated electrode cartridge only for RNA assays. In addition, we recommend for each chip to load an internal RNA control (total RNA preparation with a known RIN>9). If you encounter contamination problems, soak the electrode cartridge into an RNaseZap® decontamination solution (Ambion) for at least 10 min, then rinse the electrodes with RNase-free water and let them dry out for at least one night.
12. The Agilent 2100 Bioanalyzer is very sensitive to vibrations and this may affect your results. Therefore make sure that no vibrations will occur during the run.
13. The RNA quantity may be decreased to a minimal starting amount of 10–50 ng without considerably affecting coverage and calculation of the RiboMethScore.
14. Fragmentation time should be adjusted for each tRNA preparation depending on the quality and on the species used. We recommend testing 3–4 different times of fragmentation to

define the appropriate conditions for hydrolysis. We have already established that the fragmentation time for tRNA of good quality extracted from *E. coli* is around 10 min while the ones extracted from *S. cerevisiae* is 12 min [16]. The optimal size distribution is around 20–50 nt.

15. Ethanol quantity is increased compared to the manufacturer's recommendations in order not to loose the small RNA fragments during the RNA binding to the silica membrane.
16. Do not leave the heated adapter on ice for more than 5–10 min before proceeding to the next step; this may impact your library preparation.
17. We recommend proceeding immediately with PCR amplification. However, if it is not possible, inactivate the RT by heating for 15 min at 70 °C and cool down the reaction at 4 °C for 1–3 h or safely store the reactions at −20 °C for overnight.
18. Make sure to use only combinations of compatible primers for barcoding. Most Illumina sequencers use a green laser (or LED) to read G and T nucleotides and a red laser (or LED) to read A and C nucleotides. Within each sequencing cycle, at least one nucleotide for each color channel must be read in the index to ensure proper reading of the barcode sequence. Use as a reference the following guide (ScriptSeq™ Index PCR primers, Illumina) for verification of barcode compatibility or check compatibility with Illumina Experimental Manager software.
19. This quantification step is crucial. Make sure to quantify all your libraries properly since an under- or overestimated quantification will interfere with subsequent sequencing reads proportion and quality.
20. The High Sensitivity DNA gel-dye mix is stable for 1 month at 4 °C protected from light.
21. MINLEN parameter can vary depending on the length of the analyzed RNA, 17 nt is suitable for rRNA, but it may be shorter for tRNAs, 8 nt as here.
22. Tests with a training dataset demonstrated that with stringency parameter = 7, Trimmomatic removes the adapter with a minimal size of 10 nts. Thus, only trimmed and adapter-free reads of <40 nt were taken for alignment.

Acknowledgement

This work was supported by joint ANR-DFG grant HTRNAMod (ANR-13-ISV8-0001/HE 3397/8-1) to MH and YM, and AO Lorraine University-Lorraine Region "Aberrant RNA methylation in cancer" funding to YM.

References

1. Helm M, Alfonzo JD (2014) Posttranscriptional RNA modifications: playing metabolic games in a cell's chemical Legoland. Chem Biol 21(2):174–185
2. Helm M, Motorin Y (2017) Detecting RNA modifications in the epitranscriptome: predict and validate. Nat Rev Genet 18(5):275–291
3. Rana AK, Ankri S (2016) Reviving the RNA world: an insight into the appearance of RNA methyltransferases. Front Genet 7:99
4. Towns WL, Begley TJ (2012) Transfer RNA methytransferases and their corresponding modifications in budding yeast and humans: activities, predications, and potential roles in human health. DNA Cell Biol 31(4):434–454
5. Motorin Y, Helm M (2011) RNA nucleotide methylation. Wiley Interdiscip Rev RNA 2 (5):611–631
6. Gilbert WV, Bell TA, Schaening C (2016) Messenger RNA modifications: form, distribution, and function. Science 352(6292):1408–1412
7. Yue Y, Liu J, He C (2015) RNA N6-methyladenosine methylation in post-transcriptional gene expression regulation. Genes Dev 29(13):1343–1355
8. Sarin LP, Leidel SA (2014) Modify or die?—RNA modification defects in metazoans. RNA Biol 11(12):1555–1567
9. Maden BE (2000) Tetrahydrofolate and tetrahydromethanopterin compared: functionally distinct carriers in C1 metabolism. Biochem J 350(Pt 3):609–629
10. Maden BE (2001) Mapping 2′-O-methyl groups in ribosomal RNA. Methods 25 (3):374–382
11. Yu YT, Shu MD, Steitz JA (1997) A new method for detecting sites of 2′-O-methylation in RNA molecules. RNA 3(3):324–331
12. Dong Z-W, Shao P, Diao L-T, Zhou H, Yu C-H, Qu L-H (2012) RTL-P: a sensitive approach for detecting sites of 2′-O-methylation in RNA molecules. Nucleic Acids Res 40 (20):e157
13. Chan CTY, Dyavaiah M, DeMott MS, Taghizadeh K, Dedon PC, Begley TJ (2010) A quantitative systems approach reveals dynamic control of tRNA modifications during cellular stress. PLoS Genet [Internet] [cited 2017 May 17];6(12)
14. Marchand V, Ayadi L, El Hajj A, Blanloeil-Oillo F, Helm M, Motorin Y (2017) High-throughput mapping of 2′-O-Me residues in RNA using next-generation sequencing (illumina RiboMethSeq protocol). Methods Mol Biol 1562:171–187
15. Marchand V, Blanloeil-Oillo F, Helm M, Motorin Y (2016) Illumina-based RiboMeth-Seq approach for mapping of 2′-O-Me residues in RNA. Nucleic Acids Res 44(16):e135
16. Marchand V, Pichot F, Thüring K, Ayadi L, Freund I, Dalpke A et al (2017) Next-generation sequencing-based RiboMethSeq protocol for analysis of tRNA 2′-O-methylation. Biomolecules [Internet] [cited 2017 Jul 12];7(1)
17. Schmitt ME, Brown TA, Trumpower BL (1990) A rapid and simple method for preparation of RNA from Saccharomyces cerevisiae. Nucleic Acids Res 18(10):3091–3092
18. Wilfinger WW, Mackey K, Chomczynski P (1997) Effect of pH and ionic strength on the spectrophotometric assessment of nucleic acid purity. BioTechniques 22(3):474–476, 478–481

Bibliography:

1. Watson JD, Crick FH. Molecular structure of nucleic acids. A structure for deoxyribose nucleic acid. 1953. Rev Investig Clin Organo Hosp Enfermedades Nutr. avr 2003;55(2):108-9.

2. Dahm R. Discovering DNA: Friedrich Miescher and the early years of nucleic acid research. Hum Genet. janv 2008;122(6):565-81.

3. Quinodoz S, Guttman M. Long non-coding RNAs: An emerging link between gene regulation and nuclear organization. Trends Cell Biol. nov 2014;24(11):651-63.

4. Rutenberg-Schoenberg M, Sexton AN, Simon MD. The Properties of Long Noncoding RNAs that Regulate Chromatin. Annu Rev Genomics Hum Genet. 21 avr 2016;

5. Sacco LD, Baldassarre A, Masotti A. Bioinformatics Tools and Novel Challenges in Long Non-Coding RNAs (lncRNAs) Functional Analysis. Int J Mol Sci. 23 déc 2011;13(1):97-114.

6. Hutchison CA. DNA sequencing: bench to bedside and beyond. Nucleic Acids Res. 1 sept 2007;35(18):6227-37.

7. Holley RW, Apgar J, Everett GA, Madison JT, Marquisee M, Merrill SH, et al. STRUCTURE OF A RIBONUCLEIC ACID. Science. 19 mars 1965;147(3664):1462-5.

8. Sanger F, Brownlee GG, Barrell BG. A two-dimensional fractionation procedure for radioactive nucleotides. J Mol Biol. sept 1965;13(2):373-98.

9. Brownlee GG, Sanger F. Nucleotide sequences from the low molecular weight ribosomal RNA of Escherichia coli. J Mol Biol. 14 févr 1967;23(3):337-53.

10. Cory S, Marcker KA, Dube SK, Clark BF. Primary structure of a methionine transfer RNA from Escherichia coli. Nature. 7 déc 1968;220(5171):1039-40.

11. Dube SK, Marcker KA, Clark BF, Cory S. Nucleotide sequence of N-formyl-methionyl-transfer RNA. Nature. 20 avr 1968;218(5138):232-3.

12. Goodman HM, Abelson J, Landy A, Brenner S, Smith JD. Amber suppression: a nucleotide change in the anticodon of a tyrosine transfer RNA. Nature. 16 mars 1968;217(5133):1019-24.

13. Adams JM, Jeppesen PG, Sanger F, Barrell BG. Nucleotide sequence from the coat protein cistron of R17 bacteriophage RNA. Nature. 6 sept 1969;223(5210):1009-14.

14. Min Jou W, Haegeman G, Ysebaert M, Fiers W. Nucleotide sequence of the gene coding for the bacteriophage MS2 coat protein. Nature. 12 mai 1972;237(5350):82-8.

15. Fiers W, Contreras R, Duerinck F, Haegeman G, Iserentant D, Merregaert J, et al. Complete nucleotide sequence of bacteriophage MS2 RNA: primary and secondary structure of the replicase gene. Nature. 8 avr 1976;260(5551):500-7.

16. Wu R. Nucleotide sequence analysis of DNA. Nature New Biol. 19 avr 1972;236(68):198-200.

17. Wu R, Kaiser AD. Structure and base sequence in the cohesive ends of bacteriophage lambda DNA. J Mol Biol. 14 août 1968;35(3):523-37.

18. Sanger F, Coulson AR. A rapid method for determining sequences in DNA by primed synthesis with DNA polymerase. J Mol Biol. 25 mai 1975;94(3):441-8.

19. Maxam AM, Gilbert W. A new method for sequencing DNA. Proc Natl Acad Sci U S A. févr 1977;74(2):560-4.

20. Sanger F, Nicklen S, Coulson AR. DNA sequencing with chain-terminating inhibitors. Proc Natl Acad Sci U S A. déc 1977;74(12):5463-7.

21. Smith LM, Fung S, Hunkapiller MW, Hunkapiller TJ, Hood LE. The synthesis of oligonucleotides containing an aliphatic amino group at the 5' terminus: synthesis of fluorescent DNA primers for use in DNA sequence analysis. Nucleic Acids Res. 11 avr 1985;13(7):2399-412.

22. Ansorge W, Sproat BS, Stegemann J, Schwager C. A non-radioactive automated method for DNA sequence determination. J Biochem Biophys Methods. déc 1986;13(6):315-23.

23. Ansorge W, Sproat B, Stegemann J, Schwager C, Zenke M. Automated DNA sequencing: ultrasensitive detection of fluorescent bands during electrophoresis. Nucleic Acids Res. 11 juin 1987;15(11):4593-602.

24. Prober JM, Trainor GL, Dam RJ, Hobbs FW, Robertson CW, Zagursky RJ, et al. A system for rapid DNA sequencing with fluorescent chain-terminating dideoxynucleotides. Science. 16 oct 1987;238(4825):336-41.

25. Kambara H, Nishikawa T, Katayama Y, Yamaguchi T. Optimization of Parameters in a DNA Sequenator Using Fluorescence Detection. Bio/Technology. juill 1988;6(7):816.

26. Swerdlow H, Gesteland R. Capillary gel electrophoresis for rapid, high resolution DNA sequencing. Nucleic Acids Res. 25 mars 1990;18(6):1415-9.

27. Hunkapiller T, Kaiser RJ, Koop BF, Hood L. Large-scale and automated DNA sequence determination. Science. 4 oct 1991;254(5028):59-67.

28. Mardis ER. Next-generation sequencing platforms. Annu Rev Anal Chem Palo Alto Calif. 2013;6:287-303.

29. Dressman D, Yan H, Traverso G, Kinzler KW, Vogelstein B. Transforming single DNA molecules into fluorescent magnetic particles for detection and enumeration of genetic variations. Proc Natl Acad Sci U S A. 22 juill 2003;100(15):8817-22.

30. Kim JB, Porreca GJ, Song L, Greenway SC, Gorham JM, Church GM, et al. Polony multiplex analysis of gene expression (PMAGE) in mouse hypertrophic cardiomyopathy. Science. 8 juin 2007;316(5830):1481-4.

31. Leamon JH, Lee WL, Tartaro KR, Lanza JR, Sarkis GJ, deWinter AD, et al. A massively parallel PicoTiterPlate based platform for discrete picoliter-scale polymerase chain reactions. Electrophoresis. nov 2003;24(21):3769-77.

32. Fedurco M, Romieu A, Williams S, Lawrence I, Turcatti G. BTA, a novel reagent for DNA attachment on glass and efficient generation of solid-phase amplified DNA colonies. Nucleic Acids Res. 9 févr 2006;34(3):e22.

33. Harris TD, Buzby PR, Babcock H, Beer E, Bowers J, Braslavsky I, et al. Single-molecule DNA sequencing of a viral genome. Science. 4 avr 2008;320(5872):106-9.

34. Voelkerding KV, Dames SA, Durtschi JD. Next-generation sequencing: from basic research to diagnostics. Clin Chem. avr 2009;55(4):641-58.

35. Bentley DR, Balasubramanian S, Swerdlow HP, Smith GP, Milton J, Brown CG, et al. Accurate whole human genome sequencing using reversible terminator chemistry. Nature. 6 nov 2008;456(7218):53-9.

36. Drmanac R, Sparks AB, Callow MJ, Halpern AL, Burns NL, Kermani BG, et al. Human genome sequencing using unchained base reads on self-assembling DNA nanoarrays. Science. 1 janv 2010;327(5961):78-81.

37. Tomkinson AE, Vijayakumar S, Pascal JM, Ellenberger T. DNA ligases: structure, reaction mechanism, and function. Chem Rev. févr 2006;106(2):687-99.

38. Goodwin S, McPherson JD, McCombie WR. Coming of age: ten years of next-generation sequencing technologies. Nat Rev Genet. 17 2016;17(6):333-51.

39. Margulies M, Egholm M, Altman WE, Attiya S, Bader JS, Bemben LA, et al. Genome sequencing in microfabricated high-density picolitre reactors. Nature. 15 sept 2005;437(7057):376-80.

40. Nyrén P, Lundin A. Enzymatic method for continuous monitoring of inorganic pyrophosphate synthesis. Anal Biochem. déc 1985;151(2):504-9.

41. Rothberg JM, Hinz W, Rearick TM, Schultz J, Mileski W, Davey M, et al. An integrated semiconductor device enabling non-optical genome sequencing. Nature. 20 juill 2011;475(7356):348-52.

42. Guo J, Xu N, Li Z, Zhang S, Wu J, Kim DH, et al. Four-color DNA sequencing with 3'-O-modified nucleotide reversible terminators and chemically cleavable fluorescent dideoxynucleotides. Proc Natl Acad Sci U S A. 8 juill 2008;105(27):9145-50.

43. Ju J, Kim DH, Bi L, Meng Q, Bai X, Li Z, et al. Four-color DNA sequencing by synthesis using cleavable fluorescent nucleotide reversible terminators. Proc Natl Acad Sci U S A. 26 déc 2006;103(52):19635-40.

44. Harismendy O, Ng PC, Strausberg RL, Wang X, Stockwell TB, Beeson KY, et al. Evaluation of next generation sequencing platforms for population targeted sequencing studies. Genome Biol. 2009;10(3):R32.

45. Rieber N, Zapatka M, Lasitschka B, Jones D, Northcott P, Hutter B, et al. Coverage bias and sensitivity of variant calling for four whole-genome sequencing technologies. PloS One. 2013;8(6):e66621.

46. Forgetta V, Leveque G, Dias J, Grove D, Lyons R, Genik S, et al. Sequencing of the Dutch elm disease fungus genome using the Roche/454 GS-FLX Titanium System in a comparison of multiple genomics core facilities. J Biomol Tech JBT. avr 2013;24(1):39-49.

47. Dohm JC, Lottaz C, Borodina T, Himmelbauer H. Substantial biases in ultra-short read data sets from high-throughput DNA sequencing. Nucleic Acids Res. sept 2008;36(16):e105.

48. Nakamura K, Oshima T, Morimoto T, Ikeda S, Yoshikawa H, Shiwa Y, et al. Sequence-specific error profile of Illumina sequencers. Nucleic Acids Res. juill 2011;39(13):e90.

49. Minoche AE, Dohm JC, Himmelbauer H. Evaluation of genomic high-throughput sequencing data generated on Illumina HiSeq and genome analyzer systems. Genome Biol. 8 nov 2011;12(11):R112.

50. Braslavsky I, Hebert B, Kartalov E, Quake SR. Sequence information can be obtained from single DNA molecules. Proc Natl Acad Sci U S A. 1 avr 2003;100(7):3960-4.

51. Bowers J, Mitchell J, Beer E, Buzby PR, Causey M, Efcavitch JW, et al. Virtual terminator nucleotides for next-generation DNA sequencing. Nat Methods. août 2009;6(8):593-5.

52. van Dijk EL, Auger H, Jaszczyszyn Y, Thermes C. Ten years of next-generation sequencing technology. Trends Genet TIG. sept 2014;30(9):418-26.

53. Clarke J, Wu H-C, Jayasinghe L, Patel A, Reid S, Bayley H. Continuous base identification for single-molecule nanopore DNA sequencing. Nat Nanotechnol. avr 2009;4(4):265-70.

54. Ip CLC, Loose M, Tyson JR, de Cesare M, Brown BL, Jain M, et al. MinION Analysis and Reference Consortium: Phase 1 data release and analysis. F1000Research. 2015;4:1075.

55. Viehweger A, Krautwurst S, Lamkiewicz K, Madhugiri R, Ziebuhr J, Hölzer M, et al. Nanopore direct RNA sequencing reveals modification in full-length coronavirus genomes. bioRxiv. 30 nov 2018;483693.

56. Depledge DP, Srinivas KP, Sadaoka T, Bready D, Mori Y, Placantonakis DG, et al. Direct RNA sequencing on nanopore arrays redefines the transcriptional complexity of a viral pathogen. Nat Commun. 14 févr 2019;10(1):754.

57. Robertson G, Schein J, Chiu R, Corbett R, Field M, Jackman SD, et al. De novo assembly and analysis of RNA-seq data. Nat Methods. nov 2010;7(11):909-12.

58. Trapnell C, Williams BA, Pertea G, Mortazavi A, Kwan G, van Baren MJ, et al. Transcript assembly and quantification by RNA-Seq reveals unannotated transcripts and isoform switching during cell differentiation. Nat Biotechnol. mai 2010;28(5):511-5.

59. Han Y, Gao S, Muegge K, Zhang W, Zhou B. Advanced Applications of RNA Sequencing and Challenges. Bioinforma Biol Insights. 15 nov 2015;9(Suppl 1):29-46.

60. Camarena L, Bruno V, Euskirchen G, Poggio S, Snyder M. Molecular mechanisms of ethanol-induced pathogenesis revealed by RNA-sequencing. PLoS Pathog. 1 avr 2010;6(4):e1000834.

61. Griffith M, Griffith OL, Mwenifumbo J, Goya R, Morrissy AS, Morin RD, et al. Alternative expression analysis by RNA sequencing. Nat Methods. oct 2010;7(10):843-7.

62. Picardi E, Horner DS, Chiara M, Schiavon R, Valle G, Pesole G. Large-scale detection and analysis of RNA editing in grape mtDNA by RNA deep-sequencing. Nucleic Acids Res. août 2010;38(14):4755-67.

63. Wilhelm BT, Briau M, Austin P, Faubert A, Boucher G, Chagnon P, et al. RNA-seq analysis of 2 closely related leukemia clones that differ in their self-renewal capacity. Blood. 13 janv 2011;117(2):e27-38.

64. Wang ET, Sandberg R, Luo S, Khrebtukova I, Zhang L, Mayr C, et al. Alternative isoform regulation in human tissue transcriptomes. Nature. 27 nov 2008;456(7221):470-6.

65. Maher CA, Kumar-Sinha C, Cao X, Kalyana-Sundaram S, Han B, Jing X, et al. Transcriptome sequencing to detect gene fusions in cancer. Nature. 5 mars 2009;458(7234):97-101.

66. Berger MF, Levin JZ, Vijayendran K, Sivachenko A, Adiconis X, Maguire J, et al. Integrative analysis of the melanoma transcriptome. Genome Res. avr 2010;20(4):413-27.

67. Supper J, Gugenmus C, Wollnik J, Drueke T, Scherf M, Hahn A, et al. Detecting and visualizing gene fusions. Methods San Diego Calif. janv 2013;59(1):S24-28.

68. Conde L, Bracci PM, Richardson R, Montgomery SB, Skibola CF. Integrating GWAS and expression data for functional characterization of disease-associated SNPs: an application to follicular lymphoma. Am J Hum Genet. 10 janv 2013;92(1):126-30.

69. Lee FCY, Ule J. Advances in CLIP Technologies for Studies of Protein-RNA Interactions. Mol Cell. 1 févr 2018;69(3):354-69.

70. Turchinovich A, Weiz L, Langheinz A, Burwinkel B. Characterization of extracellular circulating microRNA. Nucleic Acids Res. 1 sept 2011;39(16):7223-33.

71. Vickers KC, Palmisano BT, Shoucri BM, Shamburek RD, Remaley AT. MicroRNAs are Transported in Plasma and Delivered to Recipient Cells by High-Density Lipoproteins. Nat Cell Biol. avr 2011;13(4):423-33.

72. Zhang H, Freitas D, Kim HS, Fabijanic K, Li Z, Chen H, et al. Identification of distinct nanoparticles and subsets of extracellular vesicles by asymmetric flow field-flow fractionation. Nat Cell Biol. mars 2018;20(3):332-43.

73. György B, Szabó TG, Pásztói M, Pál Z, Misják P, Aradi B, et al. Membrane vesicles, current state-of-the-art: emerging role of extracellular vesicles. Cell Mol Life Sci. août 2011;68(16):2667-88.

74. Momen-Heravi F, Getting SJ, Moschos SA. Extracellular vesicles and their nucleic acids for biomarker discovery. Pharmacol Ther. déc 2018;192:170-87.

75. Greening DW, Simpson RJ. Understanding extracellular vesicle diversity - current status. Expert Rev Proteomics. nov 2018;15(11):887-910.

76. Zaborowski MP, Balaj L, Breakefield XO, Lai CP. Extracellular Vesicles: Composition, Biological Relevance, and Methods of Study. Bioscience. 1 août 2015;65(8):783-97.

77. Théry C, Witwer KW, Aikawa E, Alcaraz MJ, Anderson JD, Andriantsitohaina R, et al. Minimal information for studies of extracellular vesicles 2018 (MISEV2018): a position statement of the International Society for Extracellular Vesicles and update of the MISEV2014 guidelines. J Extracell Vesicles. 2018;7(1):1535750.

78. Dostert G, Mesure B, Menu P, Velot É. How Do Mesenchymal Stem Cells Influence or Are Influenced by Microenvironment through Extracellular Vesicles Communication? Front Cell Dev Biol. 2017;5:6.

79. Crescitelli R, Lässer C, Szabó TG, Kittel A, Eldh M, Dianzani I, et al. Distinct RNA profiles in subpopulations of extracellular vesicles: apoptotic bodies, microvesicles and exosomes. J Extracell Vesicles. 2013;2.

80. Saraste A, Pulkki K. Morphologic and biochemical hallmarks of apoptosis. Cardiovasc Res. févr 2000;45(3):528-37.

81. Hristov M, Erl W, Linder S, Weber PC. Apoptotic bodies from endothelial cells enhance the number and initiate the differentiation of human endothelial progenitor cells in vitro. Blood. 1 nov 2004;104(9):2761-6.

82. Al-Nedawi K, Meehan B, Rak J. Microvesicles: messengers and mediators of tumor progression. Cell Cycle Georget Tex. 1 juill 2009;8(13):2014-8.

83. Holme PA, Solum NO, Brosstad F, Røger M, Abdelnoor M. Demonstration of platelet-derived microvesicles in blood from patients with activated coagulation and fibrinolysis using a filtration technique and western blotting. Thromb Haemost. nov 1994;72(5):666-71.

84. van Niel G, D'Angelo G, Raposo G. Shedding light on the cell biology of extracellular vesicles. Nat Rev Mol Cell Biol. avr 2018;19(4):213-28.

85. Colombo M, Raposo G, Théry C. Biogenesis, secretion, and intercellular interactions of exosomes and other extracellular vesicles. Annu Rev Cell Dev Biol. 2014;30:255-89.

86. Blanc L, Vidal M. New insights into the function of Rab GTPases in the context of exosomal secretion. Small GTPases. 04 2018;9(1-2):95-106.

87. Cocucci E, Racchetti G, Meldolesi J. Shedding microvesicles: artefacts no more. Trends Cell Biol. févr 2009;19(2):43-51.

88. Turola E, Furlan R, Bianco F, Matteoli M, Verderio C. Microglial microvesicle secretion and intercellular signaling. Front Physiol. 2012;3:149.

89. D'Souza-Schorey C, Clancy JW. Tumor-derived microvesicles: shedding light on novel microenvironment modulators and prospective cancer biomarkers. Genes Dev. 15 juin 2012;26(12):1287-99.

90. McMahon HT, Boucrot E. Membrane curvature at a glance. J Cell Sci. 15 mars 2015;128(6):1065-70.

91. Kozlov MM, Campelo F, Liska N, Chernomordik LV, Marrink SJ, McMahon HT. Mechanisms shaping cell membranes. Curr Opin Cell Biol. août 2014;29:53-60.

92. Raposo G, Stoorvogel W. Extracellular vesicles: exosomes, microvesicles, and friends. J Cell Biol. 18 févr 2013;200(4):373-83.

93. Hessvik NP, Llorente A. Current knowledge on exosome biogenesis and release. Cell Mol Life Sci CMLS. 2018;75(2):193-208.

94. Savelyeva AV, Kuligina EV, Bariakin DN, Kozlov VV, Ryabchikova EI, Richter VA, et al. Variety of RNAs in Peripheral Blood Cells, Plasma, and Plasma Fractions. BioMed Res Int [Internet]. 2017 [cité 30 nov 2018];2017. Disponible sur: https://www.ncbi.nlm.nih.gov/pmc/articles/PMC5239830/

95. Rennert RC, Hochberg FH, Carter BS. ExRNA in Biofluids as Biomarkers for Brain Tumors. Cell Mol Neurobiol. avr 2016;36(3):353-60.

96. Muralidharan-Chari V, Clancy JW, Sedgwick A, D'Souza-Schorey C. Microvesicles: mediators of extracellular communication during cancer progression. J Cell Sci. 15 mai 2010;123(Pt 10):1603-11.

97. De Toro J, Herschlik L, Waldner C, Mongini C. Emerging roles of exosomes in normal and pathological conditions: new insights for diagnosis and therapeutic applications. Front Immunol. 2015;6:203.

98. Chen CC, Liu L, Ma F, Wong CW, Guo XE, Chacko JV, et al. Elucidation of Exosome Migration across the Blood-Brain Barrier Model In Vitro. Cell Mol Bioeng. déc 2016;9(4):509-29.

99. Matsumoto J, Stewart T, Banks WA, Zhang J. The Transport Mechanism of Extracellular Vesicles at the Blood-Brain Barrier. Curr Pharm Des. 2017;23(40):6206-14.

100. Anderson HC. Vesicles associated with calcification in the matrix of epiphyseal cartilage. J Cell Biol. avr 1969;41(1):59-72.

101. Pan BT, Johnstone RM. Fate of the transferrin receptor during maturation of sheep reticulocytes in vitro: selective externalization of the receptor. Cell. juill 1983;33(3):967-78.

102. Akers JC, Gonda D, Kim R, Carter BS, Chen CC. Biogenesis of extracellular vesicles (EV): exosomes, microvesicles, retrovirus-like vesicles, and apoptotic bodies. J Neurooncol. mai 2013;113(1):1-11.

103. Beach A, Zhang H-G, Ratajczak MZ, Kakar SS. Exosomes: an overview of biogenesis, composition and role in ovarian cancer. J Ovarian Res. 25 janv 2014;7:14.

104. Möbius W, Ohno-Iwashita Y, van Donselaar EG, Oorschot VMJ, Shimada Y, Fujimoto T, et al. Immunoelectron microscopic localization of cholesterol using biotinylated and non-cytolytic perfringolysin O. J Histochem Cytochem Off J Histochem Soc. janv 2002;50(1):43-55.

105. White IJ, Bailey LM, Aghakhani MR, Moss SE, Futter CE. EGF stimulates annexin 1-dependent inward vesiculation in a multivesicular endosome subpopulation. EMBO J. 11 janv 2006;25(1):1-12.

106. Wubbolts R, Leckie RS, Veenhuizen PTM, Schwarzmann G, Möbius W, Hoernschemeyer J, et al. Proteomic and biochemical analyses of human B cell-derived exosomes. Potential implications for their function and multivesicular body formation. J Biol Chem. 28 mars 2003;278(13):10963-72.

107. Trajkovic K, Hsu C, Chiantia S, Rajendran L, Wenzel D, Wieland F, et al. Ceramide triggers budding of exosome vesicles into multivesicular endosomes. Science. 29 févr 2008;319(5867):1244-7.

108. Brouwers JF, Aalberts M, Jansen JWA, van Niel G, Wauben MH, Stout TAE, et al. Distinct lipid compositions of two types of human prostasomes. Proteomics. mai 2013;13(10-11):1660-6.

109. Balkom BWM van, Eisele AS, Pegtel DM, Bervoets S, Verhaar MC. Quantitative and qualitative analysis of small RNAs in human endothelial cells and exosomes provides insights into localized RNA processing, degradation and sorting. J Extracell Vesicles [Internet]. 29 mai 2015 [cité 3 mars 2016];4(0). Disponible sur: http://www.journalofextracellularvesicles.net/index.php/jev/article/view/26760

110. Willms E, Johansson HJ, Mäger I, Lee Y, Blomberg KEM, Sadik M, et al. Cells release subpopulations of exosomes with distinct molecular and biological properties. Sci Rep. 2 mars 2016;6:22519.

111. Andreu Z, Yáñez-Mó M. Tetraspanins in extracellular vesicle formation and function. Front Immunol. 2014;5:442.

112. Gutiérrez-Vázquez C, Villarroya-Beltri C, Mittelbrunn M, Sánchez-Madrid F. Transfer of extracellular vesicles during immune cell-cell interactions. Immunol Rev. janv 2013;251(1):125-42.

113. Villarroya-Beltri C, Baixauli F, Gutiérrez-Vázquez C, Sánchez-Madrid F, Mittelbrunn M. SORTING IT OUT: REGULATION OF EXOSOME LOADING. Semin Cancer Biol. oct 2014;28:3-13.

114. van der Vlist EJ, Arkesteijn GJA, van de Lest CHA, Stoorvogel W, Nolte-'t Hoen ENM, Wauben MHM. CD4(+) T cell activation promotes the differential release of distinct populations of nanosized vesicles. J Extracell Vesicles. 2012;1.

115. Bobrie A, Colombo M, Krumeich S, Raposo G, Théry C. Diverse subpopulations of vesicles secreted by different intracellular mechanisms are present in exosome preparations obtained by differential ultracentrifugation. J Extracell Vesicles. 2012;1.

116. Harding C, Stahl P. Transferrin recycling in reticulocytes: pH and iron are important determinants of ligand binding and processing. Biochem Biophys Res Commun. 15 juin 1983;113(2):650-8.

117. Lippincott-Schwartz J, Fambrough DM. Cycling of the integral membrane glycoprotein, LEP100, between plasma membrane and lysosomes: kinetic and morphological analysis. Cell. 5 juin 1987;49(5):669-77.

118. Hannafon BN, Ding W-Q. Intercellular Communication by Exosome-Derived microRNAs in Cancer. Int J Mol Sci. 9 juill 2013;14(7):14240-69.

119. Dioufa N, Clark AM, Ma B, Beckwitt CH, Wells A. Bi-directional exosome-driven intercommunication between the hepatic niche and cancer cells. Mol Cancer [Internet]. 14 nov 2017 [cité 3 mai 2019];16. Disponible sur: https://www.ncbi.nlm.nih.gov/pmc/articles/PMC5686836/

120. Taylor DD, Gercel-Taylor C. The origin, function, and diagnostic potential of RNA within extracellular vesicles present in human biological fluids. Front Genet [Internet]. 30 juill 2013 [cité 13 janv 2016];4. Disponible sur: http://www.ncbi.nlm.nih.gov/pmc/articles/PMC3726994/

121. Hong BS, Cho J-H, Kim H, Choi E-J, Rho S, Kim J, et al. Colorectal cancer cell-derived microvesicles are enriched in cell cycle-related mRNAs that promote proliferation of endothelial cells. BMC Genomics. 25 nov 2009;10:556.

122. Zhang J, Li S, Li L, Li M, Guo C, Yao J, et al. Exosome and Exosomal MicroRNA: Trafficking, Sorting, and Function. Genomics Proteomics Bioinformatics. févr 2015;13(1):17-24.

123. Xiang X, Poliakov A, Liu C, Liu Y, Deng Z, Wang J, et al. Induction of myeloid-derived suppressor cells by tumor exosomes. Int J Cancer. 1 juin 2009;124(11):2621-33.

124. Robbins PD, Morelli AE. Regulation of immune responses by extracellular vesicles. Nat Rev Immunol. mars 2014;14(3):195-208.

125. Wolfers J, Lozier A, Raposo G, Regnault A, Théry C, Masurier C, et al. Tumor-derived exosomes are a source of shared tumor rejection antigens for CTL cross-priming. Nat Med. mars 2001;7(3):297-303.

126. Admyre C, Johansson SM, Paulie S, Gabrielsson S. Direct exosome stimulation of peripheral human T cells detected by ELISPOT. Eur J Immunol. juill 2006;36(7):1772-81.

127. Admyre C, Bohle B, Johansson SM, Focke-Tejkl M, Valenta R, Scheynius A, et al. B cell-derived exosomes can present allergen peptides and activate allergen-specific T cells to proliferate and produce TH2-like cytokines. J Allergy Clin Immunol. déc 2007;120(6):1418-24.

128. Rosenberger L, Ezquer M, Lillo-Vera F, Pedraza PL, Ortúzar MI, González PL, et al. Stem cell exosomes inhibit angiogenesis and tumor growth of oral squamous cell carcinoma. Sci Rep. 24 janv 2019;9(1):663.

129. Rak J. Microparticles in cancer. Semin Thromb Hemost. nov 2010;36(8):888-906.

130. Hood JL, San RS, Wickline SA. Exosomes released by melanoma cells prepare sentinel lymph nodes for tumor metastasis. Cancer Res. 1 juin 2011;71(11):3792-801.

131. Luga V, Zhang L, Viloria-Petit AM, Ogunjimi AA, Inanlou MR, Chiu E, et al. Exosomes mediate stromal mobilization of autocrine Wnt-PCP signaling in breast cancer cell migration. Cell. 21 déc 2012;151(7):1542-56.

132. Jan AT, Malik MA, Rahman S, Yeo HR, Lee EJ, Abdullah TS, et al. Perspective Insights of Exosomes in Neurodegenerative Diseases: A Critical Appraisal. Front Aging Neurosci [Internet]. 29 sept 2017 [cité 3 mai 2019];9. Disponible sur: https://www.ncbi.nlm.nih.gov/pmc/articles/PMC5626860/

133. Crenshaw BJ, Gu L, Sims B, Matthews QL. Exosome Biogenesis and Biological Function in Response to Viral Infections. Open Virol J. 28 sept 2018;12:134-48.

134. Bunggulawa EJ, Wang W, Yin T, Wang N, Durkan C, Wang Y, et al. Recent advancements in the use of exosomes as drug delivery systems. J Nanobiotechnology. 16 oct 2018;16(1):81.

135. Aryani A, Denecke B. Exosomes as a Nanodelivery System: a Key to the Future of Neuromedicine? Mol Neurobiol. mars 2016;53(2):818-34.

136. Ha D, Yang N, Nadithe V. Exosomes as therapeutic drug carriers and delivery vehicles across biological membranes: current perspectives and future challenges. Acta Pharm Sin B. juill 2016;6(4):287-96.

137. Jiang X-C, Gao J-Q. Exosomes as novel bio-carriers for gene and drug delivery. Int J Pharm. 15 avr 2017;521(1-2):167-75.

138. Haney MJ, Klyachko NL, Zhao Y, Gupta R, Plotnikova EG, He Z, et al. Exosomes as drug delivery vehicles for Parkinson's disease therapy. J Control Release Off J Control Release Soc. 10 juin 2015;207:18-30.

139. Hood JL, Scott MJ, Wickline SA. Maximizing exosome colloidal stability following electroporation. Anal Biochem. 1 mars 2014;448:41-9.

140. Neesse A, Michl P, Frese KK, Feig C, Cook N, Jacobetz MA, et al. Stromal biology and therapy in pancreatic cancer. Gut. juin 2011;60(6):861-8.

141. Tai Y, Chen K, Hsieh J, Shen T. Exosomes in cancer development and clinical applications. Cancer Sci. août 2018;109(8):2364-74.

142. Tian Y, Li S, Song J, Ji T, Zhu M, Anderson GJ, et al. A doxorubicin delivery platform using engineered natural membrane vesicle exosomes for targeted tumor therapy. Biomaterials. févr 2014;35(7):2383-90.

143. Morse MA, Garst J, Osada T, Khan S, Hobeika A, Clay TM, et al. A phase I study of dexosome immunotherapy in patients with advanced non-small cell lung cancer. J Transl Med. 21 févr 2005;3(1):9.

144. Théry C, Amigorena S, Raposo G, Clayton A. Isolation and characterization of exosomes from cell culture supernatants and biological fluids. Curr Protoc Cell Biol. avr 2006;Chapter 3:Unit 3.22.

145. Livshits MA, Livshts MA, Khomyakova E, Evtushenko EG, Lazarev VN, Kulemin NA, et al. Isolation of exosomes by differential centrifugation: Theoretical analysis of a commonly used protocol. Sci Rep. 30 nov 2015;5:17319.

146. Deregibus MC, Figliolini F, D'Antico S, Manzini PM, Pasquino C, De Lena M, et al. Charge-based precipitation of extracellular vesicles. Int J Mol Med. nov 2016;38(5):1359-66.

147. Yakimchuk K. Exosomes: Isolation and Characterization Methods and Specific Markers. Mater Methods [Internet]. 6 mars 2019 [cité 4 mai 2019]; Disponible sur: /method/Exosomes-Isolation-and-Characterization-Methods-and-Specific-Markers.html

148. Arroyo JD, Chevillet JR, Kroh EM, Ruf IK, Pritchard CC, Gibson DF, et al. Argonaute2 complexes carry a population of circulating microRNAs independent of vesicles in human plasma. Proc Natl Acad Sci U S A. 22 mars 2011;108(12):5003-8.

149. Colhoun HM, Otvos JD, Rubens MB, Taskinen MR, Underwood SR, Fuller JH. Lipoprotein subclasses and particle sizes and their relationship with coronary artery calcification in men and women with and without type 1 diabetes. Diabetes. juin 2002;51(6):1949-56.

150. Brett SI, Lucien F, Guo C, Williams KC, Kim Y, Durfee PN, et al. Immunoaffinity based methods are superior to kits for purification of prostate derived extracellular vesicles from plasma samples. The Prostate. mai 2017;77(13):1335-43.

151. Contreras-Naranjo JC, Wu H-J, Ugaz VM. Microfluidics for exosome isolation and analysis: enabling liquid biopsy for personalized medicine. Lab Chip. 25 2017;17(21):3558-77.

152. Taylor DD, Shah S. Methods of isolating extracellular vesicles impact down-stream analyses of their cargoes. Methods San Diego Calif. 1 oct 2015;87:3-10.

153. Van Deun J, Mestdagh P, Sormunen R, Cocquyt V, Vermaelen K, Vandesompele J, et al. The impact of disparate isolation methods for extracellular vesicles on downstream RNA profiling. J Extracell Vesicles [Internet]. 18 sept 2014 [cité 24 oct 2016];3. Disponible sur: http://www.ncbi.nlm.nih.gov/pmc/articles/PMC4169610/

154. Stranska R, Gysbrechts L, Wouters J, Vermeersch P, Bloch K, Dierickx D, et al. Comparison of membrane affinity-based method with size-exclusion chromatography for isolation of exosome-like vesicles from human plasma. J Transl Med. 9 janv 2018;16(1):1.

155. Andreu Z, Rivas E, Sanguino-Pascual A, Lamana A, Marazuela M, González-Alvaro I, et al. Comparative analysis of EV isolation procedures for miRNAs detection in serum samples. J Extracell Vesicles [Internet]. 20 juin 2016 [cité 24 févr 2017];5. Disponible sur: http://www.ncbi.nlm.nih.gov/pmc/articles/PMC4916259/

156. Sharma P, Ludwig S, Muller L, Hong CS, Kirkwood JM, Ferrone S, et al. Immunoaffinity-based isolation of melanoma cell-derived exosomes from plasma of patients with melanoma. J Extracell Vesicles. 2018;7(1):1435138.

157. Zocco D, Zarovni N. Extraction and Analysis of Extracellular Vesicle-Associated miRNAs Following Antibody-Based Extracellular Vesicle Capture from Plasma Samples. Methods Mol Biol Clifton NJ. 2017;1660:269-85.

158. Mateescu B, Kowal EJK, van Balkom BWM, Bartel S, Bhattacharyya SN, Buzás EI, et al. Obstacles and opportunities in the functional analysis of extracellular vesicle RNA - an ISEV position paper. J Extracell Vesicles. 2017;6(1):1286095.

159. Li K, Rodosthenous RS, Kashanchi F, Gingeras T, Gould SJ, Kuo LS, et al. Advances, challenges, and opportunities in extracellular RNA biology: insights from the NIH exRNA Strategic Workshop. JCI Insight. 5 avr 2018;3(7).

160. Alexander RP, Chiou N-T, Ansel KM. Improved exosome isolation by sucrose gradient fractionation of ultracentrifuged crude exosome pellets. Protoc Exch [Internet]. 23 août 2016 [cité 21 oct 2016]; Disponible sur: http://www.nature.com/protocolexchange/protocols/5035

161. Li K, Wong DK, Hong KY, Raffai RL. Cushioned-Density Gradient Ultracentrifugation (C-DGUC): A Refined and High Performance Method for the Isolation, Characterization, and Use of Exosomes. Methods Mol Biol Clifton NJ. 2018;1740:69-83.

162. Ibsen SD, Wright J, Lewis JM, Kim S, Ko S-Y, Ong J, et al. Rapid Isolation and Detection of Exosomes and Associated Biomarkers from Plasma. ACS Nano. 25 juill 2017;11(7):6641-51.

163. Vestad B, Llorente A, Neurauter A, Phuyal S, Kierulf B, Kierulf P, et al. Size and concentration analyses of extracellular vesicles by nanoparticle tracking analysis: a variation study. J Extracell Vesicles. 2017;6(1):1344087.

164. Lawrie AS, Albanyan A, Cardigan RA, Mackie IJ, Harrison P. Microparticle sizing by dynamic light scattering in fresh-frozen plasma. Vox Sang. avr 2009;96(3):206-12.

165. Gercel-Taylor C, Atay S, Tullis RH, Kesimer M, Taylor DD. Nanoparticle analysis of circulating cell-derived vesicles in ovarian cancer patients. Anal Biochem. 1 sept 2012;428(1):44-53.

166. Wu Y, Deng W, Klinke DJ. Exosomes: improved methods to characterize their morphology, RNA content, and surface protein biomarkers. The Analyst. 7 oct 2015;140(19):6631-42.

167. Reimer L. Transmission Electron Microscopy: Physics of Image Formation and Microanalysis [Internet]. Berlin Heidelberg: Springer-Verlag; 1984 [cité 29 janv 2019]. (Springer Series in Optical Sciences). Disponible sur: //www.springer.com/la/book/9783662135532

168. Adrian M, Dubochet J, Lepault J, McDowall AW. Cryo-electron microscopy of viruses. Nature. 1 mars 1984;308(5954):32-6.

169. Soares Martins T, Catita J, Martins Rosa I, A. B. da Cruz e Silva O, Henriques AG. Exosome isolation from distinct biofluids using precipitation and column-based approaches. PLoS ONE [Internet]. 11 juin 2018 [cité 17 avr 2019];13(6). Disponible sur: http://www.ncbi.nlm.nih.gov/pmc/articles/PMC5995457/

170. Amorim MG, Valieris R, Drummond RD, Pizzi MP, Freitas VM, Sinigaglia-Coimbra R, et al. A total transcriptome profiling method for plasma-derived extracellular vesicles: applications for liquid biopsies. Sci Rep [Internet]. 31 oct 2017 [cité 14 août 2018];7. Disponible sur: https://www.ncbi.nlm.nih.gov/pmc/articles/PMC5663969/

171. Kowal EJK, Ter-Ovanesyan D, Regev A, Church GM. Extracellular Vesicle Isolation and Analysis by Western Blotting. Methods Mol Biol Clifton NJ. 2017;1660:143-52.

172. Lobb RJ, Becker M, Wen Wen S, Wong CSF, Wiegmans AP, Leimgruber A, et al. Optimized exosome isolation protocol for cell culture supernatant and human plasma. J Extracell Vesicles [Internet]. 17 juill 2015 [cité 6 mai 2019];4. Disponible sur: https://www.ncbi.nlm.nih.gov/pmc/articles/PMC4507751/

173. Gardiner C, Di Vizio D, Sahoo S, Théry C, Witwer KW, Wauben M, et al. Techniques used for the isolation and characterization of extracellular vesicles: results of a worldwide survey. J Extracell Vesicles. 2016;5:32945.

174. Suárez H, Gámez-Valero A, Reyes R, López-Martín S, Rodríguez MJ, Carrascosa JL, et al. A bead-assisted flow cytometry method for the semi-quantitative analysis of Extracellular Vesicles. Sci Rep. 12 2017;7(1):11271.

175. Robert S, Lacroix R, Poncelet P, Harhouri K, Bouriche T, Judicone C, et al. High-sensitivity flow cytometry provides access to standardized measurement of small-size microparticles--brief report. Arterioscler Thromb Vasc Biol. avr 2012;32(4):1054-8.

176. Chandler WL, Yeung W, Tait JF. A new microparticle size calibration standard for use in measuring smaller microparticles using a new flow cytometer. J Thromb Haemost JTH. juin 2011;9(6):1216-24.

177. Enderle D, Spiel A, Coticchia CM, Berghoff E, Mueller R, Schlumpberger M, et al. Characterization of RNA from Exosomes and Other Extracellular Vesicles Isolated by a Novel Spin Column-Based Method. PLoS ONE [Internet]. 28 août 2015 [cité 6 mai 2019];10(8). Disponible sur: https://www.ncbi.nlm.nih.gov/pmc/articles/PMC4552735/

178. Hoy AM, Buck AH. Extracellular small RNAs: what, where, why?: Figure 1. Biochem Soc Trans. 1 août 2012;40(4):886-90.

179. Eldh M, Lötvall J, Malmhäll C, Ekström K. Importance of RNA isolation methods for analysis of exosomal RNA: evaluation of different methods. Mol Immunol. avr 2012;50(4):278-86.

180. Park NJ, Zhou H, Elashoff D, Henson BS, Kastratovic DA, Abemayor E, et al. Salivary microRNA: discovery, characterization, and clinical utility for oral cancer detection. Clin Cancer Res Off J Am Assoc Cancer Res. 1 sept 2009;15(17):5473-7.

181. Hanke M, Hoefig K, Merz H, Feller AC, Kausch I, Jocham D, et al. A robust methodology to study urine microRNA as tumor marker: microRNA-126 and microRNA-182 are related to urinary bladder cancer. Urol Oncol. déc 2010;28(6):655-61.

182. Zubakov D, Boersma AWM, Choi Y, van Kuijk PF, Wiemer EAC, Kayser M. MicroRNA markers for forensic body fluid identification obtained from microarray screening and quantitative RT-PCR confirmation. Int J Legal Med. mai 2010;124(3):217-26.

183. Irion U, St Johnston D. bicoid RNA localization requires specific binding of an endosomal sorting complex. Nature. 1 févr 2007;445(7127):554-8.

184. Emerman AB, Blower MD. The RNA-binding complex ESCRT-II in Xenopus laevis eggs recognizes purine-rich sequences through its subunit, Vps25. J Biol Chem. 10 2018;293(32):12593-605.

185. Kosaka N, Iguchi H, Yoshioka Y, Takeshita F, Matsuki Y, Ochiya T. Secretory mechanisms and intercellular transfer of microRNAs in living cells. J Biol Chem. 4 juin 2010;285(23):17442-52.

186. Villarroya-Beltri C, Gutiérrez-Vázquez C, Sánchez-Cabo F, Pérez-Hernández D, Vázquez J, Martin-Cofreces N, et al. Sumoylated hnRNPA2B1 controls the sorting of miRNAs into exosomes through binding to specific motifs. Nat Commun [Internet]. 20 déc 2013 [cité 9 déc 2015];4. Disponible sur: http://www.nature.com/doifinder/10.1038/ncomms3980

187. Koppers-Lalic D, Hackenberg M, Bijnsdorp IV, van Eijndhoven MAJ, Sadek P, Sie D, et al. Nontemplated nucleotide additions distinguish the small RNA composition in cells from exosomes. Cell Rep. 25 sept 2014;8(6):1649-58.

188. Pigati L, Yaddanapudi SCS, Iyengar R, Kim D-J, Hearn SA, Danforth D, et al. Selective release of microRNA species from normal and malignant mammary epithelial cells. PloS One. 2010;5(10):e13515.

189. Valadi H, Ekström K, Bossios A, Sjöstrand M, Lee JJ, Lötvall JO. Exosome-mediated transfer of mRNAs and microRNAs is a novel mechanism of genetic exchange between cells. Nat Cell Biol. juin 2007;9(6):654-9.

190. Batagov AO, Kurochkin IV. Exosomes secreted by human cells transport largely mRNA fragments that are enriched in the 3′-untranslated regions. Biol Direct. 7 juin 2013;8:12.

191. Yeri A, Courtright A, Reiman R, Carlson E, Beecroft T, Janss A, et al. Total Extracellular Small RNA Profiles from Plasma, Saliva, and Urine of Healthy Subjects. Sci Rep. 17 2017;7:44061.

192. Yuan T, Huang X, Woodcock M, Du M, Dittmar R, Wang Y, et al. Plasma extracellular RNA profiles in healthy and cancer patients. Sci Rep. 20 janv 2016;6:19413.

193. Li M, Zeringer E, Barta T, Schageman J, Cheng A, Vlassov AV. Analysis of the RNA content of the exosomes derived from blood serum and urine and its potential as biomarkers. Philos Trans R Soc B Biol Sci [Internet]. 26 sept 2014 [cité 11 oct 2016];369(1652). Disponible sur: http://www.ncbi.nlm.nih.gov/pmc/articles/PMC4142023/

194. Guo Y, Vickers K, Xiong Y, Zhao S, Sheng Q, Zhang P, et al. Comprehensive evaluation of extracellular small RNA isolation methods from serum in high throughput sequencing. BMC Genomics [Internet]. 7 janv 2017 [cité 14 août 2018];18. Disponible sur: https://www.ncbi.nlm.nih.gov/pmc/articles/PMC5219650/

195. Freedman JE, Gerstein M, Mick E, Rozowsky J, Levy D, Kitchen R, et al. Diverse human extracellular RNAs are widely detected in human plasma. Nat Commun. 2016;7:11106.

196. Max KEA, Bertram K, Akat KM, Bogardus KA, Li J, Morozov P, et al. Human plasma and serum extracellular small RNA reference profiles and their clinical utility. Proc Natl Acad Sci U S A. 5 juin 2018;115(23):E5334-43.

197. Huang X, Yuan T, Tschannen M, Sun Z, Jacob H, Du M, et al. Characterization of human plasma-derived exosomal RNAs by deep sequencing. BMC Genomics. 2013;14:319.

198. Umu SU, Langseth H, Bucher-Johannessen C, Fromm B, Keller A, Meese E, et al. A comprehensive profile of circulating RNAs in human serum. RNA Biol. 01 2018;15(2):242-50.

199. Danielson KM, Rubio R, Abderazzaq F, Das S, Wang YE. High Throughput Sequencing of Extracellular RNA from Human Plasma. PloS One. 2017;12(1):e0164644.

200. Cheng HH, Yi HS, Kim Y, Kroh EM, Chien JW, Eaton KD, et al. Plasma processing conditions substantially influence circulating microRNA biomarker levels. PloS One. 2013;8(6):e64795.

201. Tosar JP, Cayota A, Eitan E, Halushka MK, Witwer KW. Ribonucleic artefacts: are some extracellular RNA discoveries driven by cell culture medium components? J Extracell Vesicles. 2017;6(1):1272832.

202. Khare D, Goldschmidt N, Bardugo A, Gur-Wahnon D, Ben-Dov IZ, Avni B. Plasma microRNA profiling: Exploring better biomarkers for lymphoma surveillance. PLoS ONE [Internet]. 13 nov 2017 [cité 17 avr 2019];12(11). Disponible sur: http://www.ncbi.nlm.nih.gov/pmc/articles/PMC5683633/

203. Tang Y-T, Huang Y-Y, Zheng L, Qin S-H, Xu X-P, An T-X, et al. Comparison of isolation methods of exosomes and exosomal RNA from cell culture medium and serum. Int J Mol Med. sept 2017;40(3):834-44.

204. Ding M, Wang C, Lu X, Zhang C, Zhou Z, Chen X, et al. Comparison of commercial exosome isolation kits for circulating exosomal microRNA profiling. Anal Bioanal Chem. juin 2018;410(16):3805-14.

205. Helwa I, Cai J, Drewry MD, Zimmerman A, Dinkins MB, Khaled ML, et al. A Comparative Study of Serum Exosome Isolation Using Differential Ultracentrifugation and Three Commercial Reagents. PLoS ONE [Internet]. 23 janv 2017 [cité 17 avr 2019];12(1). Disponible sur: http://www.ncbi.nlm.nih.gov/pmc/articles/PMC5256994/

206. Patel GK, Khan MA, Zubair H, Srivastava SK, Khushman M, Singh S, et al. Comparative analysis of exosome isolation methods using culture supernatant for optimum yield, purity and downstream applications. Sci Rep [Internet]. 29 mars 2019 [cité 18 avr 2019];9. Disponible sur: http://www.ncbi.nlm.nih.gov/pmc/articles/PMC6441044/

207. Ainsztein AM, Brooks PJ, Dugan VG, Ganguly A, Guo M, Howcroft TK, et al. The NIH Extracellular RNA Communication Consortium. J Extracell Vesicles. 2015;4:27493.

208. Galvanin A, Dostert G, Ayadi L, Marchand V, Velot É, Motorin Y. Diversity and heterogeneity of extracellular RNA in human plasma. Biochimie. 17 mai 2019;

209. Mitchell AJ, Gray WD, Hayek SS, Ko Y-A, Thomas S, Rooney K, et al. Platelets confound the measurement of extracellular miRNA in archived plasma. Sci Rep. 13 2016;6:32651.

210. Mateescu B, Kowal EJK, Balkom BWM van, Bartel S, Bhattacharyya SN, Buzás EI, et al. Obstacles and opportunities in the functional analysis of extracellular vesicle RNA – an ISEV position paper. J Extracell Vesicles. 1 janv 2017;6(1):1286095.

211. Beutler E, Gelbart T, Kuhl W. Interference of heparin with the polymerase chain reaction. BioTechniques. août 1990;9(2):166.

212. Lacroix R, Judicone C, Mooberry M, Boucekine M, Key NS, Dignat-George F, et al. Standardization of pre-analytical variables in plasma microparticle determination: results of the International Society on Thrombosis and Haemostasis SSC Collaborative workshop. J Thromb Haemost JTH. 2 avr 2013;

213. Yokota M, Tatsumi N, Nathalang O, Yamada T, Tsuda I. Effects of heparin on polymerase chain reaction for blood white cells. J Clin Lab Anal. 1999;13(3):133-40.

214. Royo F, Schlangen K, Palomo L, Gonzalez E, Conde-Vancells J, Berisa A, et al. Transcriptome of extracellular vesicles released by hepatocytes. PloS One. 2013;8(7):e68693.

215. Lai X, Wang M, McElyea SD, Sherman S, House M, Korc M. A microRNA signature in circulating exosomes is superior to exosomal glypican-1 levels for diagnosing pancreatic cancer. Cancer Lett. 1 mai 2017;393:86.

216. Dejima H, Iinuma H, Kanaoka R, Matsutani N, Kawamura M. Exosomal microRNA in plasma as a non-invasive biomarker for the recurrence of non-small cell lung cancer. Oncol Lett. mars 2017;13(3):1256-63.

217. Maruoka S, Gon Y, Shikano S, Shintani Y, Koyama D, Sekiyama T, et al. Exosomal microRNAs in the serum are potential real-time biomarkers for allergic inflammation in the airway of mice. Eur Respir J. 1 sept 2014;44(Suppl 58):P1010.

218. Sumrin A, Moazzam S, Khan AA, Ramzan I, Batool Z, Kaleem S, et al. Exosomes as Biomarker of Cancer. Braz Arch Biol Technol [Internet]. 2018 [cité 17 mai 2019];61. Disponible sur: http://www.scielo.br/scielo.php?script=sci_abstract&pid=S1516-89132018000100309&lng=en&nrm=iso&tlng=en

219. Liu T, Zhang Q, Zhang J, Li C, Miao Y-R, Lei Q, et al. EVmiRNA: a database of miRNA profiling in extracellular vesicles. Nucleic Acids Res. 8 janv 2019;47(D1):D89-93.

220. Li D-B, Liu J-L, Wang W, Luo X-M, Zhou X, Li J-P, et al. Plasma Exosomal miRNA-122-5p and miR-300-3p as Potential Markers for Transient Ischaemic Attack in Rats. Front Aging Neurosci [Internet]. 2018 [cité 17 mai 2019];10. Disponible sur: https://www.frontiersin.org/articles/10.3389/fnagi.2018.00024/full

221. Sharma R, Huang X, Brekken RA, Schroit AJ. Detection of phosphatidylserine-positive exosomes for the diagnosis of early-stage malignancies. Br J Cancer. août 2017;117(4):545-52.

222. Xi X, Li T, Huang Y, Sun J, Zhu Y, Yang Y, et al. RNA Biomarkers: Frontier of Precision Medicine for Cancer. Non-Coding RNA [Internet]. 20 févr 2017 [cité 17 mai 2019];3(1). Disponible sur: https://www.ncbi.nlm.nih.gov/pmc/articles/PMC5832009/

223. Wang K, Li H, Yuan Y, Etheridge A, Zhou Y, Huang D, et al. The complex exogenous RNA spectra in human plasma: an interface with human gut biota? PloS One. 2012;7(12):e51009.

224. Ramakrishnaiah V, Thumann C, Fofana I, Habersetzer F, Pan Q, de Ruiter PE, et al. Exosome-mediated transmission of hepatitis C virus between human hepatoma Huh7.5 cells. Proc Natl Acad Sci U S A. 6 août 2013;110(32):13109-13.

225. Nour AM, Modis Y. Endosomal vesicles as vehicles for viral genomes. Trends Cell Biol. août 2014;24(8):449-54.

226. Smit JM, Moesker B, Rodenhuis-Zybert I, Wilschut J. Flavivirus Cell Entry and Membrane Fusion. Viruses. 22 févr 2011;3(2):160-71.

227. Hamel R, Dejarnac O, Wichit S, Ekchariyawat P, Neyret A, Luplertlop N, et al. Biology of Zika Virus Infection in Human Skin Cells. J Virol. 17 juin 2015;89(17):8880-96.

228. Longatti A. The Dual Role of Exosomes in Hepatitis A and C Virus Transmission and Viral Immune Activation. Viruses. 17 déc 2015;7(12):6707-15.

229. Anderson MR, Kashanchi F, Jacobson S. Exosomes in Viral Disease. Neurotherapeutics. juill 2016;13(3):535-46.

230. Arroyo JD, Chevillet JR, Kroh EM, Ruf IK, Pritchard CC, Gibson DF, et al. Argonaute2 complexes carry a population of circulating microRNAs independent of vesicles in human plasma. Proc Natl Acad Sci U S A. 22 mars 2011;108(12):5003-8.

231. Kowalski MP, Krude T. Functional roles of non-coding Y RNAs. Int J Biochem Cell Biol. sept 2015;66:20-9.

232. Dhahbi JM, Spindler SR, Atamna H, Boffelli D, Mote P, Martin DIK. 5′-YRNA fragments derived by processing of transcripts from specific YRNA genes and pseudogenes are abundant in human serum and plasma. Physiol Genomics. 1 nov 2013;45(21):990-8.

233. Ninomiya S, Kawano M, Abe T, Ishikawa T, Takahashi M, Tamura M, et al. Potential Small Guide RNAs for tRNase ZL from Human Plasma, Peripheral Blood Mononuclear Cells, and Cultured Cell Lines. PLoS ONE [Internet]. 2 mars 2015 [cité 29 mai 2016];10(3). Disponible sur: http://www.ncbi.nlm.nih.gov/pmc/articles/PMC4346264/

234. Christov CP, Trivier E, Krude T. Noncoding human Y RNAs are overexpressed in tumours and required for cell proliferation. Br J Cancer. 11 mars 2008;98(5):981-8.

235. Hoagland MB, Keller EB, Zamecnik PC. Enzymatic carboxyl activation of amino acids. J Biol Chem. janv 1956;218(1):345-58.

236. Hoagland MB, Stephenson ML, Scott JF, Hecht LI, Zamecnik PC. A soluble ribonucleic acid intermediate in protein synthesis. J Biol Chem. mars 1958;231(1):241-57.

237. Hoagland MB, Zamecnik PC, Stephenson ML. Intermediate reactions in protein biosynthesis. 1957. Biochim Biophys Acta. 1989;1000:106-7.

238. RajBhandary UL, Köhrer C. Early days of tRNA research: discovery, function, purification and sequence analysis. J Biosci. oct 2006;31(4):439-51.

239. Holley RW. Structure of an alanine transfer ribonucleic acid. JAMA. 22 nov 1965;194(8):868-71.

240. Shepherd J, Ibba M. Bacterial transfer RNAs. FEMS Microbiol Rev. mai 2015;39(3):280-300.

241. Hori H, Tomikawa C, Hirata A, Toh Y, Tomita K, Ueda T, et al. Transfer RNA Synthesis and Regulation. In: eLS [Internet]. American Cancer Society; 2014 [cité 9 mai 2019]. Disponible sur: https://onlinelibrary.wiley.com/doi/abs/10.1002/9780470015902.a0000529.pub3

242. Fournier MJ, Ozeki H. Structure and organization of the transfer ribonucleic acid genes of Escherichia coli K-12. Microbiol Rev. déc 1985;49(4):379-97.

243. Deutscher MP, Lin JJ, Evans JA. Transfer RNA metabolism in Escherichia coli cells deficient in tRNA nucleotidyltransferase. J Mol Biol. 25 déc 1977;117(4):1081-94.

244. Lizano E, Scheibe M, Rammelt C, Betat H, Mörl M. A comparative analysis of CCA-adding enzymes from human and E. coli: differences in CCA addition and tRNA 3'-end repair. Biochimie. mai 2008;90(5):762-72.

245. Robertson HD, Webster RE, Zinder ND. Purification and properties of ribonuclease III from Escherichia coli. J Biol Chem. 10 janv 1968;243(1):82-91.

246. McDowall KJ, Lin-Chao S, Cohen SN. A+U content rather than a particular nucleotide order determines the specificity of RNase E cleavage. J Biol Chem. 8 avr 1994;269(14):10790-6.

247. Nicholson AW. Function, mechanism and regulation of bacterial ribonucleases. FEMS Microbiol Rev. juin 1999;23(3):371-90.

248. Gegenheimer P, Apirion D. Processing of procaryotic ribonucleic acid. Microbiol Rev. déc 1981;45(4):502-41.

249. Plautz G, Apirion D. Processing of RNA in Escherichia coli is limited in the absence of ribonuclease III, ribonuclease E and ribonuclease P. J Mol Biol. 15 juill 1981;149(4):813-9.

250. Cudny H, Deutscher MP. Apparent involvement of ribonuclease D in the 3' processing of tRNA precursors. Proc Natl Acad Sci U S A. févr 1980;77(2):837-41.

251. Ghosh RK, Deutscher MP. Purification of potential 3' processing nucleases using synthetic tRNA precursors. Nucleic Acids Res. oct 1978;5(10):3831-42.

252. Altman S. Biosynthesis of transfer RNA in Escherichia coli. Cell. janv 1975;4(1):21-9.

253. Kirsebom LA. RNase P RNA-mediated catalysis. Biochem Soc Trans. nov 2002;30(Pt 6):1153-8.

254. Harris ME, Christian EL. Recent insights into the structure and function of the ribonucleoprotein enzyme ribonuclease P. Curr Opin Struct Biol. juin 2003;13(3):325-33.

255. Kazantsev AV, Pace NR. Bacterial RNase P: a new view of an ancient enzyme. Nat Rev Microbiol. oct 2006;4(10):729-40.

256. Torres-Larios A, Swinger KK, Pan T, Mondragón A. Structure of ribonuclease P--a universal ribozyme. Curr Opin Struct Biol. juin 2006;16(3):327-35.

257. Stark BC, Kole R, Bowman EJ, Altman S. Ribonuclease P: an enzyme with an essential RNA component. Proc Natl Acad Sci U S A. août 1978;75(8):3717-21.

258. Guthrie C, Atchison R. Biochemical Characterization of RNase P: A tRNA Processing Activity with Protein and RNA Components. Cold Spring Harb Monogr Arch. 1 janv 1980;09B(0):83-97-97.

259. Walker SC, Engelke DR. Ribonuclease P: the evolution of an ancient RNA enzyme. Crit Rev Biochem Mol Biol. avr 2006;41(2):77-102.

260. Smith JK, Hsieh J, Fierke CA. Importance of RNA-protein interactions in bacterial ribonuclease P structure and catalysis. Biopolymers. 5 déc 2007;87(5-6):329-38.

261. Guenther U-P, Yandek LE, Niland CN, Campbell FE, Anderson D, Anderson VE, et al. Hidden specificity in an apparently nonspecific RNA-binding protein. Nature. 17 oct 2013;502(7471):385-8.

262. Grosjean H. DNA and RNA Modification Enzymes : Structure, Mechanism, Function and Evolution [Internet]. CRC Press; 2009 [cité 9 mai 2019]. Disponible sur: https://www.taylorfrancis.com/books/9780429089466

263. Motorin Y, Helm M. tRNA stabilization by modified nucleotides. Biochemistry. 22 juin 2010;49(24):4934-44.

264. El Yacoubi B, Bailly M, de Crécy-Lagard V. Biosynthesis and function of posttranscriptional modifications of transfer RNAs. Annu Rev Genet. 2012;46:69-95.

265. Björk GR, Ericson JU, Gustafsson CE, Hagervall TG, Jönsson YH, Wikström PM. Transfer RNA modification. Annu Rev Biochem. 1987;56:263-87.

266. Addepalli B, Limbach PA. Pseudouridine in the Anticodon of Escherichia coli tRNATyr(QΨA) Is Catalyzed by the Dual Specificity Enzyme RluF. J Biol Chem. 14 oct 2016;291(42):22327-37.

267. Gehrig S, Eberle M-E, Botschen F, Rimbach K, Eberle F, Eigenbrod T, et al. Identification of modifications in microbial, native tRNA that suppress immunostimulatory activity. J Exp Med. 13 févr 2012;209(2):225-33.

268. Rimbach K, Kaiser S, Helm M, Dalpke AH, Eigenbrod T. 2'-O-Methylation within Bacterial RNA Acts as Suppressor of TLR7/TLR8 Activation in Human Innate Immune Cells. J Innate Immun. 2015;7(5):482-93.

269. Ibba M, Soll D. Aminoacyl-tRNA synthesis. Annu Rev Biochem. 2000;69:617-50.

270. Reynolds NM, Lazazzera BA, Ibba M. Cellular mechanisms that control mistranslation. Nat Rev Microbiol. déc 2010;8(12):849-56.

271. Ayadi L, Galvanin A, Pichot F, Marchand V, Motorin Y. RNA ribose methylation (2'-O-methylation): Occurrence, biosynthesis and biological functions. Biochim Biophys Acta Gene Regul Mech. mars 2019;1862(3):253-69.

272. Machnicka MA, Milanowska K, Osman Oglou O, Purta E, Kurkowska M, Olchowik A, et al. MODOMICS: a database of RNA modification pathways--2013 update. Nucleic Acids Res. janv 2013;41(Database issue):D262-267.

273. Schubert HL, Blumenthal RM, Cheng X. Many paths to methyltransfer: a chronicle of convergence. Trends Biochem Sci. juin 2003;28(6):329-35.

274. Boschi-Muller S, Motorin Y. Chemistry enters nucleic acids biology: enzymatic mechanisms of RNA modification. Biochem Biokhimiia. déc 2013;78(13):1392-404.

275. Kozbial PZ, Mushegian AR. Natural history of S-adenosylmethionine-binding proteins. BMC Struct Biol. 14 oct 2005;5:19.

276. Hori H. Transfer RNA methyltransferases with a SpoU-TrmD (SPOUT) fold and their modified nucleosides in tRNA. Biomolecules. 28 févr 2017;7(1):23.

277. Watanabe K, Nureki O, Fukai S, Endo Y, Hori H. Functional Categorization of the Conserved Basic Amino Acid Residues in TrmH (tRNA (Gm18) Methyltansferase) Enzymes. J Biol Chem. 11 oct 2006;281(45):34630-9.

278. Watanabe K, Nureki O, Fukai S, Ishii R, Okamoto H, Yokoyama S, et al. Roles of conserved amino acid sequence motifs in the SpoU (TrmH) RNA methyltransferase family. J Biol Chem. 18 mars 2005;280(11):10368-77.

279. Persson BC, Jäger G, Gustafsson C. The spoU gene of Escherichia coli, the fourth gene of the spoT operon, is essential for tRNA (Gm18) 2'-O-methyltransferase activity. Nucleic Acids Res. 15 oct 1997;25(20):4093-7.

280. Kumagai I, Watanabe K, Oshima T. A thermostable tRNA (guanosine-2')-methyltransferase from Thermus thermophilus HB27 and the effect of ribose methylation on the conformational stability of tRNA. J Biol Chem. 10 juill 1982;257(13):7388-95.

281. Hori H, Suzuki T, Sugawara K, Inoue Y, Shibata T, Kuramitsu S, et al. Identification and characterization of tRNA (Gm18) methyltransferase from Thermus thermophilus HB8: domain structure and conserved amino acid sequence motifs. Genes Cells Devoted Mol Cell Mech. mars 2002;7(3):259-72.

282. Nureki O, Watanabe K, Fukai S, Ishii R, Endo Y, Hori H, et al. Deep knot structure for construction of active site and cofactor binding site of tRNA modification enzyme. Struct Lond Engl 1993. avr 2004;12(4):593-602.

283. Purta E, van Vliet F, Tkaczuk KL, Dunin-Horkawicz S, Mori H, Droogmans L, et al. The yfhQ gene of Escherichia coli encodes a tRNA:Cm32/Um32 methyltransferase. BMC Mol Biol. 18 juill 2006;7:23.

284. Somme J, Van Laer B, Roovers M, Steyaert J, Versées W, Droogmans L. Characterization of two homologous 2′-O-methyltransferases showing different specificities for their tRNA substrates. RNA. août 2014;20(8):1257-71.

285. Liu R-J, Long T, Zhou M, Zhou X-L, Wang E-D. tRNA recognition by a bacterial tRNA Xm32 modification enzyme from the SPOUT methyltransferase superfamily. Nucleic Acids Res. 3 sept 2015;43(15):7489-503.

286. Benítez-Páez A, Villarroya M, Douthwaite S, Gabaldón T, Armengod M-E. YibK is the 2'-O-methyltransferase TrmL that modifies the wobble nucleotide in Escherichia coli tRNA(Leu) isoacceptors. RNA N Y N. nov 2010;16(11):2131-43.

287. Armengod M-E, Moukadiri I, Prado S, Ruiz-Partida R, Benítez-Páez A, Villarroya M, et al. Enzymology of tRNA modification in the bacterial MnmEG pathway. Biochimie. juill 2012;94(7):1510-20.

288. Kawai G, Ue H, Yasuda M, Sakamoto K, Hashizume T, McCloskey JA, et al. Relation between functions and conformational characteristics of modified nucleosides found in tRNAs. Nucleic Acids Symp Ser. 1991;(25):49-50.

289. Prusiner P, Yathindra N, Sundaralingam M. Effect of ribose O(2')-methylation on the conformation of nucleosides and nucleotides. Biochim Biophys Acta. 11 oct 1974;366(2):115-23.

290. Lane BG, Tamaoki T. Studies of the chain termini and alkali-stable dinucleotide sequences in 16 s and 28 s ribosomal RNA from L cells. J Mol Biol. 28 juill 1967;27(2):335-48.

291. Trim AR, Parker JE. Preparation, purification and analyses of thirteen alkali-stable dinucleotides from yeast ribonucleic acid. Biochem J. févr 1970;116(4):589-98.

292. Endres L, Dedon PC, Begley TJ. Codon-biased translation can be regulated by wobble-base tRNA modification systems during cellular stress responses. RNA Biol. 18 avr 2015;12(6):603-14.

293. Huang H-Y, Hopper AK. Multiple Layers of Stress-Induced Regulation in tRNA Biology. Life [Internet]. 23 mars 2016;6(2). Disponible sur: https://www.ncbi.nlm.nih.gov/pmc/articles/PMC4931453/

294. Pluta K, Lefebvre O, Martin NC, Smagowicz WJ, Stanford DR, Ellis SR, et al. Maf1p, a negative effector of RNA polymerase III in Saccharomyces cerevisiae. Mol Cell Biol. août 2001;21(15):5031-40.

295. Oler AJ, Cairns BR. PP4 dephosphorylates Maf1 to couple multiple stress conditions to RNA polymerase III repression. EMBO J. 21 mars 2012;31(6):1440-52.

296. Vannini A, Ringel R, Kusser AG, Berninghausen O, Kassavetis GA, Cramer P. Molecular basis of RNA polymerase III transcription repression by Maf1. Cell. 1 oct 2010;143(1):59-70.

297. Oficjalska-Pham D, Harismendy O, Smagowicz WJ, Gonzalez de Peredo A, Boguta M, Sentenac A, et al. General repression of RNA polymerase III transcription is triggered by protein phosphatase type 2A-mediated dephosphorylation of Maf1. Mol Cell. 9 juin 2006;22(5):623-32.

298. Roberts DN, Wilson B, Huff JT, Stewart AJ, Cairns BR. Dephosphorylation and genome-wide association of Maf1 with Pol III-transcribed genes during repression. Mol Cell. 9 juin 2006;22(5):633-44.

299. Upadhya R, Lee J, Willis IM. Maf1 is an essential mediator of diverse signals that repress RNA polymerase III transcription. Mol Cell. déc 2002;10(6):1489-94.

300. Intine RV, Sakulich AL, Koduru SB, Huang Y, Pierstorff E, Goodier JL, et al. Control of transfer RNA maturation by phosphorylation of the human La antigen on serine 366. Mol Cell. août 2000;6(2):339-48.

301. Intine RV, Tenenbaum SA, Sakulich AL, Keene JD, Maraia RJ. Differential phosphorylation and subcellular localization of La RNPs associated with precursor tRNAs and translation-related mRNAs. Mol Cell. nov 2003;12(5):1301-7.

302. Foretek D, Wu J, Hopper AK, Boguta M. Control of Saccharomyces cerevisiae pre-tRNA processing by environmental conditions. RNA N Y N. mars 2016;22(3):339-49.

303. Netzer N, Goodenbour JM, David A, Dittmar KA, Jones RB, Schneider JR, et al. Innate immune and chemically triggered oxidative stress modifies translational fidelity. Nature. 26 nov 2009;462(7272):522-6.

304. Wiltrout E, Goodenbour JM, Fréchin M, Pan T. Misacylation of tRNA with methionine in Saccharomyces cerevisiae. Nucleic Acids Res. 1 nov 2012;40(20):10494-506.

305. Kaufmann G. Anticodon nucleases. Trends Biochem Sci. févr 2000;25(2):70-4.

306. Kirchner S, Ignatova Z. Emerging roles of tRNA in adaptive translation, signalling dynamics and disease. Nat Rev Genet. févr 2015;16(2):98-112.

307. Thompson DM, Lu C, Green PJ, Parker R. tRNA cleavage is a conserved response to oxidative stress in eukaryotes. RNA N Y N. oct 2008;14(10):2095-103.

308. Masaki H, Ogawa T. The modes of action of colicins E5 and D, and related cytotoxic tRNases. Biochimie. juin 2002;84(5-6):433-8.

309. Anderson P, Ivanov P. tRNA fragments in human health and disease. FEBS Lett. 28 nov 2014;588(23):4297-304.

310. Gebetsberger J, Polacek N. Slicing tRNAs to boost functional ncRNA diversity. RNA Biol. déc 2013;10(12):1798-806.

311. Thompson DM, Parker R. Stressing out over tRNA cleavage. Cell. 23 juill 2009;138(2):215-9.

312. Fu H, Feng J, Liu Q, Sun F, Tie Y, Zhu J, et al. Stress induces tRNA cleavage by angiogenin in mammalian cells. FEBS Lett. 22 janv 2009;583(2):437-42.

313. Ivanov P, Emara MM, Villen J, Gygi SP, Anderson P. Angiogenin-induced tRNA fragments inhibit translation initiation. Mol Cell. 19 août 2011;43(4):613-23.

314. Ivanov P, O'Day E, Emara MM, Wagner G, Lieberman J, Anderson P. G-quadruplex structures contribute to the neuroprotective effects of angiogenin-induced tRNA fragments. Proc Natl Acad Sci U S A. 23 déc 2014;111(51):18201-6.

315. Saikia M, Jobava R, Parisien M, Putnam A, Krokowski D, Gao X-H, et al. Angiogenin-cleaved tRNA halves interact with cytochrome c, protecting cells from apoptosis during osmotic stress. Mol Cell Biol. juill 2014;34(13):2450-63.

316. Zamudio JR, Kelly TJ, Sharp PA. Argonaute-bound small RNAs from promoter-proximal RNA polymerase II. Cell. 27 févr 2014;156(5):920-34.

317. Maute RL, Schneider C, Sumazin P, Holmes A, Califano A, Basso K, et al. tRNA-derived microRNA modulates proliferation and the DNA damage response and is down-regulated in B cell lymphoma. Proc Natl Acad Sci U S A. 22 janv 2013;110(4):1404-9.

318. Gebetsberger J, Zywicki M, Künzi A, Polacek N. tRNA-derived fragments target the ribosome and function as regulatory non-coding RNA in Haloferax volcanii. Archaea Vanc BC. 2012;2012:260909.

319. Sørensen MA, Fehler AO, Lo Svenningsen S. Transfer RNA instability as a stress response in Escherichia coli: Rapid dynamics of the tRNA pool as a function of demand. RNA Biol. 9 mai 2018;15(4-5):586-93.

320. Noon KR, Guymon R, Crain PF, McCloskey JA, Thomm M, Lim J, et al. Influence of Temperature on tRNA Modification in Archaea: Methanococcoides burtonii (Optimum Growth Temperature [Topt], 23°C) and Stetteria hydrogenophila (Topt, 95°C). J Bacteriol. sept 2003;185(18):5483-90.

321. Kinghorn SM, O'Byrne CP, Booth IR, Stansfield I. Physiological analysis of the role of truB in Escherichia coli: a role for tRNA modification in extreme temperature resistance. Microbiol Read Engl. nov 2002;148(Pt 11):3511-20.

322. Murata M, Fujimoto H, Nishimura K, Charoensuk K, Nagamitsu H, Raina S, et al. Molecular strategy for survival at a critical high temperature in Eschierichia coli. PloS One. 2011;6(6):e20063.

323. Emilsson V, Näslund AK, Kurland CG. Thiolation of transfer RNA in Escherichia coli varies with growth rate. Nucleic Acids Res. 11 sept 1992;20(17):4499-505.

324. Thompson KM, Gottesman S. The MiaA tRNA modification enzyme is necessary for robust RpoS expression in Escherichia coli. J Bacteriol. févr 2014;196(4):754-61.

325. Han L, Kon Y, Phizicky EM. Functional importance of Ψ38 and Ψ39 in distinct tRNAs, amplified for tRNAGln(UUG) by unexpected temperature sensitivity of the s2U modification in yeast. RNA N Y N. févr 2015;21(2):188-201.

326. Preston MA, D'Silva S, Kon Y, Phizicky EM. tRNAHis 5-methylcytidine levels increase in response to several growth arrest conditions in Saccharomyces cerevisiae. RNA N Y N. févr 2013;19(2):243-56.

327. Alings F, Sarin LP, Fufezan C, Drexler HCA, Leidel SA. An evolutionary approach uncovers a diverse response of tRNA 2-thiolation to elevated temperatures in yeast. RNA N Y N. févr 2015;21(2):202-12.

328. Damon JR, Pincus D, Ploegh HL. tRNA thiolation links translation to stress responses in Saccharomyces cerevisiae. Mol Biol Cell. 15 janv 2015;26(2):270-82.

329. Chan CTY, Dyavaiah M, DeMott MS, Taghizadeh K, Dedon PC, Begley TJ. A quantitative systems approach reveals dynamic control of tRNA modifications during cellular stress. PLoS Genet. 16 déc 2010;6(12):e1001247.

330. Gu C, Begley TJ, Dedon PC. tRNA modifications regulate translation during cellular stress. FEBS Lett. 28 nov 2014;588(23):4287-96.

331. Dominissini D, Moshitch-Moshkovitz S, Schwartz S, Salmon-Divon M, Ungar L, Osenberg S, et al. Topology of the human and mouse m6A RNA methylomes revealed by m6A-seq. Nature. 29 avr 2012;485(7397):201-6.

332. Squires JE, Patel HR, Nousch M, Sibbritt T, Humphreys DT, Parker BJ, et al. Widespread occurrence of 5-methylcytosine in human coding and non-coding RNA. Nucleic Acids Res. juin 2012;40(11):5023-33.

333. Carlile TM, Rojas-Duran MF, Zinshteyn B, Shin H, Bartoli KM, Gilbert WV. Pseudouridine profiling reveals regulated mRNA pseudouridylation in yeast and human cells. Nature. 6 nov 2014;515(7525):143-6.

334. Edelheit S, Schwartz S, Mumbach MR, Wurtzel O, Sorek R. Transcriptome-wide mapping of 5-methylcytidine RNA modifications in bacteria, archaea, and yeast reveals m5C within archaeal mRNAs. PLoS Genet. juin 2013;9(6):e1003602.

335. Meyer KD, Saletore Y, Zumbo P, Elemento O, Mason CE, Jaffrey SR. Comprehensive analysis of mRNA methylation reveals enrichment in 3' UTRs and near stop codons. Cell. 22 juin 2012;149(7):1635-46.

336. Grozhik AV, Jaffrey SR. Distinguishing RNA modifications from noise in epitranscriptome maps. Nat Chem Biol. 14 2018;14(3):215-25.

337. Ryvkin P, Leung YY, Silverman IM, Childress M, Valladares O, Dragomir I, et al. HAMR: high-throughput annotation of modified ribonucleotides. RNA N Y N. déc 2013;19(12):1684-92.

338. Motorin Y, Helm M. Methods for RNA Modification Mapping Using Deep Sequencing: Established and New Emerging Technologies. Genes. 9 janv 2019;10(1).

339. Cozen AE, Quartley E, Holmes AD, Hrabeta-Robinson E, Phizicky EM, Lowe TM. ARM-seq: AlkB-facilitated RNA methylation sequencing reveals a complex landscape of modified tRNA fragments. Nat Methods. sept 2015;12(9):879-84.

340. Zheng G, Qin Y, Clark WC, Dai Q, Yi C, He C, et al. Efficient and quantitative high-throughput tRNA sequencing. Nat Methods. sept 2015;12(9):835-7.

341. Dai Q, Zheng G, Schwartz MH, Clark WC, Pan T. Selective Enzymatic Demethylation of N2 ,N2 -Dimethylguanosine in RNA and Its Application in High-Throughput tRNA Sequencing. Angew Chem Int Ed Engl. 24 2017;56(18):5017-20.

342. Schaefer M, Pollex T, Hanna K, Lyko F. RNA cytosine methylation analysis by bisulfite sequencing. Nucleic Acids Res. févr 2009;37(2):e12.

343. Carlile TM, Rojas-Duran MF, Gilbert WV. Pseudo-Seq: Genome-Wide Detection of Pseudouridine Modifications in RNA. Methods Enzymol. 2015;560:219-45.

344. Carlile TM, Rojas-Duran MF, Gilbert WV. Transcriptome-Wide Identification of Pseudouridine Modifications Using Pseudo-seq. Curr Protoc Mol Biol. 1 oct 2015;112:4.25.1-24.

345. Schwartz S, Bernstein DA, Mumbach MR, Jovanovic M, Herbst RH, León-Ricardo BX, et al. Transcriptome-wide mapping reveals widespread dynamic-regulated pseudouridylation of ncRNA and mRNA. Cell. 25 sept 2014;159(1):148-62.

346. Lovejoy AF, Riordan DP, Brown PO. Transcriptome-wide mapping of pseudouridines: pseudouridine synthases modify specific mRNAs in S. cerevisiae. PloS One. 2014;9(10):e110799.

347. Nakamoto MA, Lovejoy AF, Cygan AM, Boothroyd JC. mRNA pseudouridylation affects RNA metabolism in the parasite Toxoplasma gondii. RNA N Y N. 2017;23(12):1834-49.

348. Marchand V, Ayadi L, Ernst FGM, Hertler J, Bourguignon-Igel V, Galvanin A, et al. AlkAniline-Seq: Profiling of m7 G and m3 C RNA Modifications at Single Nucleotide Resolution. Angew Chem Int Ed Engl. 17 déc 2018;57(51):16785-90.

349. Maden BE. Mapping 2'-O-methyl groups in ribosomal RNA. Methods San Diego Calif. nov 2001;25(3):374-82.

350. Incarnato D, Anselmi F, Morandi E, Neri F, Maldotti M, Rapelli S, et al. High-throughput single-base resolution mapping of RNA 2′-O-methylated residues. Nucleic Acids Res. 17 2017;45(3):1433-41.

351. Dong Z-W, Shao P, Diao L-T, Zhou H, Yu C-H, Qu L-H. RTL-P: a sensitive approach for detecting sites of 2'-O-methylation in RNA molecules. Nucleic Acids Res. 1 nov 2012;40(20):e157.

352. Aschenbrenner J, Marx A. Direct and site-specific quantification of RNA 2'-O-methylation by PCR with an engineered DNA polymerase. Nucleic Acids Res. 05 2016;44(8):3495-502.

353. Dai Q, Moshitch-Moshkovitz S, Han D, Kol N, Amariglio N, Rechavi G, et al. Nm-seq maps 2'-O-methylation sites in human mRNA with base precision. Nat Methods. juill 2017;14(7):695-8.

354. Zhu Y, Pirnie SP, Carmichael GG. High-throughput and site-specific identification of 2'-O-methylation sites using ribose oxidation sequencing (RibOxi-seq). RNA N Y N. 2017;23(8):1303-14.

355. Birkedal U, Christensen-Dalsgaard M, Krogh N, Sabarinathan R, Gorodkin J, Nielsen H. Profiling of ribose methylations in RNA by high-throughput sequencing. Angew Chem Int Ed Engl. 7 janv 2015;54(2):451-5.

356. Marchand V, Blanloeil-Oillo F, Helm M, Motorin Y. Illumina-based RiboMethSeq approach for mapping of 2'-O-Me residues in RNA. Nucleic Acids Res. 14 juin 2016;

357. Marchand V, Pichot F, Thüring K, Ayadi L, Freund I, Dalpke A, et al. Next-Generation Sequencing-Based RiboMethSeq Protocol for Analysis of tRNA 2′-O-Methylation. Biomolecules [Internet]. 9 févr 2017 [cité 12 juill 2017];7(1). Disponible sur: http://www.ncbi.nlm.nih.gov/pmc/articles/PMC5372725/

358. Schwartz S, Motorin Y. Next-generation sequencing technologies for detection of modified nucleotides in RNAs. RNA Biol. 28 oct 2016;14(9):1124-37.

359. Dabney J, Meyer M. Length and GC-biases during sequencing library amplification: A comparison of various polymerase-buffer systems with ancient and modern DNA sequencing libraries. BioTechniques. 1 févr 2012;52(2):87-94.

360. Abnizova I, Boekhorst R te, Orlov YL. Computational Errors and Biases in Short Read Next Generation Sequencing. J Proteomics Bioinform [Internet]. 2017 [cité 11 mai 2019];10(1). Disponible sur: https://www.omicsonline.org/open-access/computational-errors-and-biases-in-short-read-next-generationsequencing-jpb-1000420.php?aid=85469

361. Schwartz S, Oren R, Ast G. Detection and Removal of Biases in the Analysis of Next-Generation Sequencing Reads. PLOS ONE. 31 janv 2011;6(1):e16685.

362. Kellner S, Ochel A, Thüring K, Spenkuch F, Neumann J, Sharma S, et al. Absolute and relative quantification of RNA modifications via biosynthetic isotopomers. Nucleic Acids Res. 13 oct 2014;42(18):e142.

363. Su D, Chan CTY, Gu C, Lim KS, Chionh YH, McBee ME, et al. Quantitative analysis of ribonucleoside modifications in tRNA by HPLC-coupled mass spectrometry. Nat Protoc. avr 2014;9(4):828-41.

364. Galvanin A, Ayadi L, Helm M, Motorin Y, Marchand V. Mapping and Quantification of tRNA 2'-O-Methylation by RiboMethSeq. Methods Mol Biol Clifton NJ. 2019;1870:273-95.

365. Kohanski MA, Dwyer DJ, Collins JJ. How antibiotics kill bacteria: from targets to networks. Nat Rev Microbiol. juin 2010;8(6):423-35.

366. AbouHaidar MG, Ivanov IG. Non-Enzymatic RNA Hydrolysis Promoted by the Combined Catalytic Activity of Buffers and Magnesium Ions. Z Für Naturforschung C. 1 août 1999;54(7-8):542-8.

367. Jacob D, Thüring K, Galliot A, Marchand V, Galvanin A, Ciftci A, et al. Absolute Quantification of Noncoding RNA by Microscale Thermophoresis. Angew Chem Int Ed Engl. 20 mars 2019;

368. Schubert T, Längst G. Studying epigenetic interactions using MicroScale Thermophoresis (MST). Biophys 2015 Vol 2 Pages 370-380 [Internet]. 13 août 2015 [cité 30 mai 2019]; Disponible sur: http://www.aimspress.com/article/10.3934/biophy.2015.3.370

369. Hauenschild R, Tserovski L, Schmid K, Thüring K, Winz M-L, Sharma S, et al. The reverse transcription signature of N-1-methyladenosine in RNA-Seq is sequence dependent. Nucleic Acids Res. 16 nov 2015;43(20):9950-64.

370. Pang YLJ, Abo R, Levine SS, Dedon PC. Diverse cell stresses induce unique patterns of tRNA up- and down-regulation: tRNA-seq for quantifying changes in tRNA copy number. Nucleic Acids Res. 16 déc 2014;42(22):e170.

371. Jung S, von Thülen T, Laukemper V, Pigisch S, Hangel D, Wagner H, et al. A single naturally occurring 2'-O-methylation converts a TLR7- and TLR8-activating RNA into a TLR8-specific ligand. PloS One. 2015;10(3):e0120498.

372. Judge AD, Bola G, Lee ACH, MacLachlan I. Design of noninflammatory synthetic siRNA mediating potent gene silencing in vivo. Mol Ther J Am Soc Gene Ther. mars 2006;13(3):494-505.

373. Robbins M, Judge A, Liang L, McClintock K, Yaworski E, MacLachlan I. 2'-O-methyl-modified RNAs act as TLR7 antagonists. Mol Ther J Am Soc Gene Ther. sept 2007;15(9):1663-9.

374. Kaiser S, Rimbach K, Eigenbrod T, Dalpke AH, Helm M. A modified dinucleotide motif specifies tRNA recognition by TLR7. RNA. sept 2014;20(9):1351-5.

375. Finlay BB, McFadden G. Anti-Immunology: Evasion of the Host Immune System by Bacterial and Viral Pathogens. Cell. 24 févr 2006;124(4):767-82.

376. Gratz N, Hartweger H, Matt U, Kratochvill F, Janos M, Sigel S, et al. Type I interferon production induced by Streptococcus pyogenes-derived nucleic acids is required for host protection. PLoS Pathog. mai 2011;7(5):e1001345.

377. Freund I, Buhl DK, Boutin S, Kotter A, Pichot F, Marchand V, et al. 2'-O-methylation within prokaryotic and eukaryotic tRNA inhibits innate immune activation by endosomal Toll-like receptors but does not affect recognition of whole organisms. RNA N Y N. juill 2019;25(7):869-80.

378. Sander LE, Davis MJ, Boekschoten MV, Amsen D, Dascher CC, Ryffel B, et al. Detection of prokaryotic mRNA signifies microbial viability and promotes immunity. Nature. 22 mai 2011;474(7351):385-9.

379. Vierbuchen T, Bang C, Rosigkeit H, Schmitz RA, Heine H. The Human-Associated Archaeon Methanosphaera stadtmanae Is Recognized through Its RNA and Induces TLR8-Dependent NLRP3 Inflammasome Activation. Front Immunol. 2017;8:1535.

380. Feng Z, Hensley L, McKnight KL, Hu F, Madden V, Ping L, et al. A pathogenic picornavirus acquires an envelope by hijacking cellular membranes. Nature. 18 avr 2013;496(7445):367-71.

381. Chapuy-Regaud S, Dubois M, Plisson-Chastang C, Bonnefois T, Lhomme S, Bertrand-Michel J, et al. Characterization of the lipid envelope of exosome encapsulated HEV particles protected from the immune response. Biochimie. oct 2017;141:70-9.

382. Ansari MA, Singh VV, Dutta S, Veettil MV, Dutta D, Chikoti L, et al. Constitutive interferon-inducible protein 16-inflammasome activation during Epstein-Barr virus latency I, II, and III in B and epithelial cells. J Virol. août 2013;87(15):8606-23.

383. Abrami L, Brandi L, Moayeri M, Brown MJ, Krantz BA, Leppla SH, et al. Hijacking multivesicular bodies enables long-term and exosome-mediated long-distance action of anthrax toxin. Cell Rep. 27 nov 2013;5(4):986-96.

384. Laganà A, Russo F, Veneziano D, Bella SD, Giugno R, Pulvirenti A, et al. Extracellular circulating viral microRNAs: current knowledge and perspectives. Front Genet. 2013;4:120.

385. Ahsan NA, Sampey GC, Lepene B, Akpamagbo Y, Barclay RA, Iordanskiy S, et al. Presence of Viral RNA and Proteins in Exosomes from Cellular Clones Resistant to Rift Valley Fever Virus Infection. Front Microbiol. 2016;7:139.

Abstract:

For less than a decade, high-throughput sequencing became a very powerful, sensitive and precise technique for the study of ribonucleic acids. During my PhD thesis, I have used this technology for in-depth characterization of the extracellular RNA (exRNA) content of human plasma. exRNA in plasma exists either in a “soluble state” as a component of ribonucleoprotein (RNP) complexes or encapsulated into extracellular vesicles (EV) of diverse origins (exosomes, microvesicles, …). In this project, I have demonstrated that whole human plasma contains mostly micro RNAs and the fragment of RNA hY4, as well as degraded ribosomal RNA. Moreover, using a rigorous strategy *via* size exclusion chromatography or consecutive proteinase K/RNase A treatments, highly purified EVs can be obtained. miRNAs and RNA hY4 fragments were nor present in majority of samples, demonstrating a huge difference between soluble exRNA and exRNA from purified EVs. The RNA content of these EVs mainly reflects RNA composition of human microbiota. In addition, I have also performed a comparative analysis of commercially available “exosome-enrichment” kits which supposed to purify human exosomes by precipitation. RNA composition of such fractions was found to be almost identical to human plasma, showing strong uncontrolled contamination by soluble RNPs. Based on this study, we were able to propose a protocol for studies in exRNA in the field of liquid biopsies with clinical sample in order to discover new diagnostic biomarkers.

Apart from the characterization of RNA, high-throughput sequencing can be used for detection and quantification of RNA post-transcriptional modifications. During my PhD thesis I have applied deep sequencing for analysis of transfer RNA (tRNA) 2’-O-methylations in model bacteria (*E. coli*) using RiboMethSeq. Under several stress conditions, such as starvation and non-lethal antibiotics concentrations, some 2’-O-methylated nucleotides show an adaptive response. While over than half of Gm18 show a global increase under all investigated stress conditions, ribomethylated residues at position 34 show an opposite effect for some antibiotic treatments: mostly for chloramphenicol and streptomycin. Each of these dynamic profiles can be linked to cell regulation in response to stress. Change at the tRNA wobble base (position 34) could be a way to regulate translation by modifying the codon usage. Concerning Gm18, its role in the escape from the human innate immune system during host invasion is currently elucidated.

Keywords: high-throughput sequencing, extracellular RNA, extracellular vesicles, tRNA modifications; 2’O-methylation

Zusammenfassung:

Für weniger als ein Jahrzehnt wurde die Hochdurchsatzsequenzierung zu einer sehr leistungsfähigen, sensitiven und präzisen Technik für die Untersuchung von Ribonukleinsäuren. Während meiner Doktorarbeit habe ich diese Technologie zur eingehenden Charakterisierung des Gehaltes an extrazellulärer RNA (exRNA) in menschlichem Plasma verwendet. exRNA im Plasma liegt entweder in einem "löslichen Zustand" als Bestandteil von Ribonukleoprotein (RNP) -Komplexen vor oder ist in extrazellulären Vesikeln (EV) unterschiedlicher Herkunft (Exosomen, Mikrovesikel, …) eingekapselt. In diesem Projekt habe ich gezeigt, dass gesamtes menschliches Plasma hauptsächlich Mikro-RNAs und das Fragment der RNA hY4 sowie abgebaute ribosomale RNA enthält. Darüber hinaus können unter Verwendung einer rigorosen Strategie mittels Größenausschlusschromatographie oder aufeinanderfolgenden Proteinase K / RNase A-Behandlungen hochgereinigte EVs erhalten werden. miRNAs und RNA-hY4-Fragmente waren in der Mehrzahl der Proben nicht vorhanden, was einen großen Unterschied zwischen löslicher exRNA und exRNA von gereinigten EVs zeigt. Der RNA-Gehalt dieser EVs spiegelt hauptsächlich die RNA-Zusammensetzung menschlicher Mikrobiota wider. Darüber hinaus habe ich auch eine vergleichende Analyse von im Handel erhältlichen Kits zur "Exosomenanreicherung" durchgeführt, mit denen menschliche Exosomen durch Ausfällung gereinigt werden sollen. Es wurde festgestellt, dass die RNA-Zusammensetzung solcher Fraktionen fast identisch mit menschlichem Plasma ist und eine starke unkontrollierte Kontamination durch lösliche RNPs zeigt. Basierend auf dieser Studie konnten wir ein Protokoll für exRNA-Studien im Bereich der Flüssigbiopsie mit klinischer Probe vorschlagen, um neue diagnostische Biomarker zu entdecken.

Neben der Charakterisierung von RNA kann die Hochdurchsatzsequenzierung zum Nachweis und zur Quantifizierung von posttranskriptionellen RNA-Modifikationen verwendet werden. Während meiner Doktorarbeit habe ich eine Tiefensequenzierung zur Analyse von Transfer-RNA (tRNA) 2'-O-Methylierungen in Modellbakterien (E. coli) mit RiboMethSeq durchgeführt. Einige 2'-O-methylierte Nukleotide reagieren unter verschiedenen Stressbedingungen, wie Hunger und nicht-letalen Antibiotika-Konzentrationen, adaptiv. Während mehr als die Hälfte von Gm18 unter allen untersuchten Stressbedingungen einen globalen Anstieg zeigt, zeigen ribomethylierte Rückstände an Position 34 für einige Antibiotika-Behandlungen einen gegenteiligen Effekt: hauptsächlich für Chloramphenicol und Streptomycin. Jedes dieser dynamischen Profile kann als Reaktion auf Stress mit der Zellregulation verknüpft werden. Eine Veränderung an der tRNA-Wobble-Base (Position 34) könnte ein Weg sein, die Translation durch Modifizieren der Codonverwendung zu regulieren. In Bezug auf Gm18 wird derzeit seine Rolle bei der Flucht aus dem angeborenen Immunsystem des Menschen während der Invasion des Wirts aufgeklärt.

Schlüsselwörter: Hochdurchsatzsequenzierung, extrazelluläre RNA, extrazelluläre Vesikel, tRNA-Modifikationen; 2'O-Methylierung